Assessment of neuroprotective treatment strategies to promote photoreceptor survival in a murine model of cone-rod dystrophy and a murine model of retinitis pigmentosa

DISSERTATION

with the aim of achieving the doctoral degree

Doctor rerum naturalium (Dr. rer. nat.)

at the Faculty of Mathematics, Informatics and Natural Sciences

Department of Biology

University of Hamburg

submitted by

Maike Herrmann

Hamburg

2026

The present work was performed at the Experimental Ophthalmology of the Department of Ophthalmology at the University Medical Centre Hamburg-Eppendorf under supervision of Prof. Dr. rer. nat. Udo Bartsch

First reviewer: Prof. Dr. Susanne Dobler

Second reviewer: Prof. Dr. Udo Bartsch

Date of Disputation: 17.06.2026

To my loving parents Dorothea and Peter

and my family, who supported me in all my decisions

“I seem to have been only like a boy playing on the seashore, and diverting myself in now and then finding a smoother pebble or a prettier shell than ordinary, whilst the great ocean of truth lay all undiscovered before me.”

— Isaac Newton

TABLE OF CONTENTS

SUMMARY

Retinal dystrophies, such as cone and cone-rod-dystrophies (CODs/CORDs) or retinitis pigmentosa (RP) are characterised by the progressive loss of photoreceptors and their functionality. Patients with severely progressed retinal dystrophies display, depending on the disorder, symptoms such as photophobia, night blindness, nystagmus, central scotomas, and reduced or absent colour vision. They often exhibit abnormal electroretinograms (ERGs), indicating the loss of rod or cone functionality. These disorders often progress slowly, leading to visual deterioration and eventually blindness. Only few treatment options are currently examined for the treatment of retinal dystrophies, e.g. utilisation recombinant proteins, encapsulated cell therapy (ECT) or injections of viral particles. Fewer still are approved by drug agencies for use in patients.

One of the most regarded forms of treatment is the introduction of cytokines or other small proteins into the vitreous cavity of the eye, often in form of direct intravitreal injections of recombinant proteins. However, due to the chronic and often progressive nature of retinal dystrophies, and fast turn-over of molecules in the vitreous humour, the application of such therapeutics has to be repeated regularly, which can be a burden on both patient and the attending physician. Hence, a sustained approach for the treatment of retinal dystrophies is highly desirable.

The present thesis analysed the neuroprotective effect of a sustained delivery of different neurotrophic factors (NTFs), such as ciliary neurotrophic factor (CNTF), glial cell line-derived neurotrophic factor (GDNF), leukemia inhibitory factor (LIF), progranulin (PGRN) and the designer cytokine hyper-interleukin-6 (hIL6) on degenerating photoreceptors of two animal models of retinal dystrophy. A sustained delivery of the different NTFs was achieved either by application of lentivirally modified neural stem cells (NSCs) or by injection of adeno-associated viruses (AAVs) (hIL6 only). Experiments were conducted in the *Atp1b2*^{Atp1b1} knock-in (ki) mouse, a novel model of a cone-rod dystrophy, and in the rd10 mouse, a well-established model of autosomal-recessive retinitis pigmentosa.

Modified NSCs were examined *in vitro* and *in vivo* to characterise their potential for adequate performance in the animals. Cells expressed the desired NTFs in sufficient amounts and could survive for a prolonged period of time, differentiating into astrocytes *in vivo*, still expressing the respective protein. The neuroprotective effect was examined in immunohistochemically treated retinal sections analysing different parameters, such as inflammation, retina thickness, and the number of both rod and cone photoreceptors at various time points after treatment. In *Atp1b2*^{Atp1b1} ki mice all applied neurotrophic factors, except for GDNF, were suitable to attenuate loss of photoreceptor cells for several months after application of the modified NSCs. In the rd10 mouse model, which mimics both genotype and phenotype of patients with an autosomal-recessive form of retinitis pigmentosa, sustained delivery of hIL6, either by NSCs or AAVs, can protect from rod photoreceptor degeneration for up to 2 months. The collected data suggests a not inconsiderable impact of neuroinflammation on the magnitude of neuroprotection, since better effects have been observed in retinas with a higher degree of inflammation.

The present results indicate that the sustained delivery of neurotrophic factors, such as CNTF, LIF, PGRN and hIL6, by means intravitreal application of lentivirally modified NSCs or AAVs, is suitable to attenuate photoreceptor loss in the retina of *Atp1b2*^{Atp1b1} ki mice and rd10 mice. The activation of pro-survival pathways such as the JAK/STAT or the RAS/MAPK pathways as well as the degree of inflammation seem to be key factors in conveying the neuroprotective effects observed in both animal models.

ZUSAMMENFASSUNG

Retinale Dystrophien, wie etwa Zapfen-Stäbchen-Dystrophien (ZSD) oder Retinitis pigmentosa (RP) sind durch einen fortschreitenden Verlust von Photorezeptoren und deren Funktionalität charakterisiert. Patienten mit weit fortgeschrittenen retinalen Dystrophien erleiden, abhängig von ihrer Erkrankung, unterschiedlichste Symptome. Dazu zählen, unter anderem, starke Lichtempfindlichkeit, Nachtblindheit, Nystagmus, zentral Skotome, und reduzierte oder fehlenden Farbwahrnehmung. Patient*innen zeigen oft abnormale Elektroretinogramme (ERGs), welche starke Indikatoren für den Verlust der Photorezeptor-Funktionalität sind. Retinale Dystrophien entwickeln sich häufig langsam, führen aber zur Verschlechterung der Sehkraft oder zur vollkommenen Erblindung. Es gibt nur wenige gut untersuchte Behandlungsansätze für diese Erkrankungen. Dazu gehören, beispielsweise, die intravitreale Gabe rekombinanter Proteine, der Einsatz von verkapselten Zellen, oder die Injektion viraler Partikel.

Eine der am häufigsten untersuchten Behandlungsoptionen ist sicherlich der Einsatz von Zytokinen oder anderer kleiner Proteine durch intravitreale Injektionen, vor allem in Form rekombinanter Proteine. Da retinale Dystrophien häufig chronisch Verlaufen und es einen hohen Umsatz an Proteinen in der Glaskörperflüssigkeit des Auges gibt, ist eine wiederholte Applikation der eingesetzten Therapeutika notwendig. Dies kann eine immense Belastung sowohl für Patient*innen als auch für die behandelnden Ärzt*innen darstellen. Daher ist eine kontinuierliche Behandlung mit dem jeweiligen Therapeutikum anzustreben.

In der vorliegenden Arbeit wurde der neuroprotektive Effekt durch die kontinuierliche Applikation verschiedener neurotropher Faktoren (NTF), wie zum Beispiel „ciliary neurotrophic factor“ (CNTF), „glial cell line-derived neurotrophic factor“ (GDNF), „leukemia inhibitory factor“ (LIF), „progranulin“ (PGRN) und des Designer-Zytokins „hyper-interleukin-6“ (hIL6), auf die Degeneration der Photorezeptoren in zwei Mausmodellen retinaler Dystrophien untersucht. Eine anhaltende Versorgung der Retina mit den neurotrophen Faktoren wurde durch die Applikation lentiviral modifizierter neuraler Stammzellen (NSCs) oder die intravitreale Injektion Adeno-assoziierter Viren (AAVs) (nur hIL6) erreicht. Die

Experimente wurden an der *Atp1b2*^{Atp1b1} knock-in (ki)- Maus, einem neueren Model einer Zapfen-Stäbchen-Dystrophie, und der rd10-Maus, einem etablierten Model einer autosomal-rezessiven Retinitis pigmentosa, durchgeführt.

Modifizierte NSCs wurden sowohl *in vivo* als auch *in vitro* auf ihr Potenzial einer adäquaten Performanz in den Tiermodellen hin untersucht. Die untersuchten Zellen exprimierten die erwünschten NTFs in ausreichender Menge und konnten über einen längeren Zeitraum im Glaskörper überleben und sogar in Astrozyten differenzieren, wobei die immer noch das gewünschte Protein exprimierten. Der neuroprotektive Effekt der NTFs wurde in immunhistochemisch behandelten Retinae anhand verschiedener Parameter untersucht, etwa dem Grad der Neuroinflammation, der Retinadicke und der Anzahl vorhandener Stäbchen und Zapfen. Dies geschah zu verschiedenen Zeitpunkten nach erfolgter Applikation von Zellen oder AAVs.

Untersuchungen zeigten einen neuroprotektiven Effekt aller eingesetzten NTFs, außer GDNF, auf die Photorezeptoren in *Atp1b2*^{Atp1b1} ki-Mäusen über mehrere Monate hinweg. Auch in rd10-Mäusen, welche in Genotyp und Phänotyp einer humanen autosomal-rezessiven Retinitis pigmentosa ähneln, konnte ein neuroprotektiver Effekt durch die Behandlung mit hIL6 – durch Zellen oder AAVs – in bis zu 2-Monaten alten Tieren festgestellt werden. Die vorliegenden Daten legen zudem einen großen Einfluss von Neuroinflammation auf den Grad der Neuroprotektion durch die Behandlung mit NTFs nahe.

Die anhaltende Behandlung retinaler Dystrophien mittels verschiedener neurotropher Faktoren, wie etwas CNTF, LIF, PGRN oder hIL6 durch intravitreale Applikation von lentiviral modifizierten Zellen oder AAVs, stellt einen vielversprechenden Ansatz zum Schutz von Photorezeptoren in *Atp1b2*^{Atp1b1} ki-Mäusen sowie rd10-Mäusen dar. Die Aktivierung verschiedener Signalwege, z.B. des JAK/STAT Signalweges oder des RAS/MAPK Signalweges, und der Grad der Inflammation scheinen dabei eine Schlüsselrolle in der Vermittlung neuroprotektiver Effekte einzunehmen.

1. INTRODUCTION

1.1. THE MAMMALIAN RETINA

1.1.1. RETINAL CELL TYPES AND THEIR ORGANISATION

The retina is a complex, light-sensitive tissue in the back of the eye, allowing for the conversion of light energy into electrical and chemical signals for subsequent processing in the visual cortex of the brain (***FIG. 1***). The transparent tissue consists of millions of cells categorized in over 100 distinct cell types in six cells classes, including five neuronal cell classes and glial cells, which can be subdivided into three different cell classes (reviewed in: Hussey et al. (2022); Peng (2023); Reichenbach and Bringmann (2020)). A considerable part of the visual processing takes place in the retina (Gollisch & Meister, 2010). The visual system is incredibly adaptive to a wide range of visual stimuli, e.g. being able to process differences of 10 log units in light intensity by multiple stages of light adaptation and modulation (Rodieck, 1998). The incoming visual information is typically processed in parallel, i.e. different information, such as contours, colour and movements are processed simultaneously by different cells in the retina and subsequently in different parts of the cortex (Wässle, 2004).

The retina is embedded in the retinal pigment epithelium (RPE), which catches stray photons to improve visual acuity by maximising the signal-to-noise ratio and minimise light damage to other cells. Additionally, the RPE phagocytises the outer segments (OS) of photoreceptors (PR), 10% of which are shed and replaced daily (Wen et al., 2012; Young, 1967). The RPE additionally recycles all-*trans*-retinal to provide the photoreceptors with a steady supply of 11-*cis*-retinal and opsins (*cf.* **1.1.2. THE PHOTOTRANSDUCTION CASCADE AND THE VISUAL CYCLE**; ***FIG. 3***). Microglia, astrocytes and Müller cells (MCs), the resident glia cells of the retina remove metabolites and excess neurotransmitters from the retina and provide neurons with neurotrophic factors (NTFs) and anti-inflammatory cytokines (Reichenbach & Bringmann, 2020). Müller cells additionally act as light cables, guiding light in the 560 nm range, corresponding to yellow-green light, directly to the outer segments of M-cones (***FIG. 1***C) (Agte et al., 2011; Hussey et al., 2022).

1.1.1.1. PHOTORECEPTORS

Photoreceptors can be distinguished into two distinct subclasses, rods and cones. They mediate scotopic and photopic vision, respectively. In the murine retina, about 97.2% of photoreceptors, estimated at ~6.4 million cells, are rods, with cones,

constituting the remaining 2.8%, estimated at ~180,000 cells (Curcio et al., 1990; Jeon et al., 1998). In contrast to the human retina, in which cones are concentrated in the macula, in the murine retina cones are relatively evenly distributed, referred to as photoreceptor mosaic. The murine retina contains three types of photoreceptors (reviewed in: Hussey et al. (2022); Krishnamoorthi et al. (2023)):

(i) rods, mediating the perception of contrasts (λ_{max}[1]: 498 nm)
(ii) S-cones, sensitive for short wavelength light (blue; λ_{max}: 420 nm)
(iii) M-cones, sensitive for medium wavelength light (green; λ_{max}: 530 nm).

Photoreceptors are comprised of three segments (***FIG. 1***C). The outer segments contains the membranous disks with the visual pigments in which the phototransduction and part of visual cycle take place (*cf.* **1.1.2. THE PHOTOTRANSDUCTION CASCADE AND THE VISUAL CYCLE**; **FIG. 3**). The inner segments (IS) contain essential organelles of the cell, e.g. mitochondria and the endoplasmic reticulum. Numerous mitochondria provide the energy required for the continual renewal of disks. The inner segment is connected to the cell soma containing the nucleus. All photoreceptor nuclei are located in the outer nuclear layer (onl) (***FIG. 1***B).

1.1.1.2. INNER RETINAL CELLS

Visual signals generated by photoreceptors are transmitted to the inner retina in which three classes of interneurons are present: horizontal cells (HCs), bipolar cells (BPs) and amacrine cells (ACs) (***FIG. 1***A). Their somata are localised in the inner nuclear layer (inl) (***FIG. 1***B). The interneurons transmit visual signals from photoreceptors to retinal ganglion cells (RGCs), pre-processing the signals they receive in the process.

Horizontal cells provide lateral processing of incoming signals from photoreceptors through negative feedback (reviewed in: Masland (2012); Wässle (2004)). Due to the interconnection of horizontal cells by gap junctions, the negative feedback can be averaged over a large area, creating a global gain control, keeping signals from the photoreceptors within operating range (Macosko et al., 2015; Masland, 2012). Recent messenger ribonucleic acid-sequencing (mRNA-seq) data

[1] maximum of light absorption spectrum

supports the notion that mice, in contrast to other mammals, possess only one type of horizontal cells (Macosko et al., 2015).

The adjusted visual information from photoreceptors is transmitted to the bipolar cells. Rod bipolar cells innervate rod photoreceptors in a 1:1 pattern, while cone bipolar cells innervate all cone photoreceptors within the reach of their dendritic arbour and mediate some cross-talk with rods (Masland, 2012). This innervation pattern allows for the tuning of the cone-bipolar cell synapse output, and the transmission of different signals from multiple cone photoreceptors to the RGCs and subsequent pre-processing of visual information in the retina itself. Recent data suggests the existence of 15 different bipolar cell types with distinctive molecular signatures in the murine retina (Masland, 2012; Shekhar et al., 2016).

Spatiotemporal processing of the visual information is provided by the highly interconnected, mostly inhibitory amacrine cells (Diamond, 2017; Yan et al., 2020). They process signals coming from bipolar cells and other amacrine cells providing feedback to their input cells and feedforward output to the retinal ganglion cells. Some amacrine cells process very specific information, e.g. starburst amacrine cells (SACs), which respond specifically to input encoding motion in specific directions. Other amacrine cell types are broader in their input and output. AII amacrine cells, for example, respond to signals from all ON and OFF bipolar cells. In fact, many amacrine cells respond to the input of multiple innervating bipolar cells and contact different RGCs (reviewed in: Diamond (2017); Masland (2012)). To date 63 different types of amacrine cells have been identified (Yan et al., 2020).

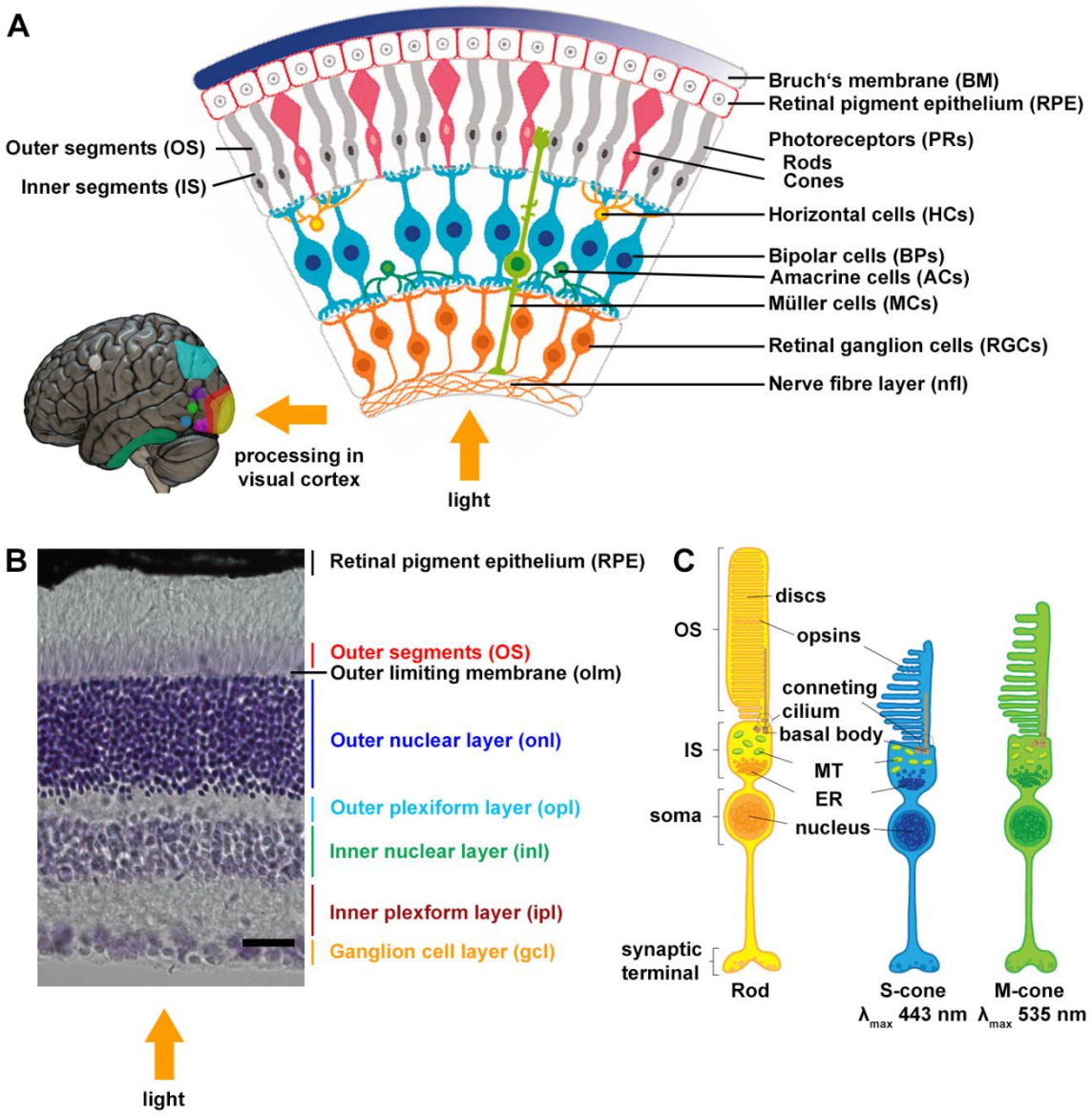

FIG. 1: SCHEMATIC OF THE MAMMALIAN RETINA.
(A) Schematic of retinal cell types and their localisation in the retina. (B) Nissl staining of an adult mouse retina with indication of the retinal layers. (C) Schematic of the murine photoreceptors. λ_{max}: maximum of light absorption spectrum; ACs: amacrine cells; BM: Bruch's membrane; BPs: bipolar cells; ER: endoplasmic reticulum; gcl: ganglion cell layer; HCs: horizontal cells; inl: inner nuclear layer; ipl: inner plexiform layer; MCs: Müller cells; MT: mitochondria; nfl: nerve fibre layer; olm: outer limiting membrane; onl: outer nuclear layer; opl: outer plexiform layer; PRs: photoreceptors; RGCs: retinal ganglion cells; RPE: retinal pigment epithelium. Scale bar in B: 25 µm.
(A) Retina schematic adapted from Ghasemi et al. (2018), © 2017, reprinted by permission of Informa UK Limited, trading as Taylor & Francis Group, https://www.tandfonline.com, and visualisation of visual cortex adapted from Ionta (2021) under Creative Commons Attribution License (CC BY). (C) Adapted from Hussey et al. (2022) under Creative Commons Attribution License (CC BY).

1.1.1.3. RETINAL GANGLION CELLS

Retinal ganglion cells, the last cells to receive input within the retina, are the retina's projecting neurons. They transmit the visual information to the tectum and diencephalon and subsequently to the primary visual cortex (V1) (***FIG. 1***A). Sanes and Masland (2015) recognised 10 subclasses of RGCs in which the ~46 different RGC

types characterised in the murine retina to date (Tran et al., 2019) can be organised. These subclasses, identified according to morphological, functional and molecular criteria include:

(i) directionally sensitive RGCs (ON-OFF- and ON-DSGCs)
(ii) αRGCs
(iii) intrinsically photosensitive RGCs (ipRGCs)
(iv) Local edge detectors (LEDs) and
(v) Junctional adhesion molecule B (JAM-B)-expressing RGCs (J-RGCs).

The somata of RGCs are usually located in the ganglion cell layer (gcl) (***FIG. 1***A,B), although the cell bodies of about 2% of the RGC population are found to be displaced in the inl (Dräger & Olsen, 1981).

The different RGC subclasses fulfil more or less specific tasks, ranging from the detection of specific motions (DSGCs, αRGCs) to edge detection (LEDs) and entrainment of the circadian clock (ipRGCs). They mostly process the already specific input they receive from the retinal interneurons. SACs, for example innervate DSGCs specifically. RGCs mostly project to the *corpus geniculatum dorsolaterale* (dLGN), located in the dorsal thalamus, and the *colliculus superior* (SC), located on the roof of the mammalian midbrain and the accessory optic system (Kerschensteiner & Feller, 2024). However, projections to at least 20 different brain areas have been found. IpRGCs project to the *nucleus suprachiasmaticus* (SCN) located in the hypothalamus, synchronising the circadian oscillator (Sanes & Masland, 2015).

1.1.2. THE PHOTOTRANSDUCTION CASCADE AND THE VISUAL CYCLE

Phototransduction in the retina begins with the entrance of a photon into the eye. This induces the photoisomerization of the chromophore 11-*cis*-retinal, a vitamin A derivative, to all-*trans*-retinal in the photoreceptor outer segment (Hussey et al., 2022). The conformational change allows an opsin, a photo-sensitive G-protein coupled receptor (GPCR), covalently bound to the chromophore by a Schiff base, to trigger the phototransduction cascade (Hubbard & Kropf, 1958). During the phototransduction, the G-protein transducin (G_t), is activated and induces the exchange of guanosine diphosphate (GDP) and guanosine triphosphate (GTP) in the transducin α-subunit (Gα), also known as guanine nucleotide-binding protein G(t) subunit α1 (GNAT1) and the subsequent dissociation of the transducin β- and γ-subunit

(Gβγ) from the now activated Gα*-GTP complex (***FIG. 2***). Two Gα* are required to activate phosphodiesterase 6 (PDE6), alleviating the inhibition of the enzyme at the γ-subunit, and allowing for the hydrolysis of cyclic guanosine monophosphate (cGMP) by guanylyl cyclase (GC). Hydrolysis of cGMP and the associated drop of cGMP levels in the cytoplasm causes cGMP-gated ion channels to close, leading to the hyperpolarisation of the cell membrane and the subsequent decrease of glutamate released towards downstream interneurons, proportional to the light intensity (Hussey et al. (2022), reviewed in: Arshavsky et al. (2002); Arshavsky and Wensel (2013); Cote et al. (2022)).

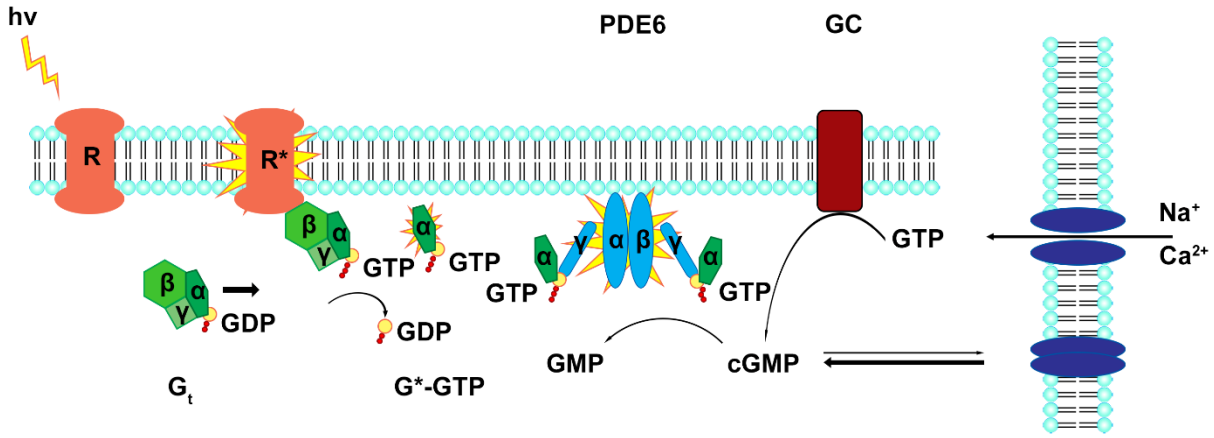

FIG. 2: SCHEMATIC OF THE PHOTOTRANSDUCTION IN THE MAMMALIAN RETINA.
The phototransduction takes place in the outer segments of photoreceptors. cGMP: cyclic guanosine monophosphate; G*: activated α subunit of G_t; GC: guanylyl cyclase; GDP: guanosine diphosphate; GMP: guanosine monophosphate; G_t: G-protein transducin; GTP: guanosine triphosphate; hv: light energy; PDE6: phosphodiesterase 6; R: rhodopsin; R*: activated rhodopsin. Adapted and redrawn after Grossniklaus et al. (2015) under Creative Commons license 3.0 AT-SA.

Several mechanisms allowing for the regeneration of 11-*cis*-retinal have been proposed (reviewed in: Swigris et al. (2025)). The canonical, light-independent visual cycle (***FIG. 3***a) involves the recovery of the photoisomerised 11-*cis*-retinal by reduction of the photoisomerised all-*trans*-retinal to all-*trans*-retinol by retinol dehydrogenase 8 (RDH8), and subsequent transfer to the RPE. After esterification by lecithin retinol acyltransferase (LRAT) and conversion to 11-*cis*-retinol by all-trans retinyl isomerase (RPE65), the molecule is oxidised to 11-*cis*-retinal and transferred to the photoreceptor outer segments. Here, the chromophore is bound to photoreceptor specific opsins, forming, for example, the rod-specific rhodopsin (RHO) (Kiser et al., 2014; Sato & Kefalov, 2024; Travis et al., 2007; Tsin et al., 2018).

A separate cone specific, light-independent visual cycle (***FIG. 3***b) has been proposed as well, taking place entirely in the neural retina, not the RPE (Mata et al., 2002; Tsin et al., 2018; Wang et al., 2009). Such a cone specific visual cycle could explain the fast regeneration of cone visual pigments, which has been reported to be ~2000-fold higher in cone photoreceptors than in rod photoreceptors in the cone-dominant, primate retina (Mata et al., 2002; Schnapf et al., 1990). However, recently, Bassetto et al. (2024) have demonstrated in mice with RPE- and MC-specific knock-out (ko) of cellular retinaldehyde-binding protein (CRALBP), a retinoid carrier involved in the regeneration of 11-*cis*-retinol and 11-*cis*-retinaldehyde, that this mechanism is only of limited importance for the regeneration of 11-*cis*-retinal in cone photoreceptors in the murine retina.

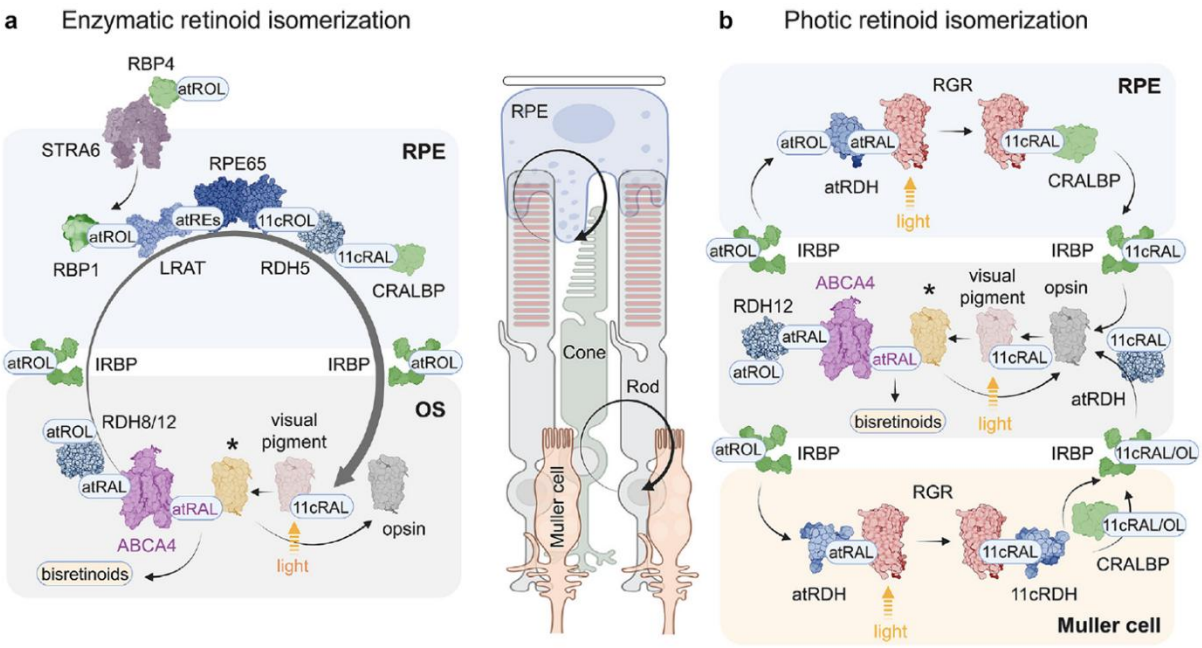

FIG. 3: CANONICAL AND PUTATIVE VISUAL CYCLES IN ROD AND CONE PHOTORECEPTORS.
Schematic representation of the (a) canonical, light-independent visual cycle or enzymatic retinoid isomerization and (b) a putative photic retinoid isomerization in the murine retina. 11cRAL: 11-cis-retinal; 11cRDH: 11-cis-retinol dehydrogenases; 11cROL: 11-cis-retinol; ABCA4: retinal-specific phospholipid-transporting ATPase 4; atRAL: all-trans-retinal; atRDH: all-trans-retinol hydrogenases; atREs: all-trans-retinyl esters; atROL: all-trans-retinol; CRALBP: cellular retinaldehyde-binding protein; IRBP: interphotoreceptor retinoid-binding protein; LRAT: lecithin retinol acyltransferase; OS: photoreceptor outer segments; RBP1: retinol-binding protein 1; RBP4: serum retinol-binding protein; RDH5: all-trans-retinol hydrogenase 5; RDH8: all-trans-retinol hydrogenase 8; RDH12: all-trans-retinol hydrogenase 12; RGR: retinal G-protein coupled receptor; RPE: retinal pigment epithelium; RPE65: all-trans retinyl isomerase; STRA6: stimulated retinoic acid-6 receptor. Adapted from Swigris et al. (2025) under Creative Commons Attribution License 4.0 (CC BY-NC).

1.2. RETINAL DISEASES

Inherited retinal dystrophies (IRDs) are a heterogeneous group of often monogenetic, progressive neurodegenerative retinal disorders. IRDs primarily affect photoreceptors and the RPE and often lead to complete loss of vision (reviewed in: Ben-Yosef (2022); Nebbioso et al. (2025)). The most common IRD is retinitis pigmentosa (RP), but cone or cone-rod dystrophies (COD or CORDs, respectively) and Stargardt disease (STGD1) are also common. Furthermore, a plethora of genetic mutations causing IRDs have been identified (>330 different genes; see https://retnet.org/, retrieved 17.01.2026), which can be involved in multiple disorders, e.g. in both RP and CORDs. The manifesting form of IRD depends on the respective mutation. Nevertheless, due to the heterogeneous nature of IRDs, for about 40% of the diseases (up to 50% for autosomal-dominant RP) the genetic cause is still unknown.

1.2.1. CONE-ROD DYSTROPHIES

As reviewed by Hamel (2007), cone-rod dystrophies are mostly non-syndromic disorders with an estimated prevalence of 1/40,000 affected people. CORDs can be inherited in an autosomal-dominant, autosomal-recessive or X-linked recessive pattern.

CORDs are characterised by the gradual and eventually complete loss of cone photoreceptors, followed by a loss of rods. Early symptoms of non-syndromic CORDs include loss of visual acuity, usually becoming apparent at an early age, photophobia, dyschromatopsia and a deviated gaze, allowing for the use of often less damaged parafoveal regions for vision. Although night blindness is often not present or less prominent than the decrease in visual acuity in early stages of CORDs, it becomes more prominent with increasing involvement of rod photoreceptors. At this point, the progression of the peripheral vision loss also becomes more apparent, making it more difficult for patients to safely move around autonomously. With the continued decrease in visual acuity, reading becomes more difficult. Nystagmus is often present. Furthermore, with increasing degeneration of photoreceptors, a-wave amplitudes in photopic and later scotopic electroretinograms (ERGs) decrease, rendering ERGs a valuable diagnostic tool (Haraguchi et al., 2023).

The aetiology of CORDs is highly complex. Most cases, approximately 5-10% of autosomal-dominant cases, are caused by mutations in the cone-rod homeobox

protein (CRX; encoded by *CRX*), which is important for photoreceptor differentiation(Hamel, 2007). Mutations in *CRX* can also provoke Leber congenital amaurosis (LCA) and in rare cases retinitis pigmentosa. Other cases of autosomal-dominant CORDs are associated with guanylyl cyclase activating protein 1 (GCAP1; encoded by *GUCA1A*). 30-60% of autosomal-recessive cases of CORDs are caused by truncating mutations in the retinal-specific phospholipid-transporting ATPase subfamily A type 4 (ABCA4), also associated with Stargardt disease. X-linked CORDs are mostly associated with mutations of the X-linked retinitis pigmentosa GTPase regulator (RPGR). CORDs as part of syndromic diseases have been described, among others, in Bardet-Biedl syndrome (BBS), spinocerebellar ataxia type 7, and several ectodermal diseases.

1.2.2. RETINITIS PIGMENTOSA

Retinitis pigmentosa is characterised, in contrast to CORDs, by the primary degeneration of rod photoreceptors, resulting in loss of peripheral vision and subsequent symptoms like night blindness and the so-called “tunnel vision” (reviewed in: Hamel (2006); Hartong et al. (2006)). The loss of rod photoreceptors is followed by the secondary degeneration of cone photoreceptors, eventually leading to disturbances in the central vision as well. With the disease progression other symptoms, such as photophobia, dyschromatopsia, particularly affecting the perception of blue and yellow hues, macular oedema or foveomacular atrophy and cataract might occur. With increasing photoreceptor degeneration, scotopic and eventually photopic ERGs become unrecordable. In most RP forms the slow degeneration of rod photoreceptors precedes the degeneration of cone photoreceptors, however, RP cases in which the degeneration of both photoreceptor types occurs nearly simultaneously have been described as well. Pigment deposits, which gave the disease its name, are a result of the infiltration of the neural retina by RPE cells as a result of photoreceptor death (Hamel, 2006).

To date, more than 100 gene loci carrying mutations leading to RP have been identified (Gopalakrishnan et al., 2023; Khaparde et al., 2024). However, the majority of cases is correlated to only a limited number of mutations in genes associated with the signal transduction pathways in rod photoreceptors. Mutations in the rhodopsin gene (*RHO*) cause ~15-25% of autosomal-dominant RP, whereas mutations in usherin (*USH2A*) are linked to Usher syndrome and other autosomal-recessive cases (Hartong

et al., 2006). Mutations in *RPGR* are associated with X-linked RP accounting for 15% of all RP cases and 80% of X-linked RP case (Hwang et al., 2025). Taken together, these genes account for ~30% of all RP cases, whereas in ~40% of cases the causative gene is still unknown (Hartong et al., 2006). Generally, due to the tight regulation of the rod environment any mutations in a protein associated with

(i) the rod signal transduction (e.g. RHO, phosphodiesterase 6 subunits (PDE6A, PDE6B), subunits of the rod cGMP gated channel (CNG))
(ii) cytoskeleton proteins (e.g. peripherin 1 and 2(PRPH1, PRPH2), rod outer segment membrane protein 1 (ROM1))
(iii) protein trafficking (e.g. RPGR, oxygen-regulated protein 1 and 2 (RP1, RP2))
(iv) photoreceptor differentiation (e.g. CRX, neural retina-specific leucine zipper protein (NRL))
(v) the composition of extracellular matrices (ECM) (e.g. usherin) or
(vi) the composition of lipids (e.g. ABCA4),

among others, can result in a form of RP (Hamel, 2006).

Retinitis pigmentosa affects ~1/4,000 people (Hamel, 2006). RP can occur either in a non-syndromic form or as part of a syndromic disease. Examples for syndromic diseases are Usher syndrome, in which co-morbidity occurs between RP and neurosensory deafness, BBS, or neuronal ceroid lipofuscinosis (NCL), in which retinal degeneration is associated with mental decline, seizures, and ataxia (Hamel, 2006).

1.3. THERAPIES

To date, although countless research efforts to find treatments for retinal dystrophies have been undertaken, only few therapeutics have been successful in clinical trials. This is not only due to the vast genetic and phenotypic heterogeneity of IRDs, but also due to the low prevalence of the different diseases. Other obstacles in the examination of relevant therapeutics are the isolation of the eyes by the blood-retina-barrier (BRB), which makes a systemic administration of many drugs impossible, and the relative short half-life time of many therapeutics within the eye.

1.3.1. THE BLOOD-RETINA-BARRIER AND ITS IMPLICATIONS FOR TARGET DELIVERY

A major disadvantage in the treatment of retinal diseases is the highly protected status of brain and retina due to their isolation from the cardiovascular system by the blood-brain-barrier (BBB) and BRB respectively, complicating the treatment of neurodegenerative diseases (Brent, 1990; Streilein, 1999; Streilein et al., 2000). The BRB consists of tight junctions between endothelial cells, retinal capillaries and junctional complexes of the RPE and the pigment epithelial cells of the pars plana. It is selectively permeable for lipophilic molecules. While this prevents harmful substances from entering the eye, it also impedes therapeutics from reaching the retina (Ham et al., 2023). Therefore, a local administration, rather than a systemic one is necessary for the delivery of therapeutics for the treatment of retinal disorders. A local administration can be achieved by either the intravitreal or subretinal application of different drugs, such as recombinant proteins, viral vectors, e.g. lentiviruses (LV), adenoviruses (AD) or adeno-associated viruses (AAV), drug-loaded nanoparticles (NP) or hydrogels, or using encapsulated cell therapy (ECT; see below). Due to the relatively low risk profile and the possibility of a sustained administration of NTFs, the projects presented in this thesis focused on treatment options utilising intravitreal application of NTF-overexpressing cells and NTF-encoding AAV vectors.

1.3.2. ENCAPSULATED CELL THERAPY

The encapsulated cell therapy uses small devices made from biocompatible, semi-permeable polymer membranes containing drug-secreting cells that are sutured to the pars plana, as illustrated in ***FIG. 4*** for the Revakinagene taroretcel-lwey ECT device (ENCELTO™; Neurotech Pharmaceuticals, Inc., Cumberland, RI, USA; Chew et al. (2025)). The ECT device has been recently approved by the U.S. Food and Drug Administration (FDA) for treatment of patients with macular telangiectasia type 2 (MacTel). MacTel is characterised by capillary abnormalities in the fovea and perifovea, leading to loss of photoreceptor nuclei layers in the onl.

The capsule contains scaffolding made from polyethylene terephthalate filaments which allow for genetically modified RPE cells, expressing ciliary neurotrophic factor (CNTF), to attach to. Through the semi-permeable membrane, cells are provided with nutrients and oxygen from the vitreous and secrete the NTF. The implants stably secrete therapeutically relevant doses of CNTF for up to 14.5 years, with an estimated half-life time the cells of 4.25 years (Kauper et al., 2012; Kauper et

al., 2025). The therapeutic potential of the implant has also been examined in patients with retinitis pigmentosa and Usher syndrome type 2 or 3 (NCT01530659), Ischemic optic neuropathy (NCT01411657) and achromatopsia (NCT01648452), but phase III trials were not successful. The implant is currently being tested on glaucoma patients (NCT04577300).

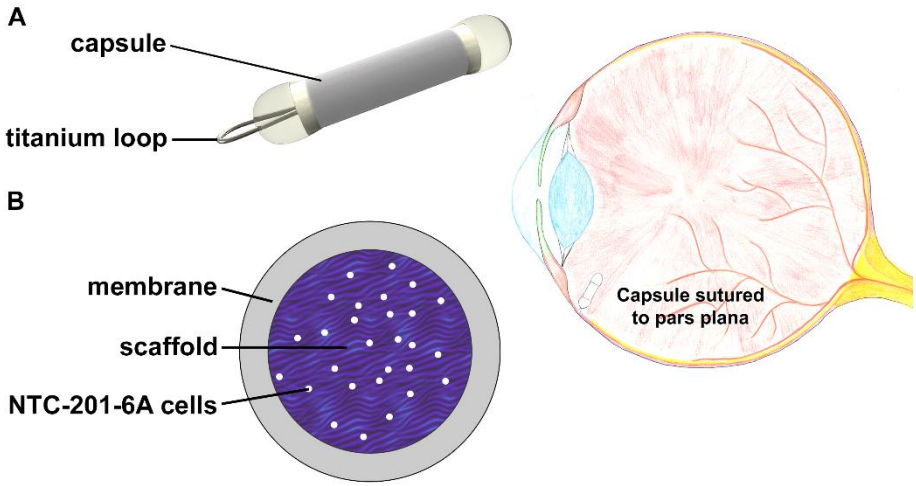

FIG. 4: THE REVAKINAGENE TARORETCEL-LWEY ECT DEVICE.
(A) Schematic of a Revakinagene taroretcel-lwey capsule (ENCELTO™; length: ca. 6.5 mm including titanium loop) loaded with RPE cells overexpressing CNTF. A titanium loop allows for the implantation of the capsule in the pars plana. (B) The capsule is composed of a biocompatible, semi-permeable polymer membrane, allowing for the supply of the cells with nutrients and oxygen and the secretion of CNTF. The capsule contains scaffolding made from polyethylene terephthalate filaments, which allows the cells to attach to. CNTF: ciliary neurotrophic factor; RPE: retinal pigment epithelium. Adapted from Kauper et al. (2025) and Kedarisetti et al. (2022) under Creative Commons Attribution License (CC BY).

1.3.3. USAGE OF VIRAL PARTICLES IN IRD TREATMENT

Gene therapies usually denote methods to alter gene expression or properties of cells. These methods encompass the gene replacement of defective genes, gene editing using, e.g. Clustered Regularly Interspaced Short Palindromic Repeats (CRISPR)/CRISPR-associated endonuclease 9 (Cas9) to repair genomes, or gene silencing to downregulate gene expression. The most common vectors used in gene therapy are viral vectors, such as lentiviruses, adenoviruses or AAVs. Other delivery methods such as chemical transfection, electroporation or microinjections are also suitable to transfer deoxyribonucleic acid (DNA) or ribonucleic acid (RNA) into cells (Khaparde et al., 2024). These methods of causative gene therapy require specific knowledge on the disease-causing mutation, or at least of the causative gene, and, hence, genetic analysis.

It is also possible to express biological therapeutics, such as NTFs, in diseased tissues using viral particles. In the present study, intravitreal injections using AAV vectors encoding hyper-interleukin-6 (hIL6) was performed to analyse the effect of the designer cytokine on the progression of photoreceptor degeneration in a murine model of autosomal-recessive retinitis pigmentosa and in a murine model of a cone-rod dystrophy.

Self-complementary AAVs with a shH10 serotype, showing a pronounced tropism for Müller cells and, to a lower degree, for photoreceptors, RPE cells and RGCs and with a high transduction efficiency were used (Gonzalez-Cordero et al., 2018; Klimczak et al., 2009; Pellissier et al., 2014).

A limiting factor in gene therapy is the relatively small packaging capacity of AAVs (~4.7 kilobases (kb)) (***FIG. 5***). In genetically modified AAVs, the replication (rep) and capsid (cap) genes of the viral genome are often displaced in a different plasmid to allow for bigger inserts of target proteins.

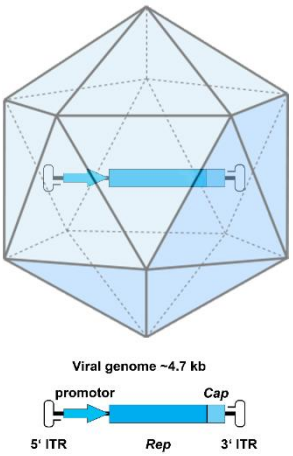

FIG. 5: SCHEMATIC REPRESENTATION OF AN ADENO-ASSOCIATED VIRUS (AAV).
AAVs are comprised of an icosahedral capsid containing the ~4.7 kilobases long viral genome. The genome consists of a promotor, the *rep* and *cap* genes, flanked on either side by inverted terminal repeats (ITRs). In genetically modified AAVs, *rep* and *cap* are often displaced in a different plasmid to allow for bigger inserts of target proteins. For a fully functional AAV, replication genes from adeno viruses in a helper plasmid are needed cap: capsid gene; ITR: inverted terminal repeats; kb: kilobases; rep: replication gene.

Although the outcomes of many pre-clinical gene therapy studies in different animal models were promising, and many clinical trials have been undertaken (reviewed in: Georgiou et al. (2021); Khaparde et al. (2024)), to date, only one gene therapy (Voretigene Neparvovec-rzyl; Luxturna®, Novartis Pharma GmbH, Nürnberg, Germany) has been approved for the treatment of RP and LCA type 2 by the European

Medicines Agency (EMA) and the FDA. The gene therapy employs an AAV serotype 2 (AAV2) encoding for *RPE65* (injection of $5\times 10^{11}\ vg/ml$), allowing to express a functional all-trans-retinyl-palmitate hydrolase in RPE cells (https://www.ema.europa.eu/en/medicines/human/EPAR/luxturna, https://www.fda.gov/vaccines-blood-biologics/cellular-gene-therapy-products/luxturna, retrieved on 17.01.2026).

Studies have shown stable expression of *RPE65* over a prolonged period and an improvement in mobility of treated patients under low light conditions over 4 years. Interestingly, the best corrected visual acuity (BCVA) initially improved over the first three years, before reverting to injection baseline, measured ≤90 days before treatment (Maguire et al., 2019), at the 4-year examination. Luxturna was not anticipated to affect cone photoreceptors in the examined diseases, which mainly affect rods (Maguire et al., 2021; Russell et al., 2017). The improvement in BCVA might be attributable to the improvement in rod photoreceptor viability and subsequent improvement of cone photoreceptor health and less irregular opsin trafficking due to the presence of functional 11-*cis*-retinal (Kono, 2015; Russell et al., 2017). The observed decline in BCVA at the 4-year examination was attributed to the retinal detachment in one patient, whereas the improvement of the BCVA in other patients remained stable (Maguire et al., 2021). Of note, recently, some reports of a worsening of the retinal degeneration and neuroinflammation in patients treated with Luxturna have been reported (Gange et al., 2022; Kessel et al., 2022; Rebelo Neves et al., 2023; Sengillo et al., 2022).

1.4. THE *ATP1B2*^{ATP1B1} KI MOUSE MODEL OF A CONE-ROD DYSTROPHY

1.4.1. THE SODIUM-POTASSIUM-ATPASE

1.4.1.1. SUBUNITS OF THE SODIUM-POTASSIUM-ATPASE

The sodium-potassium-ATPase (Na,K-ATPase or NKA; ***FIG. 6***), is a member of the superfamily of P-type ATPases. The heterodimeric ion pump consists of a catalytic α-subunit (α1-α4; encoded by *Atp1a1-Atp1a4*; ~112 kDa) and a β-subunit (β1-β3; encoded by *Atp1b1-Atp1b3*; ~33 kDa), which functions as a chaperone and ensures maturation of functional NKA. The β-subunit also mediates the intracellular transport and integration of the α-subunit into the cell membrane (Blanco & Mercer, 1998; Contreras et al., 2024). Furthermore, a so-called FXYD subunit (FXYD1-FXYD7; encoded by *Fxyd1-7*; ~10 kDa), modulates the kinetic properties of the NKA when

associated with the αβ heterodimer (Mishra et al., 2011). The NKA has a stoichiometry of 1α: 1β (:1FXYD, if present) under normal conditions (Fedosova et al., 2021).

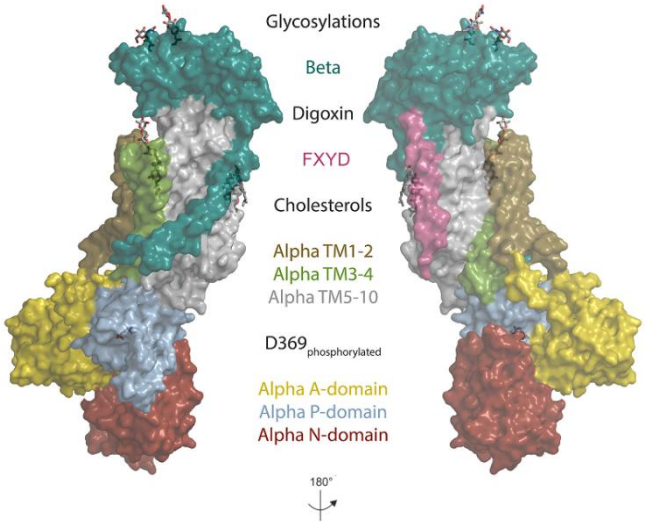

FIG. 6: STRUCTURE OF THE SODIUM-POTASSIUM-ATPASE (NA,K-ATPASE OR NKA).
The heterodimeric ion pump NKA is comprised of a catalytic α-subunit consisting of ten transmembrane (TM) domains and a β-subunit, functioning as a chaperone, consisting of a transmembrane and a large extracellular domain. Although the modulating FXYD is often associated with the NKA, it is not mandatory for proper functioning of the enzyme. Alpha: α-subunit of the NKA; Beta: β-subunit of the NKA; D369: aspartic acid 369; NKA: sodium-potassium-ATPase; TM: transmembrane domain.
NKA subunits and subunit domains are represented in colours as indicated, glycosylation residues, digoxin, cholesterols and phosphorylated D369 are represented as sticks. Adapted from Clausen et al. (2017) with surface representation of digoxin bound α1-subunit structure from Laursen et al. (2015) under Creative Commons Attribution License (CC BY).

NKAs are ubiquitously expressed and serve critical functions in the mammalian cells, such as the transmembrane ion transport of sodium ions (Na^+) and potassium ions (K^+) (***FIG. 7***) and, as a result, the maintenance of cellular volume and resting potential (Contreras et al., 2024).

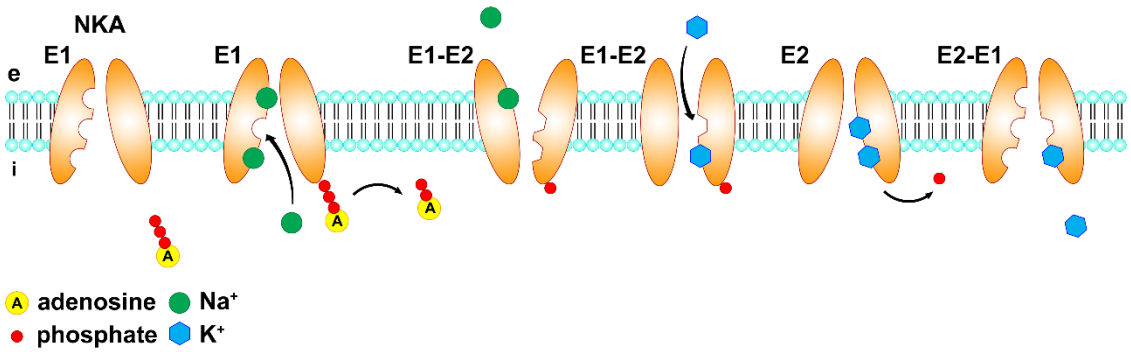

FIG. 7: TRANSMEMBRANE ION TRANSPORT FACILITATED BY NKA.
The NKA facilitates the transmembrane transport of three Na^+ into the extracellular space and two K^+ into the cytoplasm by hydrolysis of ATP. The enzyme converts between two distinct conformational states, E1 and E2. E1-E2 and E2-E1 denote intermediate states. A: adenosine; ATP: adenosine triphosphate; e: extracellular space; i: intracellular space; K^+: potassium ion; Na^+: sodium ion; NKA: Na,K-ATPase. Adapted and redrawn from Contreras et al. (2024); Suhail et al. (2010) under Creative Commons Attribution License (CC BY).

The enzymatic activity of the NKA is dependent on energy provided by adenosine triphosphate (ATP) hydrolysis, using one molecule of ATP for each transport of three Na^+ out of the cells, and two K^+ into the cells. It is estimated that photoreceptors use approximately 10^8 ATPs/photoreceptor/s, most of which can be ascribed to the consumption of ATP by the NKA (Ingram et al., 2020; Okawa et al., 2008). A dysregulation or dysfunction of the NKA is associated with several diseases, ranging from hypertension and cancer to neurological disorders (Bartsch et al., 2025; Contreras et al., 2024).

The transmembrane ion transport is facilitated by the α-subunit, transitioning between the conformational states E1, opening towards the cytoplasm, and E2, opening towards the extracellular side (***FIG. 7***), in the presence of magnesium ions (Mg^{2+}). An α-subunit consists of ten transmembrane domains (TM; αTM1-10; ***FIG. 6*** olive green, green, grey) with αTM1-6, referred to as core group, forming the NKAs pore, and αTM7-10, referred to as support group, regulating the properties of the core group. Two intracellular loops operate as functional domains. The shorter intracellular loop (αTM2-αTM3) contains the actuator (A-domain, ***FIG. 6*** yellow), the longer intracellular loop (αM4-αTM5) contains the nucleotide binding domain (N-domain, red), which undergoes phosphorylation, and the phosphorylation domain (P-domain, blue-grey), which is essential for Mg^{2+} binding (Contreras et al., 2024; Fedosova et al., 2021). However, detailed insights into the exact mechanisms of the ion transport by the NKAs α-subunits remain elusive.

In contrast, β-subunits consist of only a single transmembrane domain, and a large extracellular domain positioned in close proximity to parts of the α-subunit support group (αM7 and αM10). β-subunits support proper folding and intracellular transport of the α-subunits to their designated position in the plasma membrane and modulate the α-subunits affinity for Na^+ and K^+ (Contreras et al., 2024). Another crucial function of the β-subunits is to mediate cell-cell adhesion, likely mediated by multiple N-glycans and E-cadherins (Contreras et al., 1999; Páez et al., 2019; Rajasekaran et al., 2001; Roldán et al., 2022; Vagin et al., 2007). The β2-subunit of the NKA was first characterised as a cell recognition molecule termed Adhesion Molecule On Glia (AMOG) and was shown to mediate interactions between neurons and astrocytes *in vitro* (Antonicek et al., 1987). Later, cDNA cloning and sequence analysis revealed that AMOG shares about 40% amino acid identity with β1 and is identical to a putative NKA subunit in rat and human tissues termed β2-subunit (Gloor et al., 1990; Martin-Vasallo

et al., 1989). The dual function of AMOG/β2 as both adhesion molecule and subunit of the NKA was deduced by several observations:

(i) The addition of AMOG/β2 antibodies to astrocytes *in vitro* affected the activity of the NKA (Gloor et al., 1990)

(ii) AMOG/β2, derived from the injection of the respective cRNA into oocytes of *Xenopus laevis* DAUDIN 1802, combined with the endogenous α1-subunit of *X. laevis* formed a functional NKA (Schmalzing et al., 1992)

(iii) AMOG/β2 supported the migration of neurons along Bergmann glia processes and mediated the neuron-astrocyte interaction *in vitro* (Antonicek et al., 1987) and

(iv) AMOG/β2 promoted neurite outgrowth of cerebellar and hippocampal neurons *in vitro* (Müller-Husmann et al., 1993).

A more recent discovery was the γ-subunit, which has now been identified as FXYD2, a member of the FXYD family (Contreras et al., 2024; Geering, 2006). FXYD6, which has been shown to reduce the affinity of NKA to Na^+, is widely expressed in the nervous tissue, whereas FXYD7, enhancing the affinity of NKA to Na^+, is only expressed in the brain (Contreras et al., 2024; Hou et al., 2023; Kadowaki et al., 2004; Meyer et al., 2020). The FXYD subunit, consisting of a single transmembrane domain, acts as a modulator of the NKA via posttranslational modifications, such as phosphorylation (Contreras et al., 2024).

Although it has been shown that any α-subunit can associate with any β-subunit to form a functional heterodimer (Schmalzing et al., 1992), the expression of the different subunits and subsequently the different heterodimers *in vivo* is highly regulated, depending on cell type and tissue. Whereas α1 and β1 are ubiquitously expressed, likely fulfilling a housekeeping role in different tissues, other α-subunits exhibit a more tissue-specific expression and associate preferentially with specific β-subunits (***TAB. 1***) (Fedosova et al., 2021; Tokhtaeva et al., 2012). Of particular interest in the context of this thesis is the expression of the α3β2 heterodimer in mammalian photoreceptors (Schneider & Kraig, 1990; Schneider et al., 1991; Wetzel et al., 1999). It has previously been shown that, whereas both subunits are strongly expressed and co-localised in the inner segments of photoreceptors in C57BL/6J mice (wild-type (WT) mice), α3 partially loses its plasma membrane association in the absence of β2 expression in the $Atp1b2^{Atp1b1}$ knock-in (ki) mouse (hereafter referred to as *β2/β1* ki),

a novel mouse model with a cone-rod dystrophy-like phenotype (Bartsch et al., 2025). However, complete loss of α3-subunit membrane association is prevented, presumably because it forms heterodimers with the transgenic β1-subunit which is expressed instead of endogenous β2-subunit in this mutant mouse. The low expression level of the α3-subunit in the *β2/β1* ki mouse is likely the result of the comparatively low expression level of *Atp1b1* transcripts in the mouse model, which amounts to only 10-20% of the original expression levels of *Atp1b2* transcripts in wild-type mice (Weber et al., 1998). The low expression of *Atp1b1* transcripts has been ascribed to a low stability of the primary transcript.

Additionally, a low expression of the β3-subunit has been found by *in situ* hybridisation in the photoreceptors of both wild-type and *β2/β1* ki mice. The low β3 expression likely contributes to the normal development of photoreceptors in young *Atp1b2* ko mice (hereafter referred to as *β2* ko) in the absence of a α3β2 heterodimer in photoreceptors and in young *β2/β1* ki mice showing low expression levels of a α3β1 heterodimer in photoreceptors (Bartsch et al., 2025; Magyar et al., 1994; Molthagen et al., 1996).

TAB. 1: TISSUE-SPECIFIC EXPRESSION OF THE NA,K-ATPASE SUBUNITS.

NKA SUBUNIT	TISSUE-SPECIFIC EXPRESSION	PREFERENTIAL ASSOCIATION
α1	ubiquitous expression	β1 (Tokhtaeva et al., 2012)
α2	muscle, nervous system	β2 (Tokhtaeva et al., 2012)
α3	neurons	β2 in retina (Bartsch et al., 2025)
α4	testes	β3 (Fedosova et al., 2021)
β1	ubiquitous expression	α1 (Tokhtaeva et al., 2012)
β2	brain, retina, muscle	α2, α3 in retina (Bartsch et al., 2025; Tokhtaeva et al., 2012)
β3	lung, testis, skeletal muscle, liver, retina	α1 (Zhang et al., 2019)

1.4.1.2. INTERACTION PARTNERS OF THE NA,K-ATPASE

The Na,K-ATPase is known to interact with a plethora of different proteins. In the context of the *β2/β1* ki mouse model, the interactions of NKA with retinoschisin (RS1) and with the voltage-gated potassium channel (K_V) subunits K_V2.1 and K_V8.2 are of particular interest.

Retinoschisin is a 24 kDa cell adhesion protein implicated in maintaining the structural integrity of the retina. The 224 amino acid (aa) precursor protein contains a

specific Rs1 domain, implicated in the oligomerisation of the retinoschisin monomers, and a discoidin domain, likely serving as a ligand binding site and mediating the cell adhesive properties. The protein forms a homo-octameric complex (***FIG. 8***A) which adheres to the extracellular surfaces of photoreceptors and the cell membrane of bipolar cells upon secretion. In humans, the protein is encoded by the *RS1* gene located on Xp22.1. Loss-of-function mutations in *RS1* are associated with X-linked juvenile retinoschisis (XLRS, OMIM #312700), a form of macular degeneration found in young males, with a prevalence of 1/5,000-1/20,000 (Orphanet, 2024), and over 551 unique XLRS-associated variants (according to Leiden Open Variation Database (LOVD, https://databases.lovd.nl/shared/genes/RS1; retrieved 17.01.2026). XLRS is characterised by a bilateral foveal schisis[2] and formation of intraretinal cystic cavities. The abnormal retinal morphology leads to central scotomas, and a decrease in the signal transmission between photoreceptors and bipolar cells, resulting in a reduced b/a-wave amplitude ratio in scotopic ERGs (Molday, 2007; Plossl et al., 2017).

Although retinoschisin has been shown to directly interact with the β2-subunit of the NKA, the mechanism anchoring RS1 to the cell surface of photoreceptor and bipolar cells has remained elusive for quite some time. Molday et al. (2007) proposed the formation of a complex composed of RS1, β2 and sterile alpha and TIR motif-containing protein 1 (SARM1) based on immunoprecipitation experiments (***FIG. 8***A). Newer studies however propose a SARM1-independent mechanism (Friedrich et al., 2011; Molday et al., 2007), in which the protein-protein interactions is rather mediated by a patch of hydrophobic amino acids located on the surface of the β2-subunit in the so-called patch II (***FIG. 8***B), stabilising the interaction between the proteins (Plossl et al., 2019). In this model SARM1 merely acts as an adaptor protein.

Recently, the voltage-gated potassium channel subunits K_V2.1 and K_V8.1 have been identified as additional interaction partners of the NKA (Schmid et al., 2022). K_V8.1 exhibits modulatory properties of K_V channels but is otherwise electrically silent and unable to assemble functional K_V channels on its own. The subunit does, however, form heterotetrameric channels together with K_V2.1 (Bartsch et al., 2025; Bocksteins, 2016; Bocksteins & Snyders, 2012; Schmid et al., 2022; Vega-Saenz de Miera, 2004). The K_V channels are localised in the inner segments of photoreceptors and mediate, together with the NKA, a large portion of the photoreceptors dark current, the constant

[2] Splitting of retinal layers, in some cases the retinal periphery is affected as well

ion flux in photoreceptors in darkness, keeping the cells depolarised. Mice deficient in $K_V2.1$ additionally lack cell membrane association of $K_V8.2$. In $K_V8.2$ deficient mice, $K_V2.1$ homotetramers instead of the described heterotetramers assembled from both subunits have been found. Both mouse models exhibit dysfunctional and degenerating photoreceptors. Photoreceptor degeneration associated with decreased levels of $K_V2.1$ and $K_V8.2$ at inner photoreceptor segments has also been described in retinoschisin-deficient $Rs1h^{-/y}$ mice, in *β2* ko and *β2/β1* ki (Bartsch et al., 2025; Inamdar et al., 2021; Jiang et al., 2021; Schmid et al., 2022). These results indicate a strong interaction between the α3 and β2 of the NKA, RS1, $K_V2.1$ and $K_V8.2$. Loss of RS1 or β2 results in decreased protein levels of the different components of this complex at the photoreceptor inner segments and negatively impacts the ionic milieu and in consequence the health of photoreceptors.

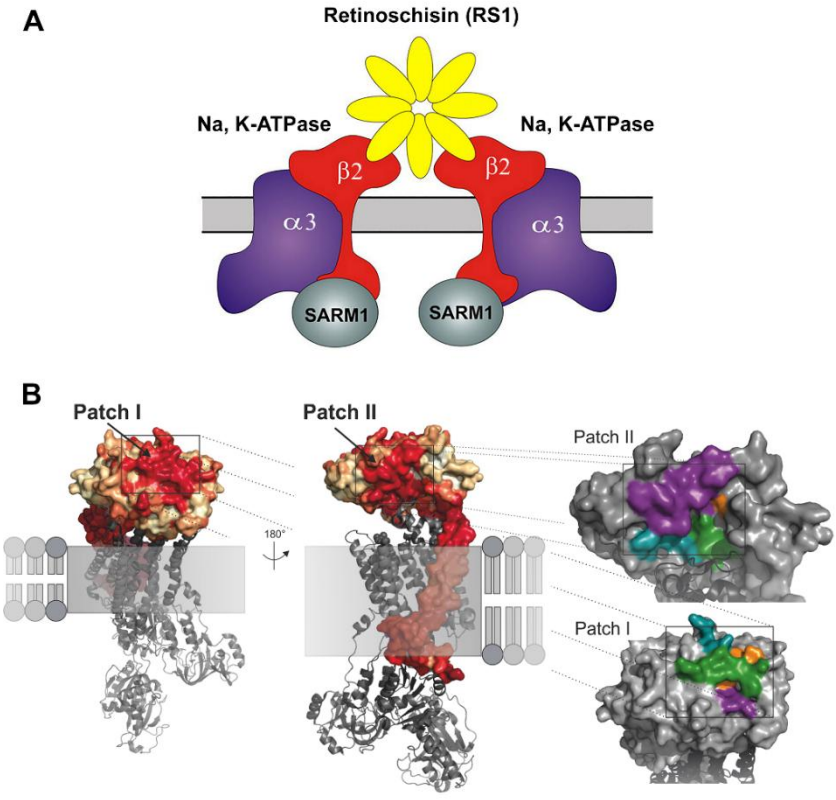

FIG. 8: THE RS1-NA,K-ATPASE-SARM1 COMPLEX.
(A) Schematic representation of the complex formed by retinoschisin (RS1) and the β2 subunit of the NKA. Although SARM1 was shown to co-precipitate with RS1, the β2 subunit and the α3 subunit of the NKA, Molday et al. (2007)found no direct interaction between RS1 and SARM1 in immunoprecipitation experiments. Hence, it is likely that SARM1 interacts exclusively with the intracellular domains of the NKA, but not RS1. (B) Hydrophobic surface patches I and II of the β2 subunit identified as putative binding sites for RS1 by Plossl et al. (2019). Since directed mutations in patch I did not interfere with the binding of RS1, but mutagenesis of T240 of the β2 subunit, located in patch II, prevented binding, it was concluded that interaction with patch II rather than patch I mediates the protein-protein interaction between RS1 and β2. α3: α3 subunit of the NKA; β2: β2 subunit of the NKA; NKA: Na,K-ATPase; RS1: retinoschisin; SARM1: sterile alpha and TIR motif-containing protein 1; T240: Threonine 240. Adapted from Molday et al. (2007) and Plossl et al. (2019) under Creative Commons Attribution License (CC BY).

1.4.1.3. DISEASES RELATED TO MUTATIONS IN THE NKA

Since the Na,K-ATPase plays a crucial role in many cell processes, mutations in the NKA subunits can have detrimental effects on the viability and function of cells. Knock-out experiments have shown that mice with a complete knock-out of most α-subunits are not viable for prolonged periods of time. Animals lacking the ubiquitously expressed α1 subunit only develop to the blastocyst stage (Barcroft et al., 2004), whereas a lack of the α2 isoform leads to death immediately after birth (Ikeda et al., 2004; Isaksen & Lykke-Hartmann, 2016) and animals lacking α3 die shortly thereafter (Moseley et al., 2007). In contrast, a knock-out of α4 does not affect the viability or general phenotype of mice but leads to complete infertility of males, in line with the expression of this subunit in sperm (***TAB. 1***) (Jimenez et al., 2010). As described in detail later (*cf.* **1.4.2. THE PHENOTYPE OF *ATP1B2ATP1B1 KNOCK-IN MICE***), β2-deficient mouse pups die pre-maturely at postnatal day (P) 17-18, after development of a severe neurological phenotype (Magyar et al., 1994).

While not affecting the viability of mice, haploinsufficiency of the different α isoforms ($\alpha1^{+/-}$, $\alpha2^{+/-}$ and $\alpha3^{+/-}$) affects behaviour, learning, memory formation and motor function (Moseley et al., 2007). In humans, several diseases are associated with mutations in α- or β-subunits. A selection of disorders can be found in ***TAB. 2***. Most diseases are caused by or correlated to mutations in the α-subunit and are often associated with migraine or motor dysfunctions, such as seizures or paraplegia (reviewed in: Benarroch (2011); Biondo et al. (2021); Kinoshita et al. (2022)).

To date, only one disorder, the small fibre neuropathy (SFN), a form of diabetic neuropathy, has been associated with mutations in a β-subunit. More specifically, Alsaloum et al. (2021) have provided first evidence that β3 might be indirectly involved in the pathogenesis of SFN by dysregulating the trafficking of voltage-gated sodium channel α subunits (Na_V). Furthermore, impaired NKA activity, due to mitochondrial dysfunction, might play a role in the degeneration of chronically demyelinated axons in multiple sclerosis (MS) (Benarroch, 2011). In MS lesions, $Na_V1.6$ channels, usually located in the nodes of Ranvier, are redistributed along the demyelinated axons, allowing for a consistent influx of Na^+ and the secondary activation of the co-expressed Na^+/Ca^{2+} exchanger (NCX), amplified by the dysregulation of Na^+ flux out of the cell due to dysfunctional NKAs.

TAB. 2: SELECTED NEUROLOGICAL DISORDERS ASSOCIATED WITH MUTATION IN NKA-RELATED GENES.

NEUROLOGICAL DISORDERS	CAUSATIVE GENE	REVIEWED IN*
PRIMARY ALDOSTERONISM (PA)	α1	Biondo et al. (2021)
CHARCOT-MARIE-TOOTH TYPE 2 (CMT2)	α1	Biondo et al. (2021)
COMPLEX SPASTIC PARAPLEGIA (CSP)	α1	Biondo et al. (2021)
HYPOMAGNESEMIA W/SEIZURES AND COGNITIVE DELAY	α1	Biondo et al. (2021)
EPILEPTIC SEIZURES	α1	Biondo et al. (2021)
FAMILIAL HEMIPLEGIC MIGRAINE TYPE 2 (FHM2)	α2	Benarroch (2011)
SPORADIC HEMIPLEGIC MIGRAINE (SHM)	α2	Benarroch (2011)
AUTOSOMAL-DOMINANT CONE-ROD-DYSTROPHY	α3	G. H. Zhou et al. (2020)[1]
CEREBELLAR ATAXIA, AREFLEXIA, PES CAVUS, OPTIC ATROPHY, AND SENSORINEURAL HEARING LOSS SYNDROME (CAPOS)	α3	Biondo et al. (2021)
RAPID-ONSET DYSTONIA-PARKINSONISM (RDP)	α3	Benarroch (2011)
ALTERNATING HEMIPLEGIA OF CHILDHOOD (AHC)	α3	Biondo et al. (2021)
EPILEPSY	α3	Benarroch (2011)
BIPOLAR DISORDER	α3	Kinoshita et al. (2022)
SMALL FIBRE NEUROPATHY (SFN)	β2	Alsaloum et al. (2021)[1]
ISOLATED DOMINANT HYPOMAGNESEMIA (IDH)	FXYD2	Biondo et al. (2021)

*unless otherwise stated
[1] original work

1.4.2. THE PHENOTYPE OF *ATP1B2*^{ATP1B1} *KNOCK-IN MICE*

Inactivation of the *Atp1b2* gene in mice (first described by Magyar et al. (1994)) results in a severe neurological phenotype. Changes in the behavioural phenotype of *β2* ko mice were observed from P15, at which point mice showed reduced righting behaviour and orientation, which worsened rapidly. *β2* ko mice developed tremors in the hind legs, kept their eyes mostly closed, and were unable to feed or drink with increasing age. Animals died prematurely at P17 or P18, a few days after the development of the first behavioural changes. Furthermore, *β2* ko mice exhibited significantly enlarged lateral and third ventricles and a spongiform degeneration of brain stem, thalamus, striatum and spinal cord, characterized by swollen astrocytic end

feet and vacuoles in close proximity to blood vessels. Apart from a few degenerating Purkinje cells and a few small-sized degenerating cells in the internal granular layer of the cerebellum, the cerebellum, the cerebral cortex and the hippocampus were not affected in *β2* ko mice. Interestingly, significant neuronal degeneration was restricted to the retina in this mouse model. The mutant exhibited a rapidly progressive degeneration of photoreceptor cells and significantly shortened photoreceptor inner and outer segments, resulting in a reduced thickness of the onl. The neuropathological phenotype was attributed to the impaired functionality of the NKA (Magyar et al., 1994; Molthagen et al., 1996).

To examine whether *Atp1b1* can compensate for the lack of *Atp1b2*, the *β2/β1* ki mouse was generated by Weber et al. (1998). In this mouse model, the expression of *Atp1b2* is abolished and replaced by a fusion protein, consisting of 18 amino acids of the NKA β2-subunit N-terminal and aa 14 to 304 of the β1-subunit. The knocked-in transgene prevented the severe brain pathology and the premature death observed in the *β2* ko mouse, and slowed– but did not prevent– the degeneration of the highly metabolically active photoreceptor cells (Country, 2017; Warrant, 2009; Weber et al., 1998). Other retinal cell types, which endogenously express β1, but not β2, were unaffected in this mouse model (Bartsch et al., 2025). The results indicate that the low expression of β3 and the low-level expression of transgenic β1 are insufficient to compensate for the lack of the normally strongly expressed β2-subunit in photoreceptor cells.

As described in Bartsch et al. (2025), *β2/β1* ki mice exhibit an early onset and rapidly progressing loss of cone photoreceptors followed by a slowly progressing loss of rod photoreceptors. The loss of cone photoreceptors became apparent as early as P14, with almost no cone photoreceptors remaining by P112. Degeneration of rod photoreceptors became apparent at P56, and approximately 50% of the rod population was lost at P168. In accordance with these observations, the photoreceptor layer thickness was reduced starting from an early age, but a significant reduction in retina thickness did not become evident before P112 when a significant fraction of rods was lost. A reduction of the thickness of the inner nuclear layer or a loss of other retinal nerve cell types such as bipolar cell or retinal ganglion cells was not observed in the mutant.

The retinas of *β2/β1* ki mice also exhibited neuroinflammation which advanced with increasing age of the animals. Expression of inflammation markers, such as glial

fibrillary acidic protein (GFAP), a marker for reactive astrogliosis, ionized calcium-binding adapter molecule 1 (IBA1) and cluster of differentiation 68 (CD68), both markers for reactive microgliosis was increased from an early age. Expression of GFAP and IBA1 in the mutant retina was increased from P14, while expression of CD68 was increased from P28 compared to the expression in WT retinas. Of note, most IBA1-positive microglia were found in their resident, ramified state, in which they monitor the surrounding tissue to maintain homeostasis (Rashid et al., 2018), instead of in their activated, amoeboid form, in which the microglia secrete endogenous cytokines and trophic factors, but also different cytotoxic substances, such as proteases. This results in the release of free radicals, such as reactive nitrogen and oxygen species (Hailer, 2008; Hanisch, 2002). Amoeboid microglia were mostly located in the subretinal space, i.e. between the RPE and the photoreceptor outer segments.

Although protein levels of RS1 were markedly reduced by a factor of ~20 in *β2/β1* ki mice compared to WT mice, and cell surface association of the protein was lost, a schisis-like phenotype, a characteristic morphological abnormality in XLRS, was not observed at any age in the mutant mice. Expression of SARM1 was not affected in *β2/β1* ki mice (***FIG. S1***; Bartsch et al. (2025), *unpublished data*), in accordance with findings in the *β2* ko mouse (Friedrich et al., 2011).

Expression levels of $K_V2.1$ and $K_V8.2$ were downregulated in the inner segments of the photoreceptors, likely contributing to a severe ion imbalance in photoreceptors, rendering ERGs a fruitless endeavour (Bartsch et al., 2025).

1.5. AN ANIMAL MODEL OF AUTOSOMAL-RECESSIVE RETINITIS PIGMENTOSA

1.5.1. THE ROD-SPECIFIC PHOSPHODIESTERASE 6

The rod-specific phosphodiesterase 6, a central protein of the visual cascade (*cf.* **1.1.2. THE PHOTOTRANSDUCTION CASCADE AND THE VISUAL CYCLE**), is a membrane-associated heterotetrameric enzyme. A PDE6 α-subunit (PDE6A) and a β-subunit (PDE6B) form a catalytic heterodimer, which associates with two homomeric inhibitory γ-subunits (***FIG. 9***A) (reviewed in: Han et al. (2013)). The catalytic domain consists of 16 α-helices consisting of ~270 aa residues. The active site forms a hydrophobic pocket that contains zinc ions (Zn^{2+}) and Mg^{2+}, binds the phosphate group of cGMP and facilitates its hydrolysis (reviewed in: Cote et al. (2022)). The catalytic subunits contain two so-called GAF domains, GAFa and GAFb, which are found in cGMP-binding phosphodiesterases, cyanobacterial Adenylyl cyclases and transcription factor

FhlA. In PDE6, in contrast to other phosphodiesterases, the GAFa domain binds cGMP and enables the dimerization of the catalytic subunits (***FIG. 9***B). The structurally largely disordered inhibitory γ-subunits contain 87 aa residues, and are organised into four sub-domains, namely an unfolded N-terminal, a loosely folded central polycationic region, a glycine-rich region and the C-terminal. Upon binding of Gα*-GTP the inhibitory restriction of the γ-subunits is released and cGMP is hydrolysed, facilitating the closure of ion channels and preventing influx of Na^+ and Ca^{2+}. The loose, asymmetric structure of the γ-subunits allows for a plethora of functions, including inhibition of cGMP hydrolysis, the modulation of cGMP affinity to GAFa and the provision of substrate sites for adenosine diphosphate (ADP)-ribosylation and phosphorylation (reviewed in: Cote et al. (2022)). While each of the γ-subunits is primarily associated with either PDE6A or PDE6B, both are also able to interact with the other catalytic subunit (Gulati et al., 2019).

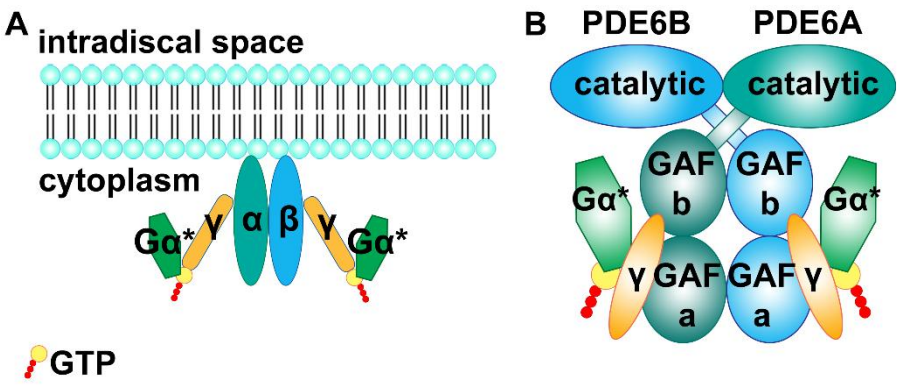

FIG. 9: SCHEMATIC REPRESENTATION OF PDE6.
(A) PDE6, a heterotetrameric enzyme consisting of one α-subunit (PDE6A), one β-subunit (PDE6B) and two γ-subunits, is located in the cytoplasm of photoreceptor disks and directly interacts with the activated Gα*-GTP complex. (B) PDE6A and PDE6B consist of a catalytic domain, as well as GAFa and GAFb which bind cGMP and enable dimerization of PDE6A and PDE6B. Gα*-GTP binds to the enzymes γ-subunits, alleviating their inhibitory effect. α: PDE6A; β: PDE6B; γ: γ-subunit of PDE6; Gα*: activated (GTP-bound) α-subunit of transducin; GAFa: cGMP-binding phosphodiesterases, cyanobacterial Adenylyl cyclases and transcription factor FhlA a; GAFb: cGMP-binding phosphodiesterases, cyanobacterial Adenylyl cyclases and transcription factor FhlA b; GTP: guanosine triphosphate; PDE6; phosphodiesterase 6; PDE6A: α-subunit of PDE6; PDE6B: β-subunit of PDE6. Adapted and redrawn after Aplin and Cerione (2024) under Creative Commons Attribution License (CC BY).

Many IRDs, such as retinitis pigmentosa, cone dystrophies, congenital stationary night blindness and achromatopsia, are associated with mutations in the phototransduction cascade (Remmer et al., 2015; Tsang & Sharma, 2018; Verbakel et al., 2018). In the context of this work, the implications of dysfunctions of PDE6 and

consequently the phototransduction cascade leading to retinitis pigmentosa are of utmost interest.

1.5.2. THE PHENOTYPE OF THE RD10 MOUSE MODEL

The phenotype of the 'retinal degeneration 10' mouse model (hereafter referred to as rd10 mouse) was first described by Chang et al. (2002) as a putative model of autosomal-recessive retinitis pigmentosa (arRP). The retinal degeneration in this model is caused by a spontaneous missense mutation in exon 13 of the *Pde6b* gene, located on chromosome 5, reducing the expression of PDE6B by ~60%, not allowing for the normal function of rod photoreceptors. The mutation results in protein mislocalisation and instability, resulting in an accumulation of cGMP. The enzyme becomes unable to degrade the second messenger, resulting in an increased Ca^{2+} influx via cGMP gated calcium channels and the subsequent degeneration of rod photoreceptors and eventually in the secondary loss of cone photoreceptors (Chang et al., 2007; Wang et al., 2018). In humans, mutations in the *PDE6B* gene lead to an aggressive form of arRP with an early onset, found in about 5% of RP patients (Danciger et al., 1995; Han et al., 2013; McLaughlin et al., 1993).

Rd10 mice exhibit a primary degeneration of rod photoreceptors, followed by a secondary degeneration of cones and cells of the inner retina (Barhoum et al., 2008; Gargini et al., 2007). First morphological changes accompanying the photoreceptor degeneration occur around P16, and significant photoreceptor loss becomes apparent at P18-P20 with a clear progression of the degeneration from centre to periphery, which becomes less apparent in older animals (Chang et al., 2007; Gargini et al., 2007; Yang et al., 2024). Rod degeneration peaks at P25, with almost no rods being left at P60. Thereafter, only one row of photoreceptor nuclei remains, consisting entirely of cone photoreceptors (Barhoum et al., 2008; Gargini et al., 2007; Pennesi et al., 2012). In 9-month-old animals, only few scattered cone photoreceptors remain in the retina of this mouse model (Gargini et al., 2007). Sclerotic vessels are present in 4-week-old animals(Chang et al., 2002). In contrast to the 'retinal degeneration 1' mouse (rd1 mouse; first described as 'rodless retina' by Keeler (1924, 1966)), another, even faster progressing model of arRP, photoreceptor degeneration in the rd10 mouse begins when photoreceptor cells are mature, making it an ideal animal to develop treatment options for arRP (Gargini et al., 2007; Otani et al., 2004; Rex et al., 2004). With increasing age of the mutant mice, rhodopsin immunoreactivity, usually restricted to

the rod outer segments (ROS) in healthy wild-type retinae, becomes dislocated to cell bodies and even some axons and rod spherules. By P40, the few remaining rods have lost their ROS and cone somata and endfeet, the so-called cone pedicles, are disorganised. Some cone pedicles persist even after complete degeneration of the cone photoreceptor outer and inner segments (Gargini et al., 2007).

In the inner retina of the rd10 mouse, cells innervating rod photoreceptors are affected first (Barhoum et al., 2008; Gargini et al., 2007). Most of the analysed cell types, such as horizontal cells, rod bipolar cells and AII amacrine cells were already affected in young mutants, exhibiting morphological changes from P20 onward. The retraction of the dendritic arbours of most cell types in response to the photoreceptor loss was complete by P40 at the latest. Dendritic arbours of rod bipolar cells were lost completely by this age. Only cone bipolar cells exhibited morphological changes later, around P40, with the only apparent changes being smaller somata and shortened axons (Barhoum et al., 2008). Additionally, a progressive decrease in metabotropic glutamate receptor 6 (mGluR6) expression, a marker for rod and cone ON-bipolar cells, and mislocalisation of the protein from dendritic tips of rod bipolar cells to their somata and axons was found. This progressive mislocalisation of mGluR6 indicates a loss of connectivity between photoreceptors and rod bipolar cells (Barhoum et al., 2008; Gargini et al., 2007). Furthermore, Gargini et al. (2007) reported a ~20% decrease in the number of rod bipolar cells and ~30% decrease in the number of horizontal cells in 9-month-old animals. Müller cells appeared largely unaffected morphologically, except for a shortening of the cells correlating to the retinal thinning due to photoreceptor degeneration and a probably life-long elevated expression of GFAP, indicating a reactive astrogliosis. Of note, the onset of retinal degeneration in rd10 mice can be delayed by one week, and possibly up to three months, by raising the animals in total darkness (Chang et al., 2007; Cronin et al., 2012; Sundar et al., 2020).

ERGs in the rd10 model are always abnormal, exhibiting much slower, lower and delayed responses in both a-waves and b-waves under both scotopic and photopic conditions compared to wild-type mice (Chang et al., 2007; Gargini et al., 2007).

To date, the rd10 mouse is one of the most widely used animal models to understand pathomechanisms of RP and to develop treatment options for this disease.

1.6. NEUROTROPHIC FACTORS AND THEIR RECEPTORS

1.6.1. CNTF

Ciliary neurotrophic factor, encoded by the *Cntf* gene, is a small protein with a molecular weight of ~30 kDa composed of about 200 amino acids. The protein is a member of the interleukin-6 (IL6) superfamily of neuropoietic cytokines involved in the survival, proliferation, differentiation and function of neurons and other cells in the nervous system— along with leukemia inhibitory factor (LIF; *cf.* **1.6.3. LIF**), IL6 (*cf.* **1.6.5. HYPER-IL6**), IL-11, IL-27, oncostatin M (OSM), cardiotrophin 1 (CT-1), and cardiotrophin-like cytokine factor 1 (CLCF1) (Murakami et al., 2004). Most members of the IL6 superfamily share a common structure consisting of four α-helices and bind to the receptor subunit LIF receptor β (LIFRβ). All members of the protein family induce intracellular signalling cascades via the signal transducer glycoprotein 130 kDa (gp130).

To initiate signalling, CNTF interacts with its specific receptor CNTF receptor α (CNTFRα), LIFRβ and gp130 (***FIG. 10***), to form a tripartite, hexameric receptor complex with a stoichiometry of 2 CNTF: 2 CNTFRα: 1 gp130: 1 LIFRβ (Boulton et al., 1994; Davis et al., 1991; De Serio et al., 1995). CNTFRα is unable to directly induce signalling due to a lack of a transmembrane or intracellular domain. Sortilin (SORT1) has been suggested to be able to facilitate binding of CNTF to LIFRβ and gp130 (Larsen et al., 2010).

CNTF is known to initiate signalling using two main pathways, the so-called classic signalling and the so-called trans-signalling. In classic signalling, CNTF binds to CNTFRα, which is anchored to the membrane via glycosylphosphatidylinositol (GPI), before interacting with the receptor subunit LIFRβ and gp130. Trans-signalling, on the other hand, is initiated by binding of CNTF to the soluble isoform of CNTFRα (sCNTFRα), which is cleaved from its GPI anchor by phospholipase C (PLC), before binding to LIFRβ and gp130 (Rose-John, 2020; Rose-John & Heinrich, 1994; Rose-John et al., 1993; Schuster et al., 2003). Hence, trans-signalling allows to induce signalling in a wider range of cells that do not express membrane-bound CNTFRα (Rose-John & Heinrich, 1994).

To date, the localisation of CNTFRα in the retina remains unresolved. While some studies have found CNTFRα localised in the outer and inner segments of photoreceptors (Beltran et al., 2005; Hertle et al., 2008; Rhee & Yang, 2003), others

have reported expression of CNTFRα in Müller cells, horizontal cells, amacrine cells and RGCs, but not in photoreceptors (Kirsch et al., 1997; Wahlin et al., 2004).

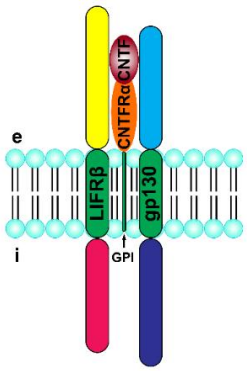

FIG. 10: SCHEMATIC REPRESENTATION OF THE TRIPARTITE CNTF RECEPTOR COMPLEX.
In classic signalling, CNTF first binds to its specific receptor CNTFRα, before the resulting complex binds to LIFRβ and gp130 in order to initiate further signalling, for example via the JAK/STAT3 signalling pathway. In trans-signalling CNTF binds to the soluble sCNTFRα, which is cleaved from its GPI anchor. This allows for induction of signalling on a wider range of cells. CNTF: ciliary neurotrophic factor; (s)CNTFRα: (soluble) CNTF receptor α subunit; e: extracellular space; gp130: glycoprotein 130 kDa; GPI: glycosylphosphatidylinositol (anchor); i: intracellular space; LIFRβ: leukemia inhibitory factor receptor β-subunit.

In addition to activating the intracellular signalling cascades via CNTFRα, CNTF can also initiate signalling via interaction with the membrane-bound or soluble IL6 receptor ((s)IL6Rα), adding additional signalling opportunities (Schuster et al., 2003).

CNTF, like other cytokines such as LIF or IL6, exerts its neurotrophic effect mainly through three distinct pathways (Askvig & Watt, 2015; Wen et al., 2012). This includes the Janus kinase (JAK)/ signal transducer and activator of transcription (STAT) signalling pathway (Wen et al., 2012), the rat sarcoma virus (RAS)/ mitogen activated protein kinase (MAPK) pathway (Boulton et al., 1994; Heinrich et al., 2003; Oh et al., 1998; Stahl & Yancopoulos, 1994) and the phosphoinositide 3-kinase (PI3K)/protein kinase B (Akt)/ mammalian target of rapamycin (mTOR) (PAM) pathway (Askvig & Watt, 2015; Guo et al., 2022).

To date, CNTF is one of the most intensively studied cytokines. It has been shown to promote the survival of different retinal cells, such as rod and cone photoreceptors and RGCs in various animal models (Bok et al., 2002; LaVail et al., 1992; LaVail et al., 1998; Li et al., 2010; McGill et al., 2007; Rhee et al., 2007; Wen et al., 1998; Wen et al., 2012). Importantly, the therapeutic potential of CNTF has been evaluated in clinical trials on patients presenting with neurodegenerative retinal disorders, such as RP (Sieving et al., 2006), geographic atrophy (GA) (Zhang et al.,

2011) or MacTel (Chew et al., 2015; Chew et al., 2025). However, regarding the application of CNTF as a putative treatment for retinal degenerations, it is important to consider that application of exogenous cytokines, such as CNTF or LIF are known to downregulate important proteins of the phototransduction cascade. This concerns, for example, proteins such as RHO, arrestin (ARR), or transducin. Downregulation of these proteins is detrimental for the visual function (Birch et al., 2013; Bok et al., 2002; Chucair-Elliott et al., 2012; Li et al., 2018; Liang et al., 2001; Schlichtenbrede et al., 2003; Wen et al., 2006; Wen et al., 2008; Wen et al., 2012; Zein et al., 2014; Zeiss et al., 2006). Additionally, in retinas treated with CNTF, Wen et al. (2006) found shorter ROS, which contain fewer discs in which signal transduction proteins such as RHO, ARR and G_t are located.

1.6.2. GDNF

Murine glial cell line-derived neurotrophic factor (GDNF), encoded by *Gdnf*, is a secreted disulphide-linked homodimer with a calculated molecular weight of ~30 kDa. The protein is the eponymous member of the GDNF family of ligands (GFL) within the transforming growth factor β (TGF-β) superfamily, which includes the proteins neurturin (NRTN), artemin (ARTN) and persephin (PSPN) (Fudalej et al., 2021). GDNF is widely expressed in the nervous system and plays a vital role in its development and function. The neurotrophic factor is implicated in the differentiation of dopaminergic neurons, increasing their dopamine uptake, the regulation of their synaptic plasticity and their axonal and dendritic elaboration (Cintrón-Colón et al., 2020). GDNF binds to the GDNF family receptor α1 (GFRα1) and the receptor tyrosine-protein kinase rearranged during transfection (RET) to induce signalling. For receptor activation a GDNF homodimer binds to GFRα1 and RET, forming complex composed of 2 GDNF: 2 GFRα1: 2 RET hexamers (Adams et al., 2021; Houghton et al., 2023; Ibáñez, 2013; Li et al., 2019; Mahato & Sidorova, 2020) (***FIG. 11***). In the retina, GFRα and RET are mainly expressed on RGCs and Müller cells (Mahato & Sidorova, 2020).

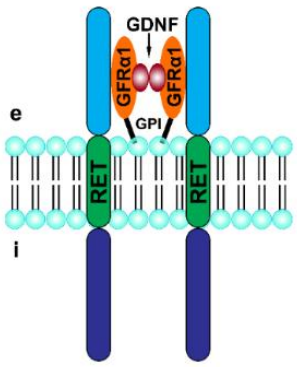

FIG. 11: SCHEMATIC OF THE GDNF-GFRα1-RET COMPLEX.
In classic signalling a glial cell-line derived neurotrophic factor (GDNF) homodimer binds to its specific receptor GDNF family receptor α1 (GFRα1), anchored to the cell plasma membrane via glycosylphosphatidylinositol (GPI). The GDNF-GFRα1 complex binds to the receptor tyrosine-protein kinase rearranged during transfection (RET), forming a 2:2:2 hexamer, in order to initiate signalling via several signalling pathways, such as RAS/MAPK, PI3K/Akt or phospholipase C-γ pathways. In trans-signalling, GFRα1 is not bound to the plasma membrane by GPI and does not need to rely on the interaction with RET, further broadening the action spectrum of GDNF. e: extracellular space; GDNF: glial cell line-derived neurotrophic factor; GFRα1: GDNF family receptor α1; GPI: glycosylphosphatidylinositol(-anchor); i: intracellular space; RET: rearranged during transfection.

Interaction with both co-receptors activates various signalling pathways, such as the RAS/MAPK, PI3K/Akt, RAS-related C3 botulinum toxin substrate (Rac)/c-Jun N-terminal kinase (JNK), and phospholipase C-γ pathways via phosphorylation of RET (Airaksinen & Saarma, 2002; Harada et al., 2002; Ibáñez & Andressoo, 2017; Mahato & Sidorova, 2020; Paratcha & Ledda, 2008). The duration and intensity of RET signalling can be modified by the partitioning of the GFRα1 co-receptors into subcompartments of the plasma membrane, such as lipid rafts, or the cleaving of the receptor into its soluble form, which enables GDNF trans-signalling (Ibáñez & Andressoo, 2017; Paratcha & Ibáñez, 2002).

Several studies have demonstrated a neuroprotective effect of GDNF on RGCs. In combination with CNTF, GDNF exerts pronounced synergistic neuroprotective effects on axotomized RGCs, significantly enhancing the neuroprotective effect of each factor alone over a prolonged period of time (Dulz et al., 2020; Flachsbarth et al., 2018; Hu et al., 2025). GDNF has also been implicated in the neuroprotection of photoreceptors, though reported effects were either relatively small or short-lived, regardless of whether the neurotrophic factor was administered using injections of the recombinant protein, virus-mediated gene transfer, or transplantations of GDNF-overexpressing neural stem cells (NSCs) (Allocca et al., 2007; Andrieu-Soler et al., 2005; Buch et al., 2006; Dalkara et al., 2011; Del Río et al., 2011; Dong et al., 2007; García-Caballero et al., 2018; Gregory-Evans et al., 2009; Hauck et al., 2006; Jmaeff

et al., 2020; Kucharska et al., 2014; McGee Sanftner et al., 2001; Ohnaka et al., 2012; Shahin et al., 2023; Wang et al., 2010; Wong et al., 2016; Wu et al., 2002). Of note, high levels of GDNF have been implicated to be detrimental to photoreceptors, accelerating their degeneration (Mahato & Sidorova, 2020).

1.6.3. LIF

The secreted cytokine LIF, encoded by *Lif*, is a member of the IL6 superfamily. Mature mouse LIF is composed of ~200 amino acids. Non-glycosylated murine LIF has a calculated molecular weight of about 20 kDa. In contrast to CNTF, LIF can directly induce signalling by binding to LIFRβ and gp130, without the need for another receptor subunit (***Fig. 12***) (Gearing et al., 1994; Schuster et al., 2003). LIF, like CNTF, activates the JAK/STAT and the RAS/MAPK signalling pathway (Joly et al., 2008; Lange et al., 2010), thereby promoting the survival of retinal nerve cell types.

LIF was first described to inhibit the proliferation of M1 murine myeloid leukemic cells (Gearing et al., 1987), but was later shown to promote the proliferation and differentiation in leukemia cells, among other cell types (Austin & Burgess, 1991; Deverman & Patterson, 2012; Hilton et al., 1991; Metcalf, 1990). The cytokine maintains the pluripotency of embryonic stem cells (ESCs) and NSCs (Bauer & Patterson, 2006; Gough & Williams, 1989; Gough et al., 1989; Hirai et al., 2011; Wulansari et al., 2021). Additionally, endogenous defence pathways and the activation of Müller cells in response to internal and external stressors are blocked in LIF-deficient mice and the expression of signalling and survival factors is kept low (Joly et al., 2008).

The expression of endogenous LIF is upregulated in various IRDs (Joly et al., 2008; Samardzija et al., 2012; Samardzija et al., 2006; Ueki et al., 2010), in response to RGC degeneration (DeParis et al., 2012; Leibinger et al., 2009; Seitz et al., 2010), and upon retinal injury (Dong et al., 2021; Joly et al., 2009; Ueki et al., 2008). The cytokine is expressed by a small subset of Müller cells in response to retinal injury (Agca et al., 2015; Joly et al., 2008).

Overall, the neuroprotective effect of LIF in neurodegenerative disorders of the retina is less well studied than that of CNTF. Nonetheless, positive outcomes of treatments with recombinant LIF (rLIF) have been reported in several animal models of retinal degeneration, such as Q344ter mice (LaVail et al., 1998), and in animal models of glaucoma and diabetic retinopathy (Agca & Grimm, 2014). However, the

neuroprotective effects were often relatively short lived (Dong et al., 2024; Frigg et al., 2005; Lange et al., 2010; Lv et al., 2023; McColm et al., 2006; Yang et al., 2018).

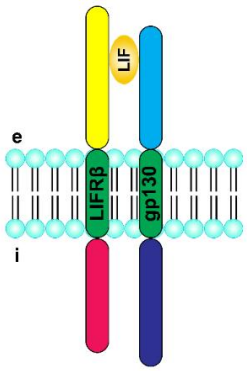

Fig. 12: SCHEMATIC OF THE LIF RECEPTOR COMPLEX.
In contrast to CNTF, LIF directly binds to LIFRβ, which is also utilised by other members of the IL6 family (OsM, CLC) before associating with the signal transducer gp130. CLC: cardiotrophin-like cytokine; e: extracellular space; gp130: glycoprotein 130 kDa; i: intracellular space; IL6: interleukin-6; LIF: leukemia inhibitory factor; LIFRβ: LIF receptor subunit β; OsM: oncostatin M.

1.6.4. PGRN

Murine progranulin (PGRN) is a 589 amino acid protein with a predicted molecular mass of 63-68 kDa. It exists as a homodimer and is a ubiquitously expressed growth factor secreted by neurons and microglia. The glycoprotein is associated with several biological processes, such as development (Daniel et al., 2003; Walsh & Hitchcock, 2017), tissue repair (He et al., 2003), inflammation (Kessenbrock et al., 2008; Life & Leavitt, 2025; Yin et al., 2010), and lysosomal function (Kleinberger et al., 2013; Life & Leavitt, 2025; Petkau et al., 2010; Takahashi et al., 2021). The pleiotropic function of PGRN is mediated by its ability to perform domain-dependent interactions with different receptors, and the subsequent induction of different signalling pathways. PGRN interacts, among others, with tumor necrosis factor receptor 1 (TNFR1) and TNFR2, toll-like receptor 9 (TLR9), SORT1 (***FIG. 13***), and pro-low-density lipoprotein receptor-related protein 1 (LRP1) and activates signalling pathways such as RAS/MAPK, PI3K/Akt, and wingless/integrase-1 (Wnt)/β-catenin signalling (Cui et al., 2019; Hu et al., 2010; Kuse et al., 2016; Paushter et al., 2018).

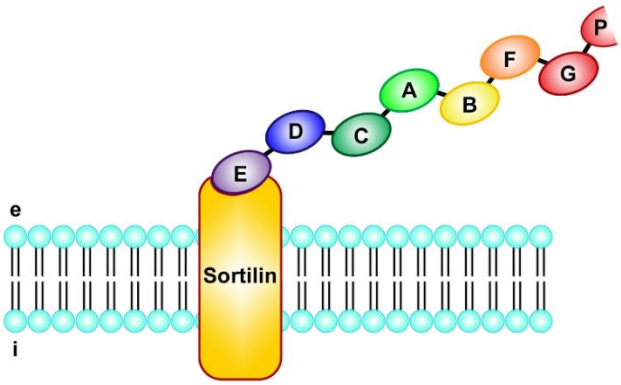

FIG. 13: PGRN-RECEPTOR COMPLEX EXEMPLIFIED.
PGRN contains 7.5 granulin domains and performs domain-dependent interactions with different receptors, enabling the induction of different signalling pathways. Here, the interaction of PGRN with sortilin is exemplified. A-E, P: Different granulin domains of PGRN; e: extracellular space; i: intracellular space; PGRN: progranulin.

Mutations in the *GRN* gene induce severe neurodegenerative diseases. A haploinsufficiency of the protein is associated with frontotemporal lobar degeneration (FTLD), a form of dementia associated with pronounced behavioural changes, progressive aphasia, and semantic disorders (Cairns et al., 2007; Hu et al., 2010; Mackenzie et al., 2009). Homozygous mutations of the protein are causative of CLN11, a subtype of a neuronal ceroid lipofuscinosis (Takahashi et al., 2021; Zin et al., 2021). NCL is a group of diseases associated with lysosomal dysfunction, leading to the accumulation of autofluorescent storage material in neurons and other cell types. The diseases are characterised by epileptic seizures, progressive motor dysfunction, cognitive decline, behavioural abnormalities, and progressive loss of vision (Hu et al., 2010; Huin et al., 2019; Neuray et al., 2020). Most NCL subtypes have a relatively early age of onset of neurological symptoms. However, the age of onset in CLN11 is variable, often occurring in mid childhood to the second or third decade of life. There is currently no cure for these fatal diseases.

Although PGRN has been implicated as a neuroprotective factor in several neurodegenerative and inflammatory diseases (Almeida et al., 2011; Cenik et al., 2011; Jian et al., 2016; Tang et al., 2011; Tsai & Boxer, 2016), the neuroprotective effect of the protein in the retina has not been studied extensively until now. One study has reported the neuroprotection of photoreceptors in $PGRN^{-/-}$ mice after systemic application of PGRN encoding-AAV vectors (Zin et al., 2021). Importantly, administration of PGRN has additionally been shown to rescue photoreceptor cells from cell death in a murine light damage model, even with relatively low doses of PGRN

inducing neuroprotective effects (Tsuruma et al., 2014). Tsuruma et al. (2014) suggested the interaction of PGRN with hepatocyte growth factor (HGF) receptor and cyclic adenosine monophosphate (cAMP)-responsive element-binding protein (CREB) via protein kinase C (PKC) pathways to mediate the neuroprotective effect.

1.6.5. HYPER-IL6

The pleiotropic cytokine IL6 is a variably glycosylated protein with a molecular weight ranging from ~22-27 kDa translated as a 212 amino acid molecule. IL6 is one of the key proteins in inflammation, regulating several inflammatory processes, the innate immune system, and is released during the acute phase response of the immune system as response to inflammation (reviewed in: Tanaka et al. (2014)). The cytokine is also implicated in tissue regeneration (Leibinger et al., 2016; Leibinger, Muller, et al., 2013).

The secreted cytokine is implicated in the pathogenesis of inflammatory diseases, such as MS, Alzheimer's disease, or rheumatoid arthritis (Alonzi et al., 1998; Okuda et al., 1998; Pedersen & Febbraio, 2012; Rose-John, 2020; Rothaug et al., 2016; Wallenius et al., 2002; Willis et al., 2020). IL6 has also been shown to promote the survival of different retinal nerve cell types, though the effectiveness has been shown to be severely restricted by the limited expression of its specific receptor IL6 receptor α (IL6Rα) on only few cell types such as hepatocytes and leukocytes (Kishimoto, 2005; Peters et al., 1998; Rose-John, 2020). In classic signalling, IL6 first binds to the membrane-bound IL6Rα, whereas trans-signalling is induced by the interaction of IL6 with the soluble isoform sIL6Rα. The receptor complex subsequently binds to gp130, initiating its homodimerization (***FIG. 14***). The hexameric IL6/(s)IL6Rα/gp130 complex initiates signalling cascades, such as the JAK/STAT, PI3K/Akt or RAS/MAPK pathway (Boulanger et al., 2003; Hibi et al., 1990; Murakami et al., 1993; Taga et al., 1989). The binding of IL6 to sILR6α, which is cleaved from its transmembrane domain by a disintegrin and metalloprotease 17 (ADAM17), allows IL6 to act on cells which lack a transmembrane IL6Rα (Fischer et al., 1997; Hibi et al., 1990; Rose-John & Heinrich, 1994; Taga et al., 1989). This ability of agonistic, activating signalling stands in stark contrast to other soluble cytokine receptors, such as the soluble interleukin 1 receptor (sIL1R) or the soluble TNFR (sTNFR), antagonistic, inhibiting signalling of their ligands (Vollmer et al., 1996). Additionally, the effective concentration needed to induce bioactivity of IL6 and IL6Rα deviates from

another by >20-fold, at 50 ng/ml and >1000 ng/ml, respectively. Hence a much greater number of IL6 receptors than IL6 would be needed for effective signalling (Kishimoto, 2005; Rose-John, 2020).

To bypass the problem of the limited receptor availability, Fischer et al. (1997) developed the designer cytokine hIL6, consisting of human IL6 covalently bound to sIL6Rα by a flexible polypeptide linker, consisting of 16 non-helical N-terminal residues and a glycine and serine rich sequence. The immunoglobulin (Ig)-like domain and C-terminal of sIL6Rα, which have been shown to be irrelevant for the biological activity (Vollmer et al., 1996; Yasukawa et al., 1990; Yawata et al., 1993), were excluded from the protein complex to keep it small (408aa; ~55kDa) due to limitations of the expression system implemented. hIL6 was chosen to be expressed in the methylotrophic yeast *Pichia pastoris*, which enables phosphorylation of molecules, resembling phosphorylation patterns in mammalian cells. Phosphorylation of proteins does not occur in the more commonly used expression system using *Saccharomyces cerevisiae* (Grinna & Tschopp, 1989; Peters et al., 1998). However, Vollmer et al. (1996) have shown that only a truncated form of sIL6Rα, missing the Ig-like domain, can be expressed in *Pichia pastoris*. The designer cytokine exhibits a significantly greater biological activity than the non-covalently bound, natural IL6/sIL6Rα complex (Peters et al., 1998) and is putatively able to interact with all cells expressing gp130, greatly extending the spectrum of target cells.

Usually, adult mammalian RGCs, like nerve cells in the mammalian central nervous system (CNS) in general, fail to regenerate their axons after traumatic injury or degeneration due to disease (Fischer, 2017; Leibinger et al., 2016; Ramon y Cajal, 1928). This failure to regenerate has been attributed to several factors, including an inhibitory environment for axonal growth cones and a non-existent intrinsic capacity for axonal regrowth (Fischer & Leibinger, 2012; Lu et al., 2014; Silver & Miller, 2004). Despite the intrinsic inability of CNS neurons to regenerate their axons, some studies have reported that exogenously administered hIL6 promotes the survival of neurons and stimulates the regeneration of injured axons. The neuroprotective effect of hIL6 is enhanced in mice deficient in Phosphatase and Tensin Homolog ($PTEN^{-/-}$), a negative regulator of the PAM pathway (Fischer, 2012). The PTEN deficiency allows for a sustained mTOR activity, which is required to bring RGCs into a regenerative state. Despite the ability of hIL6 to induce neuroprotection and axon regeneration in RGCs,

to date, no study has examined the effect of hIL6 on the survival of diseased photoreceptors.

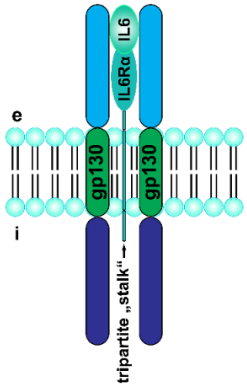

FIG. 14: SCHEMATIC OF THE IL6-IL6Rα-GP130 COMPLEX.
IL6 can interact with both the membrane-bound and the soluble form of its receptor (s)IL6Rα. Classical signalling allows for the binding of IL6 to the membrane-bound IL6Rα, inducing the homodimerization of gp130 and subsequent signalling via JAK/STAT, PI3K/Akt or RAS/MAPK pathways. Classic signalling is mostly associated with regenerative and protective processes. In trans-signalling, in which IL6 associates with sIL6R, the resulting complex can interact with gp130 on any cell, regardless of whether IL6Rα is present on the respective cell. IL6 trans-signalling is associated with autoimmune disorders and inflammation-associated cancers (Rose-John, 2020). Unlike CNTFRα or GFRα1, which are anchored to the plasma membrane by GPI, which is cleaved by phospholipase C, IL6Rα is anchored by a tripartite “stalk” consisting of an extracellular stalk region, a transmembrane domain (TM) and a intracellular domain (ICD) (Garbers & Rose-John, 2018). CNTF: ciliary neurotrophic factor; CNTFRα: ciliary neurotrophic factor receptor subunit α; e: extracellular space; GFRα1: GDNF family receptor α1; gp130: glycoprotein 130 kDa; i: intracellular space; ICD: intracellular domain; IL6: interleukin 6; (s)IL6Rα: (soluble) IL6 receptor subunit α; TM: transmembrane domain.

2. AIM OF STUDY

Aim of this study was to examine the effect of different neurotrophic factors, namely CNTF, GDNF, LIF, PGRN and hIL6 on photoreceptor survival in the *β2/β1* ki mouse, a novel animal model of autosomal-dominant cone-rod-dystrophy and in the rd10 mouse, an animal model of autosomal-recessive retinitis pigmentosa. The neurotrophic factors were introduced to the dystrophic retina by means of intravitreal application of either genetically modified NSCs or AAVs.

Genetically modified NSC lines, stably expressing the transgenes, were established from embryonal neural stem cells, modified using bi- or polycistronic lentiviral vectors coding for the NTF, a fluorescent reporter protein and an antibiotic resistance. NSCs used as control-NSCs did not express the NTF-transgene.

The neurotrophic factors were administered to the dystrophic retinas of both animal models by intravitreal injections of the lentivirally modified cell lines into young postnatal mice. hIL6 was additionally administered to the dystrophic retinas using intravitreal injections of an adeno-associated virus vector encoding the designer cytokine. AAVs with the serotype shH10, showing a pronounced tropism for Müller cells, were chosen for the application.

The neuroprotective effect of the applied neurotrophic factors was evaluated by analysis of their ability to promote photoreceptor survival. Survival of rod photoreceptor, which comprise ~97% of photoreceptors in the murine retina, l was determined by analysis of retina thickness and photoreceptor layer thickness. Additionally, cone photoreceptor survival was determined by analysis of the cone photoreceptor density. The effect of the different neurotrophic factors on the extent on neuroinflammation was also studied by analysis of the expression of the inflammation markers GFAP, IBA1 and CD68 by immunohistochemistry and Western Blot analysis. Furthermore, the impact of the designer cytokine hIL6 on the expression level of proteins of the phototransduction cascade, such as cone arrestin, and on downstream signalling pathways, such as the expression of phosphorylated STAT3, was evaluated.

3. MATERIAL AND METHODS

3.1. EXPERIMENTAL ANIMALS

Experimental procedures were carried out in two mouse models (*Mus musculus domesticus LINNAEUS 1758)* of retinal degeneration. These are the *Atp1b2*^{Atp1b1} knock-in (ki) or *β2/β1* ki mouse, a novel animal model of a cone-rod dystrophy, and the *Pde6b*^{rd10} or rd10 mouse, an animal model of an autosomal-recessive retinitis pigmentosa (for a detailed description *cf.* **1.4. THE *ATP1B2ATP1B1* KI MOUSE MODEL OF A CONE-ROD DYSTROPHY** and **1.5. AN ANIMAL MODEL OF AUTOSOMAL-RECESSIVE RETINITIS PIGMENTOSA**). Untreated, age-matched C57BL/6J (WT) mice served as control group. All experimental animals were maintained on a C57BL/6J genetic background and housed under standard conditions (21 ± 1°C, 40-60% relative humidity) with ad libitum access to food and water and on a 12/12h light/dark regiment in type II cages.

All experiments received approval from the Animal Care Committees of the University and the 'Freie und Hansestadt Hamburg, Behörde für Gesundheit und Verbraucherschutz' (reference numbers: N078/2020, N019/2023, ORG842, and ORG1089) and adhered to the EU Directive for animal experiments (2010/63/EU). All efforts were made to minimize the number of animals used and to reduce their suffering.

Animals were genotyped using polymerase chain reaction (PCR) with the appropriate primers (***TAB. 3***).

TAB. 3: PRIMERS USED FOR GENOTYPING.
For *β2/β1* ki mice, *β2/β1* ki F and *β2/β1* ki R amplify WT alleles, *β2/β1* ki R and MAG neo-3 amplify the *β2/β1* fusion transgene.

	NUCLEOTIDE SEQUENCE (5'→ 3')	GENE PRODUCT	T_A
***PDE6B*^{RD10} F**	TCT CAG AAC CCA CAT GTA CT	WT: ~100bp TG: ~150 bp	62°C
***PDE6B*^{RD10} R**	TGA TTC ATC TAG CCC ATC C		
***β2/β1* KI F**	GTG CAC CTT CGC CGC ACT GCC A	WT: ~300 bp TG: ~460 bp	65°C
***β2/β1* KI R**	CAG CTG GTC CCG GTG CGC CCC		
MAG NEO-3	GCG CAT CGC CTT CTA TCG CCT TCT		

°C: degrees Celsius; *β2/β1* ki: *Atp1b2*^{Atp1b1} knock-in mouse; bp: base pairs; F: forward primer; MAG: myelin-associated glycoprotein; *Pde6b*^{rd10}: model of an autosomal recessive retinitis pigmentosa with a mutation in the phosphodiesterase 6 β-subunit; R: reverse primer; T_A: annealing temperature; TG: transgene; WT: wild-type.

Tail biopsies were digested in Boston buffer (50mM TRIS, 50mM KCl, 2.5 mM EDTA, 0.45% NP40[3], 0.45% Tween-20[4]) with Proteinase K (2.5 U/mg, equivalent to 0.045 U final concentration; Roche, Basel, Switzerland) in a water bath at 56°C overnight. Digested biopsies were centrifuged at 12,000× g and subjected to PCR under the conditions detailed in ***TAB. 4-TAB. 7***. PCR products were separated by Agarose gel electrophoresis (2% agarose, containing 5µl/100ml RotiSafe Gel stain; Carl Roth, Karlsruhe, Germany) and bands were visualised with a ChemiImager™ 5500 Gel Imaging System (Alpha Innotech, Kasendorf, Germany). PCR-products were additionally sequenced by a commercial provider (Sanger sequencing; Eurofins Genomics, Ebersberg, Germany).

TAB. 4: PCR-MASTER MIX FOR GENOTYPING OF *β2/β1* KI MICE.

	VOLUME [µL]		FINAL CONCENTRATION
	A†	B†	
TEMPLATE	2.0	2.0	-
***β2/β1* KI F* (100 PM; EUROFINS GENOMICS, EBERSBERG, GERMANY)**	1.0	-	10 pM
***β2/β1* KI R* (100 PM; EUROFINS GENOMICS, EBERSBERG, GERMANY)**	1.0	1.0	10 pM
MAG NEO-3* (100 PM; EUROFINS GENOMICS, EBERSBERG, GERMANY)	1.0	1.0	10 pM
DNTPS (100 MM; THERMO FISCHER SCIENTIFIC)**	0.2	0.2	16µM
10X MODIFIED PCR BUFFER	2.5	2.5	1x
$MgCl_2$ (50MM)	0.75	0.75	35mM
5X Q-SOLUTION[5] (QIAGEN GMBH, HILDEN, GERMANY)	5	5	1x
DDH_2O	11.2	12.2	-
DREAMTAQ DNA POLYMERASE (5U/µL; THERMO FISCHER SCIENTIFIC)	0.6	0.6	3 U
TOTAL VOLUME	**25µl/reaction**		

Modified PCR buffer: 2 ml 1M TRIS-HCl pH8.4, 2.5 ml 1M KCl, a*d* 10ml ddH_2O (final conc.: 200mM TRIS-HCl, 250 mM KCl)
* stock solution diluted 1:10 (final conc. 10 pM)
** stock solution diluted 1:500 (final conc. 200 µM)
† Master mix A for WT alleles, B for TG alleles

dNTP: desoxyribonucleotidetriphosphate; F: forward primer; PCR: polymerase chain reaction; R: reverse primer; U: enzymatic unit.

[3] nonyl phenoxypolyethoxylethanol (Calbiochem, Merck, Darmstadt, Germany)
[4] Polysorbat 20 (Fluka, Merck)
[5] For GC rich templates

TAB. 5: PCR CONDITIONS FOR GENOTYPING OF *β2/β1* KI MICE.

	TEMPERATURE	TIME [MIN]	CYCLES
INITIAL DENATURATION	94°C	2:30	1
DENATURATION	94°C	0:30	30
ANNEALING	65°C	0:45	
ELONGATION	72°C	0:50	
FINAL EXTENSION	72°C	5:00	1
HOLDING	4°C	forever	

TAB. 6: PCR-MASTER MIX FOR GENOTYPING OF RD10 MICE.

	VOLUME [µL]	FINAL CONCENTRATION
TEMPLATE	1.0	-
***PDE6B*^{RD10} SEQ F* (100 PM; EUROFINS GENOMICS, EBERSBERG, GERMANY)**	2.5	25 pM
***PDE6B*^{RD10} SEQ R* (100 PM; EUROFINS GENOMICS, EBERSBERG, GERMANY)**	2.5	25 pM
DNTPS (100 MM; THERMO FISCHER SCIENTIFIC)**	2.5	200 µM
10X MODIFIED PCR BUFFER	2.5	1x
$MgCl_2$ (50MM)	0.7	35mM
DDH_2O	12.3	-
DREAMTAQ DNA POLYMERASE (5 U/µL; THERMO FISCHER SCIENTIFIC)	1.0	5 U
TOTAL VOLUME	**25µl/reaction**	

Modified PCR buffer: 2 ml 1 M TRIS-HCl pH8.4, 2.5 ml 1 M KCl, a*d* 10ml ddH_2O (final conc.: 200mM TRIS-HCl, 250 mM KCl)
* stock solution diluted 1:5 (final conc. 20 pM)
** stock solution diluted 1:500 (final conc. 200 µM)

dNTP: desoxyribonucleotidetriphosphate; F: forward primer; PCR: polymerase chain reaction; R: reverse primer; U: enzymatic unit.

TAB. 7: PCR CONDITIONS FOR GENOTYPING OF RD10 MICE.

	TEMPERATURE	TIME [MIN]	CYCLES
INITIAL DENATURATION	95°C	5:00	1
DENATURATION	95°C	0:45	30
ANNEALING	62°C	1:30	
ELONGATION	72°C	1:30	
FINAL EXTENSION	72°C	10:00	1
HOLDING	4°C	forever	

3.2. GENERATION OF CLONAL NEURAL STEM CELL LINES

3.2.1 GENERATION OF NEURAL STEM CELL LINES

In this thesis, clonal NSC lines overexpressing different neurotrophic factors were examined regarding their neuroprotective effect in the dystrophic retinas of *β2/β1* ki and rd10 mice. All NSC clones, with the exception of the hIL6 clone (hereafter referred to as hIL6-NSCs), were previously established. Data on the CNTF clone (hereafter referred to as CNTF-NSCs) has been published (Flachsbarth et al., 2018; Flachsbarth et al., 2014; Jankowiak et al., 2015; Jung et al., 2013).

The NSC clones (in their entirety hereafter referred to as NTF-NSCs) were generated by cloning full length cDNA of the NTFs into a polycistronic lentiviral vector. The vector was composed of either a cytomegalovirus enhancer/chicken β-actin (CAG) (for the CNTF-, GDNF-, LIF- and PGRN-encoding vectors) or an elongation factor α1 (EFα1) (for the hIL6-encoding vector) promotor, as well as an internal ribosome entry site (IRES) of the encephalomyocarditis virus, a reporter protein (enhanced green fluorescent protein (eGFP), tdTomato or Venus) and a resistance gene (blasticidin (bsd), neomycin (neo), puromycin (puro) or zeocin (zeo)). Vectors are listed in ***TAB. 8***. In the CNTF- (CNTF-NSCs, ***FIG. 15***Aa), PGRN- (PGRN-NSCs, ***FIG. 15***Ab) and hIL6- (hIL6-NSCs, ***FIG. 15***Ca) encoding vectors, the reporter and resistance gene were separated by a P2A sequence of the porcine teschovirus 1 (2A). In the GDNF- (GDNF-NSCs, ***FIG. 15***Ba) and LIF- (LIF-NSCs, ***FIG. 15***Bb) encoding vectors, the reporter and resistance gene were fused. The same vectors, lacking the respective NTF-coding cDNA, were utilised to generate control NSC lines with the respective expression of the different reporter proteins (control-NSCs, ***FIG. 15***Ac, Bc, Cb).

Lentiviral particles were based on the modular “Lentiviral Gene Ontology” (LeGO) vectors and produced by transient transfection of human embryonic kidney (HEK) 293T cells as described (http://www.LentiGo-Vectors.de) (Weber et al., 2010).

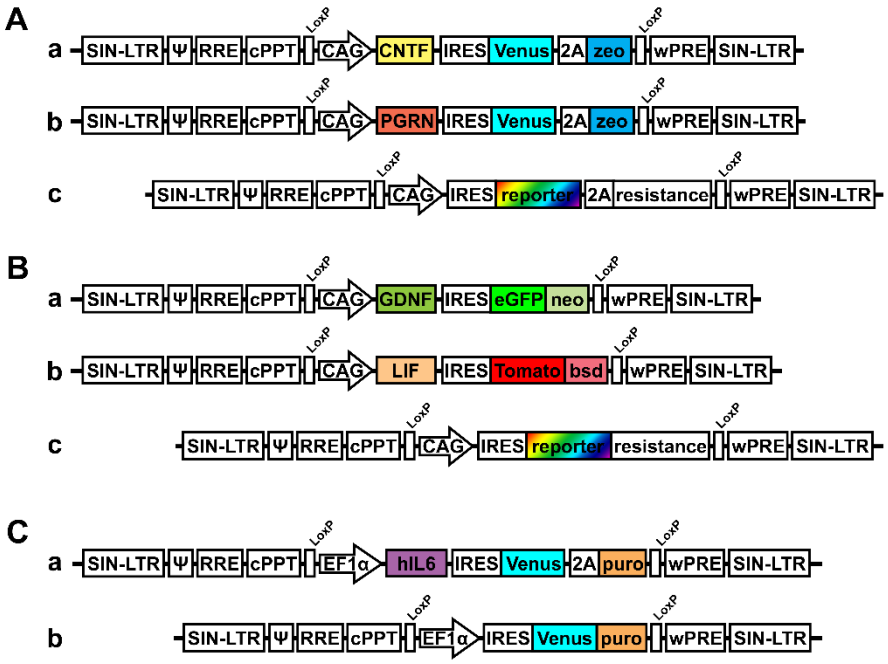

FIG. 15: SCHEMATIC REPRESENTATION OF POLYCISTRONIC LENTIVIRAL VECTORS (LEGO VECTORS) USED FOR THE GENERATION OF DIFFERENT CLONAL NTF-NSC LINES.
Different lentiviral vectors, encoding for the murine cDNA of the NTFs CNTF, GDNF, LIF, PGRN, hIL6 or, were used to transduce neural stem cells (NSCs) isolated from the cerebral cortex of embryonic C57BL/6J mice (embryonic day (E)14). An antibiotics resistance, either zeo, neo, bsd or puro, was either separated (A, C) or fused to the reporter gene (B). Identical vectors, only lacking the cDNA of the different NTFs, were used to generate control-NSCs. Ψ: packaging signal; 2A: 2A sequence of the *porcine teschovirus 1;* bsd: blasticidin; CAG: cytomegalovirus enhancer/chicken β-actin; CNTF: ciliary neurotrophic factor; cPPT: central polypurine tract; E: embryonic day; GDNF: glial cell line-derived neurotrophic factor; hIL6: hyper-interleukin-6; IRES: internal ribosome entry site; LIF: leukemia inhibitory factor; LoxP: recognition site of Cre recombinase; neo: neomycin; PGRN: progranulin; puro: puromycin; RRE: rev-responsive element; SIN-LTR: self-inactivating long-terminal repeat; wPRE: woodchuck hepatitis virus posttranscriptional regulatory element; zeo: zeocin.

To establish NSC cultures (***FIG. 16***) (Conti et al., 2005; Pollard et al., 2006), neurosphere cultures were generated from the cerebral cortex of 14-day-old C56BL/6J mouse embryos using standard protocols (Ader et al., 2004; Pressmar et al., 2001). Cortices were mechanically dissociated in sterile phosphate-buffered saline (PBS), and cells were cultivated in Dulbecco's Modified Eagle Medium (DMEM)/F12 (Gibco, Thermo Fischer Scientific, Waltham, MA, USA) containing 0.3% glucose (Carl Roth), 2 mM L-glutamine, 5 mM HEPES, 1x penicillin/streptomycin (final concentration: 100 U/mg penicillin, 100 µg/ml streptomycin) (all Sigma Aldrich), 3 mM $NaHCO_3$, supplemented with 1% N2 supplement and 1% B27 supplement (all Gibco), 10 ng/ml epidermal growth factor (EGF) and 10 ng/ml fibroblast growth factor-2 (FGF-2; both PeproTech, Thermo Fischer Scientific; medium composition hereafter referred to as NSC

medium). Shortly after isolation of cortical cells (two or three passages), free-floating neurospheres were dissociated using accutase (Gibco), and cells were further cultivated under adherent conditions in cell culture flasks coated with 0.1% Matrigel (Corning, New York, NY, USA) in NSC medium.

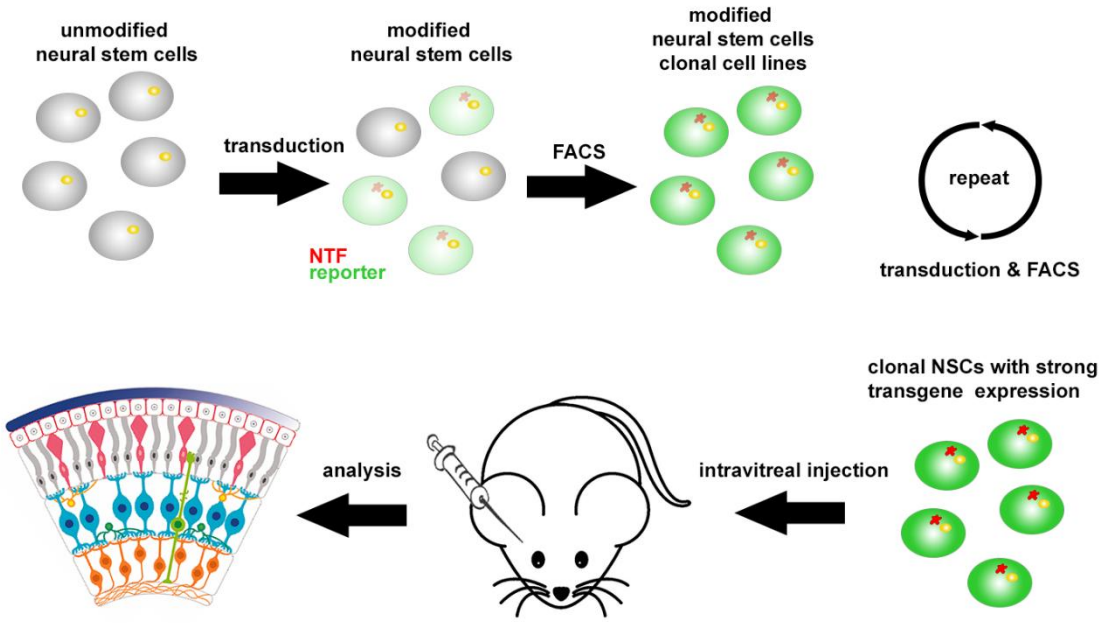

FIG. 16: SCHEMATIC REPRESENTING THE GENERATION OF GENETICALLY MODIFIED CLONAL NSC LINES. To generate clonal NSC lines used in the experimental procedures, unmodified neural stem cells were transduced with various lentiviral vectors. Successfully transduced neural stem cells were selected by FACS and clonally expanded. To obtain NSC lines with strong and homogenous expression of the reporter and neurotrophic factor, the process of transduction, FACS and subsequent clonal expansion was repeated. The generated NSC lines were then used in the subsequently described experiments. FACS: fluorescence activated cell sorting; NSCs: neural stem cells; NTF: neurotrophic factor. Schematic of retina from Ghasemi et al. (2018), © 2017, reprinted by permission of Informa UK Limited, trading as Taylor & Francis Group, https://www.tandfonline.com

The obtained neural stem cells were transduced by spinoculation in the presence of 8 µg/ml hexadimethrine bromide (Polybrene; Sigma-Aldrich) at 1100× g for 1h at room temperature followed by incubation for 1h at 37°C. Successfully transduced cells were selected by cultivation under adherent conditions in presence of the following antibiotics (all InvivoGen, San Diego, CA, USA):

LIF-NSCs:	4 µg/ml blasticidin
GDNF-NSCs:	200 µg/ml neomycin
hIL6-NSCs:	1 µg/ml puromycin
CNTF- or PGRN-NSCs:	200 µg/ml zeocin.

Clonal neural stem cell lines were generated by selecting single cells with high levels of reporter gene expression by fluorescence activated cell sorting (FACS; FACS AriaIIIu, BD Bioscience, San Diego, CA) and subsequent clonal expansion in 96-well-plates coated with 1% Matrigel (Corning). Transfection, selection of cells with high reporter gene expression and subsequent clonal expansion were repeated to obtain NSCs with strong and homogenous expression of the reporter protein and consequently strong expression of the respective NTFs.

TAB. 8: NEUROTROPHIC FACTORS, LENTIVIRAL VECTORS AND SECRETION LEVELS OF NEURAL STEM CELL CLONES.
Neurotrophic factors, polycistronic lentiviral vectors to express the respective neurotrophic factors in neural stem cells, and the amount of secreted neurotrophic factors in ng/10^5 NSCs/24 hours.

NEUROTROPHIC FACTOR	LENTIVIRAL VECTOR	SECRETION LEVEL [NG/10^5 CELLS/24H] ± SEM
CILIARY NEUROTROPHIC FACTOR (CNTF)	pCAG-mCNTF-iVenus-2A-zeo	87.2 ± 10.1 (Flachsbarth et al., 2014)
GLIAL CELL-LINE DERIVED NEUROTROPHIC FACTOR (GDNF)	pCAG-mGDNF-iGFP-neo	156.4 ± 10.0 (Flachsbarth et al., 2018)
HYPER-INTERLEUKIN-6 (HIL6)	EF1α-hIL6-iVenus-2A-puro	147 ± 7.9 (*cf*. results)
LEUKEMIA INHIBITORY FACTOR (LIF)	pCAG-mLIF-iTom-bsd	864.0 ± 26.3 (mean secretion; *cf*. results)
PROGRANULIN (PGRN)	pCAG-mPGRN-iVenus-2A-zeo	423.5 ± 26.4 (mean secretion; *cf*. results)

2A: porcine teschovirus 1 2A sequence; bsd: blasticidin; EF1α: elongation factor 1α; GFP: green fluorescent protein; h: hours; hIL6: human hyper-interleukin-6; mCNTF: murine ciliary neurotrophic factor; mGDNF: murine glial cell-derived neurotrophic factor; mLIF: murine leukemia inhibitory factor; mPGRN: murine progranulin; neo: neomycin; ng: nanogram; CAG: cytomegalovirus enhancer/chicken β-actin; puro: puromycin; zeo: zeocin.

3.2.2. CHARACTERISATION OF MODIFIED NEURAL STEM CELL LINES

To examine the expression of the neurotrophic factors, undifferentiated cells of the different NSC lines and their respective control-NSCs were characterised *in vitro* by immunocytochemistry (ICC) and Western Blot analysis. Here, previously published data on the CNTF-NSC and GDNF-NSC clones (Flachsbarth et al., 2018; Flachsbarth et al., 2014; Jankowiak et al., 2015; Jung et al., 2013) is supplemented with data on LIF-, PGRN- and hIL6-NSCs.

Undifferentiated LIF-, PGRN-, and hIL6-NSCs as well as control-NSCs were cultivated under adherent conditions for 24h on coverslips coated with 1% Matrigel (Corning) at a density of ~220,000 cells/cm^2 in NSC medium. Cultures were fixed in 4% (w/v) paraformaldehyde (PFA, Sigma-Aldrich) for 15 min and blocked in PBS (pH 7.4) containing 0.1% bovine serum albumin (BSA, Sigma-Aldrich) and 0.3% Triton X-100 (Tx-100, Fluka, Merck) (hereafter referred to as blocking medium) for 1h at room temperature. Cells were subsequently incubated with primary antibodies against LIF, PGRN or IL6 (***TAB. 10***) overnight at room temperature, washed and incubated with Cy2- and Cy3-conjugated secondary antibodies (all diluted 1:200, Jackson Immunoresearch Laboratories Inc., West Grove, PA, USA). Cell nuclei were stained with 4′,6′-diamidino-2-phenylindole (DAPI, 1: 2,000, Sigma-Aldrich) and mounted on slides using Aqua-Poly/Mount (Polysciences Inc., Warrington PA, USA). Cells were analysed with an AxioObserverZ.1 microscope equipped with an ApoTome2 (Carl Zeiss AG, Oberkochen, Germany).

Secretion levels of the neurotrophic factors were analysed by Western blot analysis of culture supernatants from the respective clonal NSC lines. LIF-, PGRN-, hIL6- and control-NSCs from low and high cell passages were seeded at a density of 5×10^5 cells/ 500µl medium on 12-well plates coated with 0.1% Matrigel and incubated at 37°C and 5% CO_2 for 24 hours. Supernatants were collected, centrifuged at 226× g and 4°C for 5 min to remove cell debris and subjected to Western Blotting. To control for fluctuations in cell populations after cultivation, cell numbers were determined again after collection of supernatants by enzymatically detaching remaining cells from the culture substrate using Accutase, again counting the cells using a Neubauer improved haemocytometer.

Culture supernatants were separated on 10% SDS-PAGE in conjunction with either recombinant murine LIF (rmLIF,10 ng/µl, Life Technologies), murine PGRN (rmPGRN, 250 ng/µl, R&D Systems, Minneapolis, MN, USA) or human IL6 (rhIL6, 500ng/µl, R&D Systems) and transferred onto nitrocellulose membranes (0.2µm pore size, Whatman, Kent, UK) at 80 V for 1.5h using a Mini-PROTEAN® Tetra electrophoresis system (Bio-Rad, Hercules, CA, USA). After transfer, membranes were blocked in Intercept Blocking buffer (1:1 diluted with TRIS-buffered saline (TBS), LI-COR Biosciences, Lincoln, NE, USA) for 1h at room temperature, incubated with the respective primary antibodies (***TAB. 10***) in

1:1 diluted Intercept Blocking buffer with 0.2% Tween 20 (Fluka) overnight at 4°C, washed and incubated with the respective IRDye® 800CW secondary antibodies (all diluted 1:20,000, LI-COR Biosciences) in TBS with 0.2% Tween 20 (Fluka) for 1h at room temperature. Immunolabeled bands were visualised using the LI-COR Odyssey® Fc Imaging system (image acquisition: 800nm, 2 minutes) and signal intensities were quantified with Empiria Studio® 1.3.0.83 software (LI-COR Biosciences) in reference to a serial dilution of the respective recombinant protein. Molecular masses of proteins were determined using the Chameleon Duo Pre-stained protein ladder (LI-COR Biosciences). All experiments were conducted in triplicate.

3.2.3. *IN VITRO* DIFFERENTIATION OF MODIFIED NEURAL STEM CELLS

Differentiation of the clonal NSC lines into astrocytes or neurons was performed as described before (Jung et al., 2013) and previously published data on the CNTF-NSC and GDNF-NSC lines (Flachsbarth et al., 2018; Flachsbarth et al., 2014; Jankowiak et al., 2015) was supplemented in the present thesis by data on the LIF-, hIL6- and PGRN-NSC clones.

Differentiation of NTF- and control-NSCs into astrocytes was induced by cultivation of undifferentiated cells on coverslips coated with 1% Matrigel (Corning) at a density of ~110,000 cells/cm^2 in NSC medium lacking EGF and FGF-2, supplemented with 1% N2 supplement, 2% B27 supplement and 1% foetal calf serum (FCS) (all Gibco) for at least 5 days. Neuronal differentiation was induced by cultivation of undifferentiated cells at the same density in NSC medium lacking EGF and supplemented with 1% N2, 2% B27 and 0.25 µl/ml FGF for at least 5 days followed by cultivation in a 1:1 mixture of NSC medium and Neurobasal™ medium (Gibco) supplemented with 0.5% penicillin and streptavidin, 0.5% glutamine, 2.5µl/ml N2 and 20µl/ml B27 for at least 4 days. Immunostainings of differentiated cells were performed as described for undifferentiated cells (*cf.* **3.2.2. CHARACTERISATION OF MODIFIED NEURAL STEM CELL LINES**). Rabbit anti-GFAP and mouse anti-microtubule-associated protein 2 (MAP2) antibodies (***TAB. 10***) were used as marker for astrocytes and neurons, respectively. These primary antibodies were visualised using the appropriate Cy5- conjugated secondary antibodies (Jackson Immunoresearch Laboratories

Inc.). Differentiated cells were analysed with an AxioObserverZ.1 microscope equipped with an ApoTome2 (Carl Zeiss AG).

3.3. AAV VECTOR PRODUCTION

Within the framework of this dissertation, intravitreal gene therapy was performed using AAV vectors encoding hIL6. AAV vectors encoding eGFP were used for control experiments. The AAV particles were produced in the Vector Facility at the University Medical Centre Eppendorf, Hamburg, Germany in the following manner:

Recombinant, self-complementary AAV vectors (scAAVs) were produced in Sf9 insect cells (*Spodoptera frugiperda* ovarian cells) using the baculovirus expression system techniques (Bac-to-Bac Expression System, Gibco). In short, to generate AAVshH10 vectors (Klimczak et al., 2009), Sf9 cells were infected with baculovirus carrying the AAV packaging plasmid pSR-AAVshH10, a modified derivate of pFastBac DUAL Expression Vector, Gibco, containing the shH10 packaging plasmid (Addgene plasmid # 64867) instead of the packaging plasmid of AAV serotype 2 (AAV2; Addgene plasmid #65214) (R. H. Smith et al. (2009); shH10 was a gift from John Flannery & David Schaffer to the Bartsch lab), a transfer plasmid, either pFastBac-1-Ultra-GFP-scCMV-hIL6 (for hIL6-AAV) or pFastBac-1-Ultra GFP-scCMV-GFP (for GFP-AAV) and the helper plasmid pMON7124.

Sf9 cells, transfected with baculovirus containing the plasmids described above using BacVector 3000 (Novagen, Madison, WI), were produced according to the “titerless infected-cells preservation and scale-up (TIPS)” method in SF-900 II SFM (Gibco), containing 5mg/l gentamycin (Invitrogen, Thermo Fischer Scientific), at an initial cell density of ~3.8× 10^5 viable cells/ml under controlled conditions (27°C, ≥50% dissolved oxygen) in Applikon stirred tank bioreactors (Gentige, Gothenburg, Sweden) (Wasilko et al., 2009).

Purification and quantification of scAAVs were performed as described before (Liu et al., 2022). Cell density at transfection was at ~8.75× 10^5 viable cells/ml. After harvest, cells were resuspended in lysis buffer (50mM TRIS-HCl, 150 mM NaCl, 5 mM Mg_2Cl_2, pH 8.5) and Turbo Nuclease (Th. Geyer, Renningen, Germany) after three freeze-thaw cycles. Lysates were incubated 1h at 37°C, centrifuged to remove cell debris and AAV vectors were purified using iodixanol

step gradients (PROGEN Biotechnik GmbH, Heidelberg, Germany). Iodixanol was removed by ultracentrifugation using Amicon Ultra Cartridges (MerckMillipore, Darmstadt, Germany). Genomic titers of AAV particles were determined after alkaline treatment and neutralisation of viral particles by real-time quantitative PCR (qPCR) using qPCRBIO SY Green Mix Hi-Rox (Nippon Genetics Europe GmbH, Düren, Germany) and ABI PRISM 7900HT cycler (Applied Biosystems, Waltham, MA, USA). Vectors were quantified using the CMV promotor specific primer 5'-GGGACTTTCCTACTTGGCA and 5′-ctaccgcccatttgcgtc. qPCR was performed under the conditions listed in ***TAB. 9***. Each reaction was performed in a total volume of 10µl with 0.3 µM of each primer. The corresponding transfer plasmid was used a copy number standard, and serial dilutions of plasmid DNA was used to generate a standard curve for quantification.

TAB. 9: QPCR CONDITIONS FOR THE QUANTIFICATION OF AAV-VECTORS.

	TEMPERATURE	TIME [MIN]	CYCLES
INITIAL DENATURATION	50°C	2:00	1
DENATURATION	95°C	10:00	1
ANNEALING	95°C	0:15	35
ELONGATION	60°C	1:00	

3.4. INTRAVITREAL NSC TRANSPLANTATION AND AAV INJECTIONS

3.4.1. INTRAVITREAL TRANSPLANTATION OF NEURAL STEM CELLS

Different clonal NSC lines were intravitreally injected into either 10-day-old rd10 mice (hIL6 NSCs only) or 14-day-old *β2/β1* ki mice (CNTF, GDNF, LIF, PGRN, hIL6). As described in more detail elsewhere (Jankowiak et al., 2015; Jung et al., 2013), animals were deeply anaesthetised using either isoflurane (Baxter Deutschland GmbH, Unterschleißheim, Germany) and additional local anaesthesia (Conjucain®EDO®; Bausch + Lomb, Berlin, Germany) (for rd10 mice) or a mixture of ketamine (45.9 mg/kg body weight; Ketanest S 25mg/ml, Pfizer Pharma GmbH, Berlin, Germany) and xylazine (8.1 mg/kg body weight; Xylazin 20mg/ml, Wirtschaftsgenossenschaft deutscher Tierärzte eG, Garbsen, Germany) (for *β2/β1* ki mice). 2µl of vitreous fluid were removed using a glass micropipette connected by tubing to a syringe and replaced with 2 µl of a cell

suspension containing ~3.8×10^5 cells/µl in PBS. To co-deliver CNTF and GDNF, a 1:1 mixture of both clones (hereafter referred to as CNTF/GDNF-NSCs) was injected. The contralateral eye received the same amount of the respective control-NSC clone. After transplantation, the animals were treated with antibiotic eye drops (OFTAQUIX® (Santen Oy, Tampere, Finland) and Gent-Ophtal® (Gentamicin; Dr. Winzer Pharma GmbH, Berlin, Germany)), moisturising eye gel (Vidisic®; Bausch + Lomb Incorporated, Berlin, Germany) and were closely monitored and kept on a heating plate at approximately 37°C to maintain body temperature.

3.4.2. INTRAVITREAL INJECTION OF AAV PARTICLES

In addition to hIL6-NSCs, rd10 mice were treated with scAAVshH10-CMV-hIL6 (hereafter referred to as AAVshH10-hIL6). Injections of AAVshH10-hIL6 and scAAVshH10-CMV-GFP (hereafter referred to as AAVshH10-GFP), used as a control, were performed as described before (Liu et al., 2022). Analogous to NSC transplantation, for AAV injections 9-day-old rd10 mice were deeply anaesthetised using isoflurane (Baxter), 1µl of vitreous fluid was removed and replaced by either AAVshH10-hIL6 in PBS (1.2×10^{13} viral genomes (vg)/ml) or AAVshH10-GFP (1.5×10^{12} vg/ml). After injections, animals received the same care as described above (see **3.4.1. INTRAVITREAL TRANSPLANTATION OF NEURAL STEM CELLS**).

TAB. 10: PRIMARY ANTIBODIES USED IN IMMUNOCYTOCHEMISTRY, IMMUNOHISTOCHEMISTRY AND WESTERN BLOTTING.

ANTIGEN	DILUTION	SUPPLIER	CATALOGUE NUMBER
CONE-ARRESTIN (CAR)	1:2,000 (IHC) 1:500 (WB)	Millipore	AB15282
CLUSTER OF DIFFERENTIATION 68 (CD68)	1:1,000 (IHC)	Bio-Rad Laboratories, Kidlington, UK	MCA1957
GLIAL FIBRILLARY ACIDIC PROTEIN (GFAP)	1:500 (IHC) 1:5,000 (WB)	Dako Cytomation GmbH, Hamburg, Germany	Z0334
GLIAL FIBRILLARY ACIDIC PROTEIN (GFAP)	1:100 (IHC)	Sigma-Aldrich	G3893
GREEN FLUORESCENT PROTEIN (GFP)	1:100 (IHC)	R&D Systems	AF4240
INTERLEUKIN-6 (IL6)	1:800 (IHC/ICC) 1:1,000 (WB)	Abcam, Cambridge, UK	Ab6672
BIOTINYLATED INTERLEUKIN-6-RECEPTOR α (IL6Rα)	1:100 s(ICC) 1:100 (IHC)	R&D Systems	BAF227
IONIZED CALCIUM-BINDING ADAPTER MOLECULE 1 (IBA1)	1:2,000 (IHC) 1:1,000 (WB)	Abcam	Ab178846
LEUKEMIA INHIBITORY FACTOR (LIF)	1:200 (IHC/ICC) 1:500 (WB)	R&D Systems	AB-449-NA
PHOSPHO P44/42 MITOGEN-ACTIVATED PROTEIN KINASE (pMAPK)	1:1,000 (IHC)	Cell Signaling Technology, Leiden, The Netherlands	4370S
MICROTUBULE-ASSOCIATED PROTEIN 2 (MAP2)	1:200 (IHC)	Sigma-Aldrich	M4403
OPSIN M (OPS M)	1:500 (IHC)	Millipore	AB5405
OPSIN BLUE (OPS S)	1:500 (IHC)	Millipore	AB5407
PROGRANULIN (PGRN)	1:1,000 (IHC/ICC) 1:250 (WB)	R&D Systems	MAB2557
RED FLUORESCENT PROTEIN (RFP)/ DSRED	1:500 (IHC/ICC)	Rockland Immunochemicals, Philadelphia, PA, USA	600-401-379
RHODOPSIN (RHO)	1:500 (IHC) 1:1000 (WB)	Abcam	Ab221664
PHOSPHORYLATED SIGNAL TRANSDUCER AND ACTIVATOR OF TRANSCRIPTION 3 (TYR705) (pSTAT3)	1:1,000 (WB)	Cell Signaling Technology	9131

ICC: immunocytochemistry, IHC: Immunohistochemistry, WB: Western blotting.

3.4.3. IMMUNOHISTOCHEMICAL ANALYSIS OF TREATED RETINAE

Treated animals were sacrificed by deep anaesthesia using O_2/CO_2 (20% O_2, 80% CO_2), followed by inhalation of 100% CO_2 and cervical dislocation at P28, P35, P42 or P56 (rd10 mice), and P56 or P112 (*β2/β1* ki mice). Eyes were processed and immunohistochemically treated as described before (Atiskova et al., 2019; Jankowiak et al., 2015; Jung et al., 2013). The temporal cornea was removed and eyes were immersion fixed in 4% (w/v) PFA (Sigma-Aldrich), cryo-protected in a sucrose series (7.5%, 15% and 30% sucrose in PBS, pH 7.4), embedded in Tissue-Tek® O.C.T. Compound (Sakura Finetek Germany GmbH, Umkirch, Germany) and sectioned at a thickness of 25 µm in the temporal-nasal plane using a cryostat (CM1950, Leica Mikrosysteme Vertrieb, Wetzlar, Germany). For quantitative analysis central sections in the plane of the optic disc were selected for immunohistochemistry. Sections were incubated in blocking medium for 1h at room temperature, and subsequently incubated with different primary antibodies (***TAB. 10***) overnight at room temperature, washed in PBS and incubated with the appropriate Cy3-conjugated secondary antibodies (all diluted 1:200, Jackson Immunoresearch Laboratories, Inc.) overnight at 4°C, washed and mounted onto slides using Aqua-Poly/Mount (Polysciences, Inc.). Inner and outer segments of cone photoreceptor cells were visualised by incubating the sections with biotinylated peanut agglutinin (PNA; 1:5,000; Vector Laboratories, Newark, CA, USA), followed by Cy3-conjugated streptavidin (1:500; Jackson Immunoresearch Laboratories, Inc.). Cell nuclei were labelled with DAPI (Sigma-Aldrich). Retinas treated with NTF-NSCs or AAVshH10-hIL6 and the contralateral control retinas were processed in parallel to allow for direct comparison of signal intensities. For experiments with hIL6-NSCs and AAVshH10-hIL6, age-matched untreated rd10 mice and untreated wild-type mice were analysed as an additional reference.

3.4.4. IMMUNOCYTOCHEMICAL ANALYSIS OF NEURAL STEM CELLS *IN VIVO*

In vivo analysis of intravitreally grafted cells was performed at the latest analysis time point after the NSC transplantation, at P56 for rd10 mice, and P112 for *β2/β1* ki mice. As described elsewhere (Dulz et al., 2020; Flachsbarth et al., 2018; Flachsbarth et al., 2014; Jankowiak et al., 2015; Jung et al., 2013) lenses

were carefully extracted from the eyecups and fixed in 4% (w/v) PFA for 30 minutes before incubation for 1h at room temperature in blocking buffer followed by incubation with primary antibodies against LIF, PGRN or IL6Rα in conjunction with either rabbit anti- red fluorescent protein (RFP) or goat anti-GFP antibodies, depending on reporter protein expressed by the respective NSC clone, and anti-GFAP antibodies overnight at room temperature. After washing, incubation with the respective secondary antibodies for 4h at room temperature and counterstaining of cell nuclei with DAPI (Sigma-Aldrich), lenses were further fixed in 4% (w/v) PFA for 30 minutes. Lenses were pinned to a petri dish with silicon base using fine insect needles (INSECT PINS® Minutiens 0.10 mm; Austerlitz, Slavkov u Brna, Czech Republic) and kept submerged in PBS. Confocal z-stacks of donor cells attached to the posterior pole of the lenses were acquired using an Olympus Fluoview FV1000 laser-scanning confocal microscope with an UMPlanFl 20x/0.5W objective. z-stacks were processed using the FV110-ASW software (Olympus Deutschland GmbH, Hamburg, Germany). Images of lenses treated with NTF-NSCs and the respective control-NSCs were acquired using the same microscope settings to allow for comparison of signal intensities.

3.4.5. WESTERN BLOT ANALYSIS OF RETINAS TREATED WITH HIL6 NSCS AND AAVS

To investigate the impact of hIL6 on the expression of proteins involved in phototransduction, activation of intracellular signalling cascades and neuroinflammation in the rd10 retinas, the expression of cone-arrestin (CAR), phosphorylated signal transducer and activator of transcription 3 (pSTAT3), ionized calcium-binding adapter molecule 1 (IBA1) and GFAP (***TAB. 10***) in treated and control retinas were examined by Western Blotting of retinal tissue as described before (Atiskova et al., 2019). Total protein homogenates of retinas from P28 rd10 mice treated with AAVshH10-hIL6 or AAVshH10-GFP and age-matched untreated rd10 or untreated wild-type mice were prepared by homogenisation in lysis buffer (50mM TRIS-HCl pH7.5, 150mM NaCl, 1% Tx-100, 4% 25x protease inhibitor cocktail (cOmplete™ Mini; Roche)), incubation on ice for 30 minutes and centrifugation at $20{,}000 \times g$ for 10 minutes. Protein concentrations of homogenates were determined by bicinchoninic acid assay (BSA; Pierce™ BCA protein Assay, Thermo Fischer Scientific) using a DS-11 µVolume spectrophotometer (DeNovix, Wilmington, DE, USA) with BSA (20

mg/ml, Thermo Fischer Scientific) serving as protein standard. The BSA standard series (0-0.9 mg/ml) was prepared by dilution of BSA in lysis buffer. Collected retinal tissue samples were diluted in lysis buffer (1:10). Samples and the BSA standard series were mixed with reagent A and reagent B (50:1) according to manufacturer instructions, incubated for 30 min at 37°C, followed by analysis of the calorimetric density at 562 nm.

Total protein homogenates were reduced by addition of dithiothreitol (DTT, 32 µg/µl; Carl Roth) in 4x protein sample loading buffer (LI-COR). After denaturing at 95°C for 10 min and short centrifugation, samples (10 µg protein/lane) were separated by 10% (for CAR, GFAP, pSTAT3) or 15% (for IBA1) SDS-PAGE at 200V for 1-2h and transferred onto nitrocellulose membranes (Mini-PROTEAN® Tetra electrophoresis system; Bio-Rad, Hercules, CA, USA). After transfer, membranes were blocked in either 5% non-fat dry milk (for CAR) in TBS or diluted Intercept Blocking buffer (LI-COR Biosciences) (for IBA1, GFAP, pSTAT3) and processed as described earlier (see **3.2.2. CHARACTERISATION OF MODIFIED NEURAL STEM CELL LINES**). Signals of immunolabeled bands were visualised as described above at 800 nm for 2 minutes. Experiments were performed in triplicate.

To process membranes for total protein staining (TPS), which served as loading control, membranes were dried for 40-60 minutes at room temperature and washed for 5 min in TBS before incubation with Revert™ 700 Total Protein Stain (LI-COR Biosciences) according to the manufacturer's instructions. Excess reagent was removed by incubation with the Revert™ 700 Wash solution (LI-COR) twice for 30 seconds. TPS signals were visualised as described (see **3.2.2. CHARACTERISATION OF MODIFIED NEURAL STEM CELL LINES**) at 700 nm for 30 seconds.

3.5. MORPHOMETRIC ANALYSIS

For morphometric analyses, optical sections with a thickness of 1.45 µm were taken across the whole length of central retinal sections (i.e. from the nasal to the temporal periphery in the plane of the optic nerve head) using an AxioObserverZ.1 microscope equipped with an ApoTome2 (Carl Zeiss AG). The retina thickness, measured from the RPE to the inner limiting membrane (ilm), and the photoreceptor layer thickness, measured from the RPE to, and including,

the opl, were determined at nine equidistant positions in both the nasal and temporal half of the retina. The number of rows of photoreceptor cell nuclei, a measure for the number of rod photoreceptor cells, was determined at the same positions. Micrographs for the qualitative documentation of the different immunostainings were taken close to the optic disc using the same microscope settings for each antigen.

Morphometric analyses of retina thickness, photoreceptor layer thickness and number of rows of photoreceptor cell nuclei were performed using Image J v. 1.53t (Rasband, W.S., Image J, U.S. National Institutes of Health, Bethesda, MD, USA) and Fiji v. 2.14.0/1.54f (Schindelin et al., 2012). Quantifications of PNA-positive cone inner segments in direct contact with the onl, IBA1-positive microglia in *β2/β1* ki mice treated with CNTF-, GDNF-, LIF- or PGRN- NSCs and cluster of differentiation 68 (CD68)-positive macrophages in hIL6-treated animals were performed across the entire retina using Zen Pro v. 3.4.91.0 (Carl Zeiss AG). Only IBA1- and CD68-positive cells with clearly visible nuclei were counted. Analysis was performed on at least 6 animals for each treatment and age group.

3.6. STATISTICAL ANALYSIS

All statistical analyses were performed using GraphPad Prism V5.02 (GraphPad Software, San Diego, CA, USA). Statistical analyses of retinal thickness, photoreceptor layer thickness, number of rows of photoreceptor cell nuclei and cell densities of PNA-, IBA1-, and CD68-positive cells were performed using a two-way ANOVA followed by a Bonferroni post-hoc test.

For statistical analysis of Western Blot data, signal intensities of immunoreactive bands in the different experimental groups were normalised using TPS. Data were analysed using a repeated measures one-way ANOVA followed by a Bonferroni post-hoc test. For all statistical tests p-values <0.05 were considered statistically significant.

4. RESULTS

4.1. Project I: Protection of photoreceptor cells with various neurotrophic factors in a novel mouse model exhibiting a cone-rod dystrophy-like phenotype

4.1.1. *IN VITRO* CHARACTERISATION OF THE MODIFIED CLONAL NSC LINES

The effect of different NTFs — namely CNTF, GDNF, LIF and PGRN — on photoreceptors survival was examined in the *β2/β1* ki mouse, an animal model with a cone-rod dystrophy-like phenotype. *β2/β1* ki mice were subjected to intravitreal transplantations of lentivirally modified NSC lines. These NSC lines expressed the NTFs together with a fluorescent reporter protein under control of the CAG promotor. Control-NSCs expressed a reporter protein but no NTF. For further information on the lentiviral vectors used to generate the NSC lines, see **TAB. *8*** and ***FIG. 15***. Clonal NSC lines with high transgene expression levels were generated by repeated transductions, each followed by selection of single cells with strong expression of the reporter protein by FACS and subsequent clonal expansion (***FIG. 16***).

Expression of transgenes in the CNTF-NSC and GDNF-NSC lines has been analysed in previous studies (Dulz et al., 2020; Flachsbarth et al., 2018; Hu et al., 2025). In the present thesis, a detailed analysis of the transgene expression in the LIF-NSC and PGRN-NSC lines was performed using immunocytochemistry and Western blot analysis.

Immunocytochemical analysis of LIF-NSCs, PGRN-NSCs and the respective control-NSCs revealed expression of the reporter proteins tdTomato (LIF-NSCs and control-NSCs) (**FIG. *17***A) and Venus (PGRN-NSCs and control-NSCs) (***FIG. 17***C) in all cells. Furthermore, the analysis revealed co-expression, as indicated by arrow heads, of tdTomato and LIF in LIF-NSCs (***FIG. 17***Ac) and Venus and PGRN in PGRN-NSCs (***FIG. 17***Cc), while control-NSCs expressed neither NTF (***FIG. 17***Ae,Ce). Additionally, the transgene was expressed in *in vitro* and in *in vivo* differentiated astrocytes (**FIG. S2** and ***FIG. S3***, respectively).The amount of secreted LIF or PGRN in culture supernatants from different cell passages was quantified by Western blot analysis. Recombinant murine LIF (rmLIF) or recombinant murine PGRN (rmPGRN) were loaded as a reference. Analysis revealed a secretion of 881.6 ± 20.4 ng LIF/10^5 cells/24h at passage 45 and 846.3 ± 46.3 ng LIF/10^5 cells/24h at passage 53 for LIF-NSCs (***FIG. 17***B).

PGRN-NSCs secreted 464.0 ± 29.1 ng PGRN/10^5 cells/24h at passage 46 and 383.0 ± 29.2 ng PGRN/10^5 cells/24h at passage 58 (***FIG. 17***D). Neither LIF nor PGRN were detectable in supernatants harvested from the respective control-NSC clones.

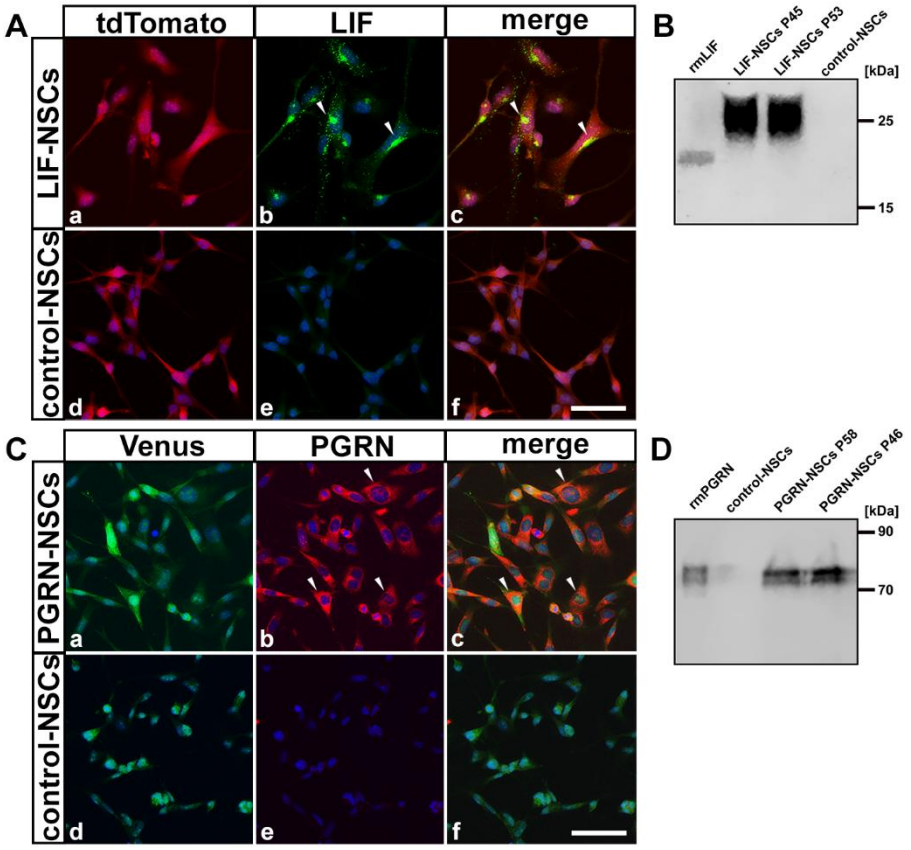

FIG. 17: EXPRESSION OF LIF AND PGRN IN NEURAL STEM CELLS.
(A) Expression of LIF (b,e) and the reporter protein tdTomato (a,d) in undifferentiated LIF-NSCs (a-c) and control-NSCs (d-f). (B) Western blot analysis of culture supernatants from LIF-NSCs at passage 45 and 53 and control-NSCs. Recombinant murine LIF was loaded as a reference. (C) Expression of PGRN (b,e) and the reporter protein Venus (a,d) in undifferentiated PGRN-NSCs (a-c) and control-NSCs (d-f). (D) Western blot analysis of culture supernatants from PGRN-NSCs at passage 46 and 58 and control-NSCs. Recombinant murine PGRN was loaded as a reference. A co-expression of the respective transgene and reporter protein is indicated by arrow heads. kDa: kilodalton; LIF: leukemia inhibitory factor; NSCs: neural stem cells; P: passage; PGRN: progranulin; rmLIF: recombinant murine leukemia inhibitory factor; rmPGRN: recombinant murine progranulin. Scale bar in Af (for Aa-Af) and Bf (for Ba-Bf): 50 µm.

4.1.2. TREATMENT WITH CYTOKINES INCREASES NEUROINFLAMMATION IN *Atp1b2*^{Atp1b1} KI RETINAS

To examine the neuroinflammation in dystrophic *β2/β1* ki retinas after transplantation of NTF-NSCs and control-NSCs, the expression of GFAP, IBA1 and CD68 was analysed.

The presence of reactive astrogliosis was assessed by examination of the GFAP expression. GFAP expression was increased in NTF-treated retinas compared to the respective control retinas regardless of the applied NTF (i.e. CNTF, GDNF, CNTF/GDNF, LIF or PGRN; ***FIG. 18***Aa-f, Ba-d). However, reactive astrogliosis was more pronounced in retinas treated with the cytokines CNTF and LIF than in retinas treated with GDNF-NSCs, PGRN-NSCs or control-NSCs in 2-month-old animals (***FIG. 18***) and 4-month-old animals (***FIG. S4***).

There was a marginal increase in the number of CD68-positive macrophages in *β2/β1* ki retinas treated with NTF-NSCs compared to those treated with control-NSCs (for P56, see: ***FIG. 18***Am-r, Bi-l; for P112, see ***FIG. S4***) Most CD68-positve macrophages were observed in retinas treated with CNTF- (***FIG. 18***An), CNTF/GDNF- (***FIG. 18***Ar) and LIF-NSCs (***FIG. 18***Bj). CD68-positive macrophages were primarily located in the subretinal space.

Ramified IBA1-positive cells were observed in all retinal layers (***FIG. 18***Ag-l, Be-h) in both NTF-treated and control-retinas, whereas IBA1-positive cells with an amoeboid-like morphology were found in the subretinal space. Of note, more IBA1-positive cells were observed in retinas treated with CNTF (***FIG. 18***Ah), CNTF/GDNF (***FIG. 18***Al) and LIF (***FIG. 18***Bf), than in retinas treated with GDNF (***FIG. 18***Aj) or PGRN (***FIG. 18***Bh). Quantitative analyses confirmed a significantly increased density of IBA1-positive cells in retinas treated with LIF-, CNTF- and CNTF/GDNF-NSCs compared to control retinas, both in 2-month-old animals (***FIG. 18***Ca) and 4-month-old animals (***FIG. 18***Cb). A sustained intravitreal administration of GDNF or PGRN did not increase the density of IBA1-positive cells compared to the respective control retinas (***FIG. 18***Ca,b). Retinas of 2-month old *β2/β1* ki mice treated with CNTF-, CNTF/GDNF-, or LIF-NSCs contained ~2-fold more IBA1-positive cells compared to retinas with grafted control-NSCs (***TAB. 11***). In 4-month-old *β2/β1* ki mice, retinas treated with CNTF-NSCs, CNTF/GDNF-NSCs, or LIF-NSCs contained ~1.7-fold more IBA1-positive microglia than the control retinas.

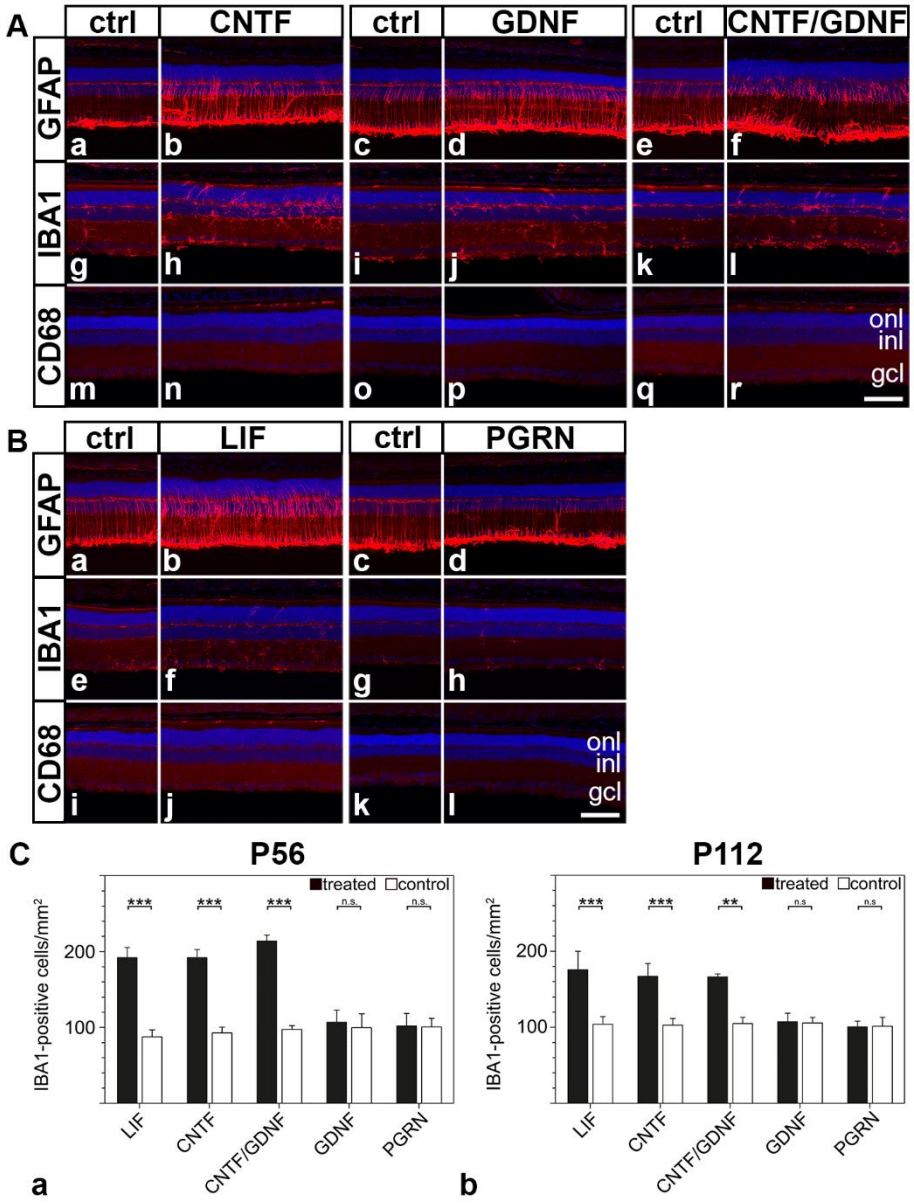

FIG. 18: ANALYSIS OF NEUROINFLAMMATION IN NTF-TREATED *β2/β1* KI RETINAS.

Reactive astrogliosis (Aa-f, Ba-d) and reactive microgliosis (Ag-r, Be-l) were assessed by immunohistochemistry in 2-month-old *β2/β1* ki mice treated with NTF-NSCs and control-NSCs. (C) The density of IBA1-positive cells in retinas treated with LIF-, CNTF-, CNTF/GDNF-, GNDF- or PGRN-NSCs (filled bars) and control-NSCs (open bars) in 2-month- (Ca) and 4-month-old (Cb) animals. Each bar represents the mean ± SEM from six retinas. **: p<0.01, ***: p<0.001, n.s.: not significant according to a two-way ANOVA followed by a Bonferroni post-hoc test. *β2/β1* ki: *Atp1b2*^{Atp1b1} knock-in mice; CD68: cluster of differentiation 68; CNTF: ciliary neurotrophic factor; ctrl: control; gcl: ganglion cell layer; GDNF: glial cell line-derived neurotrophic factor; GFAP: glial fibrillary acidic protein; IBA1: ionized calcium-binding adapter molecule 1; inl: inner nuclear layer; LIF: leukemia inhibitory factor; NSCs: neural stem cells; NTF: neurotrophic factor; onl: outer nuclear layer; P: postnatal day; PGRN: progranulin. Scale bar in Ar (for Aa-Ar) and Bl (for Ba-Bl): 100 µm.

TAB. 11: DENSITY OF IBA1-POSITIVE CELLS AND FOLD-CHANGES COMPARED TO CONTROLS IN RETINAS *β2/β1* KI MICE TREATED WITH NTF- OR CONTROL-NSCS.

	NEUROTROPHIC FACTOR	IBA1-POSITIVE CELLS/MM^2 IN TREATED RETINAS	IBA1-POSITIVE CELLS/MM^2 IN CONTROL RETINAS	FOLD-CHANGE COMPARED TO CONTROL
P56	CNTF	192.0 ± 9.7	92.2 ± 7.0	**2.1**
	GDNF	106.8 ± 14.4	99.7 ± 16.6	**1.0**
	CNTF/GDNF	213.9 ± 7.3	97.3 ± 4.7	**2.2**
	LIF	191.9 ± 12.2	90.2 ± 7.8	**2.1**
	PGRN	101.9 ± 15.2	100.7 ± 10.3	**1.0**
P112	CNTF	167.2 ± 15.2	102.7 ± 8.2	**1.6**
	GDNF	107.4 ± 10.1	106.3 ± 6.5	**1.0**
	CNTF/GDNF	185.9 ± 9.9	105.1 ± 7.3	**1.8**
	LIF	175.6 ± 22.5	103.9 ± 9.2	**1.7**
	PGRN	100.7 ± 6.8	101.4 ± 10.6	**1.0**

CNTF: ciliary neurotrophic factor; GDNF: glial cell line-derived neurotrophic factor; IBA1: ionized calcium-binding adapter molecule 1; LIF: leukemia inhibitory factor; P: postnatal day; PGRN: progranulin.

4.1.3. NEUROTROPHIC FACTORS ATTENUATE PHOTORECEPTOR LOSS IN THE *Atp1b2^{Atp1b1}* KI MOUSE

The impact of the intravitreally grafted NTF-NSC clones on photoreceptor survival was analysed in 2- and 4-month-old *β2/β1* ki mice. The examination points were chosen according to analysis of the *β2/β1* ki phenotype, as described by Bartsch et al. (2025). Significant loss of rod and cone photoreceptors was apparent in 2-month-old *β2/β1* ki retinas and became significantly more pronounced in 4-month-old animals.

4.1.3.1. RETINAL THINNING

About 97% of the photoreceptor population in the murine retina is comprised of rod photoreceptors, with the remaining 3% of the cell population consisting of cone photoreceptors (Carter-Dawson & LaVail, 1979; Jeon et al., 1998). Hence, retina thickness, photoreceptor layer thickness and the number of rows of photoreceptor cell nuclei represent useful measures to estimate the number of surviving rod photoreceptor cells in the *β2/β1* ki mice.

In 2-month-old animals the retina thickness was ~20% (LIF-NSCs: 190.25 ± 7.08 µm; CNTF-NSCs: 177.88 ± 6.81 µm; CNTF/GDNF-NSCs: 184.00 ± 2.92 µm; control-NSCs: 155.17 ± 2.77 µm), and the photoreceptor layer thickness ~30% greater (LIF-NSCs: 80.02 ± 3.44 µm; CNTF-NSCs: 70.77 ± 1.51 µm; CNTF/GDNF-NSCs: 66.33 ± 1.56 µm; control-NSCs: 55.18 ± 0.79 µm) in retinas treated with LIF-, CNTF- or CNTF/GDNF-NSCs compared to retinas treated with control-NSCs (***FIG. 19***a,c). In 4-month-old animals, retina thickness (LIF-NSCs: 156.70 ± 2.25 µm; control-NSCs: 133.59 ± 3.61 µm) and photoreceptor layer thickness (LIF-NSCs: 56.12 ± 1.23 µm; control-NSCs: 47.00 ± 2.17 µm) was significantly greater in LIF-treated retinas. In this age group, significantly thicker retinas or photoreceptor layers were no longer observed in retinas treated with CNTF or CNTF/GDNF-NSCs when compared to control retinas (***FIG. 19***b,d) In addition, no significant differences in retina thickness or photoreceptor layer thickness were observed in either age group in retinas treated with GDNF-NSCs or PGRN-NSCs compared to control-NSCs.

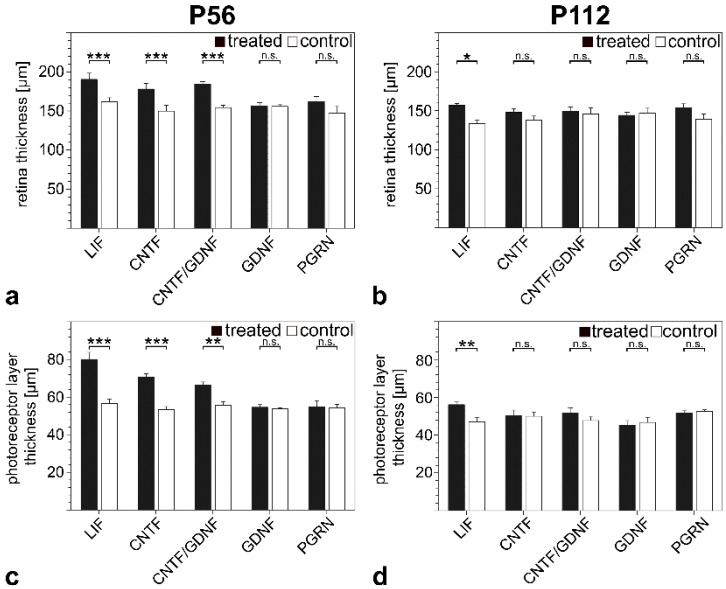

FIG. 19: RETINA THICKNESS AND PHOTORECEPTOR LAYER THICKNESS IN *β2/β1* KI RETINAS TREATED WITH NTF- OR CONTROL-NSCS.
Retina thickness (a,b) and photoreceptor layer thickness (c,d) were analysed in *β2/β1* ki mouse retinas treated with either NTF-NSCs (filled bars) or control-NSCs (open bars) in 2-month-old (a,c) and 4-month-old (b,d) mice. Each bar represents the mean ± SEM from six retinas. *: p<0.05, **: p<0.01, ***: p<0.001, n.s.: not significant according to a two-way ANOVA followed by a Bonferroni post-hoc test. CNTF: ciliary neurotrophic factor; GDNF: glial cell line-derived neurotrophic factor; LIF: leukemia inhibitory factor; PGRN: progranulin.

4.1.3.2. ROD PHOTORECEPTORS

The number of rows of photoreceptor cell nuclei (RPN) is a measure for the number of rod photoreceptors in the murine retina. Analysis revealed significantly more RPN in both 2- (***FIG. 20***a) and 4-month-old animals (***FIG. 20***b) treated with LIF-, CNTF- and CNTF/GDNF-NSCs, and in 2-month-old animals treated with PGRN-NSCs compared to retinas treated with control-NSCs (***TAB. 12***). In 4-month-old animals the protective effect of PGRN on rod photoreceptor survival was diminished. A neuroprotective effect of GDNF-NSCs alone on rod photoreceptor survival was not observed in either age group. The strongest effect on rod photoreceptor survival was observed in retinas of 2- and 4-month-old animals treated with the cytokines LIF and CNTF. In 2-month-old animals, retinas treated with LIF-NSCs and CNTF-NSCs contained significantly more RPN than those treated with CNTF/GDNF-NSCs (***FIG. S5***). In 4-month-old animals, no significant difference in RPN between retinas treated with LIF-NSCs, CNTF-NSCs and CNTF/GDNF-NSCs was observed. Furthermore, in both 2- and 4-month-old animals, retinas treated with CNTF-, CNTF/GDNF- and LIF contained significantly more RPN than those treated with GDNF or PGRN.

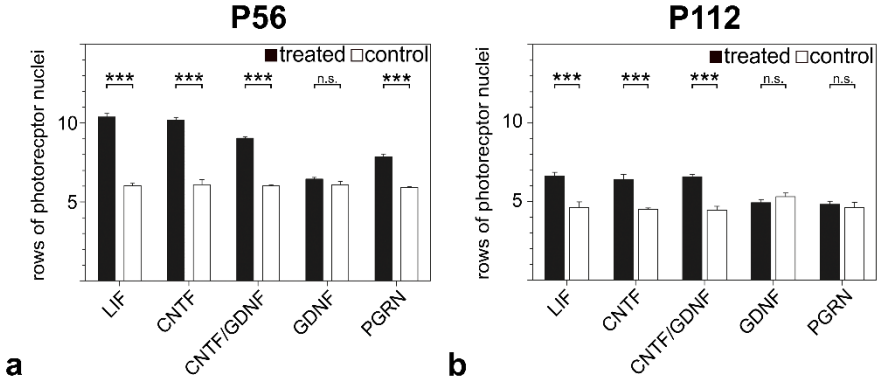

FIG. 20: THE NUMBER OF ROWS OF PHOTORECEPTOR NUCLEI IN 2- AND 4-MONTH-OLD *β2/β1* KI MICE TREATED WITH NTF- AND CONTROL-NSCS.
The number of RPN was determined in retinas of 2-month-old (a) and 4-month-old animals treated with NTF-NSCs (filled bars) or control-NSCs (open bars). Each bar represents the mean ± SEM from six retinas. ***: $p<0.001$, n.s.: not significant according to a two-way ANOVA followed by a Bonferroni post-hoc test. CNTF: ciliary neurotrophic factor; GDNF: glial cell line-derived neurotrophic factor; LIF: leukemia inhibitory factor; PGRN: progranulin; RPN: number of rows of photoreceptor nuclei.

TAB. 12: THE NUMBER OF ROWS OF PHOTORECEPTOR NUCLEI IN *β2/β1* KI RETINAS TREATED WITH NTF- OR CONTROL-NSCS.

	NEUROTROPHIC FACTOR	RPN IN TREATED RETINAS	RPN IN CONTROL RETINAS	FOLD-CHANGE COMPARED TO CONTROL
P56	CNTF	10.2 ± 0.1	6.5 ± 0.3	**1.6**
	GDNF	6.5 ± 0.09	6.1 ± 0.2	**1.1**
	CNTF/GDNF	9.3 ± 0.09	6.0 ± 0.07	**1.5**
	LIF	10.4 ± 0.2	6.0 ± 0.1	**1.7**
	PGRN	7.9 ± 0.2	5.9 ± 0.03	**1.3**
P112	CNTF	6.4 ± 0.3	4.5 ± 0.08	**1.4**
	GDNF	4.9 ± 0.2	5.3 ± 0.2	**0.9**
	CNTF/GDNF	6.6 ± 0.2	4.5 ± 0.2	**1.5**
	LIF	6.6 ± 0.2	4.6 ± 0.3	**1.4**
	PGRN	4.8 ± 0.2	4.6 ± 0.3	**1.0**

CNTF: ciliary neurotrophic factor; GDNF: glial cell line-derived neurotrophic factor; LIF: leukemia inhibitory factor; P: postnatal day; PGRN: progranulin; RPN: rows of photoreceptor nuclei.

4.1.3.3. CONE PHOTORECEPTORS

As described before (*cf.* **1.4.2. THE PHENOTYPE OF *ATP1B2ATP1B1 KNOCK-IN MICE***), the *β2/β1* ki mouse exhibits a cone-rod dystrophy-like phenotype. Hence, in the context of this project, the examination of cone photoreceptor survival in retinas treated with NTF-NSCs was of particular interest. To determine the density of cone photoreceptors in treated and control retinas, the number of PNA-positive cone inner segments (hereafter referred to as PNA-positive CIS) in direct contact with the onl was quantified across the entire length of central retina sections. All applied NTFs, with the only exception of GDNF, significantly attenuated the loss of cone photoreceptors in the retina of both 2- and 4-month-old *β2/β1* ki mice, as indicated by immunohistochemical (***FIG. 21***A,B) and quantitative analysis (***FIG. 21***C).

In 2-month-old animals, retinas treated with CNTF-, CNTF/GDNF- and LIF-NSCs contained ~3-fold more cone photoreceptor cells than retinas treated with control-NSCs (***TAB. 13***). Retinas treated with PGRN-NSCs contained about 1.5-fold more cone photoreceptor cells compared to control retinas. In contrast to retinas treated with CNTF-, CNTF/GDNF-, LIF- or PGRN-NSCs, GDNF-NSCs did not promote the survival of cone photoreceptors (***FIG. 21***A,B; ***TAB. 13***).

TAB. 13: THE DENSITY OF CONE PHOTORECEPTORS AND FOLD-CHANGES IN THE RETINA OF *β2/β1* KI MICE TREATED WITH NTF- AND CONTROL-NSCS.

	NEUROTROPHIC FACTOR	CONES/1000 µM IN TREATED RETINAS	CONES/1000 µM IN CONTROL RETINAS	FOLD-CHANGE COMPARED TO CONTROL
P56	CNTF	75.5 ± 3.6	26.7 ± 1.4	**2.8**
	GDNF	23.0 ± 1.7	22.7 ± 2.2	**0.95**
	CNTF/GDNF	67.7 ± 4.9	22.9 ± 2.6	**3.0**
	LIF	78.8 ±2.0	25.5 ± 2.3	**3.1**
	PGRN	42.0 ± 2.2	27.7 ± 3.0	**1.5**
P112	CNTF	51.0 ± 2.2	16.2 ± 0.6	**3.1**
	GDNF	9.4 ± 1.1	8.0 ± 1.0	**1.2**
	CNTF/GDNF	45.4 ± 3.2	14.6 ± 1.3	**3.1**
	LIF	31.4 ± 2.5	12.3 ± 2.0	**2.6**
	PGRN	35.9 ± 1.5	12.8 ± 2.0	**2.8**

CNTF: ciliary neurotrophic factor; GDNF: glial cell line-derived neurotrophic factor; LIF: leukemia inhibitory factor; P: postnatal day; PGRN: progranulin.

Similar effects of the different NTFs on cone photoreceptor survival were observed in 4-month-old animals (***TAB. 13***). Retinas treated with CNTF- and CNTF/GDNF-NSCs contained ~3-fold more cones, and retinas treated with LIF contained ~2.5-fold more cones than the respective control retinas. Retinas treated with PGRN-NSCs contained ~2.8-fold more cones compared to control-retinas. As in 2-month-old animals, GDNF-NSCs had no effect on the progression of cone photoreceptor degeneration (***FIG. 21***C; ***TAB. 13***).

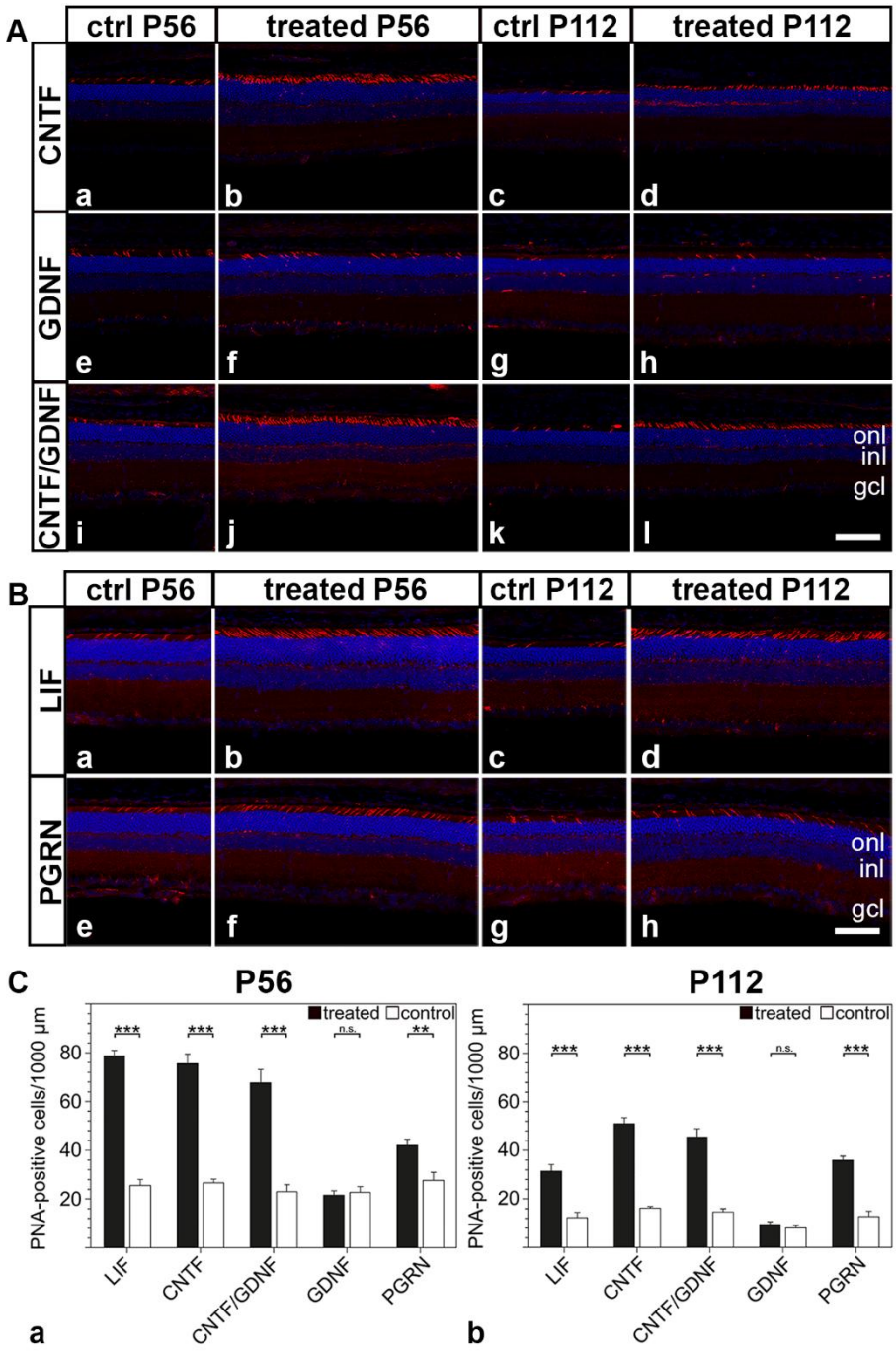

FIG. 21: THE CYTOKINES CNTF AND LIF, AS WELL AS THE GROWTH FACTOR PGRN ARE SUITABLE TO ATTENUATE THE LOSS OF CONE PHOTORECEPTORS IN 2- AND 4-MONTH-OLD *β2/β1* KI MICE.
Analysis of PNA-positive cone inner segments in retinas of 2- and 4-month-old *β2/β1* ki mice treated with CNTF-, GDNF- and CNTF/GDNF-NSCs (A) or LIF- and PGRN-NSCs (B) and control-NSCs. (C) Statistical analysis of PNA-positive cone inner and outer segments in retinas of 2-month-old (a) and 4-month-old (b) *β2/β1* ki retinas treated with NTF-NSCs (filled bars), or control-NSCs (open bars). Each bar represents the mean ± SEM from six retinas. Statistical analyses were performed using a two-way ANOVA followed by a Bonferroni post-hoc test. **: $p<0.01$, ***: $p<0.001$, n.s.: not significant. CNTF: ciliary neurotrophic factor; ctrl: control; gcl: ganglion cell layer; GDNF: glial cell line-derived neurotrophic factor; inl: inner nuclear layer; LIF: leukemia inhibitory factor; onl: outer nuclear layer; P: postnatal day; PGRN: progranulin; PNA: biotinylated peanut agglutinin. Scale bar in Al (for Aa-Al), Bh (for Ba-Bh): 100µm.

Furthermore, retinas of 2-month-old animals treated with LIF, CNTF and CNTF/GDNF contained significantly more cone photoreceptor cells than retinas of 4-month-old animals treated with the same NTFs (***FIG. S6***). Interestingly, retinas of 2- and 4-month-old animals treated with PGRN-NSCs contained approximately the same number of cones (P56: 42.0 ±2.2 PNA-positive CIS/1000 µm, P112: 35.9 ± 1.5 PNA-positive CIS/1000 µm; $p>0.05$ according to a two-way ANOVA followed by a Bonferroni post-hoc test) corresponding to a decrease of ~15% (***Tab. 14***). In animals treated with CNTF, CNTF/GDNF or LIF, on the other hand, retinas of older animals contained ~30% less PNA-positive cones compared to younger animals ($p<0.001$ according to a two-way ANOVA followed by a Bonferroni post-hoc test, ***Tab. 14***; ***FIG. 21***C; ***FIG. S6***;), indicating that PGRN was the most effective NTF in slowing the progression of cone degeneration.

Tab. 14: COMPARISON OF THE NUMBER OF CONES PRESENT IN TREATED *β2/β1* KI RETINAS BETWEEN AGE GROUPS.

	CONES/1000 µM IN TREATED RETINAS P56	CONES/1000 µM IN TREATED RETINAS P112	ΔCONES/1000 µM COMPARED TO P56
CNTF	75.5 ± 3.6	51.0 ± 2.2	**-32%**
GDNF	23.0 ± 1.7	9.4 ± 1.1	**-59%**
CNTF/GDNF	67.7 ± 4.9	45.4 ± 3.2	**-33%**
LIF	78.8 ±2.0	31.4 ± 2.5	**-60%**
PGRN	42.0 ± 2.2	35.9 ± 1.5	**-15%**

Δ: difference; CNTF: ciliary neurotrophic factor; GDNF: glial cell line-derived neurotrophic factor; LIF: leukemia inhibitory factor; P: postnatal day; PGRN: progranulin

4.2. PROJECT II: HYPER-IL6 ATTENUATES PHOTORECEPTOR LOSS IN AN AUTOSOMAL-RECESSIVE RETINITIS PIGMENTOSA AND A CONE-ROD DYSTROPHY MOUSE MODEL

In a second project, the neuroprotective effect of the novel designer cytokine hyper-IL6, a fusion protein consisting of the cytokine IL6 and the soluble isoform of its receptor, sIL6Rα (Fischer et al., 1997), was examined in two mouse models of photoreceptor degeneration. The impact of the hIL6 on photoreceptor survival was assessed in the *Pde6b*^{rd10} mouse (in the following referred to as rd10 mouse), a model of autosomal-recessive retinitis pigmentosa (Chang et al., 2002), and in the *β2/β1* ki mouse, a model of a cone-rod dystrophy (Bartsch et al., 2025). The designer cytokine was administered to the dystrophic retinas by intravitreal transplantation of hIL6-NSCs or intravitreal injections of a self-complementary AAVshH10-hIL6.

4.2.1. *IN VITRO* CHARACTERISATION OF HIL6-EXPRESSING NEURAL STEM CELLS

The expression of hIL6 in a newly generated clonal NSC line (hIL6-NSCs) was studied by immunocytochemistry in undifferentiated and differentiated cells as well as quantitative Western blot analysis.

Immunocytochemical analysis of undifferentiated cells revealed co-expression of perinuclearly located hIL6 and the cytoplasmic expression of the reporter protein Venus in all hIL6-NSCs, indicated by arrow heads (**FIG. *22*Aa-c**). Control-NSCs expressed the reporter protein, but not hIL6 (***FIG. 22*Ad-f**).

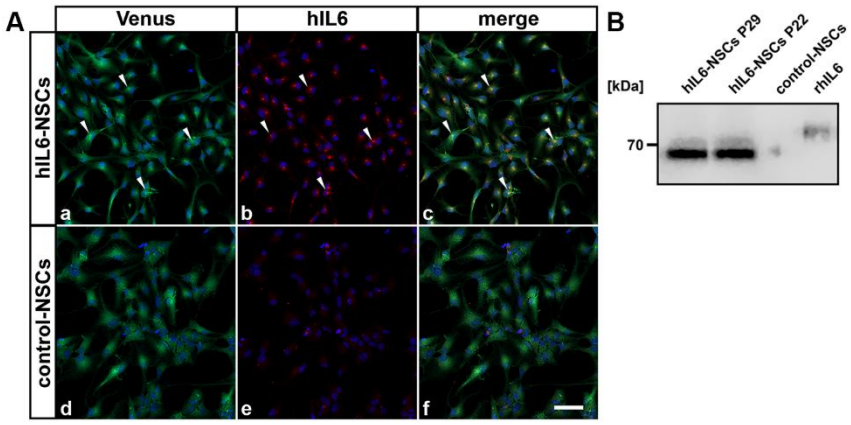

FIG. 22: *IN VITRO* CHARACTERISATION OF HIL6- AND CONTROL-NSCS.
(A) Expression of hIL6 and the reporter protein Venus in undifferentiated hIL6-NSCs (a-c) and control-NSCs (d-f). Co-expression of hIL6 and Venus is indicated by arrow heads. (B) Western blot analysis of culture supernatants obtained from hIL6-NSCs at passage 22 and 29 and control-NSCs. Recombinant human hIL6 was loaded as a reference. hIL6: hyper-interleukin-6; kDa: kilodalton; NSCs: neural stem cells; P: passage; rhIL6: recombinant human hIL6. Scale bar in Af: 50 µm.

Quantitative Western blot analysis of culture supernatants (***FIG. 22***B) obtained from the hIL6-NSC clone consistently revealed strong expression of the cytokine. hIL6-NSCs secreted 146.57 ± 7.93 ng hIL6/10^5 cells/24h at passage 22 and 128.76 ± 7.59 ng hIL6/10^5 cells/24h at passage 29. No hIL6 was detected in supernatants obtained from control-NSCs.

Additionally, the transgene expression was examined in *in vitro* differentiated cell types. hIL6-NSCs and control-NSCs were cultivated in different culture media to induce a preferential differentiation into either astrocytes or neurons. Astrocytes (**FIG. *23***Aa-d) and neurons (**FIG. *23***Ba-d) co-expressed the reporter protein Venus throughout the cytoplasm and hIL6 in a perinuclear pattern. Astrocytes and neurons derived from control-NSCs (**FIG. *23***Ae-h, Be-h) were positive for the reporter protein but lacked expression of the hIL6 transgene.

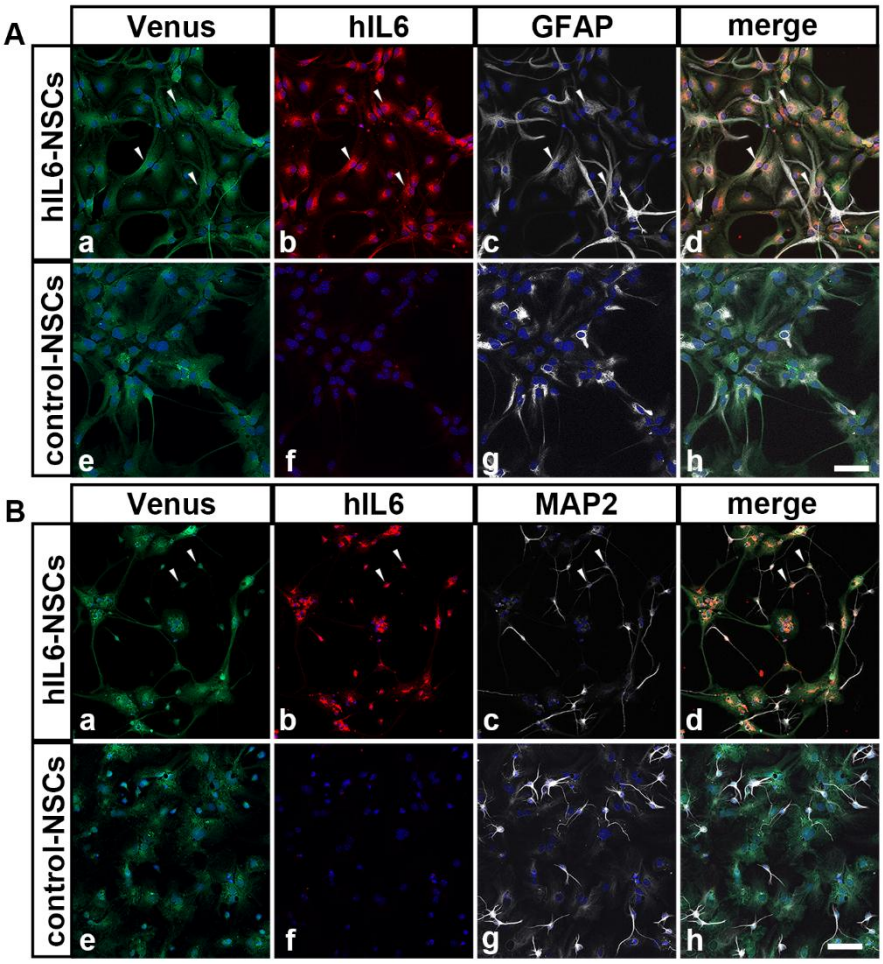

FIG. 23: TRANSGENE EXPRESSION IN ASTROCYTES AND NEURONS DERIVED FROM HIL6-NSCS AND CONTROL-NSCS *IN VITRO*.
(A) *In vitro* differentiated astrocytes derived from hIL6-NSCs (a-d) and control-NSCs (e-h). (B) *In vitro* differentiated neurons derived from hIL6-NSCs (a-d) and control-NSCs (e-h). GFAP: glial fibrillary acidic protein; hIL6: hyper-interleukin-6; MAP2: mitogen-associated protein 2; NSCs: neural stem cells. Scale bar in Ah (for Aa-h) and Bh (for Ba-h): 50 µm.

4.2.2. *IN VIVO* CHARACTERIZATION OF INTRAVITREALLY TRANSPLANTED NEURAL STEM CELL CLONES

The fate of intravitreally grafted hIL6- and control-NSCs in terms of survival, differentiation and transgene expression was analysed at the latest analysis time point, i.e. 46 days and 70 days after cell transplantation in rd10 mice and *β2/β1* ki mice, respectively. In both mouse models, grafted cells were attached to the posterior pole of the lenses where they had formed a monolayer of astrocytes (for rd10 mice, see ***FIG. 24***Aa,b, for *β2/β1* ki mice, see ***FIG. S7***Aa,b). The grafted hIL6-NSCs co-expressed hIL6 and the reporter protein for 46 days after transplantation in treated rd10 mice (***FIG. 24***Ba,b) and for 70 days after transplantation in treated *β2/β1* ki mice (***FIG. S7***Ba,b). In comparison, astrocytes derived from control-NSCs expressed the reporter protein (***FIG. 24***Bc) and GFAP (**FIG. 24**Ad; ***FIG. S7***Ac,d), but not hIL6 (***FIG. 24***Bd; ***FIG. S7***Bc,d).

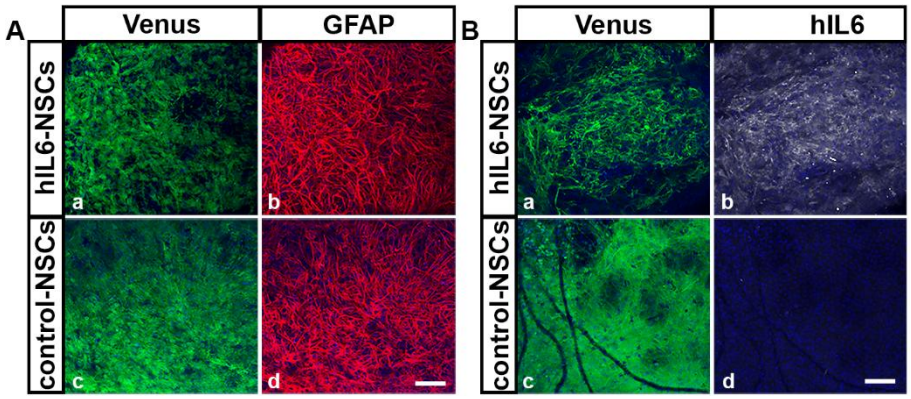

FIG. 24: IN VIVO CHARACTERISATION OF INTRAVITREALLY GRAFTED HIL6-NSCS AND CONTROL-NSCS IN RD10 MICE.
(A) Differentiation of intravitreally grafted hIL6-NSCs (a,b) and control-NSCs (c,d). (B) Expression of the reporter protein Venus and hIL6 in hIL6-NSCs (a,b) and control-NSCs (c,d). GFAP: glial fibrillary acidic protein; hIL6: hyper-interleukin-6; NSCs: neural stem cells. Scale bar in Ad (for Aa-d) and Bd (for Ba-d): 100 µm.

4.2.3. TRANSGENE EXPRESSION AFTER INTRAVITREAL INJECTIONS OF AAV VECTORS

Transgene expression after intravitreal injections of AAVshH10-hIL6 and AAVshH10-GFP in rd10 mice was evaluated at the latest analysis time point. Immunostainings of 2-month-old rd10 retinas, 47 days after the AAV injection, revealed expression of hIL6 throughout the retina (**FIG. 25**a). GFP was expressed in cell bodies located in the ganglion cell layer and in radially oriented cell

processes spanning the entire retina (**FIG. 25**b). A similar expression pattern of hIL6 and GFP was observed in 3-months-old *β2/β1* ki retinas (***FIG. S8***).

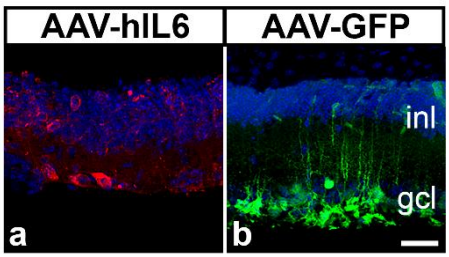

FIG. 25: EXPRESSION OF TRANSGENES AFTER INTRAVITREAL INJECTIONS OF AAVSHH10-HIL6 AND AAVSHH10-GFP IN THE RETINA OF 2-MONTH-OLD RD10 MICE.
Expression of hIL6 (a) and GFP (b) in retinas of rd10 mice treated with AAVshH10-hIL6 and AAVshH10-GFP, respectively. AAV: adeno-associated virus; gcl: ganglion cell layer; GFP: green fluorescent protein; hIL6: hyper-interleukin-6; inl: inner nuclear layer. Scale bar in b: 50 µm.

4.2.4. NEUROINFLAMMATION IN HIL6-TREATED RETINAS

4.2.4.1. HIL6 TREATMENT PROMOTES NEUROINFLAMMATION IN THE RETINA OF RD10 MICE

IL6 is a pro-inflammatory cytokine. Hence, the extent of reactive astrogliosis and reactive microgliosis induced by the grafted hIL6-NSCs or the injected AAVshH10-hIL6 was examined by analysing the expression of GFAP, IBA1 and CD68 (***FIG. 26***).

Strong expression of the inflammation markers was observed in retinas treated with either hIL6-NSCs or AAVshH10-hIL6 when compared to the contralateral control retinas, age-matched untreated rd10 retinas (also referred to as mutant mice (MUT)) or age-matched untreated wild-type retinas (***FIG. 26***). However, the extent of inflammation decreased with the increasing age of the animals as indicated by immunohistochemistry (***FIG. S9***) and quantification of the density of CD68-positive macrophages (***FIG.* 26**C).

GFAP expression was strongly increased throughout the examination period (P28 (***FIG. 26***A) through P56 (***FIG. S9***)) in retinas treated with both hIL6-NSCs (***FIG. 26***Ab) and AAVshH10-hIL6 (***FIG. 26***Ad) compared to retinas treated with control-NSCs (***FIG. 26***Aa), AAVshH10-GFP (***FIG. 26***Ac) or age-matched MUT (***FIG. 26***Ae) and WT retinas (***FIG. 26***Af).

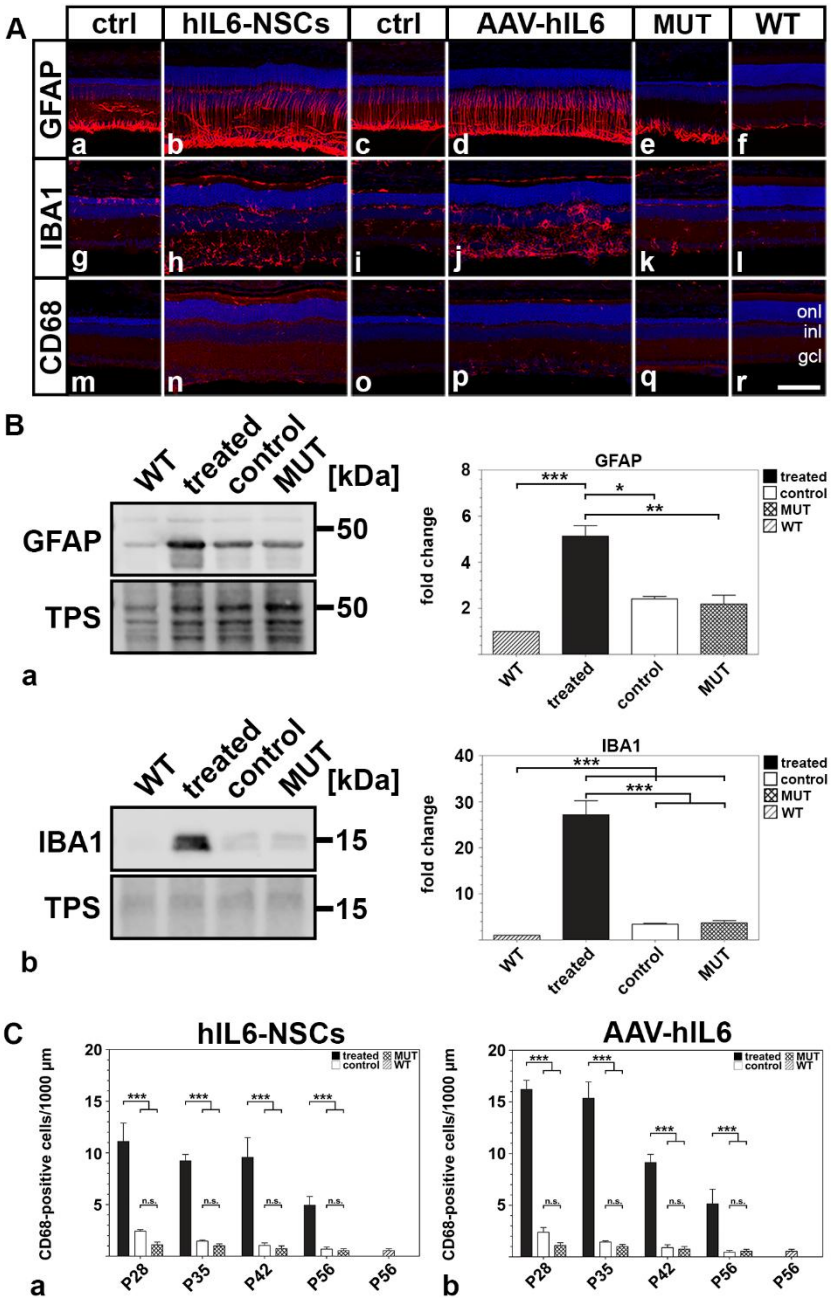

FIG. 26: TREATMENT WITH HIL6 INCREASED NEUROINFLAMMATION IN THE RETINA OF RD10 MICE.
(A) Reactive astrogliosis (a-f) and microgliosis (g-r) were assessed in 1-month-old rd10 mice treated with hIL6-NSCs (b,h,n) or AAVshH10-hIL6 (d,j,p) and their contralateral control retinas treated with control-NSCs (a,g,m) or AAVshH10-GFP (c,i,o), as well as age-matched untreated rd10 (MUT) (e,k,q) and wild-type (WT) mice (f,l,r,). (B) Quantitative Western blot analysis of GFAP (a) and IBA1 (b) in 1-month-old AAV-treated retinas (filled bars), control retinas (open bars), untreated MUT (cross-hatched bars) and untreated WT retinas (hatched bars). TPS was used as a standard. *: p<0.05; **: p<0.01; ***: p<0.001; n.s.: not significant according to one-way ANOVA followed by Bonferroni post-hoc test. (C) The density of CD68-positive macrophages in NSC- (a) or AAV-treated (b) rd10 retinas (filled bars), control retinas treated with either control-NSCs or AAVshH10-GFP (open bars), and age-matched MUT retinas (cross-hatched bars). Values for untreated 2-month-old WT mice (hatched bars) are shown as a reference. Each bar represents the mean ± SEM from eight retinas. ***: p<0.001, n.s.: not significant according to a two-way ANOVA followed by a Bonferroni post-hoc test. AAV: adeno-associated virus; CD68: cluster of differentiation 68; ctrl: control; gcl: ganglion cell layer; GFAP: glial fibrillary acidic protein; hIL6: hyper-interleukin-6; inl: inner nuclear layer; IBA1: ionized calcium-binding adapter molecule 1; kDa: kilodalton; MUT: mutant (here: rd10) NSCs: neural stem cells; onl: outer nuclear layer; P: postnatal day; TPS: total protein stain; WT: wild-type. Scale bar in Ar: 100 µm.

Quantitative Western blot analysis confirmed significantly elevated GFAP levels in 1-month-old rd10 retinas treated with AAVshH10-hIL6, the expression being ~2.2-fold higher than in rd10 retinas treated with AAVshH10-GFP or in MUT retinas, and ~5-fold higher than in untreated wild-type retinas (**FIG. *26***Ba).

Similar to GFAP, expression of IBA1 was strongly increased in 1-month-old rd10 retinas treated with hIL6-NSCs (***FIG. 26***Ah) or hIL6-AAVs (***FIG. 26***Aj; for 2-month-old retinas, see ***FIG. S9***) compared to control retinas (***FIG. 26***Ag and i, respectively), and age-matched MUT (***FIG. 26***Ak) or WT retinas (***FIG. 26***Al). IBA1 expression in 1-month-old rd10 mice treated with AAVshH10-hIL6 was markedly increased by ~7.7-fold when compared with AAVshH10-GFP-treated or MUT retinas, and by ~27-fold when compared to untreated WT retinas (***FIG.* 26**Bb).

Qualitative analysis of CD68 expression (***FIG. 26***Am-r) and quantitative analysis of the density of CD68-positive cells (**FIG. 26**C) revealed that retinas treated with hIL6-NSCs (***FIG. 26***Ca) or AAVshH10-hIL6 (***FIG. 26***Cb) contained significantly more CD68-positive macrophages than the respective control retinas or untreated MUT and WT retinas. Furthermore, AAV-treated retinas contained significantly more CD68-positive cells than NSC-treated retinas until P35 (***Tab. S1***). From P42 onward, retinas treated with hIL6-NSCs and AAVshH10-hIL6 contained about the same number of CD68-positive cells. Retinas treated with either control-NSCs or AAVshH10-GFP also contained more CD68-positive macrophages than untreated rd10 or WT retinas until P42 (***Tab. S2***).

4.2.4.2. NEUROINFLAMMATION IN *ATP1B2*^{ATP1B1} KI MICE TREATED WITH HIL6

Similar to the results observed in rd10 retinas, *β2/β1* ki retinas treated with hIL6 exhibited a more pronounced GFAP- and IBA1-expression compared to retinas treated with control-NSCs or AAVshH10-GFP and age-matched, untreated *β2/β1* ki retinas (MUT) and wild-type retinas (***FIG. S10***). The expression of GFAP was increased in *β2/β1* ki retinas treated with hIL6-NSCs and control-NSCs or AAVshH10-hIL6 and AAVshH10-GFP compared to age-matched MUT and WT retinas.

Conversely, apparent differences in the number of CD68-positive macrophages could not be observed between hIL6-treated *β2/β1* ki retinas of either age group compared to the respective controls.

4.2.5. hIL6 EXERTS NEUROPROTECTIVE EFFECTS ON PHOTORECEPTORS

4.2.5.1. hIL6 ATTENUATES PHOTORECEPTOR LOSS IN THE RETINA OF RD10 MICE

hIL6 has been shown to attenuate the loss of RGCs and to promote axonal regeneration in a mouse model of optic nerve injury (Leibinger et al., 2016). Nonetheless, to the best of our knowledge, to date no study has examined whether hIL6 promotes the survival of photoreceptor cells.

Retinas of rd10 mice treated with hIL6-NSCs or AAVshH10-hIL6 were significantly thicker and had thicker photoreceptor layers than the respective control retinas or untreated rd10 retinas until the last analysis time point, i.e. P56 (**FIG. *27***; **FIG. *28***a-d).

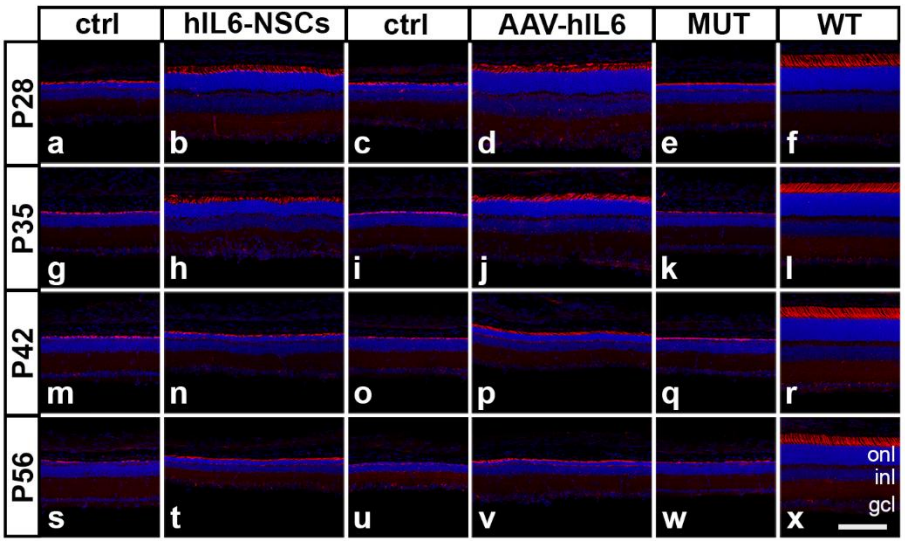

FIG. 27: hIL6 PROMOTES THE SURVIVAL OF PHOTORECEPTOR CELLS IN THE RETINA OF RD10 MICE. Representative images of retinal sections from animals treated with control-NSCs, hIL6-NSCs, AAVshH10-GFP, or AAVshH10-hIL6 and from age-matched MUT and untreated WT mice. Cone inner and outer segments were labelled with PNA. AAV: adeno-associated virus; ctrl: control; gcl: ganglion cell layer; GFP: green fluorescent protein; hIL6: hyper-interleukin-6; inl: inner nuclear layer; MUT: mutant (here: rd10); NSCs: neural stem cells; onl: outer nuclear layer; P: postnatal day; PNA: biotinylated peanut agglutinin; WT: wild-type. Scale bar: 100 µm.

Photoreceptor layers of retinas treated with hIL6-NSCs or AAVshH10-hIL6 were significantly thicker than the photoreceptor layers of control retinas at all ages analysed (**FIG. *28***c,d). Quantitative analysis revealed that the photoreceptor layer in 1-month-old animals treated with hIL6-NSCs was ~2-fold thicker than in control retinas. Retinas treated with AAVshH10-hIL6 were ~3.7-fold thicker than those treated with AAVshH10-GFP or age-matched rd10 mice. In 2-month-old animals, retinas treated with either hIL6-NSCs or AAVshH10-hIL6 were ~2-fold thicker than the contralateral control retinas.

Furthermore, there was no significant difference in the thickness of the photoreceptor layers between control retinas and age-matched MUT mice, with the only exception of NSC-treated rd10 mice at P28 (**FIG. *28***c,d). Labelling of cone inner and outer segments with PNA revealed similar densities of cones in hIL6-treated retinas, control retinas and untreated MUT and WT retinas at all ages analysed (***FIG. 27***).

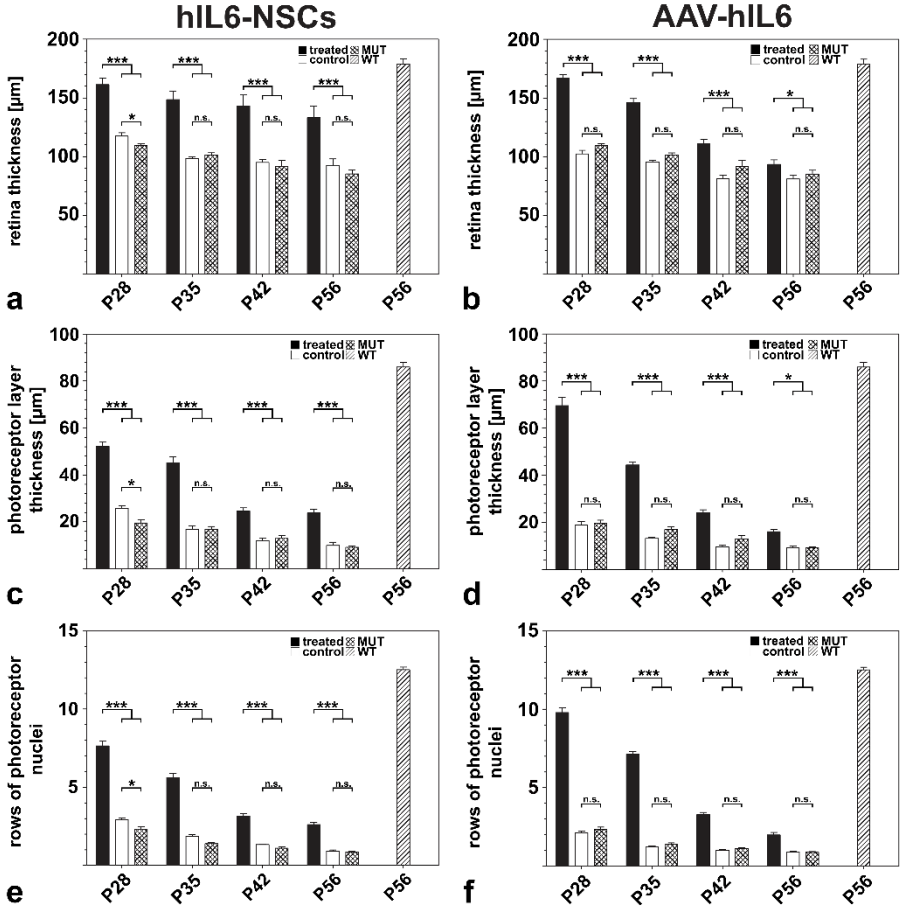

FIG. 28: QUANTITATIVE ANALYSIS OF RETINA AND PHOTORECEPTOR LAYER THICKNESS AND DETERMINATION OF THE NUMBER OF ROWS OF PHOTORECEPTOR NUCLEI IN THE RETINA OF RD10 MICE. Retina thickness (a,b), photoreceptor layer thickness (c,d) and the number of rows of photoreceptor nuclei (e,f) in retinas treated with hIL6-NSCs or AAVshH10-hIL6 (filled bars), control-NSCs or AAVshH10-GFP (open bars) and age-matched MUT mice (cross-hatched bars). Values from untreated 2-month-old WT mice (hatched bars) are shown as a reference. Each bar represents the mean ± SEM from eight retinas. *: $p<0.05$, ***: $p<0.001$, n.s.: not significant according to a two-way ANOVA followed by a Bonferroni post-hoc test. AAV: adeno-associated virus; hIL6: hyper-interleukin-6; MUT: mutant (here: rd10); NSCs: neural stem cells; P: postnatal day; WT: wild-type.

To examine the progression of rod photoreceptor degeneration, the number of rows of photoreceptor cell nuclei (RPN) was analysed. Throughout the examination period, rd10 retinas treated with hIL6 contained significantly more

RPN than the respective control retinas (***TAB. 15***). Importantly, retinas of 2-month-old rd10 mice treated with hIL6-NSCs contained ~2.8-fold more RPN than control retinas (***FIG. 28***e). Retinas treated with AAVshH10-hIL6 contained about ~2.2-fold more RPN than the contralateral control retinas or untreated MUT retinas (***Fig. 28***f). The strongest protective effect on rod photoreceptors was observed in 5-week-old animals. In these animals the onl of retinas treated with hIL6-NSCs containing ~3-fold more RPN and retinas treated with AAVshH10-hIL6 containing ~5.7-fold more RPN than the respective control retinas. In 1-month-old retinas, the neuroprotective effects of AAVshH10-hIL6 were more pronounced compared to those conferred by the hIL6-NSC clone as indicated by a greater photoreceptor layer thickness (AAVs: 69.6 ± 3.3 µm, NSCs: 52.2 ± 1.9 µm; $p<0.001$ according to a two-way ANOVA followed by Bonferroni post-hoc test) and a higher number of RPN (AAVs: 9.8 ± 0.3 RPN, NSCs: 7.6 ± 0.3 RPN; $p<0.001$ according to a two-way ANOVA followed by Bonferroni post-hoc test) (**FIG. 28**). Retinas of rd10 mice treated with AAVshH10-hIL6 were also thicker than retinas treated with hIL6-NSCs, however not significantly so (AAVs: 167.0 ± 2.6 µm, NSCs: 161.3 ± 5.0 µm). Retina thinning, photoreceptor layer thinning and photoreceptor degeneration progressed faster in retinas treated with AAVshH10-hIL6 than in retinas treated with hIL6-NSCs (**FIG. 28**). From P42 onward no significant differences in the examined parameters between retinas treated with AAVshH10-hIL6 and hIL6-NSCs were observed.

TAB. 15: THE NUMBER OF ROWS OF PHOTORECEPTOR NUCLEI IN RD10 KI RETINAS TREATED WITH HIL6-NSCS AND AAVSHH10-HIL6.

	AGE	RPN IN TREATED RETINAS	RPN IN CONTROL RETINAS[1]	FOLD-CHANGE COMPARED TO CONTROL
hIL6-NSCs	P28	7.6 ± 0.3	2.94 ± 0.1	**2.6**
	P35	5.6 ± 0.3	1.9 ± 0.1	**3.0**
	P42	3.2 ± 0.2	1.3 ± 0.03	**2.4**
	P56	2.6 ± 0.1	0.9 ± 0.07	**2.8**
AAVshH10-hIL6	P28	9.7 ± 0.3	2.1 ± 0.1	**4.6**
	P35	7.1 ± 0.2	1.2 ± 0.03	**5.7**
	P42	3.3 ± 0.1	1.0 ± 0.06	**3.3**
	P56	2.0 ± 0.1	0.9 ± 0.05	**2.2**

[1] for purposes of a clear depiction, data on the RPN of retinas treated with control-NSCs or AAVshH10-GFP was chosen for this table. For most treatment groups, except for 1-month-old animals treated with hIL6-NSCs, statistical analysis confirmed no significant differences between treated control retinas and untreated control retinas. AAVshH10: adeno-associated virus serotype shH10; hIL6: hyper-interleukin-6; NSC: neural stem cells; P: postnatal day; RPN: rows of photoreceptor nuclei.

4.2.5.2. hIL6 ATTENUATES PHOTORECEPTOR LOSS IN THE RETINA OF *Atp1b2*^{Atp1b1} KI MICE

Retina thickness was not significantly different between *β2/β1* ki retinas treated with hIL6-NSCs or AAVshH10-hIL6 and the respective control retinas or untreated MUT retinas at P56 and P84 (***FIG. 29***a,b). However, the photoreceptor layer of 2-month-old *β2/β1* ki mice treated with hIL6-NSCs or AAVshH10-hIL6 was significantly thicker than the photoreceptor layer in control retinas or untreated MUT retinas (***FIG. 29***c,d). This difference in photoreceptor layer thickness was no longer evident in 3-month-old animals (***FIG. 29***c,d).

Retinas treated with hIL6-NSCs or AAVshH10-hIL6 contained significantly more RPN than the control retinas (***FIG. 29****e,f*). On average, retinas of 2-month-old *β2/β1* ki mice treated with either hIL6-NSCs or AAVshH10-hIL6 contained ~8.4 RPN compared to ~5.3 RPN in control retinas and age-matched untreated MUT retinas (hIL6-NSCs: 8.3 ± 0.3 RPN, AAVshH10-hIL6: 8.6 ± 0.2 RPN; control retinas: 5.3 ± 0.1 RPN, MUT: 5.4 ± 0.1 RPN). Retinas of 3-month-old *β2/β1* ki mice contained ~7.6 RPN compared to ~5.2 RPN in control retinas and untreated retinas (hIL6-NSCs: 7.8 ± 0.2 RPN, AAVshH10-hIL6: 7.4 ± 0.2 RPN; control retinas: 5.1 ± 0.1 RPN; MUT: 5.3 ± 0.1). No differences in the number of photoreceptor nuclei were observed between retinas treated with control-NSCs or AAVshH10-GFP and age-matched MUT mice.

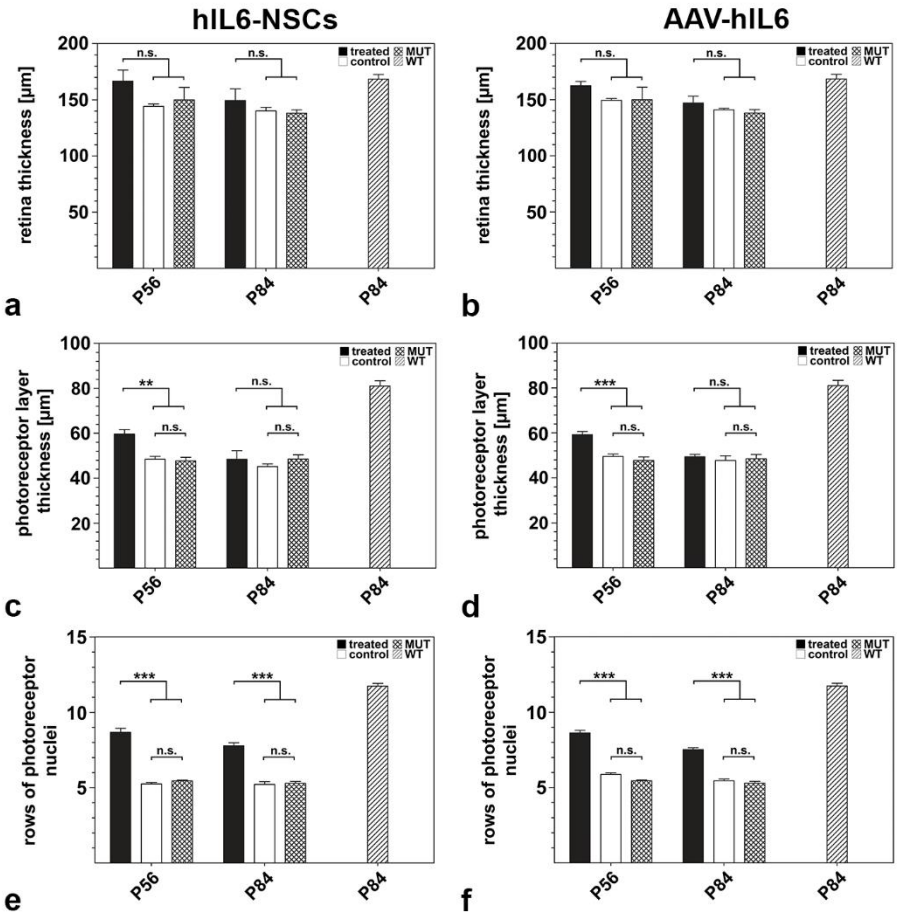

FIG. 29: QUANTITATIVE ANALYSIS OF RETINA AND PHOTORECEPTOR LAYER THICKNESS AND DETERMINATION OF THE NUMBER OF ROWS OF PHOTORECEPTOR NUCLEI IN THE RETINA OF *β2/β1* KI MICE. Analysis of retina thickness (a,b), photoreceptor layer thickness (c,d) and the number of rows of photoreceptor nuclei (e,f) in retinas treated with hIL6-NSCs or AAVshH10-hIL6 (filled bars), control-NSCs or AAVshH10-GFP (open bars) and age-matched MUT mice (cross-hatched bars). Values from untreated 3-month-old WT mice (hatched bars) are shown as a reference. Each bar represents the mean ± SEM from six retinas. **: p<0.01, ***: p<0.001, n.s.: not significant according to a two-way ANOVA followed by a Bonferroni post-hoc test. AAV: adeno-associated virus; hIL6: hyper-interleukin-6; MUT: mutant (here: *β2/β1* ki); NSCs: neural stem cells; P: postnatal day; WT: wild-type.

Since the *β2/β1* ki mouse exhibits a cone-rod dystrophy-like phenotype, the number of PNA-positive CIS in direct contact with the onl was determined (**FIG. 30**;***FIG. S11***). Retinas treated with hIL6 contained more PNA-positive CIS compared to controls and untreated age-matched MUTs. Specifically, retinas from 2-month-old animals contained ~2.7-fold more PNA-positive CIS (hIL6-NSCs: 61.5 ± 4.5 PNA-positive CIS/1000 µm; AAVshH10-hIL6: 58.0 ± 0.7 PNA-positive CIS/1000 µm) than control retinas (control-NSCs: 23.9 ± 2.1 PNA-positive CIS/1000 µm, AAVshH10-GFP: 20.9 ± 3.4 PNA-positive CIS/1000 µm) and ~3-fold more PNA-positive CIS than MUT retinas (20.0 ± 4.3 PNA-positive CIS/1000 µm). In 3-month-old *β2/β1* ki mice, retinas treated with hIL6-NSCs contained

~1.5-fold more PNA-positive CIS than the contralateral control retinas (hIL6-NSCs: 24.8 ± 2.0 PNA-positive CIS/1000 µm; control-NSCs: 15.9 ± 2.1 PNA-positive CIS/1000 µm). Retinas treated with AAVshH10-hIL6 contained ~2.6-fold more PNA-positive CIS than the control retinas (AAVshH10-hIL6: 47.3 ± 1.7 PNA-positive CIS/1000 µm; AAVshH10-GFP: 18.4 ± 2.2 PNA-positive CIS/1000 µm). In age-matched, untreated MUT retinas a similar number of PNA-positive CIS compared to retinas treated with control-NSCs or AAVshH10-GFP was observed (MUT: 18.5 ± 2.3 PNA-positive CIS/1000 µm; control-NSCs: 15.9 ± 2.1 PNA-positive CIS/1000 µm; AAVshH10-GFP: 18.4 ± 2.2 PNA-positive CIS/1000 µm). In comparison, retinas of WT mice contained 122.4 ± 0.9 PNA-positive CIS/1000 µm.

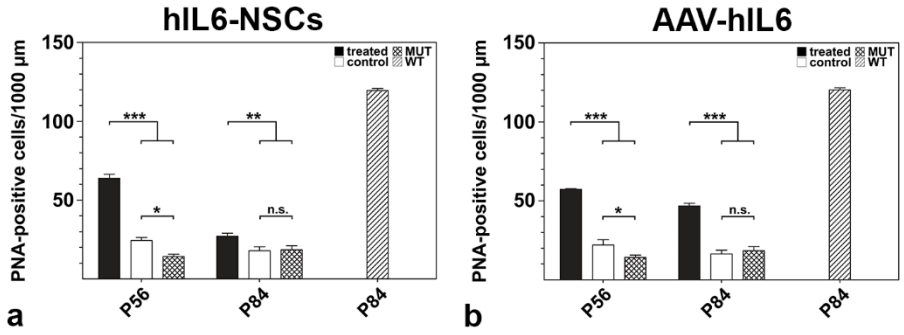

FIG. 30: HIL6 ATTENUATES CONE PHOTORECEPTOR LOSS IN THE RETINAS OF *β2/β1* KI MICE.
Quantitative analysis of PNA-positive cone inner segments in *β2/β1* ki retinas treated with hIL6-NSCs (a) or AAVshH10-hIL6 (b). Each bar represents the mean ± SEM from six retinas. Values from untreated 3-month-old WT mice (hatched bars) are shown as a reference. *: p<0.05; **: p<0.01, ***: p<0.001, n.s.: not significant according to two-way ANOVA followed by Bonferroni post-hoc test. AAV: adeno-associated virus; hIL6: hyper-interleukin 6; MUT: mutant (here: *β2/β1* ki); NSCs: neural stem cells; P: postnatal day; PNA: biotinylated peanut agglutinin; WT; wild-type.

4.2.6. HIL6 INFLUENCES THE EXPRESSION OF PROTEINS INVOLVED IN PHOTOTRANSDUCTION AND CELL SIGNALLING IN RD10 MICE

Cytokines such as CNTF, LIF and IL6 have been shown to downregulate proteins involved in phototransduction, such as RHO and CAR (Wen et al., 2006; Wen et al., 2008). Therefore, the expression of CAR in rd10 retinas treated with hIL6-NSCs and AAVshH10-hIL6 was examined by immunohistochemistry and Western blot analysis.

Qualitative analysis of CAR expression revealed that, compared to rd10 retinas treated with control-NSCs (***Fig. 31***Aa,g,m,s), AAVshH10-GFP (***Fig. 31***Ac,i,o,u) or untreated MUT (***Fig. 31***Ae,k,q,w) and WT retinas (***Fig. 31***Af,l,r,x), expression of CAR was downregulated in hIL6-treated retinas. The

downregulation of CAR appeared to progress until P35 (***Fig. 31***Ah,j), before expression levels stabilised until the last observation point at P56 (***Fig. 31***At,v).

Quantitative Western blot analysis confirmed a significant downregulation of CAR in hIL6-treated rd10 retinas (***Fig. 31***B). In 1-month-old retinas treated with AAVshH10-hIL6, expression of CAR was reduced by 84% when compared to AAVshH10-GFP or untreated rd10 retinas, and by 90% when compared to untreated WT retinas.

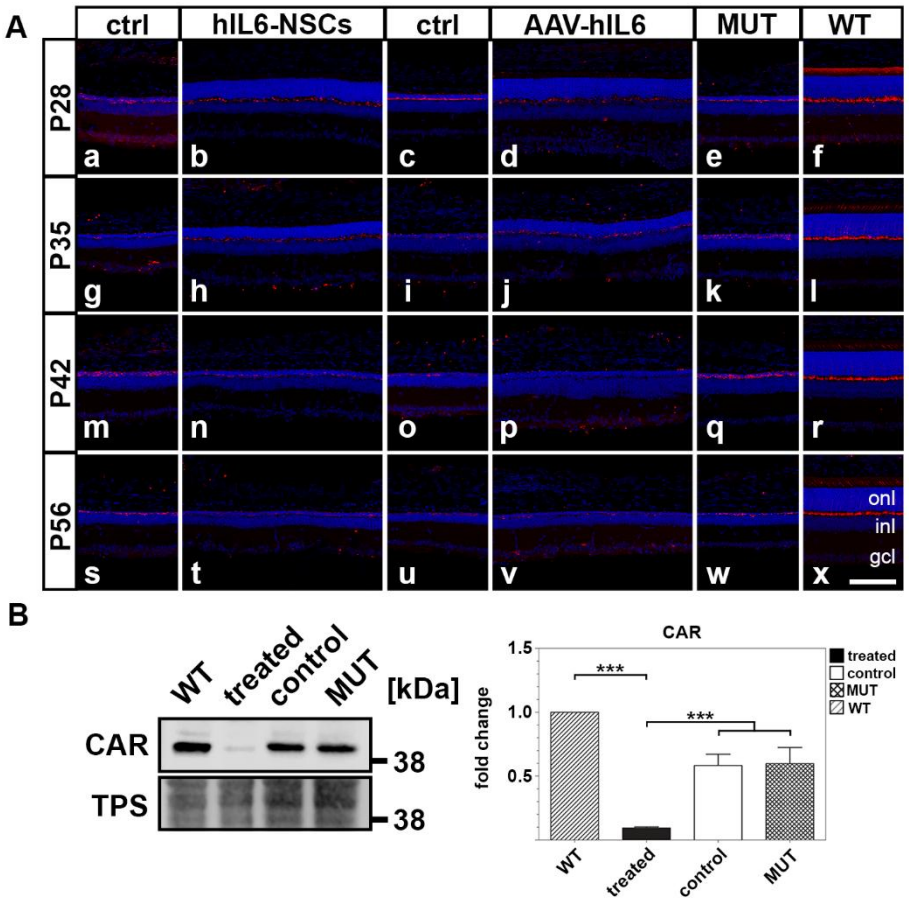

Fig. 31: hIL6 dysregulates the expression of cone-arrestin in rd10 mice.
(A) Immunohistochemical analysis of cone-arrestin (CAR) expression in retinas treated with control-NSCs, hIL6-NSCs. AAVshH10-GFP, AAVshH10-hIL6 as well as age-matched MUT and WT retinas. (B) Quantitative Western blot analysis of cone-arrestin expression in 1-month-old rd10 retinas treated with AAVshH10-hIL6 (filled bars) or AAVshH10-GFP (open bars) as well as untreated MUT (cross-hatched bars) and WT retinas (hatched bars). ***: $p<0.001$ according to a one-way ANOVA followed by Bonferroni post-hoc test. AAV: adeno-associated virus; gcl: ganglion cell layer; hIL6: hyper-interleukin-6; kDa: kilodalton; inl: inner nuclear layer; MUT: mutant (here: rd10 mice); NSCs: neural stem cells; onl: outer nuclear layer; P: postnatal day; TPS: total protein stain; WT: wild-type. Scale bar in Ax: 100 µm.

Cytokines, such as IL6, trigger the activation of the MAPK signalling pathway by phosphorylation of the kinase. Accordingly, levels of phosphorylated MAPK (pMAPK) were strongly increased in retinas of 1-month-old rd10 mice

treated with either hIL6-NSCs (***FIG. 32***Ab) or AAVshH10-hIL6 (***FIG. 32***Ad) compared to control retinas (***FIG. 32***Aa and c, respectively) or age-matched MUT (***FIG. 32***Ae) and WT retinas (***FIG. 32***Af). However, pMAPK levels in hIL6-treated retinas decreased with the increasing age of the animals (***FIG. 32***Ag-l).

Since IL6 does not only signal via the RAS/MAPK pathway but also via the JAK/STAT pathway, the expression of the phosphorylated signal transducer and activator of transcription 3 (pSTAT3) was analysed by quantitative Western blot analysis (***FIG. 32***B). Analysis of 1-month-old retinas treated with AAVshH10-hIL6 revealed a ~6-fold increase of pSTAT3 compared to AAVshH10-GFP and a ~7-fold increase compared to untreated MUT retinas. Compared to WT retinas, expression of pSTAT3 was increased ~58-fold in AAVshH10-hIL6 retinas and ~9-fold in control retinas and untreated MUT retinas (***FIG. 32***B).

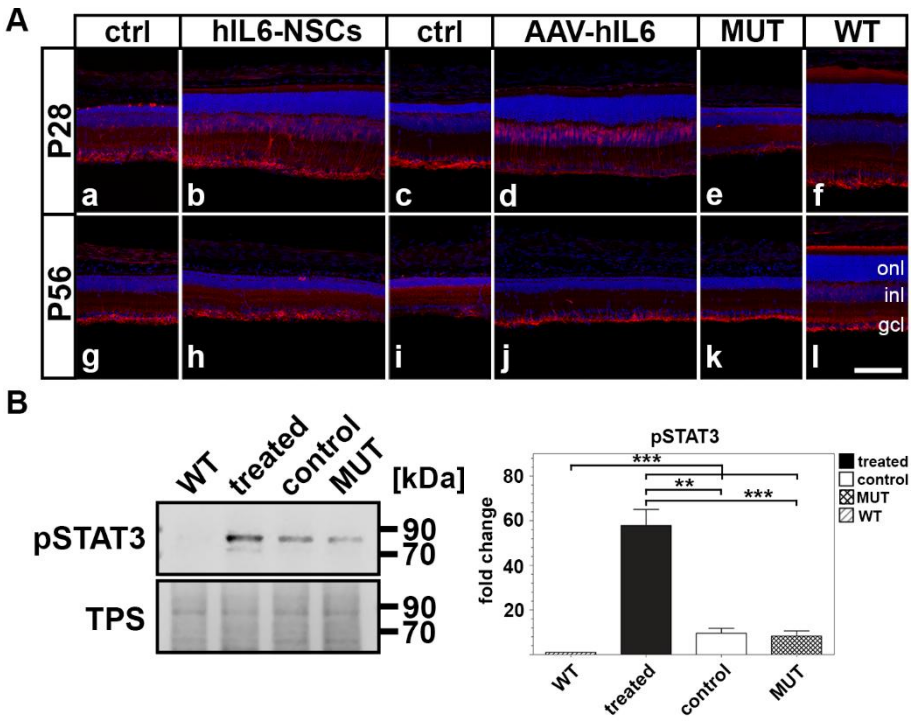

FIG. 32: TREATMENT OF RD10 RETINAS WITH HIL6-NSCS OR HIL6-AAVS STIMULATES INTRACELLULAR SIGNALLING.
(A) The effect of hIL6 on downstream signalling cascades was examined by analysing pMAPK expression in retinas treated with hIL6-NSCs or AAVshH10-hIL6, respective control retinas as well as age-matched untreated rd10 and WT retinas. (B) Quantitative Western blot analysis of pSTAT3 expression in 1-month-old AAVshH10-hIL6-treated retinas (filled bar), control retinas (open bars), untreated age-matched MUT (cross-hatched bars) and untreated WT retinas (hatched bars). **: $p<0.01$; ***: $p<0.001$ according to one-way ANOVA followed by a Bonferroni post-hoc test. AAV: adeno-associated virus; ctrl: control; gcl: ganglion cell layer; hIL6: hyper-interleukin-6; inl: inner nuclear layer; kDa: kilodalton; MUT: mutant (here: rd10); NSCs: neural stem cells; onl: outer nuclear layer; P: postnatal day; pMAPK: phospho p44/42 mitogen-activated protein kinase (Thr202/Tyr204); pSTAT3: phosphorylated signal transducer and activator of transcription 3 (Tyr705); TG: transgenic mice (here: rd10), TPS: total protein stain; WT: wild-type. Scale bar in AI: 100 µm.

5. DISCUSSION

5.1. PROJECT I: PROTECTION OF PHOTORECEPTOR CELLS WITH VARIOUS NEUROTROPHIC FACTORS IN A NOVEL MOUSE MODEL EXHIBITING A CONE-ROD DYSTROPHY-LIKE PHENOTYPE

5.1.1. PHOTORECEPTOR DEGENERATION IN THE *Atp1b2^{Atp1b1}* KI MOUSE

The *Atp1b2^{Atp1b1}* ki mouse (hereafter referred to as *β2/β1* ki mouse) (Weber et al., 1998) is a murine model exhibiting a cone-rod dystrophy-like phenotype with an early onset and rapid progression of photoreceptor degeneration. In this model, the β2-subunit of the sodium-potassium-ATPase (Na,K-ATPase or NKA) is replaced by the β1-subunit, resulting in a dysfunction of the vital enzyme. The dysfunction leads to the degeneration of photoreceptors, which normally express high levels of β2. Inner retinal cells, such as bipolar cells and retinal ganglion cells (RGCs) do not degenerate (Bartsch et al., 2025) (*cf.* **1.4.2. THE PHENOTYPE OF *ATP1B2ATP1B1 KNOCK-IN MICE***). The apoptosis of cone photoreceptors and later of rod photoreceptors observed in *β2/β1* ki mice is associated with a dysregulation of the cellular ion homeostasis caused by a reduced function and expression of the NKA. In the *β2/β1* ki mouse, transgenic *Atp1b1* transcripts amount to ~10-20% of *Atp1b2* transcripts found in wild-type mice (Weber et al., 1998).

A major function of the NKA is the transmembrane transport of sodium (Na^+) and potassium (K^+) ions (Contreras et al., 2024). Consequently, a dysfunction of the enzyme leads to the depletion of K^+, an intracellular accumulation of Na^+ and a subsequent membrane depolarisation, resulting in calcium ion (Ca^{2+}) accumulation and cytotoxicity (Yu, 2003). The ionic homeostasis is further disrupted by a reduced expression of the voltage-gated potassium channels $K_V2.1$ and $K_V8.2$, which have recently been shown to interact with the α3β2 isozyme expressed in photoreceptors (Bartsch et al., 2025; Schmid et al., 2022). $K_V2.1$ and $K_V8.2$ form heterotetrameric channels, located in the inner segments of murine photoreceptors. They, together with the NKA, carry a substantial part of the outward dark current (Fortenbach et al., 2021; Inamdar et al., 2021). Hence, the decreased expression of the K_V subunits associated with the genetically modified NKA likely contributes to the photoreceptor degeneration in the *β2/β1* ki mouse by aggravation of the ion imbalance (Fortenbach et al., 2021; Vierra et al., 2019). Of note, due to the impaired ionic homeostasis in the

photoreceptors and the subsequent lack of an outward dark current, a recording of ERGs in the *β2/β1* ki mouse is unattainable.

5.1.2. BENEFITS OF A SUSTAINED DELIVERY OF NEUROTROPHIC FACTORS

Cone-rod dystrophies are progressive in nature and require constant monitoring and treatment (reviewed in: Ben-Yosef (2022); Nebbioso et al. (2025)). However, most of the currently investigated treatments, such as the administration of recombinant neurotrophic factors, exhibit only short-term efficacy; for example, the half-life time of exogenous CNTF in the vitreous humour has been determined to be around one to three minutes (Dittrich et al., 1994; Kauper et al., 2012). Hence, treatment requires a frequent application of therapeutics, putting an immense burden on patient and attending physician. To reduce this burden, novel treatment strategies should allow for a sustained delivery of therapeutics.

In this project, a non-causative therapeutic approach was chosen, which aimed to promote photoreceptor survival in the *β2/β1* ki mouse by means of intravitreal delivery of different neurotrophic factors (NTFs). For the intravitreal delivery, a stem cell-based approach was chosen, allowing for a sustained delivery of the NTFs over a prolonged period.

The generated clonal NSC lines stably expressed CNTF, GDNF (both characterised earlier, *cf*. Dulz et al. (2020); Flachsbarth et al. (2018); Hu et al. (2025)), LIF or PGRN over a prolonged period of time *in vitro* and differentiated into astrocytes and neurons *in vitro* and into astrocytes *in vivo* (Dulz et al., 2020; Hu et al., 2025). CNTF, CNTF/GDNF, LIF and PGRN attenuated the loss of photoreceptors for up to 3.5 months after intravitreal application of the NSCs. No neuroprotective effect of GDNF on photoreceptors was observed in the *β2/β1* ki mouse.

5.1.3. NEUROINFLAMMATION IN *Atp1b2*^{Atp1b1} KI RETINAS TREATED WITH NTF-NSCS

To determine the extent of inflammation induced by the examined NTFs, expression of the inflammation markers GFAP, IBA1 and CD68 was analysed by immunohistochemistry. Retinas treated with the pro-inflammatory CNTF and LIF (Leibinger, Andreadaki, et al., 2013; Xue et al., 2011), as well as retinas treated

with CNTF/GDNF-NSCs, exhibited an increased expression of all inflammation markers, indicating the presence of reactive astrogliosis and reactive microgliosis in these retinas. In retinas treated with the anti-inflammatory GDNF (Duarte Azevedo et al., 2020) alone or PGRN, which can act both pro-inflammatory and anti-inflammatory (Amado et al., 2010; Arrant et al., 2018; Cui et al., 2019; Zhu et al., 2002; Zin et al., 2021), only the expression of GFAP was increased. This increase in expression of GFAP in the otherwise inconspicuous GDNF- and PGRN-treated retinas can be attributed to

(i) the ongoing degeneration of photoreceptors, which is associated with an increase in neuroinflammation in neurodegeneration in general and in the *β2/β1* ki mouse (Bartsch et al., 2025) specifically, and
(ii) the injection of the NSCs themselves, which have been shown to contribute to neuroinflammation in both unmodified and modified state (Wei et al., 2021).

Along this line, part of the elevated GFAP expression in retinas treated with CNTF-, CNTF/GDNF- and LIF-NSCs can be attributed to the neurodegeneration and the intravitreal injections of the NSCs as well. Additionally, in these treated retinas, the extent of reactive astrogliosis increased with age, due to the continued exposure of the retinas to the exogenous, pro-inflammatory cytokines.

Inflammation has been identified to play an important role in neuroprotection in several studies (Andries et al., 2023; Leibinger, Andreadaki, et al., 2013; London et al., 2011; Prinz et al., 2021; Rashid et al., 2019; Xue et al., 2011). However, the degree of inflammation and its duration are important factors to consider in neuroprotection. Chronic inflammation, as it occurs in neurodegenerative diseases such as Alzheimer's disease, Parkinson's disease or amyotrophic lateral sclerosis (ALS), is associated with a pathological activation of microglia and an excessive upregulation of pro-inflammatory factors, such as interleukin-1β (IL1β), IL6, interleukin-12 (IL12), tumor necrosis factor α (TNFα) or inducible nitric oxide synthase (iNOS) (Calsolaro & Edison, 2016; Twarowski & Herbet, 2023). The upregulation of these factors results in tissue damage and the worsening of symptoms in neurodegenerative diseases (Gupta et al., 2003; Gupta et al., 2018; Rashid et al., 2018; Zhao et al., 2015). Acute inflammation, on the other hand, has been associated with the promotion of neuroprotection and

axon regeneration (Andries et al., 2023; Bellver-Landete et al., 2019; Gupta et al., 2018; Rashid et al., 2018).

Most IBA1-positive microglia found in the NTF-treated retinas were distributed evenly across the entire tissue in their resident, ramified state, in which they monitor the tissue and maintain homeostasis. Comparatively few microglia were observed in the subretinal space in an activated, amoeboid state, in which they can secrete endogenous cytokines, trophic factors and different cytotoxic substances such as proteases and free radicals (Hailer, 2008; Hanisch, 2002; Rashid et al., 2019). Although the overall number of IBA1-positive cells in the retina of 4-month-old animals treated with CNTF-, CNTF/GDNF- or LIF-NSCs, decreased, a higher proportion of amoeboid microglia was observed in the subretinal space. In contrast, the number of IBA1-positive cells in retinas treated with GDNF-, PGRN- or control-NSCs was stable throughout the observation period. Although the neuroprotective effect decreased with increasing age, treatment with CNTF, CNTF/GDNF and LIF was still effective in promoting photoreceptor survival in these older animals, indicating that the chronic inflammation has not affected the retina negatively.

Nevertheless, it is important to keep in mind, that this so-called M1/M2 polarisation model, distinguishing between beneficial effects of ramified microglia and detrimental effects of amoeboid microglia is highly simplified (Mosmann et al., 1986; Ransohoff, 2016). Recent studies have suggested a much greater heterogeneity of microglia, their function being dependent on the central nervous system region, sex or disease (Noh et al., 2025). Accordingly, although the observations made here fit the polarisation model, to fully determine the role of the activated microglia in this specific scenario, further investigations into their molecular make-up are needed.

5.1.4. PHOTORECEPTOR LOSS IS ATTENUATED BY TREATMENT WITH NTF-NSCS

Since the *β2/β1* ki mouse exhibits a cone-rod dystrophy-like phenotype, the impact of the examined neurotrophic factors on the photoreceptor degeneration is of special interest in the assessment of the neuroprotective effect. The effect on rod photoreceptor survival was assessed by measurement of the photoreceptor layer thickness and the quantification of the rows of photoreceptor nuclei (RPN). As Bartsch et al. (2025) have shown, the rod photoreceptor

degeneration becomes significant at postnatal day (P) 56. The degeneration of cone photoreceptors becomes significant as early as P14, with almost no cones remaining at P112.

In dystrophic *β2/β1* ki retinas treated with CNTF-, CNTF/GDNF-, or LIF-NSCs the degeneration of photoreceptors was slowed down significantly. The outer nuclear layer (onl) of the NTF-treated *β2/β1* ki retinas contained about ~1.5-fold more RPN than those of control retinas until P112 indicating a slowing of rod photoreceptor degeneration. Importantly, CNTF-, CNTF/GDNF- and LIF-treated retinas contained up to 3-fold more cone photoreceptors than the corresponding control retinas. This is congruent with findings in other animal models of retinal degeneration when treated with these NTFs (Jankowiak et al., 2015; Jung et al., 2013; LaVail et al., 1992; LaVail et al., 1998).

As described before (*cf.* **1.6.1. CNTF**), CNTF was one of the first, and possibly the best studied, cytokines to be described exerting a neuroprotective effect on photoreceptors (Bok et al., 2002; LaVail et al., 1992; LaVail et al., 1998; Li et al., 2010; McGill et al., 2007; Rhee et al., 2007; Wen et al., 1998; Wen et al., 2012) and has been shown to be an putative treatment for different human retinal degenerations in early clinical studies (Chew et al., 2019; Chew et al., 2015; Sieving et al., 2006; Talcott et al., 2011; Zhang et al., 2011). In the *β2/β1* ki mouse model a strong neuroprotective effect of both rod and cone photoreceptors was observed until the latest observation point in 4-month-old animals, 3.5 months after application of the cytokine.

Part of the observed neuroprotective effect of CNTF might be mediated through the ability of CNTF to signal in *trans* via the soluble isoform of its specific receptor CNTF receptor α (CNTFRα). This ability vastly expands the cytokines putative range to cells which might not express CNTFRα such as photoreceptors. To this date it is highly disputed, whether CNTFRα is expressed on photoreceptors (Beltran et al., 2005; Hertle et al., 2008; Rhee & Yang, 2003) or on Müller cells, horizontal cells, amacrine cells and RGCs (Kirsch et al., 1997; Wahlin et al., 2004). If CNTFRα is expressed on Müller cells, but not photoreceptors, part of the observed neuroprotective effect of CNTF is possibly mediated indirectly through trans-signalling. However, Rhee et al. (2013) have

shown, that gp130 activation in Müller cells is required for CNTF-mediated photoreceptor protection.

As described in detail earlier, ENCELTO™ (Neurotech), an encapsulated cell therapy (ECT) device using genetically modified RPE cells expressing CNTF, was recently approved by the FDA for use in MacTel patients (*cf*. **1.3.2. ENCAPSULATED CELL THERAPY**). Although a reduction of photoreceptor loss in the ellipsoid zone area was observed in patients receiving the treatment, an improvement in the best corrected visual acuity (BCVA) was not observed (Chew et al., 2025). In earlier phase I and phase II clinical studies, the ECT device was shown to prevent cell death of cone photoreceptors in retinitis pigmentosa and Usher syndrome type 2 (Talcott et al., 2011) and improve BCVA (Sieving et al., 2006; Zhang et al., 2011). Despite positive outcomes of these trials, therapy with the ENCELTO™ device was not deemed successful in phase III clinical trials in either retinitis pigmentosa, Usher syndrome type 2, ischemic optic neuropathy, achromatopsia. Examination of the effect on retinal ganglion cell survival in glaucoma patients is still underway (NCT04577300).

Studies examining the effect of a combinatorial neuroprotective treatment by simultaneous application of CNTF- and GDNF-NSCs in an optic nerve crush model have found a synergistic effect of the two neurotrophic factors on the survival of the axotomized retinal ganglion cells (Dulz et al., 2020; Flachsbarth et al., 2018; Hu et al., 2025). The synergistic neuroprotective effect of CNTF and GDNF is likely mediated by the activation of different pro-survival signalling pathways by each factor alone and the enhancement of pro-survival signalling pathways common to both factors. Furthermore, a more effective activation of indirect neuroprotective pathways of both NTFs simultaneously might also contribute to the synergistic effects on the lesioned ganglion cells. For instance, both factors have been shown to induce the expression of other NTFs in Müller cells (Dulz et al., 2020; Flachsbarth et al., 2018; Hu et al., 2025). In order to examine whether both NTFs exert a synergistic effect on photoreceptors as well, a co-application of both CNTF and GDNF was performed.

In contrast to axotomized retinal ganglion cells in the optic nerve crush model, CNTF and GDNF had no synergistic effect on the survival of photoreceptor cells in the *β2/β1* ki mouse. On the contrary, the co-application of

CNTF- and GDNF-NSCs resulted in a slightly reduced efficacy compared to the treatment with CNTF-NSCs alone. This might be a consequence of the reduced number of CNTF-NSCs in the CNTF/GDNF cell suspension (~3.8×10^5 cells instead of ~7.6×10^5 cells applied intravitreally) in combination with the failure of GDNF-NSCs to exert a neuroprotective effect on the photoreceptors (see below).

Another NTF exhibiting promising, although often short lived, neuroprotective effects in animal models of retinitis pigmentosa (RP), retinal ischemia, glaucoma and diabetic retinopathy (DR) is LIF (Agca & Grimm, 2014; Dong et al., 2024; Frigg et al., 2005; Lange et al., 2010; LaVail et al., 1998; Lv et al., 2023; McColm et al., 2006; Yang et al., 2018). Nonetheless, as of date, and to the best of our knowledge, no clinical trials examining the efficacy and the safety of LIF for the treatment of neurodegenerative disorders have been performed.

LIF likely exerts its neuroprotective effect on photoreceptors in a similar fashion as CNTF, as both cytokines mainly signal through a similar combination of receptors, namely LIFRβ and gp130 (*cf.* **1.6.1. CNTF** and **1.6.3. LIF**). Both cytokines activate the JAK/STAT signalling pathway and the RAS/MAPK signalling pathway (Boulton et al., 1994; Bürgi et al., 2009; Heinrich et al., 2003; Joly et al., 2008; Oh et al., 1998; Stahl & Yancopoulos, 1994; Ueki et al., 2008).

Even though CNTF and LIF exert strong neuroprotective effects on both rod and cone photoreceptors in the retina of *β2/β1* ki mice, they also have been shown to diminish photoreceptor function, both in animal models and patients (Birch et al., 2013; Bok et al., 2002; Chucair-Elliott et al., 2012; Liang et al., 2001; Schlichtenbrede et al., 2003; Wen et al., 2006; Wen et al., 2008; Wen et al., 2012), due to the aforementioned downregulating effect on several proteins of the visual cascade (*cf.* **1.6.1. CNTF**) (Li et al., 2018; McGill et al., 2007). However, the downregulation of proteins of the phototransduction cascade, such as rhodopsin, arrestin and the α subunit of transducin, GNAT1, might be somewhat beneficial to photoreceptors, especially regarding their energy consumption (Country, 2017; Warrant, 2009) and protection from oxidative stress. A downregulation of these proteins has been shown to cause desensitisation of photoreceptors, protecting them from light damage. The desensitisation results in the shortening of cone and rod outer segments, similar to the light-induced shortening of outer segments

observed in animal models of light damage (Wen et al., 2006; Wen et al., 2008). Rod outer segment (ROS) disks have to be renewed constantly (~10%/day), which is highly energy intensive. Hence, less photoreceptor disks have to be replaced in the shortened ROS, and the energy costs of the replacement are massively reduced. This might contribute to the protection of photoreceptors and might be of great advantage in the *β2/β1* ki mouse model in which the homeostasis of ions and energy is perturbed (Bosch et al., 1993; LaVail, 1976, 1980). Further investigation would be needed to elucidate this hypothesis.

In contrast to retinas treated with CNTF-NSCs, CNTF/GDNF-NSCs or LIF-NSCs, PGRN-NSCs only attenuated both rod and cone photoreceptor loss in 2-month-old animals. However, although PGRN was not able to attenuate the loss of rod photoreceptors in older animals, the degeneration of cone photoreceptors was slowed considerably. In contrast to retinas treated with the other NTFs, which saw a decline in the number of PNA-positive cones around ~30-60% of cone photoreceptors between P56 and P112, the number of PNA-positive cones in retinas treated with PGRN was relatively stable. The mean difference in the number of PNA-positive cones between retinas of 2-month-old and 4-month-old animals treated with PGRN-NSCs was only ~15%. This indicates PGRN to be the most effective in slowing the progression of cone photoreceptor degeneration out of the examined NTFs.

Tsuruma et al. (2014) proposed that the activation of cyclic AMP-responsive element-binding protein (CREB) via the protein kinase C (PKC) signalling pathway mediates the neuroprotective effect of PGRN in a light damage model. It is also plausible that the neuroprotective effect of PGRN in the *β2/β1* ki mouse might be mediated, in addition to the activation of the JAK/STAT and PI3K/AKT pathway (Cui et al., 2019; Paushter et al., 2018), by its interaction with the Wnt/β-catenin signalling pathway and the neurogenic locus notch homolog proteins (Notch)-signalling, which both have been implicated in regenerative effects in the nervous system and cell survival (Altmann et al., 2016; Kuse et al., 2016; Osakada et al., 2007; Tanaka et al., 2019; Xiao et al., 2014). However, the putative regenerative effects of the Wnt/β-catenin signalling pathway and the Notch signalling pathway have been shown to be relatively short lived (Kuse et al., 2016; Osakada et al., 2007).

Furthermore, the anti-inflammatory properties of PGRN (Kessenbrock et al., 2008; Tanaka et al., 2019) limit an endogenous cytokine release from microglia and consequently, the exertion of additional neuroprotective effects via the activation of the very same cells. Anti-inflammatory effects of PGRN are mediated by its interaction with tumor necrosis factor receptor (TNFR), death receptor 3 (DR3), sortilin (SORT1) and pro-low-density lipoprotein receptor-related protein 1 (LRP1), which are all associated with lysosomal activity (Cui et al., 2019; Hu et al., 2010; Paushter et al., 2018).

A number of, albeit often small, neuroprotective effects of GDNF on photoreceptors have been described in a number of models, utilising various delivery methods (Andrieu-Soler et al., 2005; Buch et al., 2006; Dalkara et al., 2011; Del Río et al., 2011; Dong et al., 2007; García-Caballero et al., 2018; Gregory-Evans et al., 2009; Hauck et al., 2006; Kucharska et al., 2014; McGee Sanftner et al., 2001; Ohnaka et al., 2012; Shahin et al., 2023; Wang et al., 2010; Wong et al., 2016). However, observed effects were either relatively short lived (Allocca et al., 2007; Andrieu-Soler et al., 2005; Wong et al., 2016; Wu et al., 2002) or the observed effect size was relatively small (Andrieu-Soler et al., 2005; Frasson et al., 1999; García-Caballero et al., 2018; McGee Sanftner et al., 2001; Ohnaka et al., 2012; Touchard et al., 2012; Wang et al., 2010; Wong et al., 2016) and functional benefits were often absent. Some studies only examined a small number of animals (Dalkara et al., 2011; Lawrence et al., 2004).

No neuroprotective effect of GDNF on photoreceptors was observed in *β2/β1* ki mice. One limiting factor is the expression of GFRα and RET in the retina only on RGCs and Müller cells (Delyfer et al., 2005; Mahato & Sidorova, 2020), restricting the impact of GDNF to an indirect effect on the photoreceptor cells. And while trans-signalling of GDNF via the soluble isoform of GDNF family receptor α1 (sGFR1α1) is possible, this too is restricted by the expression of the co-receptor rearranged during transfection (RET), which is restricted in its localisation (Paratcha et al., 2001). Additionally, an indirect neuroprotective effect might also be conferred by activation of glial L-glutamate/L-aspartate transporter (GLAST) (Delyfer et al., 2005). The effect of GDNF on GLAST was not examined in this study.

Furthermore, one might speculate that the insufficient neuroprotective effect of GDNF in this particular mouse model comes down to a dysregulation of Ca^{2+}-homeostasis, due to the lack of proper function of the NKA (Yu, 2003). GDNF, and especially the binding of the GDNF-GFRα1-complex to RET, was shown to be highly dependable on proper regulation of Ca^{2+} in the intracellular environment, due to Ca^{2+} being necessary to induce autophosphorylation of RET (Anders et al., 2001; Lundborg et al., 2011; Mahato & Sidorova, 2020; Nozaki et al., 1998). Further experiments would be needed to further elucidate this hypothesis.

Additionally, the neuroprotective effect of GDNF has been shown to be dose dependent. While Lipinski et al. (2011) found that recombinant human GDNF (rhGDNF) only exerts an effect at high doses (200 ng/ml) in retina explants of *Rho*$^{-/-}$ mice, Touchard et al. (2012) reported adverse effects of their rGDNF-vector on photoreceptor layer thickness and inner segments after sustained release of 66.7 ± 8.1 pg/24h in the dystrophic Royal College of Surgeon's (RCS) rat model of RP. Overall, reported doses of GDNF in used in studies reporting positive neuroprotective effects in different models were relatively low, often in the low nanogram or even picogram range (Allocca et al., 2007; Andrieu-Soler et al., 2005; Frasson et al., 1999; Gamm et al., 2007; Gregory-Evans et al., 2009; Lawrence et al., 2004; Touchard et al., 2012; Wu et al., 2002). On the other hand, the GDNF-NSCs described here secreted up to 156.4 ± 4.8 ng GDNF/10^5 cells/24h *in vitro* (Flachsbarth et al., 2018) with 7.6×10^5 cells being intravitreally injected. Though the intravitreal concentration of GDNF could not be determined, the secreted amount of GDNF in this setup might be too high to exert neuroprotective effects on photoreceptors. The same NSCs clone used here was previously shown to protect axotomized RGCs from degeneration in multiple independent studies (Dulz et al., 2020; Flachsbarth et al., 2018; Hu et al., 2025).

5.2. PROJECT II: HYPER-IL6 ATTENUATES PHOTORECEPTOR LOSS IN AN AUTOSOMAL-RECESSIVE RETINITIS PIGMENTOSA AND A CONE-ROD DYSTROPHY MOUSE MODEL

5.2.1. THE DESIGNER CYTOKINE HYPER-IL6 AS A NEUROTROPHIC FACTOR

The designer cytokine hyper-IL6 (hIL6), consisting of human IL6 covalently bound to its soluble receptor sIL6Rα by a flexible peptide linker, allows for the direct activation of the ubiquitously expressed signal transducer gp130 (Fischer, 2017; Fischer et al., 1997; Leibinger et al., 2016; Rose-John, 2020; Taga & Kishimoto, 1997). Indeed, the expression of gp130 on any given cell has been shown to be about 10-20 times higher than the expression of IL6Rα (Peters et al., 1998). This direct interaction of hIL6 and gp130 should allow for a stronger neuroprotective effect compared to IL6 alone, as gp130 is expressed on all cells except granulocytes (Calabrese & Rose-John, 2014; Hibi et al., 1990; Saito et al., 1992; Wilkinson et al., 2018). Furthermore, hIL6 is 10- to 100-fold more active, and was retained for longer periods of time in blood plasma of intraperitoneally injected mice than IL6, contributing to its stronger biological activity (Peters et al., 1998; Peters et al., 1996). This prolonged plasma half-life of the designer cytokine was attributed to a reduced degradation or internalisation of hIL6 due to its size, resulting in a less efficient plasma clearance (Peters et al., 1998; Peters et al., 1996). Indeed, hIL6 effectively promoted neurite outgrowth of adult RGCs and dorsal root ganglion (DRG) neurons *in vitro*, exhibited significant neuroprotective effects on injured RGCs and promoted axon regeneration of axotomized RGCs *in vivo* (Leibinger et al., 2016). The neuroprotective effects were increased in Phosphatase and Tensin Homolog knock-out (ko) ($PTEN^{-/-}$) mice, due to an inhibition of cytokine supressing signalling in this mutant (Allan et al., 1990; Park et al., 2009; Park et al., 2008; P. D. Smith et al., 2009; Sun et al., 2011). Considering these results, hIL6 is a promising candidate drug for neuroprotection in animal models of photoreceptor degeneration. To test this hypothesis, the neuroprotective effects of intravitreally injected hIL6-NSCs and AAVshH10-hIL6 were examined in rd10 mice and *β2/β1* ki mice. To the best of our knowledge, to date no studies on the neuroprotective effect of hIL6 on photoreceptors have been published.

5.2.2. AAVS AS A VECTOR FOR SUSTAINED CYTOKINE DELIVERY

hIL6-NSCs and AAVshH10-hIL6 and appropriate control NSCs and AAVs were intravitreally injected into rd10 and *β2/β1* ki mice prior to the onset of the retinal dystrophy. Characterisation of the hIL6-NSCs confirmed proper expression of the hIL6 transgene in undifferentiated cells and in *in vitro* differentiated astrocytes and neurons. hIL6 was also expressed in intravitreally grafted hIL6-NSCs, which attached to the posterior pole of the lens and differentiated into astrocytes in both rd10 mice and *β2/β1* ki mice.

Additionally, the transduction efficiency of AAVsH10-hIL6 and AAVshH10-GFP was analysed. The shH10 serotype was selected for experiments due to its pronounced tropism for Müller cells and high transduction efficiency (Gonzalez-Cordero et al., 2018; Klimczak et al., 2009; Pellissier et al., 2014). And indeed, Müller cells in the retina of rd10 mice and *β2/β1* ki mice and additionally RGCs in *β2/β1* ki mice, were successfully transduced with high efficiency by both AAVshH10-hIL6 and AAVshH10-GFP. Of note, although both rd10 mice and *β2/β1* ki mice were treated with the same AAV vector at the same age (P9), the observed transduction efficiency was higher in retinas of *β2/β*1 ki mice than in retinas of rd10 mice. Like stem cells, AAVs are a well-established tool for the application of therapeutics in animal models for the development of treatment strategies for various neurodegenerative diseases. AAVs allow for a sustained release of nucleic acids or proteins with relatively low safety risks compared to other viral vectors such as adenoviral or lentiviral vectors (Klimczak et al., 2009). They possess a relatively low immunogenicity compared to adenoviruses (Mays et al., 2014; Naso et al., 2017) and do not integrate in the genome as frequent as lentiviruses (Chen et al., 2020; Jüttner et al., 2019). AAVs are therefore considered one of the safest viral vehicles for gene therapy (Naso et al., 2017).

5.2.3. HIL6 PROMOTES NEUROINFLAMMATION IN THE RETINA

IL6 is deemed one of the most important pro-inflammatory cytokines (Kishimoto, 2005). The pleiotropic protein is involved in a plethora of physiological and pathological processes, from development, homeostasis and regulation of lipid, glucose and iron metabolism, to the maturation of cells such as megakaryocytes and the specific differentiation of naïve $CD4^+$ T cells (reviewed in: Millrine et al. (2022); Omodaka et al. (2014)). The most important function of

IL6, however, is its role in inflammation, inducing acute phase proteins, acting as an alert system for the immune system, and activating multiple pro-inflammatory signalling pathways (Heinrich et al., 1990; Kishimoto et al., 1992).

The pro-inflammatory properties of IL6, and consequently of hIL6, are reflected in the massive upregulation of the inflammation markers GFAP, IBA1 and CD68 in the retinas of rd10 mice and *β2/β1* ki mice treated with either hIL6-NSCs or AAVshH10-hIL6. The elevated GFAP expression in untreated rd10 mice and *β2/β1* ki mice can be attributed to the inflammation induced by the degeneration of photoreceptors in these mouse models, whereas the GFAP expression in retinas treated with control-NSCs or AAVshH10-GFP is further elevated compared to untreated controls due to the treatment itself (*cf.* **5.1.3. NEUROINFLAMMATION IN *ATP1B2ATP1B1* KI RETINAS TREATED WITH NTF-NSCS** and Wei et al. (2021)). Most IBA1-positive microglia cells in hIL6-treated rd10 and *β2/β1* ki retinas were distributed across the retina in their ramified state, rather than in their amoeboid state located in the subretinal space. This indicates an acute inflammation which has not yet become chronic. Furthermore, an increased number of CD68-positive macrophages, for which IL6 is a chemoattractant (Kobayashi & Mizisin, 2000), was observed in addition to elevated levels of GFAP and IBA1. Additionally, part of the neuroinflammation in the retinas treated with hIL6 can also be ascribed to the fact that an exogenous human protein was injected, which, in itself, triggers an immune response (reviewed in: Chaplin (2010)).

Of note, the neuroinflammation in hIL6-treated rd10 retinas subsided rather than increased with increasing age of the animals. The observed decrease in neuroinflammation might be the result of a desensitisation of cells caused by several regulating mechanisms, restricting the extend and duration of the hIL6 signalling (Jones & Jenkins, 2018; Peters et al., 1996). A dysregulated gp130 activation is associated with pathophysiological consequences on the homeostasis of the immune system and subsequent susceptibility to infection, among others. Multiple mechanisms might contribute to a negative regulation of IL6:

(i) internalisation of gp130 or its ligands (e.g. IL6), but not IL6Rα (Heinrich et al., 2003)

(ii) the deactivation of receptors and signalling intermediates (e.g. different STAT proteins) by protein tyrosine phosphatases (Stark & Darnell, 2012)

(iii) translational repression and degradation of mRNAs encoding cytokines and cytokine receptors via micro RNAs (miRNA) (Villarino et al., 2017) and

(iv) induction of cytokine inhibitors (e.g. protein inhibitor of activated STAT (PIAS), suppressor of cytokine signalling (SOCS)) by STAT (Yoshimura et al., 2007).

In the context of the role of IL6 in the immune system, the applied dose of hIL6 should be carefully considered, as an excessive application of the cytokine has the potential to trigger unwanted adverse effects (Chen et al., 2019; Ferreros & Trapero, 2022; Li et al., 2024; Maude & Barrett, 2016; Mehta et al., 2020; Nasonov & Samsonov, 2020; Rose-John et al., 2023; Tanaka et al., 2014; Waage et al., 1989; Wang et al., 2020; Wu & McGoogan, 2020; F. Zhou et al., 2020). However, the immunologic privilege and separation of the eye from the cardiovascular system by the BRB (Brent, 1990; Streilein, 1999; Streilein et al., 2000) might be an effective protection from such adverse effects of high doses of hIL6.

5.2.4. hIL6 attenuates photoreceptor loss in a retinitis pigmentosa and a cone-rod dystrophy mouse model

Retinas of rd10 and *β2/β1* ki mice treated with hIL6-NSCs or AAVshH10-hIL6 contained significantly more photoreceptors than retinas treated with control-NSCs or AAVshH10-GFP and retinas of untreated rd10 and *β2/β1* ki mice.

For the evaluation of the neuroprotective effect of hIL6 on photoreceptors in rd10 mice the number of rows of photoreceptor nuclei (RPN) in the outer nuclear layer is of special interest, since it is a measure for the number of rods, which represent ~97% of all photoreceptors in the retina (Jeon et al., 1998). Rod photoreceptors are the first to degenerate in this model of autosomal-recessive retinitis pigmentosa. Cone photoreceptors, on the other hand, degenerate relatively late in the disease progression and are largely unaffected within the examination period of the present study. Indeed, at P60 the last remaining photoreceptors found in the retina have been determined to be cone

photoreceptors. Some cone photoreceptors are still being viable in 9-month-old animals (Barhoum et al., 2008; Gargini et al., 2007).

Rd10 retinas, treated with hIL6-NSCs contained about 3-fold more and rd10 retinas treated with AAVshH10-hIL6 contained about 5-fold more photoreceptor nuclei than control retinas, respectively. Although the hIL6 treatment did not stop retinal degeneration in this mouse model, it was slowed down considerably. In the oldest examined animals (P56), the onl contained ~2.6 RPN in hIL6-NSCs treated retinas and ~2.0 RPN in AAVshH10-hIL6 treated retinas, compared to a single row of photoreceptor nuclei attributable to the remaining cone photoreceptors in control retinas. In contrast, the number of rod photoreceptors in control retinas was already strongly reduced in 1-month-old animals. At P28, retinas treated with control-NSCs contained ~2.9 rows of photoreceptor nuclei, retinas treated with AAVshH10-GFP contained ~2.2 rows of photoreceptor nuclei. hIL6-treated retinas of 1-month-old rd10 mice, on the other hand, contained 7.6 rows of photoreceptor nuclei when treated with hIL6-NSCs and 9.7 rows of photoreceptor nuclei when treated with AAVshH10-hIL6.

Photoreceptor loss in *β2/β1* ki mice treated with hIL6-NSCs and AAVshH10-hIL6 was attenuated for up to three months, as evidenced by a higher number of RPN and PNA-positive cones, when compared to control retinas. Retinas of 2-month-old animals treated with hIL6 contained ~1.6-fold more RPN and 2.7-fold more PNA-positive cones. Retinas of 3-month-old animals contained ~1.5-fold more RPN and ~1.5-fold more PNA-positive cones.

The neuroprotective effect of hIL6 is likely mediated mainly by two mechanisms:

(i) the activation of pro-survival signalling pathways such as the JAK/STAT pathway, the PI3K/AKT pathway and the RAS/MAPK pathway (Heinrich et al., 2003) and

(ii) the activation of astrocytes and Müller cells and the subsequent secretion of additional cytokines and growth factors by the glia cells (Rashid et al., 2019).

However, as described before (cf. **5.2.1. THE DESIGNER CYTOKINE HYPER-IL6 AS A NEUROTROPHIC FACTOR**), studies on the effect of hIL6 on RGCs in WT and PTEN$^{-/-}$ ONC models suggest, that the designer cytokine does not achieve its full

putative neuroprotective effect in mice with normal PTEN expression. PTEN, together with SOCS3, is one of the prime regulators of the negative feedback loops in cytokine signalling. In mice with a RGC specific conditional PTEN knock-out treated with hIL6, phosphorylation of AKT was found to be much stronger than in WT mice, suggesting a dampened effect of hIL6 in the presence of PTEN (Leibinger et al., 2016).

Nonetheless, if hIL6 application is also beneficial for visual function remains to be determined. The application of exogenous cytokine, such as CNTF and LIF, was shown in multiple studies to be detrimental for visual function (Birch et al., 2013; Bok et al., 2002; Chucair-Elliott et al., 2012; Liang et al., 2001; Schlichtenbrede et al., 2003; Wen et al., 2006; Wen et al., 2008; Wen et al., 2012). In accordance with these findings, expression of cone-arrestin (CAR) in the retina of 1-month-old rd10 mice treated with AAVshH10-hIL6 was down-regulated by ~84% compared to expression in untreated rd10 mice. Compared to wild-type mice CAR was down-regulated by ~90%.

5.2.5. hIL6 INFLUENCES THE EXPRESSION OF PROTEINS INVOLVED IN MAJOR SIGNALLING CASCADES IN RD10 MICE

Immunohistochemical and Western blot analysis of rd10 mice treated with hIL6 revealed massive upregulation of both pMAPK and pSTAT3, respectively. Although pMAPK expression in 2-month-old animals was decreased from levels observed in 1-month-old animals, data suggests a sustained activation of the RAS/MAPK pathway in retinas treated with hIL6-NSCs or AAVshH10-hIL6. Expression of pMAPK was mostly restricted to the inner endfeet and somata of Müller cells and a few astrocytes located in the inner retina. These observations are in accordance with the expression patterns found previously in retinas treated with hIL6 or CNTF (Leibinger et al., 2016; Muller et al., 2009). Expression of pMAPK appears to be slightly increased in retinas treated with hIL6-NSCs compared to those treated with AAVshH10-hIL6.

Likewise, the upregulation of pSTAT3 in hIL6-treated retinas by 58-fold compared to WT demonstrates a strong activation of the JAK/STAT pathway. Interesting in this context is the apparent dichotomy found in the functional redundancy of IL6-related cytokines through the activation of the common signal transducer gp130 and the subsequent activation of common signalling pathways

on one hand (Tanaka et al., 2014), and the heterogeneity of STAT signalling on the other hand (Villarino et al., 2017). Although multiple cytokines can activate the same STAT proteins, their observed downstream effect can vary widely. IL6 and IL10, for example, share STAT3 as a common primary signalling target, but exhibit pro-inflammatory and anti-inflammatory properties, respectively. This discrepancy can be explained by differences in duration and intensity of the STAT3 signalling as well as the additional activation of auxiliary STATs and the activation of different sets of genes (Hirahara et al., 2015; O'Shea & Murray, 2008; Wan et al., 2015).

pSTAT3-expression was also increased 9.5-fold in the retinas of 1-month-old rd10 mice treated with AAVshH10-GFP and 8.3-fold in in retinas of untreated, age-matched rd10 mice. This increase is likely induced by the increased neuroinflammation observed in these retinas and caused by the endogenous expression of cytokines induced by the ongoing photoreceptor degeneration alone (untreated rd10) or in combination with the treatment itself (rd10 retinas treated with AAVshH10-GFP). The increase in expression of pSTAT3, in combination with the increase in expression of pMAPK, might explain the increased photoreceptor layer thickness and number of RPN found in retinas of 1-month-old rd10 mice treated with hIL6-NSCs.

Taken together the results demonstrate that a cell-based or AAV-mediated administration of the cytokine hIL6 promotes the survival of rod photoreceptors in a murine model of autosomal-recessive retinitis pigmentosa and in a murine model of an autosomal-dominant cone-rod dystrophy. To the best of our knowledge, this is the first study demonstrating the neuroprotective effect of hIL6 on photoreceptor cells.

5.3. GENERAL REMARKS

Due to the overall low prevalence of IRDs, with retinitis pigmentosa affecting only 1/4,000 people (Hamel, 2006) and cone-rod dystrophies affecting 1/40,000 people (Hamel, 2007), their heterogeneous aetiology, and the notion that the causative genetic mutation is often unknown, it is highly difficult to develop specific treatment options for each malady. Therefore, the development of mutation-independent, broader approaches, not treating the causative mutation, but rather attempting to promote the survival of the affected retinal cell types, represents a promising strategy for the development of treatment of such rare diseases. Results of the present thesis demonstrate that a sustained delivery of different neuroprotective factors using lentivirally modified stem cells or gene therapy effectively rescues rod and cone photoreceptor cells from cell death in two mouse models of IRDs.

5.3.1. DISEASES ASSOCIATED WITH NKA DYSFUNCTION

As described before (*cf.* **1.4.1.3. DISEASES RELATED TO MUTATIONS IN THE NKA**), several diseases are associated with mutations in the different NKA subunits, particularly in *ATP1A1*, *ATP1A2*, and *ATP1A3*. Until recently the only condition described to be caused by a dysfunction of the NKA and affecting the visual system was the cerebella ataxia, areflexia, pes cavus, optic atrophy, sensorineural hearing loss (CAPOS) syndrome, which is caused by a mutation in the *ATP1A3* gene. However, recently a novel form of an autosomal-dominant cone-rod dystrophy was described in a family with a heterozygous missense mutation (c.1772A>T, p. D591V) in exon 13 of the *ATP1A3* gene (G. H. Zhou et al., 2020). The study has additionally analysed a transgenic mouse line that ubiquitously expressed the same *ATP1A3* mutation. The mice exhibited a normal retinal morphology and retinal function for up to three months. ERG recordings in 12-month-old animals, however, revealed significantly reduced a-wave amplitudes under photopic conditions, indicating an impaired cone function. These findings support the notion that cones are more severely affected in rods by a NKA dysfunction, as is the case in the *β2/β1* ki mouse model.

5.3.2. MANAGEMENT OF DISEASES AND OTHER TREATMENT OPTIONS

Due to the relatively low risk profile of encapsulated cell therapy and gene therapy using AAVs, these treatment options are the most widely explored for the treatment of various IRDs. However, to date only two therapies, the cell-based ENCELTO™ (Neurotech) and the AAV-based gene replacement therapy Luxturna (Novartis) have been approved by EMA and FDA for use in patients.

In addition to intraocular administration of therapeutics using a cell-based or AAVs-mediated approach, other forms of delivery systems are being explored. An example are nanoparticles made from biocompatible, biodegradable polymers containing lipophilic drug molecules. In nanoparticles a number of properties, such as solubility, target structure in the retina and cellular uptake, among others can be customised to be adapted to specific needs, for example to alter their spreading behaviour in the vitreous. However, nanoparticles tend to have low encapsulation capacity and poor drug release. These problems can be mitigated by enveloping nanoparticles in so-called hydrogels serving as secondary carriers (Ham et al., 2023).

Other ways of intraocular drug delivery include small refillable eye implants, so-called port delivery systems, subretinal injections of therapeutics and suprachoroidal injections, which allow for the injection of larger molecules, up to 70 kDa, directly to the retina through the choroid. Topical and systemic drug applications can also be suitable delivery strategies, though these do not allow for a sustained delivery of therapeutics (Ham et al., 2023). Additionally, other treatment options, such as cell replacement using pluripotent stem cells, e.g. embryonal stem cells (ESCs) or induced pluripotent stem cells (iPSCs), or optogenetic approaches, sometimes in combination with extraocular devices, are being examined (Lu & Pan, 2021; Sahel et al., 2021; Schneider et al., 2022; Singh et al., 2020).

Due to the potentially wide applicability of the neuroprotective approach examined in the present thesis, the treatments described here might be conferred to other, non-hereditary retinal dystrophies, such as age-related macular degeneration (AMD) or diabetic retinopathy (DR). While one clinical study examined the effect of CNTF in patients with AMD (NCT00447954), to the best of our knowledge no pre-clinical or clinical study is underway to examine the

effect of CNTF, GDNF, LIF, PGRN or hIL6 in other non-hereditary retinal dystrophies.

Considering the low number of treatment options for IRDs approved worldwide, some suggestions on management options have been made. Common suggestions include the protection of eyes from bright light by wearing dark or tinted glasses to protect the retina from photodamage, and thus slowing down the degeneration of photoreceptors, or to reduce photophobia by using orange- or magenta-tinted glasses (Georgiou et al., 2021; Hamel, 2006; Khaparde et al., 2024). Concomitant symptoms such as myopia, cataracts or other complications should be corrected. In some cases, a vitamin A supplementation has been shown to be beneficial by slowing down degeneration, but should be avoided in IRDs caused by mutations in *ABCA4*, such as Stargardt disease (Georgiou et al., 2021; Hamel, 2006). Vitamin A intake enhances the visual cycle and subsequent accumulation of bis-retinoid N-retinyl-N-retinylidene ethanolamine (A2E), which disturbs lysosomal function and promotes accumulation of cytotoxic substances (Allikmets, 2007; Holz et al., 1999; Mata et al., 2000) For diseases with photoreceptor degeneration due to cGMP accumulation (e.g. in COD with *GUCA1A* mutations), some clinicians suggest sleeping with lights on to prevent cGMP accumulation during the night, which causes photoreceptor damage in these diseases (Georgiou et al., 2021; Gill et al., 2019). Additionally, as IRDs can be quite restrictive in day-to-day life, patients should receive help coping with the disease in form of mobility training or psychological support.

5.3.3. CONCLUSION AND FUTURE PROSPECTS

In conclusion, the results presented in this thesis demonstrate that the neurotrophic factors CNTF, LIF, PGRN and hIL6 are suitable agents to promote photoreceptor survival in the *Atp1b2*^{Atp1b1} ki (*β2/β1* ki) mouse, a novel mouse model of a cone-rod dystrophy, and in the *Pde6b*^{rd10} (rd10) mouse, a mouse model of an autosomal-recessive retinitis pigmentosa. In eyes treated with the neurotrophic factors, retinas retained significantly more rod and/or cone photoreceptors than control retinas for a prolonged period. The neuroprotective effects were likely mediated by the activation of pro-survival pathways like the JAK/STAT pathway or the RAS/MAPK pathway, as well as by the additional release of endogenous cytokines induced by inflammation. Of note, more surviving photoreceptors were observed in retinas with a higher degree of neuroinflammation, underlining the importance of neuroinflammation in the mediation of pro-survival effects on photoreceptors.

Importantly, both the cell-based treatment as well as the AAV-mediated approach might be applicable in a clinical context. Neurotrophic factors can be continuously delivered to retina using the so-called “encapsulated cell technology”. This technology uses genetically modified cells that are enclosed in capsules made from biocompatible, semi-permeable membranes and implanted into the vitreous cavity of the patients. The neurotrophic factors expressed by the encapsulated cells can diffuse into the vitreous fluid and subsequently into the dystrophic retinas. The method has been proven to be relatively safe and allows the removal of the capsules in case of complications. An approved gene therapy for RPE65-associated retinopathies and numerous ongoing clinical trials using AAVs to express therapeutics in a variety of retinal disorders indicate that an AAV-based delivery of neuroprotective factors to dystrophic retinas can also be transferred to clinical applications. However, to the best of our knowledge, to date no clinical trials examining the neuroprotective effect of neurotrophic factors on photoreceptors using an AAV-mediated approach have been undertaken.

Taken together, the present work has demonstrated that a sustained application of CNTF, LIF, PGRN or hIL6 attenuates photoreceptor loss in animal models of two different retinal dystrophies. Contrary to some other studies, a significant neuroprotective effect of GDNF on photoreceptors was not observed.

6. References

Adams, S. E., Purkiss, A. G., Knowles, P. P., Nans, A., Briggs, D. C., Borg, A., Earl, C. P., Goodman, K. M., Nawrotek, A., Borg, A. J., McIntosh, P. B., Houghton, F. M., Kjær, S., & McDonald, N. Q. (2021). A two-site flexible clamp mechanism for RET-GDNF-GFRα1 assembly reveals both conformational adaptation and strict geometric spacing. *Structure*, *29*(7), 694-708.e697. https://doi.org/https://doi.org/10.1016/j.str.2020.12.012

Ader, M., Schachner, M., & Bartsch, U. (2004). Integration and differentiation of neural stem cells after transplantation into the dysmyelinated central nervous system of adult mice. *Eur J Neurosci*, *20*(5), 1205-1210. https://doi.org/10.1111/j.1460-9568.2004.03577.x

Agca, C., Boldt, K., Gubler, A., Meneau, I., Corpet, A., Samardzija, M., Stucki, M., Ueffing, M., & Grimm, C. (2015). Expression of leukemia inhibitory factor in Müller glia cells is regulated by a redox-dependent mRNA stability mechanism. *BMC Biol*, *13*, 30. https://doi.org/10.1186/s12915-015-0137-1

Agca, C., & Grimm, C. (2014). Leukemia inhibitory factor signaling in degenerating retinas. *Adv Exp Med Biol*, *801*, 389-394. https://doi.org/10.1007/978-1-4614-3209-8_49

Agte, S., Junek, S., Matthias, S., Ulbricht, E., Erdmann, I., Wurm, A., Schild, D., Käs, J. A., & Reichenbach, A. (2011). Müller glial cell-provided cellular light guidance through the vital guinea-pig retina. *Biophys J*, *101*(11), 2611-2619. https://doi.org/10.1016/j.bpj.2011.09.062

Airaksinen, M. S., & Saarma, M. (2002). The GDNF family: signalling, biological functions and therapeutic value. *Nat Rev Neurosci*, *3*(5), 383-394. https://doi.org/10.1038/nrn812

Allan, E. H., Hilton, D. J., Brown, M. A., Evely, R. S., Yumita, S., Metcalf, D., Gough, N. M., Ng, K. W., Nicola, N. A., & Martin, T. J. (1990). Osteoblasts display receptors for and responses to leukemia-inhibitory factor. *J Cell Physiol*, *145*(1), 110-119. https://doi.org/10.1002/jcp.1041450116

Allikmets, R. (2007). Stargardt Disease. In J. Tombran-Tink & C. J. Barnstable (Eds.), *Retinal Degenerations: Biology, Diagnostics, and Therapeutics* (pp. 105-118). Humana Press. https://doi.org/10.1007/978-1-59745-186-4_5

Allocca, M., Di Vicino, U., Petrillo, M., Carlomagno, F., Domenici, L., & Auricchio, A. (2007). Constitutive and AP20187-induced Ret activation in photoreceptors does not protect from light-induced damage. *Invest Ophthalmol Vis Sci*, *48*(11), 5199-5206. https://doi.org/10.1167/iovs.07-0140

Almeida, S., Zhou, L., & Gao, F.-B. (2011). Progranulin, a Glycoprotein Deficient in Frontotemporal Dementia, Is a Novel Substrate of Several Protein Disulfide Isomerase Family Proteins. *PLoS One*, *6*(10), e26454. https://doi.org/10.1371/journal.pone.0026454

Alonzi, T., Fattori, E., Lazzaro, D., Costa, P., Probert, L., Kollias, G., De Benedetti, F., Poli, V., & Ciliberto, G. (1998). Interleukin 6 Is Required for the Development of Collagen-induced Arthritis. *Journal of Experimental Medicine*, *187*(4), 461-468. https://doi.org/10.1084/jem.187.4.461

Alsaloum, M., Labau, J. I. R., Sosniak, D., Zhao, P., Almomani, R., Gerrits, M., Hoeijmakers, J. G. J., Lauria, G., Faber, C. G., Waxman, S. G., & Dib-Hajj, S. (2021). A novel gain-of-function sodium channel β2 subunit mutation in idiopathic small fiber neuropathy. *Journal of Neurophysiology*, *126*(3), 827-839. https://doi.org/10.1152/jn.00184.2021

Altmann, C., Vasic, V., Hardt, S., Heidler, J., Häussler, A., Wittig, I., Schmidt, M. H. H., & Tegeder, I. (2016). Progranulin promotes peripheral nerve regeneration and reinnervation: role of notch signaling. *Mol Neurodegener*, *11*(1), 69. https://doi.org/10.1186/s13024-016-0132-1

Amado, D., Mingozzi, F., Hui, D., Bennicelli, J. L., Wei, Z., Chen, Y., Bote, E., Grant, R. L., Golden, J. A., Narfstrom, K., Syed, N. A., Orlin, S. E., High, K. A., Maguire, A. M., & Bennett, J. (2010). Safety and efficacy of subretinal readministration of a viral vector in large animals to treat congenital blindness. *Sci Transl Med*, *2*(21), 21ra16. https://doi.org/10.1126/scitranslmed.3000659

Anders, J., Kjær, S., & Ibáñez, C. F. (2001). Molecular Modeling of the Extracellular Domain of the RET Receptor Tyrosine Kinase Reveals Multiple Cadherin-like Domains and a Calcium-binding Site*. *Journal of Biological Chemistry*, *276*(38), 35808-35817. https://doi.org/https://doi.org/10.1074/jbc.M104968200

Andries, L., Kancheva, D., Masin, L., Scheyltjens, I., Van Hove, H., De Vlaminck, K., Bergmans, S., Claes, M., De Groef, L., Moons, L., & Movahedi, K. (2023). Immune stimulation recruits a subset of pro-regenerative macrophages to the retina that promotes axonal

regrowth of injured neurons. *Acta Neuropathol Commun*, *11*(1), 85. https://doi.org/10.1186/s40478-023-01580-3

Andrieu-Soler, C., Aubert-Pouëssel, A., Doat, M., Picaud, S., Halhal, M., Simonutti, M., Venier-Julienne, M. C., Benoit, J. P., & Behar-Cohen, F. (2005). Intravitreous injection of PLGA microspheres encapsulating GDNF promotes the survival of photoreceptors in the rd1/rd1 mouse. *Mol Vis*, *11*, 1002-1011. http://www.molvis.org/molvis/v11/a120/v11a120-andrieu-soler.pdf

Antonicek, H., Persohn, E., & Schachner, M. (1987). Biochemical and functional characterization of a novel neuron-glia adhesion molecule that is involved in neuronal migration. *J Cell Biol*, *104*(6), 1587-1595. https://doi.org/10.1083/jcb.104.6.1587

Aplin, C., & Cerione, R. A. (2024). Probing the mechanism by which the retinal G protein transducin activates its biological effector PDE6. *Journal of Biological Chemistry*, *300*(2). https://doi.org/10.1016/j.jbc.2023.105608

Arrant, A. E., Onyilo, V. C., Unger, D. E., & Roberson, E. D. (2018). Progranulin Gene Therapy Improves Lysosomal Dysfunction and Microglial Pathology Associated with Frontotemporal Dementia and Neuronal Ceroid Lipofuscinosis. *The Journal of Neuroscience*, *38*(9), 2341-2358. https://doi.org/10.1523/jneurosci.3081-17.2018

Arshavsky, V. Y., Lamb, T. D., & Pugh, E. N., Jr. (2002). G proteins and phototransduction. *Annu Rev Physiol*, *64*, 153-187. https://doi.org/10.1146/annurev.physiol.64.082701.102229

Arshavsky, V. Y., & Wensel, T. G. (2013). Timing Is Everything: GTPase Regulation in Phototransduction. *Investigative Ophthalmology & Visual Science*, *54*(12), 7725-7733. https://doi.org/10.1167/iovs.13-13281

Askvig, J. M., & Watt, J. A. (2015). The MAPK and PI3K pathways mediate CNTF-induced neuronal survival and process outgrowth in hypothalamic organotypic cultures. *J Cell Commun Signal*, *9*(3), 217-231. https://doi.org/10.1007/s12079-015-0268-8

Atiskova, Y., Bartsch, S., Danyukova, T., Becker, E., Hagel, C., Storch, S., & Bartsch, U. (2019). Mice deficient in the lysosomal enzyme palmitoyl-protein thioesterase 1 (PPT1) display a complex retinal phenotype. *Sci Rep*, *9*(1), 14185. https://doi.org/10.1038/s41598-019-50726-8

Austin, L., & Burgess, A. W. (1991). Stimulation of myoblast proliferation in culture by leukaemia inhibitory factor and other cytokines. *J Neurol Sci*, *101*(2), 193-197. https://doi.org/10.1016/0022-510x(91)90045-9

Barcroft, L. C., Moseley, A. E., Lingrel, J. B., & Watson, A. J. (2004). Deletion of the Na/K-ATPase alpha1-subunit gene (Atp1a1) does not prevent cavitation of the preimplantation mouse embryo. *Mech Dev*, *121*(5), 417-426. https://doi.org/10.1016/j.mod.2004.04.005

Barhoum, R., Martínez-Navarrete, G., Corrochano, S., Germain, F., Fernandez-Sanchez, L., de la Rosa, E. J., de la Villa, P., & Cuenca, N. (2008). Functional and structural modifications during retinal degeneration in the rd10 mouse. *Neuroscience*, *155*(3), 698-713. https://doi.org/10.1016/j.neuroscience.2008.06.042

Bartsch, S., Atiskova, Y., Schlichting, S., Becker, E., Herrmann, M., & Bartsch, U. (2025). Atp1b2Atp1b1 Knock-In Mice Exhibit a Cone–Rod Dystrophy-Like Phenotype. *Cells*, *14*(12), 878. https://www.mdpi.com/2073-4409/14/12/878

Bassetto, M., Kolesnikov, A. V., Lewandowski, D., Kiser, J. Z., Halabi, M., Einstein, D. E., Choi, E. H., Palczewski, K., Kefalov, V. J., & Kiser, P. D. (2024). Dominant role for pigment epithelial CRALBP in supplying visual chromophore to photoreceptors. *Cell Reports*, *43*(5), 114143. https://doi.org/https://doi.org/10.1016/j.celrep.2024.114143

Bauer, S., & Patterson, P. H. (2006). Leukemia inhibitory factor promotes neural stem cell self-renewal in the adult brain. *J Neurosci*, *26*(46), 12089-12099. https://doi.org/10.1523/JNEUROSCI.3047-06.2006

Bellver-Landete, V., Bretheau, F., Mailhot, B., Vallières, N., Lessard, M., Janelle, M. E., Vernoux, N., Tremblay, M., Fuehrmann, T., Shoichet, M. S., & Lacroix, S. (2019). Microglia are an essential component of the neuroprotective scar that forms after spinal cord injury. *Nat Commun*, *10*(1), 518. https://doi.org/10.1038/s41467-019-08446-0

Beltran, W. A., Rohrer, H., & Aguirre, G. D. (2005). Immunolocalization of ciliary neurotrophic factor receptor alpha (CNTFRalpha) in mammalian photoreceptor cells. *Mol Vis*, *11*, 232-244. https://www.ncbi.nlm.nih.gov/pubmed/15827545

http://www.molvis.org/molvis/v11/a27/v11a27-beltran.pdf

Ben-Yosef, T. (2022). Inherited Retinal Diseases. *Int J Mol Sci*, *23*(21). https://doi.org/10.3390/ijms232113467

Benarroch, E. E. (2011). Na⁺, K⁺-ATPase. *Neurology*, *76*(3), 287-293. https://doi.org/doi:10.1212/WNL.0b013e3182074c2f

Biondo, E. D., Spontarelli, K., Ababioh, G., Méndez, L., & Artigas, P. (2021). Diseases caused by mutations in the Na+/K+ pump α1 gene ATP1A1. *American Journal of Physiology-Cell Physiology*, *321*(2), C394-C408. https://doi.org/10.1152/ajpcell.00059.2021

Birch, D. G., Weleber, R. G., Duncan, J. L., Jaffe, G. J., & Tao, W. (2013). Randomized trial of ciliary neurotrophic factor delivered by encapsulated cell intraocular implants for retinitis pigmentosa. *Am J Ophthalmol*, *156*(2), 283-292.e281. https://doi.org/10.1016/j.ajo.2013.03.021

Blanco, G., & Mercer, R. W. (1998). Isozymes of the Na-K-ATPase: heterogeneity in structure, diversity in function. *Am J Physiol*, *275*(5), F633-650. https://doi.org/10.1152/ajprenal.1998.275.5.F633

Bocksteins, E. (2016). Kv5, Kv6, Kv8, and Kv9 subunits: No simple silent bystanders. *Journal of General Physiology*, *147*(2), 105-125. https://doi.org/10.1085/jgp.201511507

Bocksteins, E., & Snyders, D. J. (2012). Electrically Silent Kv Subunits: Their Molecular and Functional Characteristics. *Physiology*, *27*(2), 73-84. https://doi.org/10.1152/physiol.00023.2011

Bok, D., Yasumura, D., Matthes, M. T., Ruiz, A., Duncan, J. L., Chappelow, A. V., Zolutukhin, S., Hauswirth, W., & LaVail, M. M. (2002). Effects of adeno-associated virus-vectored ciliary neurotrophic factor on retinal structure and function in mice with a P216L rds/peripherin mutation. *Exp Eye Res*, *74*(6), 719-735. https://doi.org/10.1006/exer.2002.1176

Bosch, E., Horwitz, J., & Bok, D. (1993). Phagocytosis of outer segments by retinal pigment epithelium: phagosome-lysosome interaction. *J Histochem Cytochem*, *41*(2), 253-263. https://doi.org/10.1177/41.2.8419462

Boulanger, M. J., Chow, D. C., Brevnova, E. E., & Garcia, K. C. (2003). Hexameric structure and assembly of the interleukin-6/IL-6 alpha-receptor/gp130 complex. *Science*, *300*(5628), 2101-2104. https://doi.org/10.1126/science.1083901

Boulton, T. G., Stahl, N., & Yancopoulos, G. D. (1994). Ciliary neurotrophic factor/leukemia inhibitory factor/interleukin 6/oncostatin M family of cytokines induces tyrosine phosphorylation of a common set of proteins overlapping those induced by other cytokines and growth factors. *J Biol Chem*, *269*(15), 11648-11655. https://www.sciencedirect.com/science/article/pii/S0021925819781745?via%3Dihub

Brent, L. (1990). Immunologically privileged sites. In *Pathophysiology of the blood-brain barrier* (pp. 383-402). Elsevier Amsterdam.

Buch, P. K., MacLaren, R. E., Duran, Y., Balaggan, K. S., MacNeil, A., Schlichtenbrede, F. C., Smith, A. J., & Ali, R. R. (2006). In contrast to AAV-mediated Cntf expression, AAV-mediated Gdnf expression enhances gene replacement therapy in rodent models of retinal degeneration. *Mol Ther*, *14*(5), 700-709. https://doi.org/10.1016/j.ymthe.2006.05.019

Bürgi, S., Samardzija, M., & Grimm, C. (2009). Endogenous leukemia inhibitory factor protects photoreceptor cells against light-induced degeneration. *Mol Vis*, *15*, 1631-1637. https://pmc.ncbi.nlm.nih.gov/articles/PMC2728564/pdf/mv-v15-1631.pdf

Cairns, N. J., Bigio, E. H., Mackenzie, I. R., Neumann, M., Lee, V. M., Hatanpaa, K. J., White, C. L., 3rd, Schneider, J. A., Grinberg, L. T., Halliday, G., Duyckaerts, C., Lowe, J. S., Holm, I. E., Tolnay, M., Okamoto, K., Yokoo, H., Murayama, S., Woulfe, J., Munoz, D. G.,…Mann, D. M. (2007). Neuropathologic diagnostic and nosologic criteria for frontotemporal lobar degeneration: consensus of the Consortium for Frontotemporal Lobar Degeneration. *Acta Neuropathol*, *114*(1), 5-22. https://doi.org/10.1007/s00401-007-0237-2

Calabrese, L. H., & Rose-John, S. (2014). IL-6 biology: implications for clinical targeting in rheumatic disease. *Nat Rev Rheumatol*, *10*(12), 720-727. https://doi.org/10.1038/nrrheum.2014.127

Calsolaro, V., & Edison, P. (2016). Neuroinflammation in Alzheimer's disease: Current evidence and future directions. *Alzheimers Dement*, *12*(6), 719-732. https://doi.org/10.1016/j.jalz.2016.02.010

Carter-Dawson, L. D., & LaVail, M. M. (1979). Rods and cones in the mouse retina. I. Structural analysis using light and electron microscopy. *J Comp Neurol*, *188*(2), 245-262. https://doi.org/10.1002/cne.901880204

Cenik, B., Sephton, C. F., Dewey, C. M., Xian, X., Wei, S., Yu, K., Niu, W., Coppola, G., Coughlin, S. E., Lee, S. E., Dries, D. R., Almeida, S., Geschwind, D. H., Gao, F.-B., Miller, B. L., Farese, R. V., Posner, B. A., Yu, G., & Herz, J. (2011). Suberoylanilide Hydroxamic Acid

(Vorinostat) Up-regulates Progranulin Transcription: RATIONAL THERAPEUTIC APPROACH TO FRONTOTEMPORAL DEMENTIA*. *Journal of Biological Chemistry*, *286*(18), 16101-16108. https://doi.org/https://doi.org/10.1074/jbc.M110.193433

Chang, B., Hawes, N. L., Hurd, R. E., Davisson, M. T., Nusinowitz, S., & Heckenlively, J. R. (2002). Retinal degeneration mutants in the mouse. *Vision Research*, *42*(4), 517-525. https://doi.org/https://doi.org/10.1016/S0042-6989(01)00146-8

Chang, B., Hawes, N. L., Pardue, M. T., German, A. M., Hurd, R. E., Davisson, M. T., Nusinowitz, S., Rengarajan, K., Boyd, A. P., Sidney, S. S., Phillips, M. J., Stewart, R. E., Chaudhury, R., Nickerson, J. M., Heckenlively, J. R., & Boatright, J. H. (2007). Two mouse retinal degenerations caused by missense mutations in the beta-subunit of rod cGMP phosphodiesterase gene. *Vision Res*, *47*(5), 624-633. https://doi.org/10.1016/j.visres.2006.11.020

Chaplin, D. D. (2010). Overview of the immune response. *Journal of Allergy and Clinical Immunology*, *125*(2, Supplement 2), S3-S23. https://doi.org/https://doi.org/10.1016/j.jaci.2009.12.980

Chen, H., Wang, F., Zhang, P., Zhang, Y., Chen, Y., Fan, X., Cao, X., Liu, J., Yang, Y., Wang, B., Lei, B., Gu, L., Bai, J., Wei, L., Zhang, R., Zhuang, Q., Zhang, W., Zhao, W., & He, A. (2019). Management of cytokine release syndrome related to CAR-T cell therapy. *Frontiers of Medicine*, *13*(5), 610-617. https://doi.org/10.1007/s11684-019-0714-8

Chen, W., Hu, Y., & Ju, D. (2020). Gene therapy for neurodegenerative disorders: advances, insights and prospects. *Acta Pharmaceutica Sinica B*, *10*(8), 1347-1359. https://doi.org/https://doi.org/10.1016/j.apsb.2020.01.015

Chew, E. Y., Clemons, T. E., Jaffe, G. J., Johnson, C. A., Farsiu, S., Lad, E. M., Guymer, R., Rosenfeld, P., Hubschman, J. P., Constable, I., Wiley, H., Singerman, L. J., Gillies, M., Comer, G., Blodi, B., Eliott, D., Yan, J., Bird, A., & Friedlander, M. (2019). Effect of Ciliary Neurotrophic Factor on Retinal Neurodegeneration in Patients with Macular Telangiectasia Type 2: A Randomized Clinical Trial. *Ophthalmology*, *126*(4), 540-549. https://doi.org/10.1016/j.ophtha.2018.09.041

Chew, E. Y., Clemons, T. E., Peto, T., Sallo, F. B., Ingerman, A., Tao, W., Singerman, L., Schwartz, S. D., Peachey, N. S., & Bird, A. C. (2015). Ciliary neurotrophic factor for macular telangiectasia type 2: results from a phase 1 safety trial. *Am J Ophthalmol*, *159*(4), 659-666.e651. https://doi.org/10.1016/j.ajo.2014.12.013

Chew, E. Y., Gillies, M., Jaffe, G. J., Gaudric, A., Egan, C., Constable, I., Clemons, T., Aaberg, T., Manning, D. C., Hohman, T. C., Bird, A., Friedlander, M., & MacTel, C. N.-R. i. (2025). Cell-Based Ciliary Neurotrophic Factor Therapy for Macular Telangiectasia Type 2. *NEJM Evid*, *4*(8), EVIDoa2400481. https://doi.org/10.1056/EVIDoa2400481

Chucair-Elliott, A. J., Elliott, M. H., Wang, J., Moiseyev, G. P., Ma, J. X., Politi, L. E., Rotstein, N. P., Akira, S., Uematsu, S., & Ash, J. D. (2012). Leukemia inhibitory factor coordinates the down-regulation of the visual cycle in the retina and retinal-pigmented epithelium. *J Biol Chem*, *287*(29), 24092-24102. https://doi.org/10.1074/jbc.M112.378240

Cintrón-Colón, A. F., Almeida-Alves, G., Boynton, A. M., & Spitsbergen, J. M. (2020). GDNF synthesis, signaling, and retrograde transport in motor neurons. *Cell Tissue Res*, *382*(1), 47-56. https://doi.org/10.1007/s00441-020-03287-6

Clausen, M. V., Hilbers, F., & Poulsen, H. (2017). The Structure and Function of the Na,K-ATPase Isoforms in Health and Disease. *Front Physiol*, *8*, 371. https://doi.org/10.3389/fphys.2017.00371

Conti, L., Pollard, S. M., Gorba, T., Reitano, E., Toselli, M., Biella, G., Sun, Y., Sanzone, S., Ying, Q. L., Cattaneo, E., & Smith, A. (2005). Niche-independent symmetrical self-renewal of a mammalian tissue stem cell. *PLoS Biol*, *3*(9), e283. https://doi.org/10.1371/journal.pbio.0030283

Contreras, R. G., Shoshani, L., Flores-Maldonado, C., Lázaro, A., & Cereijido, M. (1999). Relationship between Na(+),K(+)-ATPase and cell attachment. *J Cell Sci*, *112 (Pt 23)*, 4223-4232. https://doi.org/10.1242/jcs.112.23.4223

Contreras, R. G., Torres-Carrillo, A., Flores-Maldonado, C., Shoshani, L., & Ponce, A. (2024). Na(+)/K(+)-ATPase: More than an Electrogenic Pump. *Int J Mol Sci*, *25*(11). https://doi.org/10.3390/ijms25116122

Cote, R. H., Gupta, R., Irwin, M. J., & Wang, X. (2022). Photoreceptor Phosphodiesterase (PDE6): Structure, Regulatory Mechanisms, and Implications for Treatment of Retinal Diseases. *Adv Exp Med Biol*, *1371*, 33-59. https://doi.org/10.1007/5584_2021_649

Country, M. W. (2017). Retinal metabolism: A comparative look at energetics in the retina. *Brain Res*, *1672*, 50-57. https://doi.org/10.1016/j.brainres.2017.07.025

Cronin, T., Lyubarsky, A., & Bennett, J. (2012). Dark-rearing the rd10 mouse: implications for therapy. *Adv Exp Med Biol*, *723*, 129-136. https://doi.org/10.1007/978-1-4614-0631-0_18

Cui, Y., Hettinghouse, A., & Liu, C. J. (2019). Progranulin: A conductor of receptors orchestra, a chaperone of lysosomal enzymes and a therapeutic target for multiple diseases. *Cytokine Growth Factor Rev*, *45*, 53-64. https://doi.org/10.1016/j.cytogfr.2019.01.002

Curcio, C. A., Sloan, K. R., Kalina, R. E., & Hendrickson, A. E. (1990). Human photoreceptor topography. *J Comp Neurol*, *292*(4), 497-523. https://doi.org/10.1002/cne.902920402

Dalkara, D., Kolstad, K. D., Guerin, K. I., Hoffmann, N. V., Visel, M., Klimczak, R. R., Schaffer, D. V., & Flannery, J. G. (2011). AAV mediated GDNF secretion from retinal glia slows down retinal degeneration in a rat model of retinitis pigmentosa. *Mol Ther*, *19*(9), 1602-1608. https://doi.org/10.1038/mt.2011.62

Danciger, M., Blaney, J., Gao, Y. Q., Zhao, D. Y., Heckenlively, J. R., Jacobson, S. G., & Farber, D. B. (1995). Mutations in the PDE6B gene in autosomal recessive retinitis pigmentosa. *Genomics*, *30*(1), 1-7. https://doi.org/10.1006/geno.1995.0001

Daniel, R., Daniels, E., He, Z., & Bateman, A. (2003). Progranulin (acrogranin/PC cell-derived growth factor/granulin-epithelin precursor) is expressed in the placenta, epidermis, microvasculature, and brain during murine development. *Dev Dyn*, *227*(4), 593-599. https://doi.org/10.1002/dvdy.10341

Davis, S., Aldrich, T. H., Valenzuela, D. M., Wong, V. V., Furth, M. E., Squinto, S. P., & Yancopoulos, G. D. (1991). The receptor for ciliary neurotrophic factor. *Science*, *253*(5015), 59-63. https://doi.org/10.1126/science.1648265

De Serio, A., Graziani, R., Laufer, R., Ciliberto, G., & Paonessa, G. (1995). In vitro binding of ciliary neurotrophic factor to its receptors: evidence for the formation of an IL-6-type hexameric complex. *J Mol Biol*, *254*(5), 795-800. https://doi.org/10.1006/jmbi.1995.0655

Del Río, P., Irmler, M., Arango-González, B., Favor, J., Bobe, C., Bartsch, U., Vecino, E., Beckers, J., Hauck, S. M., & Ueffing, M. (2011). GDNF-induced osteopontin from Müller glial cells promotes photoreceptor survival in the Pde6brd1 mouse model of retinal degeneration. *Glia*, *59*(5), 821-832. https://doi.org/10.1002/glia.21155

Delyfer, M. N., Simonutti, M., Neveux, N., Léveillard, T., & Sahel, J. A. (2005). Does GDNF exert its neuroprotective effects on photoreceptors in the rd1 retina through the glial glutamate transporter GLAST? *Mol Vis*, *11*, 677-687. http://www.molvis.org/molvis/v11/a80/v11a80-delyfer.pdf

DeParis, S., Caprara, C., & Grimm, C. (2012). Intrinsically photosensitive retinal ganglion cells are resistant to N-methyl-D-aspartic acid excitotoxicity. *Mol Vis*, *18*, 2814-2827. https://pmc.ncbi.nlm.nih.gov/articles/PMC3519378/

Deverman, B. E., & Patterson, P. H. (2012). Exogenous leukemia inhibitory factor stimulates oligodendrocyte progenitor cell proliferation and enhances hippocampal remyelination. *J Neurosci*, *32*(6), 2100-2109. https://doi.org/10.1523/JNEUROSCI.3803-11.2012

Diamond, J. S. (2017). Inhibitory Interneurons in the Retina: Types, Circuitry, and Function. *Annu Rev Vis Sci*, *3*, 1-24. https://doi.org/10.1146/annurev-vision-102016-061345

Dittrich, F., Thoenen, H., & Sendtner, M. (1994). Ciliary neurotrophic factor: pharmacokinetics and acute-phase response in rat. *Ann Neurol*, *35*(2), 151-163. https://doi.org/10.1002/ana.410350206

Dong, A., Shen, J., Krause, M., Hackett, S. F., & Campochiaro, P. A. (2007). Increased expression of glial cell line-derived neurotrophic factor protects against oxidative damage-induced retinal degeneration. *J Neurochem*, *103*(3), 1041-1052. https://doi.org/10.1111/j.1471-4159.2007.04839.x

Dong, S., Zhen, F., Xu, H., Li, Q., & Wang, J. (2021). Leukemia inhibitory factor protects photoreceptor cone cells against oxidative damage through activating JAK/STAT3 signaling. *Annals of Translational Medicine*, *9*(2), 152. https://atm.amegroups.org/article/view/61685

Dong, S., Zhen, F., Zou, T., Zhou, Y., Wu, J., Wang, T., & Zhang, H. (2024). Leukemia Inhibitory Factor Protects against Degeneration of Cone Photoreceptors Caused by RPE65 Deficiency. *Curr Med Chem*, *31*(25), 4022-4033. https://doi.org/10.2174/0109298673240896231027053716

Dräger, U. C., & Olsen, J. F. (1981). Ganglion cell distribution in the retina of the mouse. *Investigative Ophthalmology & Visual Science*, *20*(3), 285-293.

Duarte Azevedo, M., Sander, S., & Tenenbaum, L. (2020). GDNF, A Neuron-Derived Factor Upregulated in Glial Cells during Disease. *J Clin Med*, *9*(2). https://doi.org/10.3390/jcm9020456

Dulz, S., Bassal, M., Flachsbarth, K., Riecken, K., Fehse, B., Schlichting, S., Bartsch, S., & Bartsch, U. (2020). Intravitreal Co-Administration of GDNF and CNTF Confers Synergistic and Long-Lasting Protection against Injury-Induced Cell Death of Retinal Ganglion Cells in Mice. *Cells*, *9*(9). https://doi.org/10.3390/cells9092082

Fedosova, N. U., Habeck, M., & Nissen, P. (2021). Structure and Function of Na,K-ATPase-The Sodium-Potassium Pump. *Compr Physiol*, *12*(1), 2659-2679. https://doi.org/10.1002/cphy.c200018

Ferreros, P., & Trapero, I. (2022). Interleukin Inhibitors in Cytokine Release Syndrome and Neurotoxicity Secondary to CAR-T Therapy. *Diseases*, *10*(3), 41. https://www.mdpi.com/2079-9721/10/3/41

Fischer, D. (2012). Stimulating axonal regeneration of mature retinal ganglion cells and overcoming inhibitory signaling. *Cell Tissue Res*, *349*(1), 79-85. https://doi.org/10.1007/s00441-011-1302-7

Fischer, D. (2017). Hyper-IL-6: a potent and efficacious stimulator of RGC regeneration. *Eye (Lond)*, *31*(2), 173-178. https://doi.org/10.1038/eye.2016.234

Fischer, D., & Leibinger, M. (2012). Promoting optic nerve regeneration. *Prog Retin Eye Res*, *31*(6), 688-701. https://doi.org/10.1016/j.preteyeres.2012.06.005

Fischer, M., Goldschmitt, J., Peschel, C., Brakenhoff, J. P., Kallen, K. J., Wollmer, A., Grötzinger, J., & Rose-John, S. (1997). I. A bioactive designer cytokine for human hematopoietic progenitor cell expansion. *Nat Biotechnol*, *15*(2), 142-145. https://doi.org/10.1038/nbt0297-142

Flachsbarth, K., Jankowiak, W., Kruszewski, K., Helbing, S., Bartsch, S., & Bartsch, U. (2018). Pronounced synergistic neuroprotective effect of GDNF and CNTF on axotomized retinal ganglion cells in the adult mouse. *Exp Eye Res*, *176*, 258-265. https://doi.org/10.1016/j.exer.2018.09.006

Flachsbarth, K., Kruszewski, K., Jung, G., Jankowiak, W., Riecken, K., Wagenfeld, L., Richard, G., Fehse, B., & Bartsch, U. (2014). Neural stem cell-based intraocular administration of ciliary neurotrophic factor attenuates the loss of axotomized ganglion cells in adult mice. *Invest Ophthalmol Vis Sci*, *55*(11), 7029-7039. https://doi.org/10.1167/iovs.14-15266

Fortenbach, C., Peinado Allina, G., Shores, C. M., Karlen, S. J., Miller, E. B., Bishop, H., Trimmer, J. S., Burns, M. E., & Pugh, E. N., Jr. (2021). Loss of the K+ channel Kv2.1 greatly reduces outward dark current and causes ionic dysregulation and degeneration in rod photoreceptors. *Journal of General Physiology*, *153*(2). https://doi.org/10.1085/jgp.202012687

Frasson, M., Picaud, S., Léveillard, T., Simonutti, M., Mohand-Said, S., Dreyfus, H., Hicks, D., & Sabel, J. (1999). Glial cell line-derived neurotrophic factor induces histologic and functional protection of rod photoreceptors in the rd/rd mouse. *Invest Ophthalmol Vis Sci*, *40*(11), 2724-2734. https://iovs.arvojournals.org/article.aspx?articleid=2199753

Friedrich, U., Stohr, H., Hilfinger, D., Loenhardt, T., Schachner, M., Langmann, T., & Weber, B. H. (2011). The Na/K-ATPase is obligatory for membrane anchorage of retinoschisin, the protein involved in the pathogenesis of X-linked juvenile retinoschisis. *Hum Mol Genet*, *20*(6), 1132-1142. https://doi.org/10.1093/hmg/ddq557

Frigg, R., Wenzel, A., Grimm, C., & Remé, C. E. (2005). [Survival factors in the treatment of hereditary retinal degeneration]. *Ophthalmologe*, *102*(8), 757-763. https://doi.org/10.1007/s00347-005-1244-0 (Uberlebensfaktoren in der Therapie erblicher Netzhautdegenerationen.)

Fudalej, E., Justyniarska, M., Kasarello, K., Dziedziak, J., Szaflik, J. P., & Cudnoch-Jedrzejewska, A. (2021). Neuroprotective Factors of the Retina and Their Role in Promoting Survival of Retinal Ganglion Cells: A Review. *Ophthalmic Res*, *64*(3), 345-355. https://doi.org/10.1159/000514441

Gamm, D. M., Wang, S., Lu, B., Girman, S., Holmes, T., Bischoff, N., Shearer, R. L., Sauve, Y., Capowski, E., Svendsen, C. N., & Lund, R. D. (2007). Protection of visual functions by human neural progenitors in a rat model of retinal disease. *PLoS One*, *2*(3), e338. https://doi.org/10.1371/journal.pone.0000338

Gange, W. S., Sisk, R. A., Besirli, C. G., Lee, T. C., Havunjian, M., Schwartz, H., Borchert, M., Sengillo, J. D., Mendoza, C., Berrocal, A. M., & Nagiel, A. (2022). Perifoveal Chorioretinal Atrophy after Subretinal Voretigene Neparvovec-rzyl for RPE65-Mediated Leber Congenital Amaurosis. *Ophthalmol Retina*, *6*(1), 58-64. https://doi.org/10.1016/j.oret.2021.03.016

Garbers, C., & Rose-John, S. (2018). IL6RA, Interleukin-6 Receptor Subunit Alpha. In S. Choi (Ed.), *Encyclopedia of Signaling Molecules* (pp. 2565-2570). Springer International Publishing. https://doi.org/10.1007/978-3-319-67199-4_101661

García-Caballero, C., Lieppman, B., Arranz-Romera, A., Molina-Martínez, I. T., Bravo-Osuna, I., Young, M., Baranov, P., & Herrero-Vanrell, R. (2018). Photoreceptor preservation induced by intravitreal controlled delivery of GDNF and GDNF/melatonin in rhodopsin knockout mice. *Mol Vis*, *24*, 733-745. https://pmc.ncbi.nlm.nih.gov/articles/PMC6279195/pdf/mv-v24-733.pdf

Gargini, C., Terzibasi, E., Mazzoni, F., & Strettoi, E. (2007). Retinal organization in the retinal degeneration 10 (rd10) mutant mouse: a morphological and ERG study. *J Comp Neurol*, *500*(2), 222-238. https://doi.org/10.1002/cne.21144

Gearing, D. P., Gough, N. M., King, J. A., Hilton, D. J., Nicola, N. A., Simpson, R. J., Nice, E. C., Kelso, A., & Metcalf, D. (1987). Molecular cloning and expression of cDNA encoding a murine myeloid leukaemia inhibitory factor (LIF). *The EMBO Journal*, *6*(13), 3995-4002. https://doi.org/https://doi.org/10.1002/j.1460-2075.1987.tb02742.x

Gearing, D. P., Ziegler, S. F., Comeau, M. R., Friend, D., Thoma, B., Cosman, D., Park, L., & Mosley, B. (1994). Proliferative responses and binding properties of hematopoietic cells transfected with low-affinity receptors for leukemia inhibitory factor, oncostatin M, and ciliary neurotrophic factor. *Proc Natl Acad Sci U S A*, *91*(3), 1119-1123. https://doi.org/10.1073/pnas.91.3.1119

Geering, K. (2006). FXYD proteins: new regulators of Na-K-ATPase. *Am J Physiol Renal Physiol*, *290*(2), F241-250. https://doi.org/10.1152/ajprenal.00126.2005

Georgiou, M., Fujinami, K., & Michaelides, M. (2021). Inherited retinal diseases: Therapeutics, clinical trials and end points-A review. *Clin Exp Ophthalmol*, *49*(3), 270-288. https://doi.org/10.1111/ceo.13917

Ghasemi, M., Alizadeh, E., Saei Arezoumand, K., Fallahi Motlagh, B., & Zarghami, N. (2018). Ciliary neurotrophic factor (CNTF) delivery to retina: an overview of current research advancements. *Artif Cells Nanomed Biotechnol*, *46*(8), 1694-1707. https://doi.org/10.1080/21691401.2017.1391820

Gill, J. S., Georgiou, M., Kalitzeos, A., Moore, A. T., & Michaelides, M. (2019). Progressive cone and cone-rod dystrophies: clinical features, molecular genetics and prospects for therapy. *Br J Ophthalmol*, *103*(5), 711-720. https://doi.org/10.1136/bjophthalmol-2018-313278

Gloor, S., Antonicek, H., Sweadner, K. J., Pagliusi, S., Frank, R., Moos, M., & Schachner, M. (1990). The adhesion molecule on glia (AMOG) is a homologue of the beta subunit of the Na,K-ATPase. *J Cell Biol*, *110*(1), 165-174. https://doi.org/10.1083/jcb.110.1.165

Gollisch, T., & Meister, M. (2010). Eye smarter than scientists believed: neural computations in circuits of the retina. *Neuron*, *65*(2), 150-164. https://doi.org/10.1016/j.neuron.2009.12.009

Gonzalez-Cordero, A., Goh, D., Kruczek, K., Naeem, A., Fernando, M., kleine Holthaus, S.-M., Takaaki, M., Blackford, S. J. I., Kloc, M., Agundez, L., Sampson, R. D., Borooah, S., Ovando-Roche, P., Mehat, M. S., West, E. L., Smith, A. J., Pearson, R. A., & Ali, R. R. (2018). Assessment of AAV Vector Tropisms for Mouse and Human Pluripotent Stem Cell–Derived RPE and Photoreceptor Cells. *Human Gene Therapy*, *29*(10), 1124-1139. https://doi.org/10.1089/hum.2018.027

Gopalakrishnan, P., Beryozkin, A., Banin, E., & Sharon, D. (2023). Morphological and Functional Comparison of Mice Models for Retinitis Pigmentosa. In J. D. Ash, E. Pierce, R. E. Anderson, C. Bowes Rickman, J. G. Hollyfield, & C. Grimm, *Retinal Degenerative Diseases XIX* Cham.

Gough, N. M., & Williams, R. L. (1989). The pleiotropic actions of leukemia inhibitory factor. *Cancer Cells*, *1*(3), 77-80. https://www.ncbi.nlm.nih.gov/pubmed/2518284

Gough, N. M., Williams, R. L., Hilton, D. J., Pease, S., Willson, T. A., Stahl, J., Gearing, D. P., Nicola, N. A., & Metcalf, D. (1989). LIF: a molecule with divergent actions on myeloid leukaemic cells and embryonic stem cells. *Reprod Fertil Dev*, *1*(4), 281-288. https://doi.org/10.1071/rd9890281

Gregory-Evans, K., Chang, F., Hodges, M. D., & Gregory-Evans, C. Y. (2009). Ex vivo gene therapy using intravitreal injection of GDNF-secreting mouse embryonic stem cells in a rat model of retinal degeneration. *Mol Vis*, *15*, 962-973. https://pmc.ncbi.nlm.nih.gov/articles/PMC2684563/pdf/mv-v15-962.pdf

Grinna, L. S., & Tschopp, J. F. (1989). Size distribution and general structural features of N-linked oligosaccharides from the methylotrophic yeast, Pichia pastoris. *Yeast*, *5*(2), 107-115. https://doi.org/10.1002/yea.320050206

Grossniklaus, H. E., Geisert, E. E., & Nickerson, J. M. (2015). Introduction to the Retina. *Prog Mol Biol Transl Sci*, *134*, 383-396. https://doi.org/10.1016/bs.pmbts.2015.06.001

Gulati, S., Palczewski, K., Engel, A., Stahlberg, H., & Kovacik, L. (2019). Cryo-EM structure of phosphodiesterase 6 reveals insights into the allosteric regulation of type I phosphodiesterases. *Science Advances*, *5*(2), eaav4322. https://doi.org/doi:10.1126/sciadv.aav4322

Guo, H., Chen, P., Luo, R., Zhang, Y., Xu, X., & Gou, X. (2022). The Roles of Ciliary Neurotrophic Factor - from Neuronutrition to Energy Metabolism. *Protein Pept Lett*, *29*(10), 815-828. https://doi.org/10.2174/0929866529666220905105800

Gupta, N., Brown, K. E., & Milam, A. H. (2003). Activated microglia in human retinitis pigmentosa, late-onset retinal degeneration, and age-related macular degeneration. *Exp Eye Res*, *76*(4), 463-471. https://doi.org/10.1016/s0014-4835(02)00332-9

Gupta, N., Shyamasundar, S., Patnala, R., Karthikeyan, A., Arumugam, T. V., Ling, E. A., & Dheen, S. T. (2018). Recent progress in therapeutic strategies for microglia-mediated neuroinflammation in neuropathologies. *Expert Opin Ther Targets*, *22*(9), 765-781. https://doi.org/10.1080/14728222.2018.1515917

Hailer, N. P. (2008). Immunosuppression after traumatic or ischemic CNS damage: it is neuroprotective and illuminates the role of microglial cells. *Prog Neurobiol*, *84*(3), 211-233. https://doi.org/10.1016/j.pneurobio.2007.12.001

Ham, Y., Mehta, H., Kang-Mieler, J., Mieler, W. F., & Chang, A. (2023). Novel Drug Delivery Methods and Approaches for the Treatment of Retinal Diseases. *Asia Pac J Ophthalmol (Phila)*, *12*(4), 402-413. https://doi.org/10.1097/apo.0000000000000623

Hamel, C. (2006). Retinitis pigmentosa. *Orphanet J Rare Dis*, *1*, 40. https://doi.org/10.1186/1750-1172-1-40

Hamel, C. P. (2007). Cone rod dystrophies. *Orphanet J Rare Dis*, *2*, 7. https://doi.org/10.1186/1750-1172-2-7

Han, J., Dinculescu, A., Dai, X., Du, W., Smith, W. C., & Pang, J. (2013). Review: the history and role of naturally occurring mouse models with Pde6b mutations. *Mol Vis*, *19*, 2579-2589. https://pmc.ncbi.nlm.nih.gov/articles/PMC3869645/

Hanisch, U. K. (2002). Microglia as a source and target of cytokines. *Glia*, *40*(2), 140-155. https://doi.org/10.1002/glia.10161

Harada, T., Harada, C., Kohsaka, S., Wada, E., Yoshida, K., Ohno, S., Mamada, H., Tanaka, K., Parada, L. F., & Wada, K. (2002). Microglia-Muller glia cell interactions control neurotrophic factor production during light-induced retinal degeneration. *J Neurosci*, *22*(21), 9228-9236. https://doi.org/10.1523/JNEUROSCI.22-21-09228.2002

Haraguchi, Y., Chiang, T.-K., & Yu, M. (2023). Application of Electrophysiology in Non-Macular Inherited Retinal Dystrophies. *Journal of Clinical Medicine*, *12*(21), 6953. https://www.mdpi.com/2077-0383/12/21/6953

Hartong, D. T., Berson, E. L., & Dryja, T. P. (2006). Retinitis pigmentosa. *Lancet*, *368*(9549), 1795-1809. https://doi.org/10.1016/s0140-6736(06)69740-7

Hauck, S. M., Kinkl, N., Deeg, C. A., Swiatek-de Lange, M., Schöffmann, S., & Ueffing, M. (2006). GDNF family ligands trigger indirect neuroprotective signaling in retinal glial cells. *Mol Cell Biol*, *26*(7), 2746-2757. https://doi.org/10.1128/mcb.26.7.2746-2757.2006

He, Z., Ong, C. H., Halper, J., & Bateman, A. (2003). Progranulin is a mediator of the wound response. *Nat Med*, *9*(2), 225-229. https://doi.org/10.1038/nm816

Heinrich, P. C., Behrmann, I., Haan, S., Hermanns, H. M., Müller-Newen, G., & Schaper, F. (2003). Principles of interleukin (IL)-6-type cytokine signalling and its regulation. *Biochem J*, *374*(Pt 1), 1-20. https://doi.org/10.1042/bj20030407

Heinrich, P. C., Castell, J. V., & Andus, T. (1990). Interleukin-6 and the acute phase response. *Biochem J*, *265*(3), 621-636. https://doi.org/10.1042/bj2650621

Hertle, D., Schleichert, M., Steup, A., Kirsch, M., & Hofmann, H. D. (2008). Regulation of cytokine signaling components in developing rat retina correlates with transient inhibition of rod differentiation by CNTF. *Cell Tissue Res*, *334*(1), 7-16. https://doi.org/10.1007/s00441-008-0651-3

Hibi, M., Murakami, M., Saito, M., Hirano, T., Taga, T., & Kishimoto, T. (1990). Molecular cloning and expression of an IL-6 signal transducer, gp130. *Cell*, *63*(6), 1149-1157. https://doi.org/10.1016/0092-8674(90)90411-7

Hilton, D. J., Nicola, N. A., & Metcalf, D. (1991). Distribution and comparison of receptors for leukemia inhibitory factor on murine hemopoietic and hepatic cells. *J Cell Physiol*, *146*(2), 207-215. https://doi.org/10.1002/jcp.1041460204

Hirahara, K., Onodera, A., Villarino, A. V., Bonelli, M., Sciumè, G., Laurence, A., Sun, H. W., Brooks, S. R., Vahedi, G., Shih, H. Y., Gutierrez-Cruz, G., Iwata, S., Suzuki, R., Mikami, Y., Okamoto, Y., Nakayama, T., Holland, S. M., Hunter, C. A., Kanno, Y., & O'Shea, J. J. (2015). Asymmetric Action of STAT Transcription Factors Drives Transcriptional Outputs and Cytokine Specificity. *Immunity*, *42*(5), 877-889. https://doi.org/10.1016/j.immuni.2015.04.014

Hirai, H., Karian, P., & Kikyo, N. (2011). Regulation of embryonic stem cell self-renewal and pluripotency by leukaemia inhibitory factor. *Biochem J*, *438*(1), 11-23. https://doi.org/10.1042/BJ20102152

Holz, F. G., Schütt, F., Kopitz, J., Eldred, G. E., Kruse, F. E., Völcker, H. E., & Cantz, M. (1999). Inhibition of lysosomal degradative functions in RPE cells by a retinoid component of lipofuscin. *Investigative Ophthalmology & Visual Science*, *40*(3), 737-743.

Hou, W., Cai, J., Shen, P., Zhang, S., Xiao, S., You, P., Tong, Y., Li, K., Qi, Z., & Luo, H. (2023). Identification of FXYD6 as the novel biomarker for glioma based on differential expression and DNA methylation. *Cancer Medicine*, *12*(24), 22170-22184. https://doi.org/https://doi.org/10.1002/cam4.6752

Houghton, F. M., Adams, S. E., Ríos, A. S., Masino, L., Purkiss, A. G., Briggs, D. C., Ledda, F., & McDonald, N. Q. (2023). Architecture and regulation of a GDNF-GFRα1 synaptic adhesion assembly. *Nature Communications*, *14*(1), 7551. https://doi.org/10.1038/s41467-023-43148-8

Hu, F., Padukkavidana, T., Vægter, C. B., Brady, O. A., Zheng, Y., Mackenzie, I. R., Feldman, H. H., Nykjaer, A., & Strittmatter, S. M. (2010). Sortilin-mediated endocytosis determines levels of the frontotemporal dementia protein, progranulin. *Neuron*, *68*(4), 654-667. https://doi.org/10.1016/j.neuron.2010.09.034

Hu, Y., Grodzki, L. M., & Bartsch, U. (2025). Survival and Axonal Regeneration of Retinal Ganglion Cells in a Mouse Optic Nerve Crush Model After a Cell-Based Intravitreal Co-Administration of Ciliary Neurotrophic Factor and Glial Cell Line-Derived Neurotrophic Factor at Different Post-Lesion Time Points. *Cells*, *14*(9). https://doi.org/10.3390/cells14090643

Hubbard, R., & Kropf, A. (1958). THE ACTION OF LIGHT ON RHODOPSIN. *Proc Natl Acad Sci U S A*, *44*(2), 130-139. https://doi.org/10.1073/pnas.44.2.130

Huin, V., Barbier, M., Bottani, A., Lobrinus, J. A., Clot, F., Lamari, F., Chat, L., Rucheton, B., Fluchère, F., Auvin, S., Myers, P., Gelot, A., Camuzat, A., Caillaud, C., Jornéa, L., Forlani, S., Saracino, D., Duyckaerts, C., Brice, A.,…Le Ber, I. (2019). Homozygous GRN mutations: new phenotypes and new insights into pathological and molecular mechanisms. *Brain*, *143*(1), 303-319. https://doi.org/10.1093/brain/awz377

Hussey, K. A., Hadyniak, S. E., & Johnston, R. J. (2022). Patterning and Development of Photoreceptors in the Human Retina [Review]. *Frontiers in Cell and Developmental Biology*, *Volume 10 - 2022*. https://doi.org/10.3389/fcell.2022.878350

Hwang, S., Jeon, S., Yoon, J. M., Woo, S. J., Joo, K., Choi, Y. J., Yoon, C. K., Kim, M., Lee, H. J., Byeon, S. H., Lee, C. S., Jeon, J., Kim, J. Y., Han, J., Surl, D., Sagong, M., Jeong, A., Park, T. K., Park, H. S.,…Kim, S. J. (2025). Retinitis Pigmentosa GTPase Regulator-Associated X-Linked Retinitis Pigmentosa: Molecular Genetics and Clinical Characteristics. *American Journal of Ophthalmology*, *274*, 171-183. https://doi.org/https://doi.org/10.1016/j.ajo.2025.03.001

Ibáñez, C. F. (2013). Structure and physiology of the RET receptor tyrosine kinase. *Cold Spring Harb Perspect Biol*, *5*(2). https://doi.org/10.1101/cshperspect.a009134

Ibáñez, C. F., & Andressoo, J.-O. (2017). Biology of GDNF and its receptors — Relevance for disorders of the central nervous system. *Neurobiology of Disease*, *97*, 80-89. https://doi.org/https://doi.org/10.1016/j.nbd.2016.01.021

Ikeda, K., Onimaru, H., Yamada, J., Inoue, K., Ueno, S., Onaka, T., Toyoda, H., Arata, A., Ishikawa, T. O., Taketo, M. M., Fukuda, A., & Kawakami, K. (2004). Malfunction of respiratory-related neuronal activity in Na+, K+-ATPase alpha2 subunit-deficient mice is attributable to abnormal Cl- homeostasis in brainstem neurons. *J Neurosci*, *24*(47), 10693-10701. https://doi.org/10.1523/jneurosci.2909-04.2004

Inamdar, S. M., Lankford, C. K., Poria, D., Laird, J. G., Solessio, E., Kefalov, V. J., & Baker, S. A. (2021). Differential impact of Kv8.2 loss on rod and cone signaling and degeneration. *Human Molecular Genetics*, *31*(7), 1035-1050. https://doi.org/10.1093/hmg/ddab301

Ingram, N. T., Fain, G. L., & Sampath, A. P. (2020). Elevated energy requirement of cone photoreceptors. *Proc Natl Acad Sci U S A*, *117*(32), 19599-19603. https://doi.org/10.1073/pnas.2001776117

Ionta, S. (2021). Visual Neuropsychology in Development: Anatomo-Functional Brain Mechanisms of Action/Perception Binding in Health and Disease [Review]. *Frontiers in Human Neuroscience*, *Volume 15 - 2021*. https://doi.org/10.3389/fnhum.2021.689912

Isaksen, T. J., & Lykke-Hartmann, K. (2016). Insights into the Pathology of the α2-Na(+)/K(+)-ATPase in Neurological Disorders; Lessons from Animal Models. *Front Physiol*, *7*, 161. https://doi.org/10.3389/fphys.2016.00161

Jankowiak, W., Kruszewski, K., Flachsbarth, K., Skevas, C., Richard, G., Ruther, K., Braulke, T., & Bartsch, U. (2015). Sustained Neural Stem Cell-Based Intraocular Delivery of CNTF Attenuates Photoreceptor Loss in the nclf Mouse Model of Neuronal Ceroid Lipofuscinosis. *PLoS One*, *10*(5), e0127204. https://doi.org/10.1371/journal.pone.0127204

Jeon, C. J., Strettoi, E., & Masland, R. H. (1998). The major cell populations of the mouse retina. *J Neurosci*, *18*(21), 8936-8946. https://doi.org/10.1523/jneurosci.18-21-08936.1998

Jian, J., Tian, Q.-Y., Hettinghouse, A., Zhao, S., Liu, H., Wei, J., Grunig, G., Zhang, W., Setchell, K. D. R., Sun, Y., Overkleeft, H. S., Chan, G. L., & Liu, C.-j. (2016). Progranulin Recruits HSP70 to β-Glucocerebrosidase and Is Therapeutic Against Gaucher Disease. *EBioMedicine*, *13*, 212-224. https://doi.org/https://doi.org/10.1016/j.ebiom.2016.10.010

Jiang, X., Rashwan, R., Voigt, V., Nerbonne, J., Hunt, D. M., & Carvalho, L. S. (2021). Molecular, Cellular and Functional Changes in the Retinas of Young Adult Mice Lacking the Voltage-Gated K+ Channel Subunits Kv8.2 and K2.1. *International Journal of Molecular Sciences*, *22*(9), 4877. https://www.mdpi.com/1422-0067/22/9/4877

Jimenez, T., Sánchez, G., Wertheimer, E., & Blanco, G. (2010). Activity of the Na,K-ATPase alpha4 isoform is important for membrane potential, intracellular Ca2+, and pH to maintain motility in rat spermatozoa. *Reproduction*, *139*(5), 835-845. https://doi.org/10.1530/rep-09-0495

Jmaeff, S., Sidorova, Y., Lippiatt, H., Barcelona, P. F., Nedev, H., Saragovi, L. M., Hancock, M. A., Saarma, M., & Saragovi, H. U. (2020). Small-Molecule Ligands that Bind the RET Receptor Activate Neuroprotective Signals Independent of but Modulated by Coreceptor GFRα1. *Molecular Pharmacology*, *98*(1), 1-12. https://doi.org/https://doi.org/10.1124/mol.119.118950

Joly, S., Francke, M., Ulbricht, E., Beck, S., Seeliger, M., Hirrlinger, P., Hirrlinger, J., Lang, K. S., Zinkernagel, M., Odermatt, B., Samardzija, M., Reichenbach, A., Grimm, C., & Remé, C. E. (2009). Cooperative phagocytes: resident microglia and bone marrow immigrants remove dead photoreceptors in retinal lesions. *Am J Pathol*, *174*(6), 2310-2323. https://doi.org/10.2353/ajpath.2009.090023

Joly, S., Lange, C., Thiersch, M., Samardzija, M., & Grimm, C. (2008). Leukemia inhibitory factor extends the lifespan of injured photoreceptors in vivo. *J Neurosci*, *28*(51), 13765-13774. https://doi.org/10.1523/jneurosci.5114-08.2008

Jones, S. A., & Jenkins, B. J. (2018). Recent insights into targeting the IL-6 cytokine family in inflammatory diseases and cancer. *Nat Rev Immunol*, *18*(12), 773-789. https://doi.org/10.1038/s41577-018-0066-7

Jung, G., Sun, J., Petrowitz, B., Riecken, K., Kruszewski, K., Jankowiak, W., Kunst, F., Skevas, C., Richard, G., Fehse, B., & Bartsch, U. (2013). Genetically modified neural stem cells for a local and sustained delivery of neuroprotective factors to the dystrophic mouse retina. *Stem Cells Transl Med*, *2*(12), 1001-1010. https://doi.org/10.5966/sctm.2013-0013

Jüttner, J., Szabo, A., Gross-Scherf, B., Morikawa, R. K., Rompani, S. B., Hantz, P., Szikra, T., Esposti, F., Cowan, C. S., Bharioke, A., Patino-Alvarez, C. P., Keles, Ö., Kusnyerik, A., Azoulay, T., Hartl, D., Krebs, A. R., Schübeler, D., Hajdu, R. I., Lukats, A.,…Roska, B. (2019). Targeting neuronal and glial cell types with synthetic promoter AAVs in mice, non-human primates and humans. *Nature Neuroscience*, *22*(8), 1345-1356. https://doi.org/10.1038/s41593-019-0431-2

Kadowaki, K., Sugimoto, K., Yamaguchi, F., Song, T., Watanabe, Y., Singh, K., & Tokuda, M. (2004). Phosphohippolin expression in the rat central nervous system. *Molecular Brain Research*, *125*(1), 105-112. https://doi.org/https://doi.org/10.1016/j.molbrainres.2004.03.021

Kauper, K., McGovern, C., Sherman, S., Heatherton, P., Rapoza, R., Stabila, P., Dean, B., Lee, A., Borges, S., Bouchard, B., & Tao, W. (2012). Two-year intraocular delivery of ciliary neurotrophic factor by encapsulated cell technology implants in patients with chronic retinal degenerative diseases. *Invest Ophthalmol Vis Sci*, *53*(12), 7484-7491. https://doi.org/10.1167/iovs.12-9970

Kauper, K., Nystuen, A., Orecchio, L., Gonzalez-Lopez, E., Lee, A., Duncan, J. L., Stewart, J. M., & Aaberg, T., Jr. (2025). Long-Term Durability of Ciliary Neurotrophic Factor-Releasing Revakinagene Taroretcel-lwey in Individuals With Retinal Degenerative Disorders. *Invest Ophthalmol Vis Sci*, *66*(11), 3. https://doi.org/10.1167/iovs.66.11.3

Kedarisetti, K. C., Narayanan, R., Stewart, M. W., Reddy Gurram, N., & Khanani, A. M. (2022). Macular Telangiectasia Type 2: A Comprehensive Review. *Clin Ophthalmol*, *16*, 3297-3309. https://doi.org/10.2147/OPTH.S373538

Kerschensteiner, D., & Feller, M. B. (2024). Mapping the Retina onto the Brain. *Cold Spring Harb Perspect Biol*, *16*(2). https://doi.org/10.1101/cshperspect.a041512

Kessel, L., Christensen, U. C., & Klemp, K. (2022). Inflammation after Voretigene Neparvovec Administration in Patients with RPE65-Related Retinal Dystrophy. *Ophthalmology*, *129*(11), 1287-1293. https://doi.org/10.1016/j.ophtha.2022.06.018

Kessenbrock, K., Fröhlich, L., Sixt, M., Lämmermann, T., Pfister, H., Bateman, A., Belaaouaj, A., Ring, J., Ollert, M., Fässler, R., & Jenne, D. E. (2008). Proteinase 3 and neutrophil elastase enhance inflammation in mice by inactivating antiinflammatory progranulin. *J Clin Invest*, *118*(7), 2438-2447. https://doi.org/10.1172/jci34694

Khaparde, A., Mathias, G. P., Poornachandra, B., Thirumalesh, M. B., Shetty, R., & Ghosh, A. (2024). Gene therapy for retinal diseases: From genetics to treatment. *Indian J Ophthalmol*, *72*(8), 1091-1101. https://doi.org/10.4103/ijo.Ijo_2902_23

Kinoshita, P. F., Orellana, A. M. M., Nakao, V. W., de Souza Port's, N. M., Quintas, L. E. M., Kawamoto, E. M., & Scavone, C. (2022). The Janus face of ouabain in Na+/K+-ATPase and calcium signalling in neurons. *British Journal of Pharmacology*, *179*(8), 1512-1524. https://doi.org/https://doi.org/10.1111/bph.15419

Kirsch, M., Lee, M.-Y., Meyer, V., Wiese, A., & Hofmann, H.-D. (1997). Evidence for Multiple, Local Functions of Ciliary Neurotrophic Factor (CNTF) in Retinal Development: Expression of CNTF and Its Receptor and In Vitro Effects on Target Cells. *Journal of Neurochemistry*, *68*(3), 979-990. https://doi.org/https://doi.org/10.1046/j.1471-4159.1997.68030979.x

Kiser, P. D., Golczak, M., & Palczewski, K. (2014). Chemistry of the Retinoid (Visual) Cycle. *Chemical Reviews*, *114*(1), 194-232. https://doi.org/10.1021/cr400107q

Kishimoto, T. (2005). INTERLEUKIN-6: From Basic Science to Medicine—40 Years in Immunology. *Annual Review of Immunology*, *23*(Volume 23, 2005), 1-21. https://doi.org/https://doi.org/10.1146/annurev.immunol.23.021704.115806

Kishimoto, T., Akira, S., & Taga, T. (1992). IL-6 receptor and mechanism of signal transduction. *Int J Immunopharmacol*, *14*(3), 431-438. https://doi.org/10.1016/0192-0561(92)90173-i

Kleinberger, G., Capell, A., Haass, C., & Van Broeckhoven, C. (2013). Mechanisms of granulin deficiency: lessons from cellular and animal models. *Mol Neurobiol*, *47*(1), 337-360. https://doi.org/10.1007/s12035-012-8380-8

Klimczak, R. R., Koerber, J. T., Dalkara, D., Flannery, J. G., & Schaffer, D. V. (2009). A Novel Adeno-Associated Viral Variant for Efficient and Selective Intravitreal Transduction of Rat Müller Cells. *PLoS One*, *4*(10), e7467. https://doi.org/10.1371/journal.pone.0007467

Kobayashi, H., & Mizisin, A. P. (2000). CNTFR alpha alone or in combination with CNTF promotes macrophage chemotaxis in vitro. *Neuropeptides*, *34*(6), 338-347. https://doi.org/10.1054/npep.2000.0829

Kono, M. (2015). Cone Health and Retinoids. *Prog Mol Biol Transl Sci*, *134*, 465-476. https://doi.org/10.1016/bs.pmbts.2015.06.002

Krishnamoorthi, A., Khosh Abady, K., Dhankhar, D., & Rentzepis, P. M. (2023). Ultrafast Transient Absorption Spectra and Kinetics of Rod and Cone Visual Pigments. *Molecules*, *28*(15), 5829. https://www.mdpi.com/1420-3049/28/15/5829

Kucharska, J., Del Rio, P., Arango-Gonzalez, B., Gorza, M., Feuchtinger, A., Hauck, S. M., & Ueffing, M. (2014). Cyr61 activates retinal cells and prolongs photoreceptor survival in rd1 mouse model of retinitis pigmentosa. *J Neurochem*, *130*(2), 227-240. https://doi.org/10.1111/jnc.12704

Kuse, Y., Tsuruma, K., Sugitani, S., Izawa, H., Ohno, Y., Shimazawa, M., & Hara, H. (2016). Progranulin promotes the retinal precursor cell proliferation and the photoreceptor differentiation in the mouse retina. *Sci Rep*, *6*, 23811. https://doi.org/10.1038/srep23811

Lange, C., Thiersch, M., Samardzija, M., Bürgi, S., Joly, S., & Grimm, C. (2010). LIF-dependent JAK3 activation is not essential for retinal degeneration. *J Neurochem*, *113*(5), 1210-1220. https://doi.org/10.1111/j.1471-4159.2010.06686.x

Larsen, J. V., Hansen, M., Møller, B., Madsen, P., Scheller, J., Nielsen, M., & Petersen, C. M. (2010). Sortilin Facilitates Signaling of Ciliary Neurotrophic Factor and Related Helical Type 1 Cytokines Targeting the gp130/Leukemia Inhibitory Factor Receptor β

Heterodimer. *Molecular and Cellular Biology*, *30*(17), 4175-4187. https://doi.org/10.1128/MCB.00274-10

Laursen, M., Gregersen, J. L., Yatime, L., Nissen, P., & Fedosova, N. U. (2015). Structures and characterization of digoxin- and bufalin-bound Na+,K+-ATPase compared with the ouabain-bound complex. *Proc Natl Acad Sci U S A*, *112*(6), 1755-1760. https://doi.org/10.1073/pnas.1422997112

LaVail, M. M. (1976). Rod outer segment disc shedding in relation to cyclic lighting. *Exp Eye Res*, *23*(2), 277-280. https://doi.org/10.1016/0014-4835(76)90209-8

LaVail, M. M. (1980). Circadian nature of rod outer segment disc shedding in the rat. *Invest Ophthalmol Vis Sci*, *19*(4), 407-411. https://iovs.arvojournals.org/article.aspx?articleid=2159069

LaVail, M. M., Unoki, K., Yasumura, D., Matthes, M. T., Yancopoulos, G. D., & Steinberg, R. H. (1992). Multiple growth factors, cytokines, and neurotrophins rescue photoreceptors from the damaging effects of constant light. *Proc Natl Acad Sci U S A*, *89*(23), 11249-11253. https://doi.org/10.1073/pnas.89.23.11249

LaVail, M. M., Yasumura, D., Matthes, M. T., Lau-Villacorta, C., Unoki, K., Sung, C. H., & Steinberg, R. H. (1998). Protection of mouse photoreceptors by survival factors in retinal degenerations. *Invest Ophthalmol Vis Sci*, *39*(3), 592-602. https://www.ncbi.nlm.nih.gov/pubmed/9501871

Lawrence, J. M., Keegan, D. J., Muir, E. M., Coffey, P. J., Rogers, J. H., Wilby, M. J., Fawcett, J. W., & Lund, R. D. (2004). Transplantation of Schwann cell line clones secreting GDNF or BDNF into the retinas of dystrophic Royal College of Surgeons rats. *Invest Ophthalmol Vis Sci*, *45*(1), 267-274. https://doi.org/10.1167/iovs.03-0093

Leibinger, M., Andreadaki, A., Diekmann, H., & Fischer, D. (2013). Neuronal STAT3 activation is essential for CNTF- and inflammatory stimulation-induced CNS axon regeneration. *Cell Death Dis*, *4*(9), e805. https://doi.org/10.1038/cddis.2013.310

Leibinger, M., Andreadaki, A., Gobrecht, P., Levin, E., Diekmann, H., & Fischer, D. (2016). Boosting Central Nervous System Axon Regeneration by Circumventing Limitations of Natural Cytokine Signaling. *Mol Ther*, *24*(10), 1712-1725. https://doi.org/10.1038/mt.2016.102

Leibinger, M., Müller, A., Andreadaki, A., Hauk, T. G., Kirsch, M., & Fischer, D. (2009). Neuroprotective and axon growth-promoting effects following inflammatory stimulation on mature retinal ganglion cells in mice depend on ciliary neurotrophic factor and leukemia inhibitory factor. *J Neurosci*, *29*(45), 14334-14341. https://doi.org/10.1523/jneurosci.2770-09.2009

Leibinger, M., Muller, A., Gobrecht, P., Diekmann, H., Andreadaki, A., & Fischer, D. (2013). Interleukin-6 contributes to CNS axon regeneration upon inflammatory stimulation. *Cell Death Dis*, *4*(4), e609. https://doi.org/10.1038/cddis.2013.126

Li, J., Shang, G., Chen, Y.-J., Brautigam, C. A., Liou, J., Zhang, X., & Bai, X.-c. (2019). Cryo-EM analyses reveal the common mechanism and diversification in the activation of RET by different ligands. *Elife*, *8*, e47650. https://doi.org/10.7554/eLife.47650

Li, K., Cai, J., Jiang, Z., Meng, Q., Meng, Z., Xiao, H., Chen, G., Qiao, C., Luo, L., Yu, J., Li, X., Wei, Y., Li, H., Liu, C., Shen, B., Wang, J., & Feng, J. (2024). Unveiling novel insights into human IL-6 − IL-6R interaction sites through 3D computer-guided docking and systematic site mutagenesis. *Scientific Reports*, *14*(1), 18293. https://doi.org/10.1038/s41598-024-69429-w

Li, S., Sato, K., Gordon, W. C., Sendtner, M., Bazan, N. G., & Jin, M. (2018). Ciliary neurotrophic factor (CNTF) protects retinal cone and rod photoreceptors by suppressing excessive formation of the visual pigments. *J Biol Chem*, *293*(39), 15256-15268. https://doi.org/10.1074/jbc.RA118.004008

Li, Y., Tao, W., Luo, L., Huang, D., Kauper, K., Stabila, P., Lavail, M. M., Laties, A. M., & Wen, R. (2010). CNTF induces regeneration of cone outer segments in a rat model of retinal degeneration. *PLoS One*, *5*(3), e9495. https://doi.org/10.1371/journal.pone.0009495

Liang, F.-Q., Aleman, T. S., Dejneka, N. S., Dudus, L., Fisher, K. J., Maguire, A. M., Jacobson, S. G., & Bennett, J. (2001). Long-Term Protection of Retinal Structure but Not Function Using RAAV.CNTF in Animal Models of Retinitis Pigmentosa. *Molecular Therapy*, *4*(5), 461-472. https://doi.org/https://doi.org/10.1006/mthe.2001.0473

Life, B. E., & Leavitt, B. R. (2025). Progranulin function and regulation in the CNS. *Trends Neurosci*, *48*(7), 523-537. https://doi.org/10.1016/j.tins.2025.05.004

Lipinski, D. M., Singh, M. S., & MacLaren, R. E. (2011). Assessment of cone survival in response to CNTF, GDNF, and VEGF165b in a novel ex vivo model of end-stage retinitis

pigmentosa. *Invest Ophthalmol Vis Sci*, *52*(10), 7340-7346. https://doi.org/10.1167/iovs.11-7996

Liu, J., Bassal, M., Schlichting, S., Braren, I., Di Spiezio, A., Saftig, P., & Bartsch, U. (2022). Intravitreal gene therapy restores the autophagy-lysosomal pathway and attenuates retinal degeneration in cathepsin D-deficient mice. *Neurobiol Dis*, *164*, 105628. https://doi.org/10.1016/j.nbd.2022.105628

London, A., Itskovich, E., Benhar, I., Kalchenko, V., Mack, M., Jung, S., & Schwartz, M. (2011). Neuroprotection and progenitor cell renewal in the injured adult murine retina requires healing monocyte-derived macrophages. *J Exp Med*, *208*(1), 23-39. https://doi.org/10.1084/jem.20101202

Lu, Q., & Pan, Z.-H. (2021). Optogenetic Strategies for Vision Restoration. In H. Yawo, H. Kandori, A. Koizumi, & R. Kageyama (Eds.), *Optogenetics: Light-Sensing Proteins and Their Applications in Neuroscience and Beyond* (pp. 545-555). Springer Singapore. https://doi.org/10.1007/978-981-15-8763-4_38

Lu, Y., Belin, S., & He, Z. (2014). Signaling regulations of neuronal regenerative ability. *Curr Opin Neurobiol*, *27*, 135-142. https://doi.org/10.1016/j.conb.2014.03.007

Lundborg, C., Westerlund, A., Björklund, U., Biber, B., & Hansson, E. (2011). Ifenprodil restores GDNF-evoked Ca(2+) signalling and Na(+)/K(+) -ATPase expression in inflammation-pretreated astrocytes. *J Neurochem*, *119*(4), 686-696. https://doi.org/10.1111/j.1471-4159.2011.07465.x

Lv, J., Gao, R., Wang, Y., Huang, C., & Wu, R. (2023). Protective effect of leukemia inhibitory factor on the retinal injury induced by acute ocular hypertension in rats. *Exp Ther Med*, *25*(1), 19. https://doi.org/10.3892/etm.2022.11717

Mackenzie, I. R., Neumann, M., Bigio, E. H., Cairns, N. J., Alafuzoff, I., Kril, J., Kovacs, G. G., Ghetti, B., Halliday, G., Holm, I. E., Ince, P. G., Kamphorst, W., Revesz, T., Rozemuller, A. J., Kumar-Singh, S., Akiyama, H., Baborie, A., Spina, S., Dickson, D. W.,…Mann, D. M. (2009). Nomenclature for neuropathologic subtypes of frontotemporal lobar degeneration: consensus recommendations. *Acta Neuropathol*, *117*(1), 15-18. https://doi.org/10.1007/s00401-008-0460-5

Macosko, E. Z., Basu, A., Satija, R., Nemesh, J., Shekhar, K., Goldman, M., Tirosh, I., Bialas, A. R., Kamitaki, N., Martersteck, E. M., Trombetta, J. J., Weitz, D. A., Sanes, J. R., Shalek, A. K., Regev, A., & McCarroll, S. A. (2015). Highly Parallel Genome-wide Expression Profiling of Individual Cells Using Nanoliter Droplets. *Cell*, *161*(5), 1202-1214. https://doi.org/10.1016/j.cell.2015.05.002

Maguire, A. M., Russell, S., Chung, D. C., Yu, Z.-F., Tillman, A., Drack, A. V., Simonelli, F., Leroy, B. P., Reape, K. Z., High, K. A., & Bennett, J. (2021). Durability of Voretigene Neparvovec for Biallelic RPE65-Mediated Inherited Retinal Disease: Phase 3 Results at 3 and 4 Years. *Ophthalmology*, *128*(10), 1460-1468. https://doi.org/https://doi.org/10.1016/j.ophtha.2021.03.031

Maguire, A. M., Russell, S., Wellman, J. A., Chung, D. C., Yu, Z.-F., Tillman, A., Wittes, J., Pappas, J., Elci, O., Marshall, K. A., McCague, S., Reichert, H., Davis, M., Simonelli, F., Leroy, B. P., Wright, J. F., High, K. A., & Bennett, J. (2019). Efficacy, Safety, and Durability of Voretigene Neparvovec-rzyl in RPE65 Mutation–Associated Inherited Retinal Dystrophy: Results of Phase 1 and 3 Trials. *Ophthalmology*, *126*(9), 1273-1285. https://doi.org/https://doi.org/10.1016/j.ophtha.2019.06.017

Magyar, J. P., Bartsch, U., Wang, Z. Q., Howells, N., Aguzzi, A., Wagner, E. F., & Schachner, M. (1994). Degeneration of neural cells in the central nervous system of mice deficient in the gene for the adhesion molecule on Glia, the beta 2 subunit of murine Na,K-ATPase. *J Cell Biol*, *127*(3), 835-845. https://doi.org/10.1083/jcb.127.3.835

Mahato, A. K., & Sidorova, Y. A. (2020). RET Receptor Tyrosine Kinase: Role in Neurodegeneration, Obesity, and Cancer. *Int J Mol Sci*, *21*(19). https://doi.org/10.3390/ijms21197108

Martin-Vasallo, P., Dackowski, W., Emanuel, J. R., & Levenson, R. (1989). Identification of a putative isoform of the Na,K-ATPase beta subunit. Primary structure and tissue-specific expression. *J Biol Chem*, *264*(8), 4613-4618.

Masland, R. H. (2012). The neuronal organization of the retina. *Neuron*, *76*(2), 266-280. https://doi.org/10.1016/j.neuron.2012.10.002

Mata, N. L., Radu, R. A., Clemmons, R. S., & Travis, G. H. (2002). Isomerization and Oxidation of Vitamin A in Cone-Dominant Retinas: A Novel Pathway for Visual-Pigment Regeneration in Daylight. *Neuron*, *36*(1), 69-80. https://doi.org/https://doi.org/10.1016/S0896-6273(02)00912-1

Mata, N. L., Weng, J., & Travis, G. H. (2000). Biosynthesis of a major lipofuscin fluorophore in mice and humans with ABCR-mediated retinal and macular degeneration. *Proceedings of the National Academy of Sciences*, *97*(13), 7154-7159. https://doi.org/doi:10.1073/pnas.130110497

Maude, S., & Barrett, D. M. (2016). Current status of chimeric antigen receptor therapy for haematological malignancies. *British Journal of Haematology*, *172*(1), 11-22. https://doi.org/https://doi.org/10.1111/bjh.13792

Mays, L. E., Wang, L., Lin, J., Bell, P., Crawford, A., Wherry, E. J., & Wilson, J. M. (2014). AAV8 Induces Tolerance in Murine Muscle as a Result of Poor APC Transduction, T Cell Exhaustion, and Minimal MHCI Upregulation on Target Cells. *Molecular Therapy*, *22*(1), 28-41. https://doi.org/https://doi.org/10.1038/mt.2013.134

McColm, J. R., Geisen, P., Peterson, L. J., & Hartnett, M. E. (2006). Exogenous leukemia inhibitory factor (LIF) attenuates retinal vascularization reducing cell proliferation not apoptosis. *Exp Eye Res*, *83*(2), 438-446. https://doi.org/10.1016/j.exer.2006.01.027

McGee Sanftner, L. H., Abel, H., Hauswirth, W. W., & Flannery, J. G. (2001). Glial cell line derived neurotrophic factor delays photoreceptor degeneration in a transgenic rat model of retinitis pigmentosa. *Mol Ther*, *4*(6), 622-629. https://doi.org/10.1006/mthe.2001.0498

McGill, T. J., Prusky, G. T., Douglas, R. M., Yasumura, D., Matthes, M. T., Nune, G., Donohue-Rolfe, K., Yang, H., Niculescu, D., Hauswirth, W. W., Girman, S. V., Lund, R. D., Duncan, J. L., & LaVail, M. M. (2007). Intraocular CNTF reduces vision in normal rats in a dose-dependent manner. *Invest Ophthalmol Vis Sci*, *48*(12), 5756-5766. https://doi.org/10.1167/iovs.07-0054

McLaughlin, M. E., Sandberg, M. A., Berson, E. L., & Dryja, T. P. (1993). Recessive mutations in the gene encoding the beta-subunit of rod phosphodiesterase in patients with retinitis pigmentosa. *Nat Genet*, *4*(2), 130-134. https://doi.org/10.1038/ng0693-130

Mehta, P., McAuley, D. F., Brown, M., Sanchez, E., Tattersall, R. S., & Manson, J. J. (2020). COVID-19: consider cytokine storm syndromes and immunosuppression. *The Lancet*, *395*(10229), 1033-1034.

Metcalf, D. (1990). The induction and inhibition of differentiation in normal and leukaemic cells. *Philos Trans R Soc Lond B Biol Sci*, *327*(1239), 99-109. https://doi.org/10.1098/rstb.1990.0046

Meyer, D. J., Bijlani, S., de Sautu, M., Spontarelli, K., Young, V. C., Gatto, C., & Artigas, P. (2020). FXYD protein isoforms differentially modulate human Na/K pump function. *Journal of General Physiology*, *152*(12). https://doi.org/10.1085/jgp.202012660

Millrine, D., Jenkins, R. H., Hughes, S. T. O., & Jones, S. A. (2022). Making sense of IL-6 signalling cues in pathophysiology. *FEBS Lett*, *596*(5), 567-588. https://doi.org/10.1002/1873-3468.14201

Mishra, N. K., Peleg, Y., Cirri, E., Belogus, T., Lifshitz, Y., Voelker, D. R., Apell, H. J., Garty, H., & Karlish, S. J. (2011). FXYD proteins stabilize Na,K-ATPase: amplification of specific phosphatidylserine-protein interactions. *J Biol Chem*, *286*(11), 9699-9712. https://doi.org/10.1074/jbc.M110.184234

Molday, L. L., Wu, W. W., & Molday, R. S. (2007). Retinoschisin (RS1), the protein encoded by the X-linked retinoschisis gene, is anchored to the surface of retinal photoreceptor and bipolar cells through its interactions with a Na/K ATPase-SARM1 complex. *J Biol Chem*, *282*(45), 32792-32801. https://doi.org/10.1074/jbc.M706321200

Molday, R. S. (2007). Focus on molecules: retinoschisin (RS1). *Exp Eye Res*, *84*(2), 227-228. https://doi.org/10.1016/j.exer.2005.12.013

Molthagen, M., Schachner, M., & Bartsch, U. (1996). Apoptotic cell death of photoreceptor cells in mice deficient for the adhesion molecule on glia (AMOG, the beta 2- subunit of the Na, K-ATPase). *J Neurocytol*, *25*(4), 243-255. https://doi.org/10.1007/bf02284800

Moseley, A. E., Williams, M. T., Schaefer, T. L., Bohanan, C. S., Neumann, J. C., Behbehani, M. M., Vorhees, C. V., & Lingrel, J. B. (2007). Deficiency in Na,K-ATPase alpha isoform genes alters spatial learning, motor activity, and anxiety in mice. *J Neurosci*, *27*(3), 616-626. https://doi.org/10.1523/jneurosci.4464-06.2007

Mosmann, T. R., Cherwinski, H., Bond, M. W., Giedlin, M. A., & Coffman, R. L. (1986). Two types of murine helper T cell clone. I. Definition according to profiles of lymphokine activities and secreted proteins. *J Immunol*, *136*(7), 2348-2357.

Müller-Husmann, G., Gloor, S., & Schachner, M. (1993). Functional characterization of beta isoforms of murine Na,K-ATPase. The adhesion molecule on glia (AMOG/beta 2), but not beta 1, promotes neurite outgrowth. *J Biol Chem*, *268*(35), 26260-26267. https://www.sciencedirect.com/science/article/pii/S0021925819743099?via%3Dihub

Muller, A., Hauk, T. G., Leibinger, M., Marienfeld, R., & Fischer, D. (2009). Exogenous CNTF stimulates axon regeneration of retinal ganglion cells partially via endogenous CNTF. *Mol Cell Neurosci*, *41*(2), 233-246. https://doi.org/10.1016/j.mcn.2009.03.002

Murakami, M., Hibi, M., Nakagawa, N., Nakagawa, T., Yasukawa, K., Yamanishi, K., Taga, T., & Kishimoto, T. (1993). IL-6-induced homodimerization of gp130 and associated activation of a tyrosine kinase. *Science*, *260*(5115), 1808-1810. https://doi.org/10.1126/science.8511589

Murakami, M., Kamimura, D., & Hirano, T. (2004). New IL-6 (gp130) family cytokine members, CLC/NNT1/BSF3 and IL-27. *Growth Factors*, *22*(2), 75-77. https://doi.org/10.1080/08977190410001715181

Naso, M. F., Tomkowicz, B., Perry, W. L., 3rd, & Strohl, W. R. (2017). Adeno-Associated Virus (AAV) as a Vector for Gene Therapy. *BioDrugs*, *31*(4), 317-334. https://doi.org/10.1007/s40259-017-0234-5

Nasonov, E., & Samsonov, M. (2020). The role of Interleukin 6 inhibitors in therapy of severe COVID-19. *Biomedicine & Pharmacotherapy*, *131*, 110698. https://doi.org/https://doi.org/10.1016/j.biopha.2020.110698

Nebbioso, M., Artico, M., Gharbiya, M., Mannocci, A., Limoli, P. G., Iannetta, D., & Donato, L. (2025). State of the Art on Inherited Retinal Dystrophies: Management and Molecular Genetics. *Journal of Clinical Medicine*, *14*(10), 3526. https://www.mdpi.com/2077-0383/14/10/3526

Neuray, C., Sultan, T., Alvi, J. R., Franca, M. C., Jr, Assmann, B., Wagner, M., Canafoglia, L., Franceschetti, S., Rossi, G., Santana, I., Macario, M. C., Almeida, M. R., Kamate, M., Parikh, S., Elloumi, H. Z., Murphy, D., Efthymiou, S., Maroofian, R., & Houlden, H. (2020). Early-onset phenotype of bi-allelic GRN mutations. *Brain*, *144*(2), e22-e22. https://doi.org/10.1093/brain/awaa414

Noh, M. Y., Kwon, H. S., Kwon, M. S., Nahm, M., Jin, H. K., Bae, J. S., & Kim, S. H. (2025). Biomarkers and therapeutic strategies targeting microglia in neurodegenerative diseases: current status and future directions. *Mol Neurodegener*, *20*(1), 82. https://doi.org/10.1186/s13024-025-00867-4

Nozaki, C., Asai, N., Murakami, H., Iwashita, T., Iwata, Y., Horibe, K., Klein, R. D., Rosenthal, A., & Takahashi, M. (1998). Calcium-dependent Ret activation by GDNF and neurturin. *Oncogene*, *16*(3), 293-299. https://doi.org/10.1038/sj.onc.1201548

O'Shea, J. J., & Murray, P. J. (2008). Cytokine signaling modules in inflammatory responses. *Immunity*, *28*(4), 477-487. https://doi.org/10.1016/j.immuni.2008.03.002

Oh, H., Fujio, Y., Kunisada, K., Hirota, H., Matsui, H., Kishimoto, T., & Yamauchi-Takihara, K. (1998). Activation of phosphatidylinositol 3-kinase through glycoprotein 130 induces protein kinase B and p70 S6 kinase phosphorylation in cardiac myocytes. *J Biol Chem*, *273*(16), 9703-9710. https://doi.org/10.1074/jbc.273.16.9703

Ohnaka, M., Miki, K., Gong, Y. Y., Stevens, R., Iwase, T., Hackett, S. F., & Campochiaro, P. A. (2012). Long-term expression of glial cell line-derived neurotrophic factor slows, but does not stop retinal degeneration in a model of retinitis pigmentosa. *J Neurochem*, *122*(5), 1047-1053. https://doi.org/10.1111/j.1471-4159.2012.07842.x

Okawa, H., Sampath, A. P., Laughlin, S. B., & Fain, G. L. (2008). ATP consumption by mammalian rod photoreceptors in darkness and in light. *Curr Biol*, *18*(24), 1917-1921. https://doi.org/10.1016/j.cub.2008.10.029

Okuda, Y., Sakoda, S., Bernard, C. C., Fujimura, H., Saeki, Y., Kishimoto, T., & Yanagihara, T. (1998). IL-6-deficient mice are resistant to the induction of experimental autoimmune encephalomyelitis provoked by myelin oligodendrocyte glycoprotein. *International Immunology*, *10*(5), 703-708. https://doi.org/10.1093/intimm/10.5.703

Omodaka, K., Kurimoto, T., Nakamura, O., Sato, K., Yasuda, M., Tanaka, Y., Himori, N., Yokoyama, Y., & Nakazawa, T. (2014). Artemin augments survival and axon regeneration in axotomized retinal ganglion cells. *J Neurosci Res*, *92*(12), 1637-1646. https://doi.org/10.1002/jnr.23449

Orphanet. (2024). *Prevalence of rare diseases: Bibliographic data, Number 2: Diseases listed by decreasing prevalence, incidences or number of published cases* (2). (Orphanet Report Series, Rare Diseases Collection, Issue. http://www.orpha.net/orphacom/cahiers/docs/GB/Prevalence_of_rare_diseases_by_decreasing_prevalence_or_cases.pdf

Osakada, F., Ooto, S., Akagi, T., Mandai, M., Akaike, A., & Takahashi, M. (2007). Wnt signaling promotes regeneration in the retina of adult mammals. *J Neurosci*, *27*(15), 4210-4219. https://doi.org/10.1523/jneurosci.4193-06.2007

Otani, A., Dorrell, M. I., Kinder, K., Moreno, S. K., Nusinowitz, S., Banin, E., Heckenlively, J., & Friedlander, M. (2004). Rescue of retinal degeneration by intravitreally injected adult bone marrow-derived lineage-negative hematopoietic stem cells. *J Clin Invest*, *114*(6), 765-774. https://doi.org/10.1172/jci21686

Páez, O., Martínez-Archundia, M., Villegas-Sepúlveda, N., Roldan, M. L., Correa-Basurto, J., & Shoshani, L. (2019). A Model for the Homotypic Interaction between Na+,K+-ATPase β1 Subunits Reveals the Role of Extracellular Residues 221–229 in Its Ig-Like Domain. *International Journal of Molecular Sciences*, *20*(18), 4538. https://www.mdpi.com/1422-0067/20/18/4538

https://pmc.ncbi.nlm.nih.gov/articles/PMC6770782/

Paratcha, G., & Ibáñez, C. F. (2002). Lipid rafts and the control of neurotrophic factor signaling in the nervous system: variations on a theme. *Current Opinion in Neurobiology*, *12*(5), 542-549. https://doi.org/https://doi.org/10.1016/S0959-4388(02)00363-X

Paratcha, G., & Ledda, F. (2008). GDNF and GFRalpha: a versatile molecular complex for developing neurons. *Trends Neurosci*, *31*(8), 384-391. https://doi.org/10.1016/j.tins.2008.05.003

Paratcha, G., Ledda, F., Baars, L., Coulpier, M., Besset, V., Anders, J., Scott, R., & Ibáñez, C. F. (2001). Released GFRalpha1 potentiates downstream signaling, neuronal survival, and differentiation via a novel mechanism of recruitment of c-Ret to lipid rafts. *Neuron*, *29*(1), 171-184. https://doi.org/10.1016/s0896-6273(01)00188-x

Park, K. K., Hu, Y., Muhling, J., Pollett, M. A., Dallimore, E. J., Turnley, A. M., Cui, Q., & Harvey, A. R. (2009). Cytokine-induced SOCS expression is inhibited by cAMP analogue: impact on regeneration in injured retina. *Mol Cell Neurosci*, *41*(3), 313-324. https://doi.org/10.1016/j.mcn.2009.04.002

Park, K. K., Liu, K., Hu, Y., Smith, P. D., Wang, C., Cai, B., Xu, B., Connolly, L., Kramvis, I., Sahin, M., & He, Z. (2008). Promoting axon regeneration in the adult CNS by modulation of the PTEN/mTOR pathway. *Science*, *322*(5903), 963-966. https://doi.org/10.1126/science.1161566

Paushter, D. H., Du, H., Feng, T., & Hu, F. (2018). The lysosomal function of progranulin, a guardian against neurodegeneration. *Acta Neuropathol*, *136*(1), 1-17. https://doi.org/10.1007/s00401-018-1861-8

Pedersen, B. K., & Febbraio, M. A. (2012). Muscles, exercise and obesity: skeletal muscle as a secretory organ. *Nature Reviews Endocrinology*, *8*(8), 457-465. https://doi.org/10.1038/nrendo.2012.49

Pellissier, L. P., Hoek, R. M., Vos, R. M., Aartsen, W. M., Klimczak, R. R., Hoyng, S. A., Flannery, J. G., & Wijnholds, J. (2014). Specific tools for targeting and expression in Müller glial cells. *Molecular Therapy Methods & Clinical Development*, *1*. https://doi.org/10.1038/mtm.2014.9

Peng, Y.-R. (2023). Cell-type specification in the retina: Recent discoveries from transcriptomic approaches. *Current Opinion in Neurobiology*, *81*, 102752. https://doi.org/https://doi.org/10.1016/j.conb.2023.102752

Pennesi, M. E., Michaels, K. V., Magee, S. S., Maricle, A., Davin, S. P., Garg, A. K., Gale, M. J., Tu, D. C., Wen, Y., Erker, L. R., & Francis, P. J. (2012). Long-Term Characterization of Retinal Degeneration in rd1 and rd10 Mice Using Spectral Domain Optical Coherence Tomography. *Investigative Ophthalmology & Visual Science*, *53*(8), 4644-4656. https://doi.org/10.1167/iovs.12-9611

Peters, M., Blinn, G., Solem, F., Fischer, M., Meyer zum Büschenfelde, K. H., & Rose-John, S. (1998). In vivo and in vitro activities of the gp130-stimulating designer cytokine Hyper-IL-6. *J Immunol*, *161*(7), 3575-3581.

Peters, M., Jacobs, S., Ehlers, M., Vollmer, P., Müllberg, J., Wolf, E., Brem, G., Meyer zum Büschenfelde, K. H., & Rose-John, S. (1996). The function of the soluble interleukin 6 (IL-6) receptor in vivo: sensitization of human soluble IL-6 receptor transgenic mice towards IL-6 and prolongation of the plasma half-life of IL-6. *J Exp Med*, *183*(4), 1399-1406. https://doi.org/10.1084/jem.183.4.1399

Petkau, T. L., Neal, S. J., Orban, P. C., MacDonald, J. L., Hill, A. M., Lu, G., Feldman, H. H., Mackenzie, I. R. A., & Leavitt, B. R. (2010). Progranulin expression in the developing and adult murine brain. *Journal of Comparative Neurology*, *518*(19), 3931-3947. https://doi.org/https://doi.org/10.1002/cne.22430

Plossl, K., Straub, K., Schmid, V., Strunz, F., Wild, J., Merkl, R., Weber, B. H. F., & Friedrich, U. (2019). Identification of the retinoschisin-binding site on the retinal Na/K-ATPase. *PLoS One*, *14*(5), e0216320. https://doi.org/10.1371/journal.pone.0216320

Plossl, K., Weber, B. H., & Friedrich, U. (2017). The X-linked juvenile retinoschisis protein retinoschisin is a novel regulator of mitogen-activated protein kinase signalling and apoptosis in the retina. *J Cell Mol Med*, *21*(4), 768-780. https://doi.org/10.1111/jcmm.13019

Pollard, S. M., Conti, L., Sun, Y., Goffredo, D., & Smith, A. (2006). Adherent neural stem (NS) cells from fetal and adult forebrain. *Cereb Cortex*, *16 Suppl 1*, i112-120. https://doi.org/10.1093/cercor/bhj167

Pressmar, S., Ader, M., Richard, G., Schachner, M., & Bartsch, U. (2001). The fate of heterotopically grafted neural precursor cells in the normal and dystrophic adult mouse retina. *Invest Ophthalmol Vis Sci*, *42*(13), 3311-3319.

Prinz, M., Masuda, T., Wheeler, M. A., & Quintana, F. J. (2021). Microglia and Central Nervous System-Associated Macrophages-From Origin to Disease Modulation. *Annu Rev Immunol*, *39*, 251-277. https://doi.org/10.1146/annurev-immunol-093019-110159

Rajasekaran, S. A., Palmer, L. G., Moon, S. Y., Peralta Soler, A., Apodaca, G. L., Harper, J. F., Zheng, Y., & Rajasekaran, A. K. (2001). Na,K-ATPase activity is required for formation of tight junctions, desmosomes, and induction of polarity in epithelial cells. *Mol Biol Cell*, *12*(12), 3717-3732. https://doi.org/10.1091/mbc.12.12.3717

Ramon y Cajal, S. (1928). *Degeneration and regeneration of the nervous system*. Clarendon Press.

Ransohoff, R. M. (2016). A polarizing question: do M1 and M2 microglia exist? *Nat Neurosci*, *19*(8), 987-991. https://doi.org/10.1038/nn.4338

Rashid, K., Akhtar-Schaefer, I., & Langmann, T. (2019). Microglia in Retinal Degeneration. *Front Immunol*, *10*, 1975. https://doi.org/10.3389/fimmu.2019.01975

Rashid, K., Wolf, A., & Langmann, T. (2018). Microglia Activation and Immunomodulatory Therapies for Retinal Degenerations. *Front Cell Neurosci*, *12*, 176. https://doi.org/10.3389/fncel.2018.00176

Rebelo Neves, E., Carvalho, A. L., Mesquita, T., Paiva, C., Alfaiate, M., Figueira, J., Murta, J., & Marques, J. P. (2023). Bilateral functional worsening following voretigene neparvovec therapy. *Eye (Lond)*, *37*(13), 2828-2829. https://doi.org/10.1038/s41433-023-02411-4

Reichenbach, A., & Bringmann, A. (2020). Glia of the human retina. *Glia*, *68*(4), 768-796. https://doi.org/10.1002/glia.23727

Remmer, M. H., Rastogi, N., Ranka, M. P., & Ceisler, E. J. (2015). Achromatopsia: a review. *Current Opinion in Ophthalmology*, *26*(5), 333-340. https://doi.org/10.1097/icu.0000000000000189

Rex, T. S., Allocca, M., Domenici, L., Surace, E. M., Maguire, A. M., Lyubarsky, A., Cellerino, A., Bennett, J., & Auricchio, A. (2004). Systemic but not intraocular Epo gene transfer protects the retina from light-and genetic-induced degeneration. *Mol Ther*, *10*(5), 855-861. https://doi.org/10.1016/j.ymthe.2004.07.027

Rhee, K. D., Nusinowitz, S., Chao, K., Yu, F., Bok, D., & Yang, X. J. (2013). CNTF-mediated protection of photoreceptors requires initial activation of the cytokine receptor gp130 in Muller glial cells. *Proc Natl Acad Sci U S A*, *110*(47), E4520-4529. https://doi.org/10.1073/pnas.1303604110

Rhee, K. D., Ruiz, A., Duncan, J. L., Hauswirth, W. W., Lavail, M. M., Bok, D., & Yang, X. J. (2007). Molecular and cellular alterations induced by sustained expression of ciliary neurotrophic factor in a mouse model of retinitis pigmentosa. *Invest Ophthalmol Vis Sci*, *48*(3), 1389-1400. https://doi.org/10.1167/iovs.06-0677

Rhee, K. D., & Yang, X. J. (2003). Expression of cytokine signal transduction components in the postnatal mouse retina. *Mol Vis*, *9*, 715-722. https://www.ncbi.nlm.nih.gov/pubmed/14685141

Rodieck, R. W. (1998). *The first steps in seeing*. Sinauer Associates.

Roldán, M. L., Ramírez-Salinas, G. L., Martinez-Archundia, M., Cuellar-Perez, F., Vilchis-Nestor, C. A., Cancino-Diaz, J. C., & Shoshani, L. (2022). The β(2)-Subunit (AMOG) of Human Na(+), K(+)-ATPase Is a Homophilic Adhesion Molecule. *Int J Mol Sci*, *23*(14). https://doi.org/10.3390/ijms23147753

Rose-John, S. (2020). Interleukin-6 signalling in health and disease. *F1000Res*, *9*. https://doi.org/10.12688/f1000research.26058.1

Rose-John, S., & Heinrich, P. C. (1994). Soluble receptors for cytokines and growth factors: generation and biological function. *Biochem J*, *300 (Pt 2)*(Pt 2), 281-290. https://doi.org/10.1042/bj3000281

Rose-John, S., Jenkins, B. J., Garbers, C., Moll, J. M., & Scheller, J. (2023). Targeting IL-6 trans-signalling: past, present and future prospects. *Nature Reviews Immunology*, *23*(10), 666-681. https://doi.org/10.1038/s41577-023-00856-y

Rose-John, S., Schooltink, H., Schmitz-Van de Leur, H., Müllberg, J., Heinrich, P. C., & Graeve, L. (1993). Intracellular retention of interleukin-6 abrogates signaling. *J Biol Chem*, *268*(29), 22084-22091. https://www.sciencedirect.com/science/article/pii/S0021925820806516?via%3Dihub

Rothaug, M., Becker-Pauly, C., & Rose-John, S. (2016). The role of interleukin-6 signaling in nervous tissue. *Biochimica et Biophysica Acta (BBA) - Molecular Cell Research*, *1863*(6, Part A), 1218-1227. https://doi.org/https://doi.org/10.1016/j.bbamcr.2016.03.018

Russell, S., Bennett, J., Wellman, J. A., Chung, D. C., Yu, Z.-F., Tillman, A., Wittes, J., Pappas, J., Elci, O., McCague, S., Cross, D., Marshall, K. A., Walshire, J., Kehoe, T. L., Reichert, H., Davis, M., Raffini, L., George, L. A., Hudson, F. P.,…Maguire, A. M. (2017). Efficacy and safety of voretigene neparvovec (AAV2-hRPE65v2) in patients with RPE65-mediated inherited retinal dystrophy: a randomised, controlled, open-label, phase 3 trial. *The Lancet*, *390*(10097), 849-860. https://doi.org/https://doi.org/10.1016/S0140-6736(17)31868-8

Sahel, J. A., Boulanger-Scemama, E., Pagot, C., Arleo, A., Galluppi, F., Martel, J. N., Esposti, S. D., Delaux, A., de Saint Aubert, J. B., de Montleau, C., Gutman, E., Audo, I., Duebel, J., Picaud, S., Dalkara, D., Blouin, L., Taiel, M., & Roska, B. (2021). Partial recovery of visual function in a blind patient after optogenetic therapy. *Nat Med*, *27*(7), 1223-1229. https://doi.org/10.1038/s41591-021-01351-4

Saito, M., Yoshida, K., Hibi, M., Taga, T., & Kishimoto, T. (1992). Molecular cloning of a murine IL-6 receptor-associated signal transducer, gp130, and its regulated expression in vivo. *J Immunol*, *148*(12), 4066-4071.

Samardzija, M., Wariwoda, H., Imsand, C., Huber, P., Heynen, S. R., Gubler, A., & Grimm, C. (2012). Activation of survival pathways in the degenerating retina of rd10 mice. *Exp Eye Res*, *99*, 17-26. https://doi.org/10.1016/j.exer.2012.04.004

Samardzija, M., Wenzel, A., Aufenberg, S., Thiersch, M., Remé, C., & Grimm, C. (2006). Differential role of Jak-STAT signaling in retinal degenerations. *FASEB J*, *20*(13), 2411-2413. https://doi.org/10.1096/fj.06-5895fje

Sanes, J. R., & Masland, R. H. (2015). The Types of Retinal Ganglion Cells: Current Status and Implications for Neuronal Classification. *Annual Review of Neuroscience*, *38*(Volume 38, 2015), 221-246. https://doi.org/https://doi.org/10.1146/annurev-neuro-071714-034120

Sato, S., & Kefalov, V. J. (2024). The Retina-Based Visual Cycle. *Annu Rev Vis Sci*, *10*(1), 293-321. https://doi.org/10.1146/annurev-vision-100820-083937

Schindelin, J., Arganda-Carreras, I., Frise, E., Kaynig, V., Longair, M., Pietzsch, T., Preibisch, S., Rueden, C., Saalfeld, S., Schmid, B., Tinevez, J.-Y., White, D. J., Hartenstein, V., Eliceiri, K., Tomancak, P., & Cardona, A. (2012). Fiji: an open-source platform for biological-image analysis. *Nature Methods*, *9*(7), 676-682. https://doi.org/10.1038/nmeth.2019

Schlichtenbrede, F. C., MacNeil, A., Bainbridge, J. W., Tschernutter, M., Thrasher, A. J., Smith, A. J., & Ali, R. R. (2003). Intraocular gene delivery of ciliary neurotrophic factor results in significant loss of retinal function in normal mice and in the Prph2Rd2/Rd2 model of retinal degeneration. *Gene Ther*, *10*(6), 523-527. https://doi.org/10.1038/sj.gt.3301929

Schmalzing, G., Kröner, S., Schachner, M., & Gloor, S. (1992). The adhesion molecule on glia (AMOG/beta 2) and alpha 1 subunits assemble to functional sodium pumps in Xenopus oocytes. *J Biol Chem*, *267*(28), 20212-20216. https://www.sciencedirect.com/science/article/pii/S002192581988688X?via%3Dihub

Schmid, V., Wurzel, A., Wetzel, C. H., Plossl, K., Bruckmann, A., Luckner, P., Weber, B. H. F., & Friedrich, U. (2022). Retinoschisin and novel Na/K-ATPase interaction partners Kv2.1 and Kv8.2 define a growing protein complex at the inner segments of mammalian photoreceptors. *Cell Mol Life Sci*, *79*(8), 448. https://doi.org/10.1007/s00018-022-04409-9

Schnapf, J. L., Nunn, B. J., Meister, M., & Baylor, D. A. (1990). Visual transduction in cones of the monkey Macaca fascicularis. *The Journal of Physiology*, *427*(1), 681-713. https://doi.org/https://doi.org/10.1113/jphysiol.1990.sp018193

Schneider, B. G., & Kraig, E. (1990). Na+, K(+)-ATPase of the photoreceptor: selective expression of alpha 3 and beta 2 isoforms. *Exp Eye Res*, *51*(5), 553-564. https://doi.org/10.1016/0014-4835(90)90086-a

Schneider, B. G., Shyjan, A. W., & Levenson, R. (1991). Co-localization and polarized distribution of Na,K-ATPase alpha 3 and beta 2 subunits in photoreceptor cells. *J Histochem Cytochem*, *39*(4), 507-517. https://doi.org/10.1177/39.4.1848572

Schneider, N., Sundaresan, Y., Gopalakrishnan, P., Beryozkin, A., Hanany, M., Levanon, E. Y., Banin, E., Ben-Aroya, S., & Sharon, D. (2022). Inherited retinal diseases: Linking genes, disease-causing variants, and relevant therapeutic modalities. *Progress in Retinal and Eye Research*, *89*, 101029. https://doi.org/https://doi.org/10.1016/j.preteyeres.2021.101029

Schuster, B., Kovaleva, M., Sun, Y., Regenhard, P., Matthews, V., Grötzinger, J., Rose-John, S., & Kallen, K. J. (2003). Signaling of human ciliary neurotrophic factor (CNTF) revisited. The interleukin-6 receptor can serve as an alpha-receptor for CTNF. *J Biol Chem*, *278*(11), 9528-9535. https://doi.org/10.1074/jbc.m210044200

Seitz, R., Hackl, S., Seibuchner, T., Tamm, E. R., & Ohlmann, A. (2010). Norrin mediates neuroprotective effects on retinal ganglion cells via activation of the Wnt/beta-catenin signaling pathway and the induction of neuroprotective growth factors in Muller cells. *J Neurosci*, *30*(17), 5998-6010. https://doi.org/10.1523/JNEUROSCI.0730-10.2010

Sengillo, J. D., Gregori, N. Z., Sisk, R. A., Weng, C. Y., Berrocal, A. M., Davis, J. L., Mendoza-Santiesteban, C. E., Zheng, D. D., Feuer, W. J., & Lam, B. L. (2022). Visual Acuity, Retinal Morphology, and Patients' Perceptions after Voretigene Neparovec-rzyl Therapy for RPE65-Associated Retinal Disease. *Ophthalmol Retina*, *6*(4), 273-283. https://doi.org/10.1016/j.oret.2021.11.005

Shahin, S., Tan, P., Chetsawang, J., Lu, B., Svendsen, S., Ramirez, S., Conniff, T., Alfaro, J. S., Fernandez, M., Fulton, A., Laperle, A. H., Svendsen, C. N., & Wang, S. (2023). Human Neural Progenitors Expressing GDNF Enhance Retinal Protection in a Rodent Model of Retinal Degeneration. *Stem Cells Transl Med*, *12*(11), 727-744. https://doi.org/10.1093/stcltm/szad054

Shekhar, K., Lapan, S. W., Whitney, I. E., Tran, N. M., Macosko, E. Z., Kowalczyk, M., Adiconis, X., Levin, J. Z., Nemesh, J., Goldman, M., McCarroll, S. A., Cepko, C. L., Regev, A., & Sanes, J. R. (2016). Comprehensive Classification of Retinal Bipolar Neurons by Single-Cell Transcriptomics. *Cell*, *166*(5), 1308-1323.e1330. https://doi.org/10.1016/j.cell.2016.07.054

Sieving, P. A., Caruso, R. C., Tao, W., Coleman, H. R., Thompson, D. J., Fullmer, K. R., & Bush, R. A. (2006). Ciliary neurotrophic factor (CNTF) for human retinal degeneration: phase I trial of CNTF delivered by encapsulated cell intraocular implants. *Proc Natl Acad Sci U S A*, *103*(10), 3896-3901. https://doi.org/10.1073/pnas.0600236103

Silver, J., & Miller, J. H. (2004). Regeneration beyond the glial scar. *Nat Rev Neurosci*, *5*(2), 146-156. https://doi.org/10.1038/nrn1326

Singh, R. K., Binette, F., Seiler, M., Petersen-Jones, S. M., & Nasonkin, I. O. (2020). Pluripotent Stem Cell-Based Organoid Technologies for Developing Next-Generation Vision Restoration Therapies of Blindness. *Journal of Ocular Pharmacology and Therapeutics*, *37*(3), 147-156. https://doi.org/10.1089/jop.2020.0016

Smith, P. D., Sun, F., Park, K. K., Cai, B., Wang, C., Kuwako, K., Martinez-Carrasco, I., Connolly, L., & He, Z. (2009). SOCS3 deletion promotes optic nerve regeneration in vivo. *Neuron*, *64*(5), 617-623. https://doi.org/10.1016/j.neuron.2009.11.021

Smith, R. H., Levy, J. R., & Kotin, R. M. (2009). A simplified baculovirus-AAV expression vector system coupled with one-step affinity purification yields high-titer rAAV stocks from insect cells. *Mol Ther*, *17*(11), 1888-1896. https://doi.org/10.1038/mt.2009.128

Stahl, N., & Yancopoulos, G. D. (1994). The tripartite CNTF receptor complex: activation and signaling involves components shared with other cytokines. *J Neurobiol*, *25*(11), 1454-1466. https://doi.org/10.1002/neu.480251111

Stark, G. R., & Darnell, J. E., Jr. (2012). The JAK-STAT pathway at twenty. *Immunity*, *36*(4), 503-514. https://doi.org/10.1016/j.immuni.2012.03.013

Streilein, J. W. (1999). Immunologic privilege of the eye. *Springer Semin Immunopathol*, *21*(2), 95-111. https://doi.org/10.1007/bf00810243

Streilein, J. W., Okamoto, S., Sano, Y., & Taylor, A. W. (2000). Neural control of ocular immune privilege. *Ann N Y Acad Sci*, *917*, 297-306. https://doi.org/10.1111/j.1749-6632.2000.tb05396.x

Suhail, M., Nursing, C., Center, M., Minhajpur, Allahabad, & India. (2010). Na+, K+-ATPase: Ubiquitous Multifunctional Transmembrane Protein and its Relevance to Various Pathophysiological Conditions. *J Clin Med Res (JOCMR),Canada*, *2*, 1-17.

Sun, F., Park, K. K., Belin, S., Wang, D., Lu, T., Chen, G., Zhang, K., Yeung, C., Feng, G., Yankner, B. A., & He, Z. (2011). Sustained axon regeneration induced by co-deletion of PTEN and SOCS3. *Nature*, *480*(7377), 372-375. https://doi.org/10.1038/nature10594

Sundar, J. C., Munezero, D., Bryan-Haring, C., Saravanan, T., Jacques, A., & Ramamurthy, V. (2020). Rhodopsin signaling mediates light-induced photoreceptor cell death in rd10 mice through a transducin-independent mechanism. *Hum Mol Genet*, *29*(3), 394-406. https://doi.org/10.1093/hmg/ddz299

Swigris, J., Widjaja-Adhi, M. A. K., & Golczak, M. (2025). Retinoid dynamics in vision: from visual cycle biology to retina disease treatments. *Pharmacol Ther*, *273*, 108902. https://doi.org/10.1016/j.pharmthera.2025.108902

Taga, T., Hibi, M., Hirata, Y., Yamasaki, K., Yasukawa, K., Matsuda, T., Hirano, T., & Kishimoto, T. (1989). Interleukin-6 triggers the association of its receptor with a possible signal transducer, gp130. *Cell*, *58*(3), 573-581. https://doi.org/10.1016/0092-8674(89)90438-8

Taga, T., & Kishimoto, T. (1997). Gp130 and the interleukin-6 family of cytokines. *Annu Rev Immunol*, *15*, 797-819. https://doi.org/10.1146/annurev.immunol.15.1.797

Takahashi, K., Nakamura, S., Shimazawa, M., & Hara, H. (2021). Retinal Degeneration and Microglial Dynamics in Mature Progranulin-Deficient Mice. *Int J Mol Sci*, *22*(21). https://doi.org/10.3390/ijms222111557

Talcott, K. E., Ratnam, K., Sundquist, S. M., Lucero, A. S., Lujan, B. J., Tao, W., Porco, T. C., Roorda, A., & Duncan, J. L. (2011). Longitudinal study of cone photoreceptors during retinal degeneration and in response to ciliary neurotrophic factor treatment. *Invest Ophthalmol Vis Sci*, *52*(5), 2219-2226. https://doi.org/10.1167/iovs.10-6479

Tanaka, M., Kuse, Y., Nakamura, S., Hara, H., & Shimazawa, M. (2019). Potential effects of progranulin and granulins against retinal photoreceptor cell degeneration. *Mol Vis*, *25*, 902-911. https://www.ncbi.nlm.nih.gov/pubmed/32025182

Tanaka, T., Narazaki, M., & Kishimoto, T. (2014). IL-6 in inflammation, immunity, and disease. *Cold Spring Harb Perspect Biol*, *6*(10), a016295. https://doi.org/10.1101/cshperspect.a016295

Tang, W., Lu, Y., Tian, Q.-Y., Zhang, Y., Guo, F.-J., Liu, G.-Y., Syed, N. M., Lai, Y., Lin, E. A., Kong, L., Su, J., Yin, F., Ding, A.-H., Zanin-Zhorov, A., Dustin, M. L., Tao, J., Craft, J., Yin, Z., Feng, J. Q.,…Liu, C.-j. (2011). The Growth Factor Progranulin Binds to TNF Receptors and Is Therapeutic Against Inflammatory Arthritis in Mice. *Science*, *332*(6028), 478-484. https://doi.org/doi:10.1126/science.1199214

Tokhtaeva, E., Clifford, R. J., Kaplan, J. H., Sachs, G., & Vagin, O. (2012). Subunit isoform selectivity in assembly of Na,K-ATPase α-β heterodimers. *J Biol Chem*, *287*(31), 26115-26125. https://doi.org/10.1074/jbc.M112.370734

Touchard, E., Heiduschka, P., Berdugo, M., Kowalczuk, L., Bigey, P., Chahory, S., Gandolphe, C., Jeanny, J. C., & Behar-Cohen, F. (2012). Non-viral gene therapy for GDNF production in RCS rat: the crucial role of the plasmid dose. *Gene Ther*, *19*(9), 886-898. https://doi.org/10.1038/gt.2011.154

Tran, N. M., Shekhar, K., Whitney, I. E., Jacobi, A., Benhar, I., Hong, G., Yan, W., Adiconis, X., Arnold, M. E., Lee, J. M., Levin, J. Z., Lin, D., Wang, C., Lieber, C. M., Regev, A., He, Z., & Sanes, J. R. (2019). Single-Cell Profiles of Retinal Ganglion Cells Differing in Resilience to Injury Reveal Neuroprotective Genes. *Neuron*, *104*(6), 1039-1055.e1012. https://doi.org/10.1016/j.neuron.2019.11.006

Travis, G. H., Golczak, M., Moise, A. R., & Palczewski, K. (2007). Diseases Caused by Defects in the Visual Cycle: Retinoids as Potential Therapeutic Agents. *Annual Review of Pharmacology and Toxicology*, *47*(Volume 47, 2007), 469-512. https://doi.org/https://doi.org/10.1146/annurev.pharmtox.47.120505.105225

Tsai, R. M., & Boxer, A. L. (2016). Therapy and clinical trials in frontotemporal dementia: past, present, and future. *Journal of Neurochemistry*, *138*(S1), 211-221. https://doi.org/https://doi.org/10.1111/jnc.13640

Tsang, S. H., & Sharma, T. (2018). Congenital Stationary Night Blindness. In S. H. Tsang & T. Sharma (Eds.), *Atlas of Inherited Retinal Diseases* (pp. 61-64). Springer International Publishing. https://doi.org/10.1007/978-3-319-95046-4_13

Tsin, A., Betts-Obregon, B., & Grigsby, J. (2018). Visual cycle proteins: Structure, function, and roles in human retinal disease. *Journal of Biological Chemistry*, *293*(34), 13016-13021. https://doi.org/10.1074/jbc.AW118.003228

Tsuruma, K., Yamauchi, M., Sugitani, S., Otsuka, T., Ohno, Y., Nagahara, Y., Ikegame, Y., Shimazawa, M., Yoshimura, S., Iwama, T., & Hara, H. (2014). Progranulin, a major secreted protein of mouse adipose-derived stem cells, inhibits light-induced retinal degeneration. *Stem Cells Transl Med*, *3*(1), 42-53. https://doi.org/10.5966/sctm.2013-0020

Twarowski, B., & Herbet, M. (2023). Inflammatory Processes in Alzheimer's Disease—Pathomechanism, Diagnosis and Treatment: A Review. *International Journal of Molecular Sciences*, *24*(7), 6518. https://www.mdpi.com/1422-0067/24/7/6518

Ueki, Y., Chollangi, S., Le, Y. Z., & Ash, J. D. (2010). gp130 activation in Müller cells is not essential for photoreceptor protection from light damage. *Adv Exp Med Biol*, *664*, 655-661. https://doi.org/10.1007/978-1-4419-1399-9_75

Ueki, Y., Wang, J., Chollangi, S., & Ash, J. D. (2008). STAT3 activation in photoreceptors by leukemia inhibitory factor is associated with protection from light damage. *J Neurochem*, *105*(3), 784-796. https://doi.org/10.1111/j.1471-4159.2007.05180.x

Vagin, O., Turdikulova, S., & Tokhtaeva, E. (2007). Polarized membrane distribution of potassium-dependent ion pumps in epithelial cells: different roles of the N-glycans of their beta subunits. *Cell Biochem Biophys*, *47*(3), 376-391. https://doi.org/10.1007/s12013-007-0033-6

Vega-Saenz de Miera, E. C. (2004). Modification of Kv2.1 K+ currents by the silent Kv10 subunits. *Molecular Brain Research*, *123*(1), 91-103. https://doi.org/https://doi.org/10.1016/j.molbrainres.2004.01.004

Verbakel, S. K., van Huet, R. A. C., Boon, C. J. F., den Hollander, A. I., Collin, R. W. J., Klaver, C. C. W., Hoyng, C. B., Roepman, R., & Klevering, B. J. (2018). Non-syndromic retinitis pigmentosa. *Prog Retin Eye Res*, *66*, 157-186. https://doi.org/10.1016/j.preteyeres.2018.03.005

Vierra, N. C., Kirmiz, M., van der List, D., Santana, L. F., & Trimmer, J. S. (2019). Kv2.1 mediates spatial and functional coupling of L-type calcium channels and ryanodine receptors in mammalian neurons. *Elife*, *8*, e49953. https://doi.org/10.7554/eLife.49953

Villarino, A. V., Kanno, Y., & O'Shea, J. J. (2017). Mechanisms and consequences of Jak-STAT signaling in the immune system. *Nat Immunol*, *18*(4), 374-384. https://doi.org/10.1038/ni.3691

Vollmer, P., Peters, M., Ehlers, M., Yagame, H., Matsuba, T., Kondo, M., Yasukawa, K., Büschenfelde, K. H., & Rose-John, S. (1996). Yeast expression of the cytokine receptor domain of the soluble interleukin-6 receptor. *J Immunol Methods*, *199*(1), 47-54. https://doi.org/10.1016/s0022-1759(96)00163-9

Waage, A., Brandtzaeg, P., Halstensen, A., Kierulf, P., & Espevik, T. (1989). The complex pattern of cytokines in serum from patients with meningococcal septic shock. Association between interleukin 6, interleukin 1, and fatal outcome. *J Exp Med*, *169*(1), 333-338. https://doi.org/10.1084/jem.169.1.333

Wahlin, K. J., Lim, L., Grice, E. A., Campochiaro, P. A., Zack, D. J., & Adler, R. (2004). A method for analysis of gene expression in isolated mouse photoreceptor and Müller cells. *Mol Vis*, *10*, 366-375.

Wallenius, V., Wallenius, K., Ahrén, B., Rudling, M., Carlsten, H., Dickson, S. L., Ohlsson, C., & Jansson, J.-O. (2002). Interleukin-6-deficient mice develop mature-onset obesity. *Nature Medicine*, *8*(1), 75-79. https://doi.org/10.1038/nm0102-75

Walsh, C. E., & Hitchcock, P. F. (2017). Progranulin regulates neurogenesis in the developing vertebrate retina. *Dev Neurobiol*, *77*(9), 1114-1129. https://doi.org/10.1002/dneu.22499

Wan, C. K., Andraski, A. B., Spolski, R., Li, P., Kazemian, M., Oh, J., Samsel, L., Swanson, P. A., 2nd, McGavern, D. B., Sampaio, E. P., Freeman, A. F., Milner, J. D., Holland, S. M., & Leonard, W. J. (2015). Opposing roles of STAT1 and STAT3 in IL-21 function in CD4+ T cells. *Proc Natl Acad Sci U S A*, *112*(30), 9394-9399. https://doi.org/10.1073/pnas.1511711112

Wang, F., Wu, N., Zhang, L., Ahammed, G. J., Chen, X., Xiang, X., Zhou, J., Xia, X., Shi, K., Yu, J., Foyer, C. H., & Zhou, Y. (2018). Light Signaling-Dependent Regulation of Photoinhibition and Photoprotection in Tomato. *Plant Physiol*, *176*(2), 1311-1326. https://doi.org/10.1104/pp.17.01143

Wang, J.-S., Estevez, M. E., Cornwall, M. C., & Kefalov, V. J. (2009). Intra-retinal visual cycle required for rapid and complete cone dark adaptation. *Nature Neuroscience*, *12*(3), 295-302. https://doi.org/10.1038/nn.2258

Wang, J., Yang, J., Gu, P., & Klassen, H. (2010). Effects of glial cell line-derived neurotrophic factor on cultured murine retinal progenitor cells. *Mol Vis*, *16*, 2850-2866. https://pmc.ncbi.nlm.nih.gov/articles/PMC3012652/pdf/mv-v16-2850.pdf

Wang, Z., Yang, B., Li, Q., Wen, L., & Zhang, R. (2020). Clinical Features of 69 Cases With Coronavirus Disease 2019 in Wuhan, China. *Clinical Infectious Diseases*, *71*(15), 769-777. https://doi.org/10.1093/cid/ciaa272

Warrant, E. J. (2009). Mammalian vision: rods are a bargain. *Curr Biol*, *19*(2), R69-71. https://doi.org/10.1016/j.cub.2008.11.031

Wasilko, D. J., Lee, S. E., Stutzman-Engwall, K. J., Reitz, B. A., Emmons, T. L., Mathis, K. J., Bienkowski, M. J., Tomasselli, A. G., & Fischer, H. D. (2009). The titerless infected-cells preservation and scale-up (TIPS) method for large-scale production of NO-sensitive human soluble guanylate cyclase (sGC) from insect cells infected with recombinant baculovirus. *Protein Expr Purif*, *65*(2), 122-132. https://doi.org/10.1016/j.pep.2009.01.002

Wässle, H. (2004). Parallel processing in the mammalian retina. *Nat Rev Neurosci*, *5*(10), 747-757. https://doi.org/10.1038/nrn1497

Weber, K., Mock, U., Petrowitz, B., Bartsch, U., & Fehse, B. (2010). Lentiviral gene ontology (LeGO) vectors equipped with novel drug-selectable fluorescent proteins: new building blocks for cell marking and multi-gene analysis. *Gene Ther*, *17*(4), 511-520. https://doi.org/10.1038/gt.2009.149

Weber, P., Bartsch, U., Schachner, M., & Montag, D. (1998). Na,K-ATPase subunit beta1 knock-in prevents lethality of beta2 deficiency in mice. *J Neurosci*, *18*(22), 9192-9203. https://doi.org/10.1523/jneurosci.18-22-09192.1998

Wei, N., Sun, Z., Yu, J., Jia, Y., Zheng, P., Tang, H., & Chen, J. (2021). Immunological Responses to Transgene-Modified Neural Stem Cells After Transplantation. *Front Immunol*, *12*, 697203. https://doi.org/10.3389/fimmu.2021.697203

Wen, R., Cheng, T., Song, Y., Matthes, M. T., Yasumura, D., LaVail, M. M., & Steinberg, R. H. (1998). Continuous exposure to bright light upregulates bFGF and CNTF expression in the rat retina. *Curr Eye Res*, *17*(5), 494-500. https://doi.org/10.1076/ceyr.17.5.494.5186

Wen, R., Song, Y., Kjellstrom, S., Tanikawa, A., Liu, Y., Li, Y., Zhao, L., Bush, R. A., Laties, A. M., & Sieving, P. A. (2006). Regulation of rod phototransduction machinery by ciliary neurotrophic factor. *J Neurosci*, *26*(52), 13523-13530. https://doi.org/10.1523/jneurosci.4021-06.2006

Wen, R., Song, Y., Liu, Y., Li, Y., Zhao, L., & Laties, A. M. (2008). CNTF negatively regulates the phototransduction machinery in rod photoreceptors: implication for light-induced photostasis plasticity. *Adv Exp Med Biol*, *613*, 407-413. https://doi.org/10.1007/978-0-387-74904-4_48

Wen, R., Tao, W., Li, Y., & Sieving, P. A. (2012). CNTF and retina. *Prog Retin Eye Res*, *31*(2), 136-151. https://doi.org/10.1016/j.preteyeres.2011.11.005

Wetzel, R. K., Arystarkhova, E., & Sweadner, K. J. (1999). Cellular and subcellular specification of Na,K-ATPase alpha and beta isoforms in the postnatal development of mouse retina. *J Neurosci*, *19*(22), 9878-9889. https://doi.org/10.1523/jneurosci.19-22-09878.1999

Wilkinson, A. N., Gartlan, K. H., Kelly, G., Samson, L. D., Olver, S. D., Avery, J., Zomerdijk, N., Tey, S.-K., Lee, J. S., Vuckovic, S., & Hill, G. R. (2018). Granulocytes Are Unresponsive to IL-6 Due to an Absence of gp130. *The Journal of Immunology*, *200*(10), 3547-3555. https://doi.org/10.4049/jimmunol.1701191

Willis, E. F., MacDonald, K. P. A., Nguyen, Q. H., Garrido, A. L., Gillespie, E. R., Harley, S. B. R., Bartlett, P. F., Schroder, W. A., Yates, A. G., Anthony, D. C., Rose-John, S., Ruitenberg, M. J., & Vukovic, J. (2020). Repopulating Microglia Promote Brain Repair in an IL-6-Dependent Manner. *Cell*, *180*(5), 833-846.e816. https://doi.org/https://doi.org/10.1016/j.cell.2020.02.013

Wong, F. S., Wong, C. C., Chan, B. P., & Lo, A. C. (2016). Sustained Delivery of Bioactive GDNF from Collagen and Alginate-Based Cell-Encapsulating Gel Promoted Photoreceptor Survival in an Inherited Retinal Degeneration Model. *PLoS One*, *11*(7), e0159342. https://doi.org/10.1371/journal.pone.0159342

Wu, W.-C., Lai, C.-C., Chen, S.-L., Xiao, X., Chen, T.-L., Tsai, R. J.-F., Kuo, S.-W., & Tsao, Y.-P. (2002). Gene Therapy for Detached Retina by Adeno-Associated Virus Vector Expressing Glial Cell Line–Derived Neurotrophic Factor. *Investigative Ophthalmology & Visual Science*, *43*(11), 3480-3488.

Wu, Z., & McGoogan, J. M. (2020). Characteristics of and Important Lessons From the Coronavirus Disease 2019 (COVID-19) Outbreak in China: Summary of a Report of

72 314 Cases From the Chinese Center for Disease Control and Prevention. *Jama*, *323*(13), 1239-1242. https://doi.org/10.1001/jama.2020.2648

Wulansari, N., Sulistio, Y. A., Darsono, W. H. W., Kim, C. H., & Lee, S. H. (2021). LIF maintains mouse embryonic stem cells pluripotency by modulating TET1 and JMJD2 activity in a JAK2-dependent manner. *Stem Cells*, *39*(6), 750-760. https://doi.org/10.1002/stem.3345

Xiao, W., Chen, X., & He, M. (2014). Inhibition of the Jagged/Notch pathway inhibits retinoblastoma cell proliferation via suppressing the PI3K/Akt, Src, p38MAPK and Wnt/β-catenin signaling pathways. *Mol Med Rep*, *10*(1), 453-458. https://doi.org/10.3892/mmr.2014.2213

Xue, W., Cojocaru, R. I., Dudley, V. J., Brooks, M., Swaroop, A., & Sarthy, V. P. (2011). Ciliary neurotrophic factor induces genes associated with inflammation and gliosis in the retina: a gene profiling study of flow-sorted, Müller cells. *PLoS One*, *6*(5), e20326. https://doi.org/10.1371/journal.pone.0020326

Yan, W., Laboulaye, M. A., Tran, N. M., Whitney, I. E., Benhar, I., & Sanes, J. R. (2020). Mouse Retinal Cell Atlas: Molecular Identification of over Sixty Amacrine Cell Types. *J Neurosci*, *40*(27), 5177-5195. https://doi.org/10.1523/jneurosci.0471-20.2020

Yang, H., Zhang, H., & Li, X. (2024). Navigating the future of retinitis pigmentosa treatments: A comprehensive analysis of therapeutic approaches in rd10 mice. *Neurobiol Dis*, *193*, 106436. https://doi.org/10.1016/j.nbd.2024.106436

Yang, X. F., Huang, Y. X., Lan, M., Zhang, T. R., & Zhou, J. (2018). Protective Effects of Leukemia Inhibitory Factor on Retinal Vasculature and Cells in Streptozotocin-induced Diabetic Mice. *Chin Med J (Engl)*, *131*(1), 75-81. https://doi.org/10.4103/0366-6999.221263

Yasukawa, K., Saito, T., Fukunaga, T., Sekimori, Y., Koishihara, Y., Fukui, H., Ohsugi, Y., Matsuda, T., Yawata, H., Hirano, T., & et al. (1990). Purification and characterization of soluble human IL-6 receptor expressed in CHO cells. *J Biochem*, *108*(4), 673-676. https://doi.org/10.1093/oxfordjournals.jbchem.a123261

Yawata, H., Yasukawa, K., Natsuka, S., Murakami, M., Yamasaki, K., Hibi, M., Taga, T., & Kishimoto, T. (1993). Structure-function analysis of human IL-6 receptor: dissociation of amino acid residues required for IL-6-binding and for IL-6 signal transduction through gp130. *EMBO J*, *12*(4), 1705-1712. https://doi.org/10.1002/j.1460-2075.1993.tb05815.x

Yin, F., Banerjee, R., Thomas, B., Zhou, P., Qian, L., Jia, T., Ma, X., Ma, Y., Iadecola, C., Beal, M. F., Nathan, C., & Ding, A. (2010). Exaggerated inflammation, impaired host defense, and neuropathology in progranulin-deficient mice. *J Exp Med*, *207*(1), 117-128. https://doi.org/10.1084/jem.20091568

Yoshimura, A., Naka, T., & Kubo, M. (2007). SOCS proteins, cytokine signalling and immune regulation. *Nat Rev Immunol*, *7*(6), 454-465. https://doi.org/10.1038/nri2093

Young, R. W. (1967). The renewal of photoreceptor cell outer segments. *J Cell Biol*, *33*(1), 61-72. https://doi.org/10.1083/jcb.33.1.61

Yu, S. P. (2003). Na(+), K(+)-ATPase: the new face of an old player in pathogenesis and apoptotic/hybrid cell death. *Biochem Pharmacol*, *66*(8), 1601-1609. https://doi.org/10.1016/s0006-2952(03)00531-8

Zein, W. M., Jeffrey, B. G., Wiley, H. E., Turriff, A. E., Tumminia, S. J., Tao, W., Bush, R. A., Marangoni, D., Wen, R., Wei, L. L., & Sieving, P. A. (2014). CNGB3-achromatopsia clinical trial with CNTF: diminished rod pathway responses with no evidence of improvement in cone function. *Invest Ophthalmol Vis Sci*, *55*(10), 6301-6308. https://doi.org/10.1167/iovs.14-14860

Zeiss, C. J., Allore, H. G., Towle, V., & Tao, W. (2006). CNTF induces dose-dependent alterations in retinal morphology in normal and rcd-1 canine retina. *Exp Eye Res*, *82*(3), 395-404. https://doi.org/10.1016/j.exer.2005.07.014

Zhang, K., Hopkins, J. J., Heier, J. S., Birch, D. G., Halperin, L. S., Albini, T. A., Brown, D. M., Jaffe, G. J., Tao, W., & Williams, G. A. (2011). Ciliary neurotrophic factor delivered by encapsulated cell intraocular implants for treatment of geographic atrophy in age-related macular degeneration. *Proc Natl Acad Sci U S A*, *108*(15), 6241-6245. https://doi.org/10.1073/pnas.1018987108

Zhang, S. H., Liu, D. X., Wang, L., Li, Y. H., Wang, Y. H., Zhang, H., Su, Z. K., Fang, W. G., Qin, X. X., Shang, D. S., Li, B., Han, X. N., Zhao, W. D., & Chen, Y. H. (2019). A CASPR1-ATP1B3 protein interaction modulates plasma membrane localization of Na(+)/K(+)-ATPase in brain microvascular endothelial cells. *J Biol Chem*, *294*(16), 6375-6386. https://doi.org/10.1074/jbc.RA118.006263

Zhao, L., Zabel, M. K., Wang, X., Ma, W., Shah, P., Fariss, R. N., Qian, H., Parkhurst, C. N., Gan, W. B., & Wong, W. T. (2015). Microglial phagocytosis of living photoreceptors contributes

to inherited retinal degeneration. *EMBO Mol Med*, *7*(9), 1179-1197. https://doi.org/10.15252/emmm.201505298

Zhou, F., Yu, T., Du, R., Fan, G., Liu, Y., Liu, Z., Xiang, J., Wang, Y., Song, B., Gu, X., Guan, L., Wei, Y., Li, H., Wu, X., Xu, J., Tu, S., Zhang, Y., Chen, H., & Cao, B. (2020). Clinical course and risk factors for mortality of adult inpatients with COVID-19 in Wuhan, China: a retrospective cohort study. *The Lancet*, *395*(10229), 1054-1062. https://doi.org/https://doi.org/10.1016/S0140-6736(20)30566-3

Zhou, G. H., Ma, Y., Li, M. L., Zhou, X. Y., Mou, H., & Jin, Z. B. (2020). ATP1A3 mutation as a candidate cause of autosomal dominant cone-rod dystrophy. *Hum Genet*, *139*(11), 1391-1401. https://doi.org/10.1007/s00439-020-02182-y

Zhu, J., Nathan, C., Jin, W., Sim, D., Ashcroft, G. S., Wahl, S. M., Lacomis, L., Erdjument-Bromage, H., Tempst, P., Wright, C. D., & Ding, A. (2002). Conversion of Proepithelin to Epithelins: Roles of SLPI and Elastase in Host Defense and Wound Repair. *Cell*, *111*(6), 867-878. https://doi.org/https://doi.org/10.1016/S0092-8674(02)01141-8

Zin, E. A., Han, D., Tran, J., Morisson-Welch, N., Visel, M., Kuronen, M., & Flannery, J. G. (2021). Outcomes of progranulin gene therapy in the retina are dependent on time and route of delivery. *Mol Ther Methods Clin Dev*, *22*, 40-51. https://doi.org/10.1016/j.omtm.2021.05.009

APPENDIX

I. SUPPLEMENTARY IMAGES

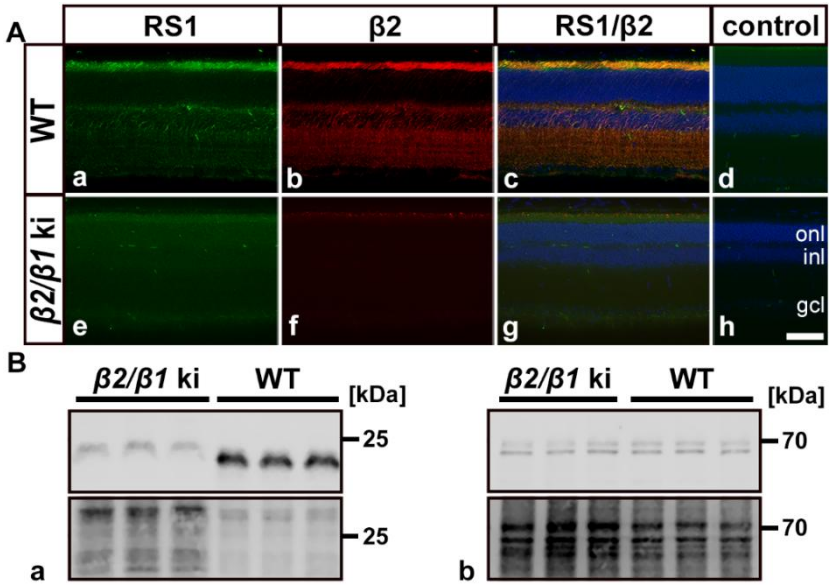

FIG. S1: EXPRESSION OF RS1 AND SARM1 IN THE RETINA OF *β2/β1* KI AND WILD-TYPE MICE. Expression of RS1 (A, Ba) and SARM1 (Bb) was examined by IHC (A) and Western blot analysis (B). β2: β2-subunit of the NKA; *β2/β1* ki: *Atp1b2*^{Atp1b1} ki mice; gcl: ganglion cell layer; inl: inner nuclear layer; kDa: kilodalton; onl: outer nuclear layer; RS1: retinoschisin; SARM1: Sterile alpha and TIR motif containing 1; WT: wild-type. Scale bar in Ah: 50 µm. Modified from Bartsch et al. (2025) with unpublished data on SARM1 expression.

I.I. SUPPLEMENTARY IMAGES PROJECT I

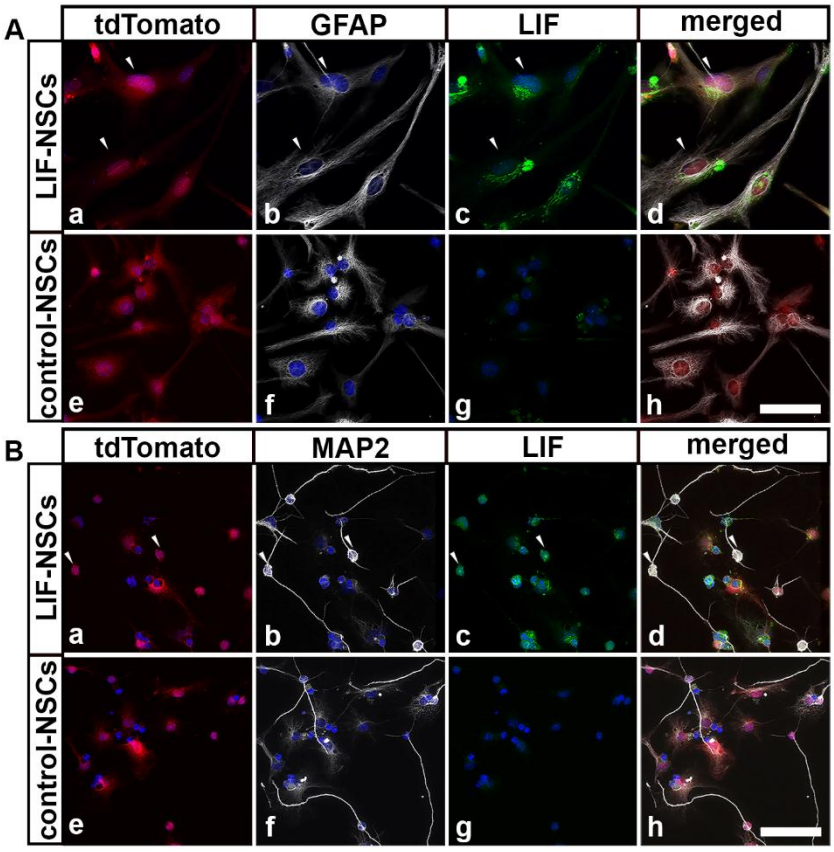

FIG. S2: DIFFERENTIATION OF LIF-NSCS. (A) Differentiation of LIF-NSCs into astrocytes. (B) Differentiation of LIF-NSCs into neurons. ctrl: control; GFAP: glial fibrillary acidic protein; LIF: leukemia inhibitory factor; MAP2: microtubule-associated protein 2; NSCs: neural stem cells. Scale bar in Ah (for A) and Bh (for B): 50 µm.

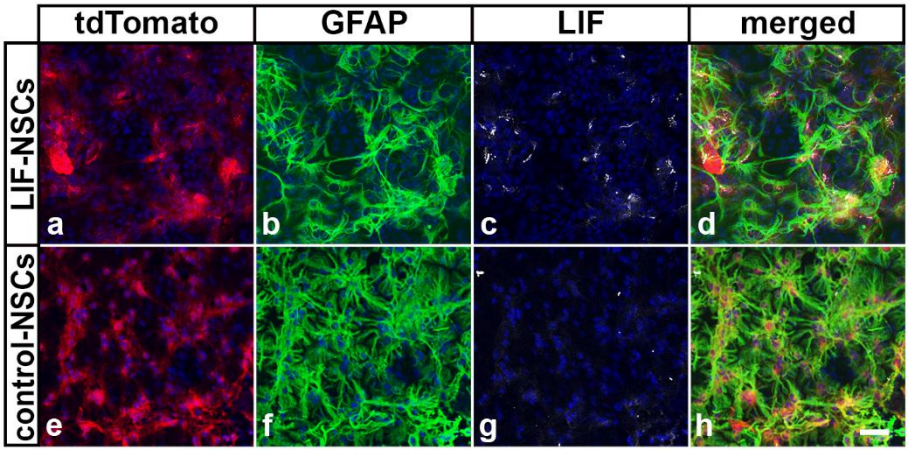

FIG. S3: IN VIVO CHARACTERISATION OF LIF-NSCS IN *β2/β1* KI MICE.
Analysis of intravitreally grafted LIF-NSCs attached to the posterior pole of lenses in 4-month-old *β2/β1* ki mice. GFAP: glial fibrillary acidic protein; LIF: leukemia inhibitory factor; NSCs: neural stem cells. Scale bar in h: 100 µm.

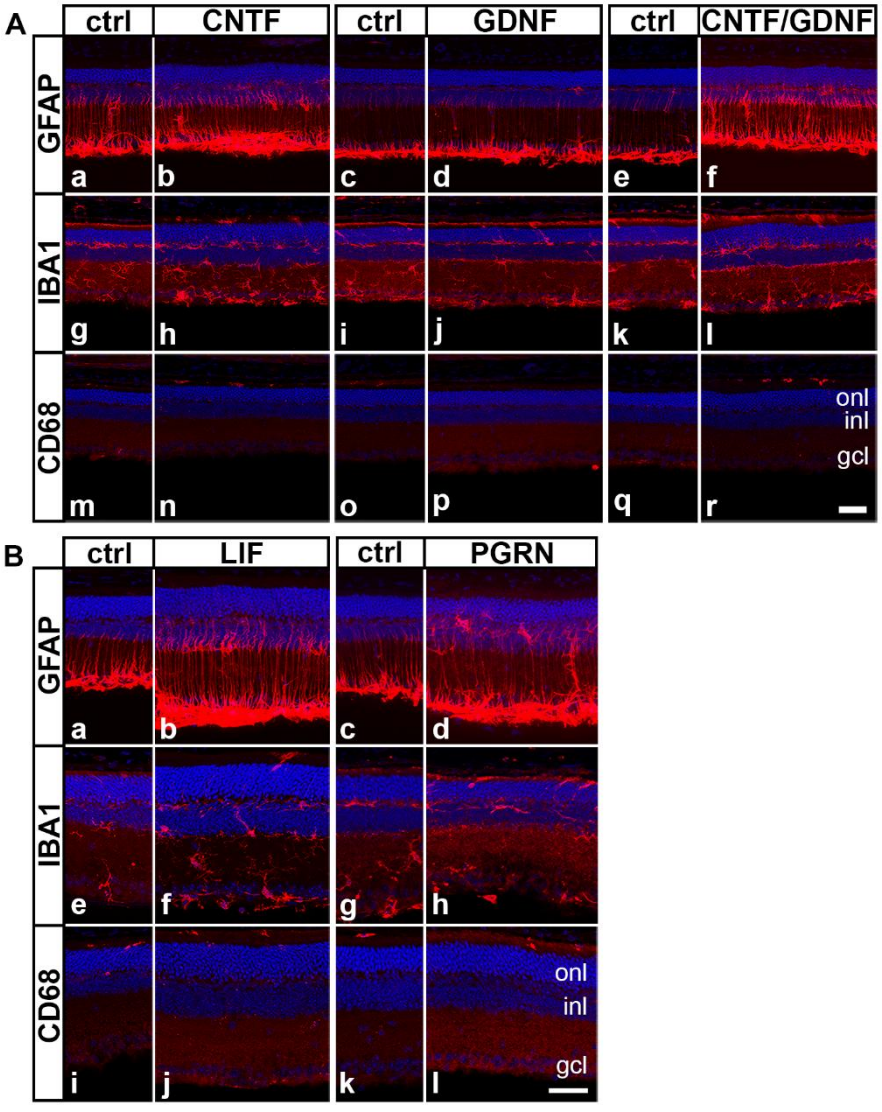

PGRN: progranulin. Scale in Ar (for A) and Bl (for B): 50 µm.

FIG. S4: INFLAMMATION IN *β2/β1* KI MICE TREATED WITH NTF-NSCS.
(A) Reactive astrogliosis and reactive microgliosis in retinas of 4-month-old animals treated with CNTF-, GDNF-, CNTF/GDNF- and control-NSCs. (B) Reactive astrogliosis and reactive microgliosis in retinas of 4-month-old animals treated with LIF-, PGRN- and control-NSCs. CD68: cluster of differentiation 68; CNTF: ciliary neurotrophic factor; ctrl: control; gcl: ganglion cell layer; GDNF: glial cell line-derived neurotrophic factor; GFAP: glial fibrillary acidic protein; IBA1: ionized calcium-binding adapter molecule 1; inl: inner nuclear layer; LIF: leukemia inhibitory factor; onl: outer nuclear layer;

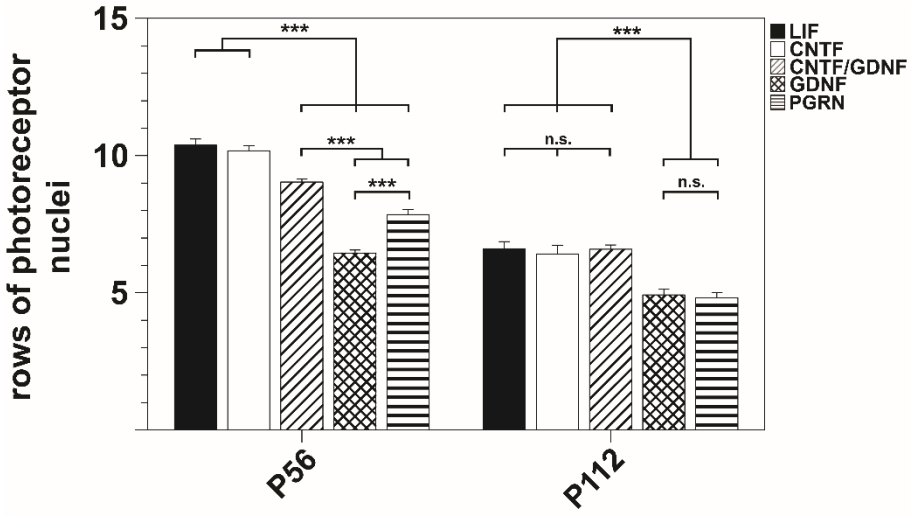

FIG. S5: *β2/β1* KI RETINAS TREATED WITH CNTF OR LIF CONTAIN MORE RPN THAN RETINAS TREATED WITH GDNF OR PGRN.
Comparative analysis of RPN in retinas of 2-month-old and 4-month-old *β2/β1* ki animals treated NTF-NSCs in animals. ***: p<0.001; n.s.: not significant according to a two-way ANOVA followed by Bonferroni post-hoc test. CNTF: ciliary neurotrophic factor; GDNF: glial cell line-derived neurotrophic factor; LIF: leukemia inhibitory factor; P: postnatal day; PGRN: progranulin.

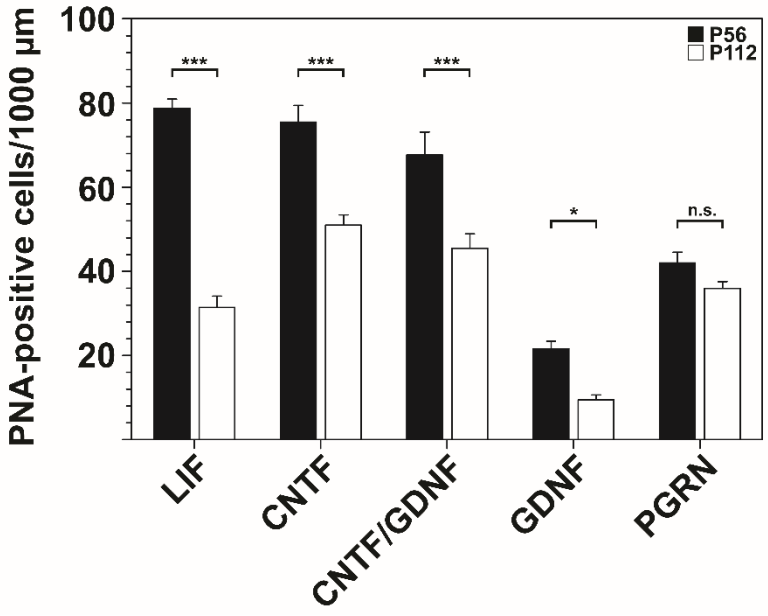

FIG. S6: RETINAS OF *β2/β1* KI MICE TREATED WITH PGRN-NSCS CONTAIN A SIMILAR NUMBER OF PNA-POSITIVE CELLS IN 2- AND 4-MONTH-OLD ANIMALS.
Comparative analysis of PNA-positive COS in retinas of 2-month-old and 4-month-old *β2/β1* ki animals treated NTF-NSCs in animals. *: p<0.05, ***: p<0.001, n.s.: not significant according to a two-way ANOVA followed by Bonferroni post-hoc test. CNTF: ciliary neurotrophic factor; GDNF: glia cell line-derived neurotrophic factor; LIF: leukemia inhibitory factor; P: postnatal day; PGRN: progranulin; PNA: biotinylated peanut agglutinin.

I.II. SUPPLEMENTARY IMAGES PROJECT II

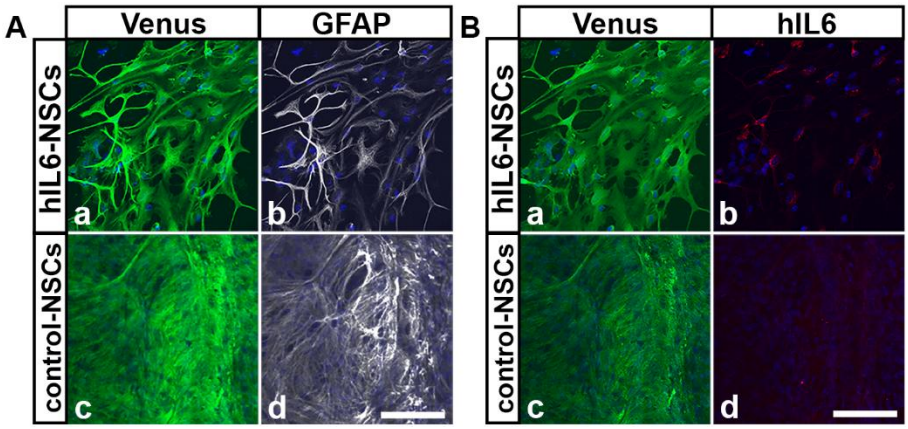

FIG. S7: *IN VIVO* CHARACTERISATION OF HIL6-NSCS IN 3-MONTH-OLD *β2/β1* KI MICE.
(A) Differentiation into astrocytes and (B) expression of hIL6 in hIL6-NSCs and control-NSCs *in vivo*. ctrl: control; GFAP: glial fibrillary acidic protein; hIL6: hyper-interleukin 6; NSCs: neural stem cells. Scale bar A and B 100µm.

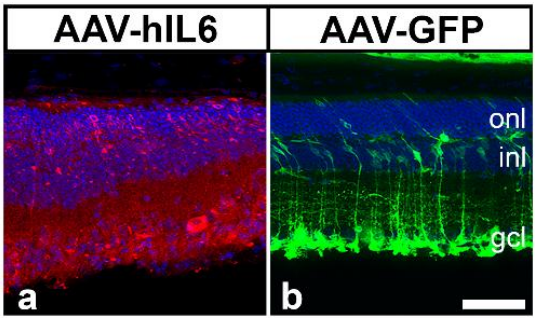

FIG. S8: EXPRESSION OF TRANSGENES AFTER INTRAVITREAL INJECTIONS OF AAVSHH10-HIL6 AND AAVSHH10-GFP IN THE RETINA OF 3-MONTH-OLD *β2/β1* KI MICE.
Retinas treated with AAVs were labelled with antibodies against hIL6 (a) or GFP (b) to examine transduction efficiency of AAVshH10-hIL6 and AAVshH10-GFP in *β2/β1* ki mice. gcl: ganglion cell layer; GFP: green fluorescent protein; hIL6: hyper-interleukin-6; inl: inner nuclear layer; onl: outer nuclear layer. Scale bar in b: 50 µm.

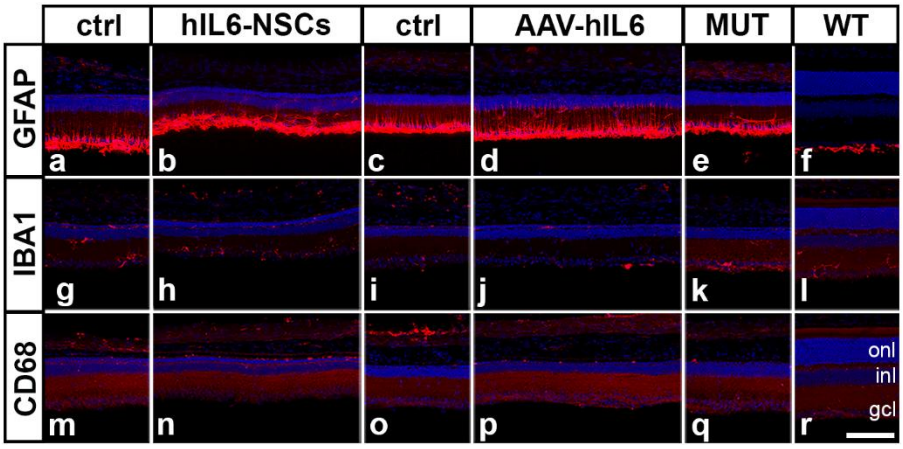

FIG. S9: ANALYSIS OF NEUROINFLAMMATION IN HIL6-TREATED RETINAS OF 2-MONTH-OLD RD10 MICE.
Assessment of reactive astrogliosis (a-f) and microgliosis (g-r) in 2- month-old rd10 mice treated with hIL6-NSCs (b,h,n) and AAVshH10-hIL6 (d,j,p) and their contralateral control retinas treated with either control-NSCs (a,g,m) or AAVshH10-GFP (c,i,o), as well as age-matched rd10 mice (untreat) (e,k,q) and wild-type mice (WT) (f,l,r).AAV: adeno-associated virus; CD68: cluster of differentiation 68; ctrl: control; gcl: ganglion cell layer; GFAP: glial fibrillary acidic protein; IBA1: ionized calcium-binding adapter molecule 1; hIL6: hyper-interleukin-6; inl: inner nuclear layer; NSCs: neural stem cells; onl: outer nuclear layer; untreat: untreated (here: rd10 mice); WT: wild-type. Scale bar in r: 100µm.

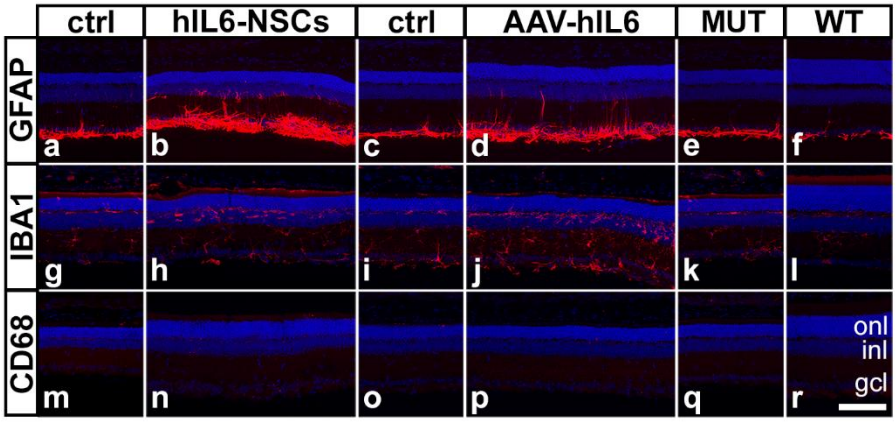

FIG. S10: NEUROINFLAMMATION OF HIL6-TREATED RETINAS OF 3-MONTH-OLD *β2/β1* KI MICE.
Assessment of reactive astrogliosis (a-f) and microgliosis (g-r) in 3- month-old *β2/β1* ki mice treated with hIL6-NSCs (b,h,n) and AAVshH10-hIL6 (d,j,p) and their contralateral control retinas treated with either control-NSCs (a,g,m) or AAVshH10-GFP (c,i,o), as well as age-matched *β2/β1* ki mice (untreat) (e,k,q) and wild-type mice (WT) (f,l,r). AAV: adeno-associated virus; CD68: cluster of differentiation 68; ctrl: control; gcl: ganglion cell layer; GFAP: glial fibrillary acidic protein; IBA1: ionized calcium-binding adapter molecule 1; hIL6: hyper-interleukin-6; inl: inner nuclear layer; NSCs: neural stem cells; onl: outer nuclear layer; untreat: untreated (here: *β2/β1* ki mice); WT: wild-type. Scale bar in r: 100µm.

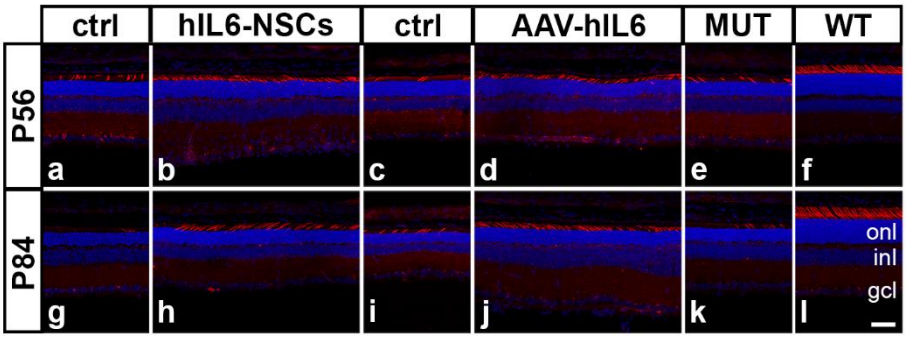

FIG. S11: PNA-POSITIVE CONE INNER AND OUTER SEGMENTS IN 2- AND 3-MONTH-OLD *β2/β1* KI MICE TREATED WITH HIL6.
Analysis of PNA-positive cone inner and outer segments in 2-month-old (a-f) and 3-month-old (g-l) *β2/β1* ki retinas treated with hIL6-NSCs and AAVshH10-hIL6, contralateral controls treated with control-NSCs and AAVshH10-GFP as well as age-matched, untreated β2/β1 ki retinas and WT retinas. AAV: adeno-associated virus; ctrl: control; gcl: ganglion cell layer; hIL6: hyper-interleukin-6; inl: inner nuclear layer; NSCs: neural stem cells; onl: outer nuclear layer; untreat: untreated (here: *β2/β1* ki); WT: wild-type. Scale bar in l: 50 µm.

II. SUPPLEMENTARY TABLES

Tab. S1: DENSITY OF CD68-POSITIVE CELLS IN RD10 RETINAS AND FOLD-CHANGES COMPARED TO HIL6-TREATMENT.

		P28		P35		P42		P56	
		CD68-POSITIVE CELLS/1000 µM	FOLD-CHANGE COMPARED TO HIL6-TREATMENT	CD68-POSITIVE CELLS/1000 µM	FOLD-CHANGE COMPARED TO HIL6-TREATMENT	CD68-POSITIVE CELLS/1000 µM	FOLD-CHANGE COMPARED TO HIL6-TREATMENT	CD68-POSITIVE CELLS/1000 µM	FOLD-CHANGE COMPARED TO HIL6-TREATMENT
HIL6-NSCs	TREATED	11.1 ± 1.7		9.2 ± 0.6		9.6 ± 1.8		4.9 ± 0.8	
	CONTROL	2.4 ± 0.1	**-4.6x**	1.5 ± 0.1	**-6.3x**	1.0 ± 0.2	**-9.2x**	0.7 ± 0.2	**-7.2x**
	MUT	1.1 ± 0.2	**-10x**	1.0 ± 0.2	**-9.2x**	0.8 ± 0.2	**-12.7x**	0.5 ± 0.2	**-9.1x**
	WT	0.07 ± 0.03	**-154x**	0.3 ± 0.04	**-35.7x**	0.3 ± 0.05	**-37.3x**	0.1 ± 0.03	**-41.9x**
AAV-HIL6	TREATED	16.2 ±0.8		15.4 ± 1.5		9.1 ± 0.7		5.1 ± 1.3	
	CONTROL	2.4 ± 0.4	**-6.8x**	1.4 ± 0.1	**-10.7x**	0.9 ± 0.3	**-10x**	0.5 ± 0.2	**-11.4x**
	MUT	1.1 ± 0.2	**-14.6x**	1.0 ± 0.2	**-15.3x**	0.8 ± 0.2	**-12.2x**	0.5 ± 0.2	**-9.5x**
	WT	0.07 ± 0.03	**-225x**	0.3 ± 0.04	**-59.4x**	0.3 ± 0.05	**-35.7x**	0.1 ± 0.03	**-43.6x**

AAV: adeno-associated virus; CD68: cluster of differentiation 68; hIL6: hyper-interleukin-6; NSCs: neural stem cells; P: postnatal day; WT: wild-type; x: fold-change.

Tab. S2: DENSITY OF CD68-POSITIVE CELLS IN CONTROL RETINAS OF RD10 MICE AND FOLD-CHANGES IN UNTREATED RETINAS COMPARED TO CONTROL RETINAS.

		P28		P35		P42		P56	
		CD68-POSITIVE CELLS/1000 µM	FOLD-CHANGE COMPARED TO TREATED CONTROLS	CD68-POSITIVE CELLS/1000 µM	FOLD-CHANGE COMPARED TO TREATED CONTROLS	CD68-POSITIVE CELLS/1000 µM	FOLD-CHANGE COMPARED TO TREATED CONTROLS	CD68-POSITIVE CELLS/1000 µM	FOLD-CHANGE COMPARED TO TREATED CONTROLS
CONTROL-NSCs		2.4 ± 0.1		1.5 ± 0.1		1.0 ± 0.2		0.7 ± 0.2	
AAV-GFP		2.4 ± 0.4		1.4 ± 0.1		0.9 ± 0.3		0.5 ± 0.2	
UNTREATED	NSCs AAVs	1.1 ± 0.2	**-2.2x** **-2.2x**	1.0 ± 0.2	**-1.5x** **-1.4x**	0.8 ± 0.2	**-1.3x** **-1.1x**	0.5 ± 0.2	**0** **0**
WT	NSCs AAVs	0.07 ± 0.03	**-34.3x** **-34.3x**	0.3 ± 0.04	**-5x** **-4.6x**	0.3 ± 0.05	**-3.3x** **-3.0x**	0.1 ± 0.03	**-5x** **-7x**

AAV: adeno-associated virus; CD68: cluster of differentiation 68; GFP: green fluorescent protein; hIL6: hyper-interleukin-6; NSCs: neural stem cells; P: postnatal day; TG: transgenic mice (here: rd10 mice); WT: wild-type; x: fold-change.

III. LIST OF ABBREVIATIONS

III.I. GENERAL ABBREVIATIONS

***β2/β1* ki**	*Atp1b2*^{Atp1b1} knock-in mice
λ_{max}	maximum of light absorption spectrum
11cRAL	11-cis-retinal
11cRDH	11-cis-retinol dehydrogenases
11cROL	11-cis-retinol
2A	P2A sequence of the porcine teschovirus-1
°C	degrees Celsius
A	adenosine
A2E	bis-retinoid N-retinyl-N-retinylidene ethanolamine
aa	amino acid
AAV2	adeno-associated virus serotype 2
AAVshH10	adeno-associated virus serotype shH10
ABCA4	retinal-specific phospholipid-transporting ATPase 4
AC	amacrine cell
AD	adenovirus
A-domain	actuator domain
ADP	adenosine diphosphate
Akt	protein kinase B, a serine/threonine kinase
ANOVA	analysis of variance
approx.	approximately
ARR	arrestin
arRP	autosomal-recessive retinitis pigmentosa
ARTN	artemin
ATP	adenosine triphosphate
Atp1b1	gene encoding for the β1-subunit of the Na,K-ATPase
Atp1b2	gene encoding for the β2-subunit of the Na,K-ATPase
atRAL	all-trans-retinal
atRDH	all-trans-retinol hydrogenases
atREs	all-trans-retinyl esters
atROL	all-trans-retinol
BBB	blood-brain-barrier
BCVA	best corrected visual acuity
BM	Bruch's membrane
BP	bipolar cell
bp	base pairs
BRB	blood-retina-barrier
BSA	bovine serum albumin
bsd	blasticidin
C	cytosine
Ca^{2+}	calcium ion, bivalent
CAG	cytomegalovirus enhancer/chicken β-actin promotor
cAMP	cyclic adenosine monophosphate
cap	structural genes encoding capsid proteins in AAVs
CAR	cone-arrestin
CAR-T	chimeric antigen receptor T
CD68	cluster of differentiation 68
cDNA	complementary deoxyribonucleic acid
CG	cardiac glycosides
cGMP	cyclic guanosine monophosphate
CIS	cone inner segments
c-Jun	transcription factor encoded by *Jun* gene
CLCF1	cardiotrophin-like cytokine factor 1
CMV	cytomegalovirus
CNG	cyclic nucleotide–gated ion channels
CNS	central nervous system
CNTF	ciliary neurotrophic factor
(s)CNTFRα	(soluble) ciliary neurotrophic factor receptor α subunit

conc.	concentration
COS	cone outer segments
CREB	cAMP-responsive element-binding protein
CRISPR-Cas9	Clustered Regularly Interspaced Short Palindromic Repeats/CRISPR-associated endonuclease 9
cRNA	complementary ribonucleic acid
CRX	cone-rod homeobox protein
CT-1	cardiotropin 1
Cy	cyanine
D	aspartic acid, proteinogenic amino acid
DAPI	4′,6-diamidino-2-phenylindole
DES1	dihydroceramide desaturase 1
DGC	displaced ganglion cells
dLGN	*corpus geniculatum dorsolaterale*
DMEM/F12	Dulbecco's modified eagle medium, nutrient mixture F-12
DNA	deoxyribonucleic acid
DPBS	Dulbecco's balanced salt solution
DRG	dorsal root ganglion
DSGC	directionally sensitive ganglion cells
E2a	gene needed for the replication of ADs
E4	gene needed for the replication of ADs
ECM	extracellular matrix
ECT	encapsulated cell therapy
EDTA	ethylenediaminetetraacetic acid, a buffer substance
EF1α	elongation factor α1 promotor
e.g.	*exemplum gratia*
EGF	epidermal growth factor
eGFP	enhanced green fluorescent protein
EMA	European Medicines Agency
ERG	electroretinography
ERGs	electroretinograms
ESC	embryonic stem cells
etc.	*et cetera*
F	forward primer
F	phenylalanine
FACS	fluorescence activated cell sorting
FCS	foetal calf serum
FDA	federal drug administration, USA
FGF	fibroblast growth factor
FTLD	frontotemporal lobar degeneration
G	guanine
Gα	α-subunit of the G-coupled protein transducin
Gα*	photoactivated α-subunit of the G-coupled protein transducin
GABA	γ-aminobutyric acid
GAF	cGMP-binding phosphodiesterases, cyanobacterial Adenylyl cyclases and transcription factor FhlA
GC	guanylyl cyclase
GCAP1	guanylyl cyclase activating protein1
gcl	ganglion cell layer
GDNF	glial cell-derived neurotrophic factor
GDP	guanosine diphosphate
GFAP	glial fibrillary acidic protein
GFL	GDNF family of ligands
GFRα1	GDNF-family receptor α1
GLAST	glial L-glutamate/L-aspartate transporter
GNAT1	guanine nucleotide-binding protein G(t) subunit α1
gp130	glycoprotein 130 kDa
GPCR	G-protein coupled receptor
GPI	glycosylphosphatidylinositol
GS	glutamate synthetase
G_t	transducin, a heterotrimeric G-protein

GTP	guanosine triphosphate
GTPase	guanosine triphosphatase
GUCA1A	guanylyl cyclase activating protein1
H	histidine
h	hour
HC	horizontal cell
HCl	hydrochloric acid
HEK293T	human embryonic kidney 293T cells
HFG	hepatocyte growth factor
hIL6	hyper-interleukin-6
IBA1	ionized calcium-binding adapter molecule 1
ICC	immunocytochemistry
ICD	intracellular domain
i.e.	*id est*
Ig	immunoglobulin
IHC	immunohistochemistry
IL1β	interleukin-1 β subunit
(s)IL1-R	(soluble) interleukin 1 receptor
IL6	interleukin-6
(s)IL6-Rα	(soluble) interleukin-6-receptor α subunit
IL11	interleukin-11
IL12	interleukin-12
IL27	interleukin-27
ilm	inner limiting membrane
inl	inner nuclear layer
iNOS	inducible nitric oxide synthase
ipl	inner plexiform layer
ipRGC	intrinsically photosensitive retinal ganglion cell
iPSCs	induced pluripotent stem cells
IRBP	interphotoreceptor retinoid-binding protein
IRES	internal ribosome entry site
IS	inner segments
iTom	tdTomato
JAK	Janus Kinase
JAM-B	junctional adhesion molecule B
JNK	c-Jun N-terminal kinase
J-RGC	JAM-B-expressing RGCs
K^+	potassium ion, monovalent
kb	kilobases
KCl	potassium chloride
kDa	kilodalton, 10^3 Daltons
ki	knock-in
ko	knock-out
K_V	voltage-gated potassium channel
K_V2.1	voltage-gated potassium channel subunit 2.1
K_V8.2	voltage-gated potassium channel subunit 8.2
l	litre
LED	local edge detector
LeGO	Lentiviral Gene Ontology
LIF	leukemia inhibitory factor
LRAT	lecithin retinol acyltransferase
LRP1	pro-low-density lipoprotein receptor-related protein 1
LV	lentivirus
µl	microliter, 10^{-6} l
µm	micrometre, 10^{-6} m
MAG	myelin-associated glycoprotein
MAP2	microtubule-associated protein 2
MAPK	mitogen-activated protein kinase
MC	Müller cells
MEK	MAPK/ERK kinase
Mg^{2+}	magnesium ions, bivalent

mGluR6	metabotropic glutamate receptor 6
min	minutes
mM	millimolar, molar concentration, 10^{-3} mol/l
mRNA	messenger RNA
miRNA	micro-RNA
mTOR	mammalian Target Of Rapamycin
MUT	mutant mice, either rd10 or *β2/β1 ki*
n	statistical sample
N-domain	nucleotide-binding domain
Na^+	sodium ion, monovalent
NaCl	sodium chloride, table salt
Na,K-ATPase	sodium-potassium ATPase
Na_V	voltage-gated sodium channel
NCL	neural ceroid lipofuscinosis
NCX	Na^+/Ca^{2+}-exchanger
neo	neomycin
nfl	nerve fibre layer
ng	10^{-9} gram, nanogram
NKA	sodium-potassium ATPase
nm	10^{-9} m(etre), nanometre
Notch (1-4)	neurogenic locus notch homolog protein (1-4)
NP	nanoparticles
NP40	nonyl phenoxypolyethoxylethanol
NRTN	neurturin
NSC	neural stem cells
NTF	neurotrophic factor
onl	outer nuclear layer
opl	outer plexiform layer
OPS M	opsin m
OPS S	opsin s
OS	outer segments
OSM	oncostatin M
P	postnatal day
PAM	PI3K/Akt/mTOR pathway
PBS	phosphate- buffered saline
PCR	polymerase chain reaction
PDE6	cGMP-specific 3',5'-cyclic phosphodiesterase 6
PDE6β	β subunit of the cGMP-specific 3',5'-cyclic phosphodiesterase
P-domain	phosphorylation domain
PFA	paraformaldehyde
pg	10^{-12} g(ram); picogram
PGRN	progranulin
pH	*potentia hydrogenii,* used to specify the acidity or basicity of aqueous solutions
PI3K	phosphatidylinositol 3-kinase
PKC	protein kinase C
PLC	phospholipase C
pMAPK	phospho p44/42 mitogen-activated protein kinase
PNA	biotinylated peanut agglutinin
PNS	peripheral nervous system
PR	photoreceptor cell
PRGR	X-linked retinitis pigmentosa GTPase regulator
PRPH2	peripherin 2
PSPN	persephin
PTEN	Phosphatase and Tensin homolog
pSTAT3	phosphorylated signal transducer and activator of transcription 3
puro	puromycin
qPCR	real-time quantitative polymerase chain reaction
R	reverse primer
rAAV	recombinant adeno-associated virus
Rac	RAS-related C3 botulinum toxin substrate

RAS	from rat sarcoma virus, a protein of the MAPK/ERK pathway
RAF	from rapidly accelerated fibrosarcoma, a protein of the MAPK/ERK pathway
RBP1	retinol-binding protein 1
RBP4	retinol-binding protein 4
RCS	Royal College of Surgeon's
rd10	"retinal degeneration 10", a model of an autosomal-recessive retinitis pigmentosa
RDH5	retinol dehydrogenase 5
RDH8	retinol dehydrogenase 8
RDH12	retinol dehydrogenase 12
rep	replication genes in AAVs
RET	proto-oncogene tyrosine-protein kinase receptor, derived from rearranged after transfection
RFP	red fluorescent protein
RGC	retinal ganglion cell
RGR	retinal G-protein coupled receptor
rh	recombinant human protein
RHO	rhodopsin
rm	recombinant murine protein
RM	repeated measures
RNA	ribonucleic acid
ROM1	rod outer segment membrane protein 1
RPS	retinal prosthesis system
ROS	rod outer segments
RP	retinitis pigmentosa
RP1	oxygen-regulated protein 1
RP2	oxygen-regulated protein 2
RPE	retinal pigment epithelium
RPE65	all-trans retinyl isomerase
rpm	rounds per minute
RPN	rows of photoreceptor nuclei
RS1	retinoschisin
Rs1	retinoschisin gene, mutations causative for XLRS
SAC	starburst amacrine cell
SARM1	sterile alpha and TIR motif- containing protein 1
sc	self-complementary
SC	*colliculi superiores*
SCN	*nucleus suprachiasmaticus*
SDS	sodium dodecyl sulphate
SDS-PAGE	sodium dodecyl sulphate- polyacrylamide gel electrophoresis
sec	seconds
shH10	adeno-associated virus serotype shH10
SEM	standard error of the mean
SORT1	sortilin
Src	proto-oncogene tyrosine-protein kinase, derived from sarcoma
STAT1	signal transducer and activator of transduction 1
STAT3	signal transducer and activator of transduction 3
STRA6	stimulated retinoic acid-6 receptor
T	threonine
T	thymine
T_A	annealing temperature
TBS-T	TRIS-buffered saline with 0.2% Tween 20
TGF-β	transforming growth factor β
TIR	Toll/interleukin 1 receptor
TLR9	toll-like receptor 9
TM	transmembrane domain
TNFα	tumor necrosis factor α
(s)TNFR1	(soluble) tumor necrosis factor receptor 1
(s)TNFR2	(soluble) tumor necrosis factor receptor 2
TPS	total protein stain

TRIS	tris(hydroxymethyl)aminomethane
Tx-100	Triton X-100
Tyr (705)	L-tyrosine 705
U	enzyme unit, measure of enzymatic activity
USH2A	usherin
V1	primary visual cortex
VA	gene needed for the replication of Ads
VG3-ACs	amacrine cells expressing VGluT3
vg/ml	viral genomes/ml, measure for AAV concentration
VGluT3	vesicular glutamate receptor 3
WB	Western Blot
Wnt	wingless/integrase 1
WT	wild-type mice
X	interchangeable amino acid in FXYD
Y	tyrosine
zeo	zeocin
ZSD	Zapfen-Stäbchen Dystrophie

III.II. ABBREVIATIONS OF DISEASES

AHC	Alternating hemiplegia of childhood
ALS	amyotrophic lateral sclerosis
AMD	age-related macular degeneration
BBS	Bardet-Biedl syndrome
CAPOS	syndrome with cerebella ataxia, areflexia, pes cavus, optic atrophy, sensorineural hearing loss
CMT2	Charcot–Marie–Tooth Type 2
CORD	cone-rod dystrophy
COVID-19	corona virus disease 2019
CRS	cytokine release syndrome
CSP	complex spastic paraplegia
DR	diabetic retinopathy
FHM2	familial hemiplegic migraine type 2
GA	geographic atrophy
HASCD	hypomagnesemia with seizures and cognitive delay
IDH	isolated dominant hypomagnesemia
IRD	inherited retinal dystrophy
LCA	Leber congenital amaurosis
MacTel	macular telangiectasia type 2
MS	multiple sclerosis
PA	primary aldosteronism
RDP	rapid-onset dystonia-parkinsonism
SFM	small fibre neuropathy
SHM	sporadic hemiplegic migraine
STGD1	Stargardt disease
XLRS	X-linked juvenile retinoschisis

IV. LIST OF FIGURES

V. LIST OF TABLES

VI. ACKNOWLEDGEMENTS

First, I would like to thank Prof. Dr. Udo Bartsch, for giving me the opportunity to work in his laboratory, for his guidance throughout the thesis and for his help whenever necessary. He gave me the opportunity to learn a lot about rigorous scientific work during my time in his laboratory.

I am also grateful to all my colleagues. I am grateful for the excellent technical support of Sabine Helbing, Stefanie Schlichting and Elke Becker. I am especially grateful to Sabine for her much-appreciated emotional support during tough times. I would also like to thank Lynn Michelle Grodzki and Susanne Bartsch for many interesting talks. Additionally, I thank Christoph Spartalis for introducing me to the lab's microscopy procedures and image analysis.

My gratitude also goes out to Prof. Dr. Susanne Dobler for examination of the dissertation and all members of the examination commission. I would also like to thank Prof. Dr. Martin Spitzer for providing the position in his clinic. I would also like to acknowledge Ingke Braren for providing the virus preparations needed for this project. A special thanks to Ali Derin and Suanne Conrad and all other animal care takers at the for their excellent animal care.

Lastly, I would like to thank my family, for their loving support during this time and sometimes much needed distraction from arising problems.

VII. PUBLICATIONS, PARTICIPATIONS AND GRANTS

VII.I. PUBLICATIONS

Bartsch, S., Atiskova, Y., Schlichting, S., Becker, E., Herrmann, M., & Bartsch, U. (2025). *Atp1b2*^{Atp1b1} Knock-In Mice Exhibit a Cone–Rod Dystrophy-Like Phenotype. Cells, 14(12), 878. https://www.mdpi.com/2073-4409/14/12/878

- Experimental procedure (Histological and Western Blot analysis of retinoschisin expression)
- Preparation, review and approval of the manuscript

Herrmann, M., Bartsch, S., Spartalis, C., Becker E., Schlichting S., Helbing S. & Bartsch, U. Protection of Photoreceptor Cells with Various Neurotrophic Factors in a Novel Mouse Model with a Cone-Rod Dystrophy-Like Phenotype. Manuscript in preparation (part of the thesis).

- All experimental work (except cloning of lentiviral vectors, cell transductions, generation of clonal cell lines by FACS and cell transplantations)
- Preparation, review and approval of the manuscript
- First author of the manuscript

Herrmann, M., Pille, J.A., Bartsch, S., Braren, I. & Bartsch, U. Hyper-IL6 Attenuates Rod Photoreceptor Loss in the Retina of Pde6b^{rd10} Mice. Manuscript in preparation (part of the thesis).

- All experimental work (except cloning of lentiviral vectors, cell transductions, generation of clonal cell lines by FACS and cell transplantations)
- Preparation, review and approval of the manuscript
- First co-author of the manuscript

VII.II. GRANTS

Maike Herrmann, Udo Bartsch
Protektion von Photorezeptoren mit lentiviral modifizierter Stammzellen- oder einer Gen-Therapie in verschiedenen Krankheitsmodellen
Ernst und Berta Grimmke Stiftung (2023)

Eidesstattliche Versicherung

Hiermit versichere ich an Eides statt, die vorliegende Dissertationsschrift selbst verfasst und keine anderen als die angegebenen Hilfsmittel und Quellen benutzt zu haben.

Sofern im Zuge der Erstellung der vorliegenden Dissertationsschrift generative Künstliche Intelligenz (gKI) basierte elektronische Hilfsmittel verwendet wurden, versichere ich, dass meine eigene Leistung im Vordergrund stand und dass eine vollständige Dokumentation aller verwendeten Hilfsmittel gemäß der Guten wissenschaftlichen Praxis vorliegt. Ich trage die Verantwortung für eventuell durch die gKI generierte fehlerhafte oder verzerrte Inhalte, fehlerhafte Referenzen, Verstöße gegen das Datenschutz- und Urheberrecht oder Plagiate.

AFFIDAVIT

I hereby declare and affirm that this doctoral dissertation is my own work and that I have not used any aids and sources other than those indicated.

If electronic resources based on generative artificial intelligence (gAI) were used in the course of writing this dissertation, I confirm that my own work was the main and value-adding contribution and that complete documentation of all resources used is available in accordance with good scientific practice. I am responsible for any erroneous or distorted content, incorrect references, violations of data protection and copyright law or plagiarism that may have been generated by the gAI.

HAMBURG, DEN 26.01.2026
city and date

Maike Herrmann